AWARD NUMBER: W81XWH-15-1-0280

TITLE: Metabolic and Epigenetic Interactions Regulate Vascular Phenotypic Change and Maintenance in Pulmonary Hypertension

PRINCIPAL INVESTIGATOR: Kurt Stenmark, MD

CONTRACTING ORGANIZATION: Regents of the University of Colorado Denver
Aurora, CO 80045

REPORT DATE: October 2016

TYPE OF REPORT: Annual

PREPARED FOR: U.S. Army Medical Research and Materiel Command
Fort Detrick, Maryland 21702-5012

REPORT DOCUMENTATION PAGE

Form Approved
OMB No. 0704-0188

1. REPORT DATE	2. REPORT TYPE	3. DATES COVERED
October 2016	Annual	15 Sep 2015 - 14 Sep 2016

4. TITLE AND SUBTITLE

Metabolic and Epigenetic Interactions Regulate Vascular Phenotypic Change and Maintenance in Pulmonary Hypertension

5a. CONTRACT NUMBER

5b. GRANT NUMBER
W81XWH-15-1-0280

5c. PROGRAM ELEMENT NUMBER

6. AUTHOR(S)

Kurt Stenmark, MD

E-Mail:kurt.stenmark@ucdenver.edu

5d. PROJECT NUMBER

5e. TASK NUMBER

5f. WORK UNIT NUMBER

7. PERFORMING ORGANIZATION NAME(S) AND ADDRESS(ES)

University of Colorado Denver
12700 E 19th Ave B133
Aurora, CO 80045-2507

8. PERFORMING ORGANIZATION REPORT NUMBER

9. SPONSORING / MONITORING AGENCY NAME(S) AND ADDRESS(ES)

U.S. Army Medical Research and Materiel Command
Fort Detrick, Maryland 21702-5012

10. SPONSOR/MONITOR'S ACRONYM(S)

11. SPONSOR/MONITOR'S REPORT NUMBER(S)

12. DISTRIBUTION / AVAILABILITY STATEMENT

Approved for Public Release; Distribution Unlimited

13. SUPPLEMENTARY NOTES

14. ABSTRACT

Changes in metabolism have been suggested to contribute to the aberrant phenotype of vascular cells including fibroblasts in pulmonary hypertension (PH). We tested the hypothesis that metabolic reprogramming to aerobic glycolysis is a critical adaptation of fibroblasts in the hypertensive vessel wall that drives proliferative and pro-inflammatory activation through a mechanism involving increased activity of the NADH-sensitive transcriptional co-repressor C-terminal binding protein 1 (CtBP1).

Using fluorescence-lifetime imaging and mass spectrometry-based metabolomics we found adventitial fibroblasts from animals and humans with severe PH (termed PH-Fibs) displayed aerobic glycolysis and increased free NADH when cultured under normoxia. We documented increased expression of CtBP1 *in vivo* and *in vitro* in fibroblasts within or from the pulmonary adventitia of humans and animals with PH. Decreasing NADH pharmacologically with a novel inhibitor of CtBP1, 4-methylthio-2-oxybutyric acid (MTOB), or blocking CtBP1 using siRNA attenuated proliferation, corrected the glycolytic reprogramming phenotype of PH-Fibs, and augmented transcription of anti-proliferative, pro-apoptotic, and anti-inflammatory genes. Treatment of hypoxic mice with MTOB decreased glycolysis, attenuated proliferation, and inflammation and reduced remodeling in the distal pulmonary vasculature. CtBP1 is thus a critical factor linking changes in cell metabolism to cell phenotype in PH and a potential therapeutic target.

15. SUBJECT TERMS

Pulmonary hypertension, hypoxia, chronic obstructive pulmonary disease, metabolism, fibroblasts, epigenetic regulation, miR-124, polypyrimidine tract-binding protein 1, alternative splicing, pyruvate kinase, glycolysis, proliferation, inflammation, CtBP1, HDAC inhibitor.

16. SECURITY CLASSIFICATION OF:			17. LIMITATION OF ABSTRACT	18. NUMBER OF PAGES	19a. NAME OF RESPONSIBLE PERSON
a. REPORT	b. ABSTRACT	c. THIS PAGE			USAMRMC
Unclassified	Unclassified	Unclassified	Unclassified	102	19b. TELEPHONE NUMBER *(include area code)*

Table of Contents

Page

1. INTRODUCTION

Despite recent advances in diagnosis and treatment, pulmonary hypertension (PH) remains a devastating disease with high mortality affecting both adult and pediatric patients. While it can arise for unknown (idiopathic) or genetic reasons, it is more frequently associated with chronic lung diseases such as Chronic Obstructive Pulmonary Disease (COPD), pulmonary fibrosis, obesity, and viral infections, disorders that are very prevalent among veterans. A lack of understanding of the factors that cause PH in patients with chronic lung disease has limited the therapeutic options for these patients. Notable is the fact that though some progress has been made in the treatment of patients with idiopathic PAH, none of the drugs shown to be useful in these patients have shown any benefit in patients with chronic hypoxic lung diseases, such as COPD, or lung fibrosis.

Pulmonary hypertension, in the aforementioned chronic lung diseases, is generally believed to be hypoxic in origin. However, PH in these patients is often irreversible or only minimally reversible with supplemental oxygen. This may be due to structural changes in the lung blood vessels in these patients. These vessels exhibit thickening and fibrotic changes due to excessive proliferation and resistance to normal senescence of resident pulmonary vascular wall cells. Recent studies also suggest that an inflammatory mechanism plays a significant role in the pathogenesis of these forms of PH. Interestingly, cells in the hypertensive lung blood vessels, including the ones we are proposing to study, endothelial cells and fibroblasts, have recently been shown to exhibit many features of cancer cells including excessive proliferation, resistance to death, and a hyper-inflammatory phenotype. It has recently been suggested that cancer cells exhibiting these same abnormal functional characteristics also exhibit dramatic changes in their metabolism and it is these metabolic changes that are the principle cause of all the abnormal cell characteristics. In this proposal, we test the hypothesis that metabolic abnormalities similar to those observed in cancer cells, exist in cells of the pulmonary vasculature and that they control the proliferative and inflammatory behavior of cells. Importantly, we also propose that these metabolic abnormalities can be targeted with specific pharmacologic therapies to reverse the cell abnormalities and mitigate pulmonary hypertension.

We propose a series of experiments, which will allow us to determine precisely how the metabolic abnormalities arise, how they direct the abnormalities of cell phenotype that contribute directly to PH, and lastly how we can interrupt this process to achieve better outcomes. We believe these studies will lay the groundwork for a new treatment strategy that targets multiple molecular abnormalities in PH simultaneously and thus, we speculate, will be potentially more effective and achieve greater benefits than the current therapeutic approaches. We also believe these studies will open the door to potential new diagnostics to assess the disease progression as well as responses to therapy.

PH is a prevalent co-morbid condition that significantly worsens morbidity and mortality in patients with a wide variety of disorders, from those who survive acute lung injury to those with pulmonary fibrosis or COPD. Identifying improved treatment strategies for these patients is our long-term goal. Based on existing data, we hypothesized that vascular remodeling in PH results from histone deacetylase (HDAC)-mediated epigenetic modifications in adventitial fibroblasts, which alter expression of miR-124 and polypyrimidine tract binding protein 1 (PTBP1) to result in sustained metabolic changes (aerobic glycolysis) that control the activated, pro-inflammatory phenotype of fibroblasts from the pulmonary hypertensive vessel wall (PH-Fibs). The long-term goals of our research are: 1) define the mechanisms controlling metabolic abnormalities in PH-Fibs that result in persistence of inflammation in PH, and 2) define whether HDAC inhibition can abrogate metabolic abnormalities and thus sustained pro-inflammatory activation in PH-Fibs, and reverse the PH process and 3) determine if we can define, using metabolomic approaches, specific metabolites that will be useful in diagnosis, assessment of severity, and responses to treatment in PH.

2. KEYWORDS

Pulmonary hypertension, hypoxia, chronic obstructive pulmonary disease, metabolism, fibroblasts, epigenetic regulation, miR-124, polypyrimidine tract-binding protein 1, alternative splicing, pyruvate kinase, glycolysis, proliferation, inflammation, C-terminal binding protein 1, heme oxygenase 1, HDAC inhibitor.

3. ACCOMPLISHMENTS

Major Goal 1: Define the metabolic profile of pulmonary hypertensive fibroblasts (bovine and human) compared to controls.

What was accomplished under this goal?

We wanted to begin the project by defining in depth the metabolic reprogramming that takes place in cells in the pulmonary hypertensive vessel as we hypothesize that these changes are directly involved in controlling the changes in proliferation and inflammation that characterize vascular remodeling in pulmonary hypertension (PH). We started by performing RNA-seq analysis to examine differentially regulated genes in PH vs. control (CO) fibroblasts. RNA-seq analysis elucidated over 1000 differentially regulated genes in PH-Fibs compared to CO-Fibs. Glycolysis/gluconeogenesis and pyruvate metabolism were identified as two of the most significantly upregulated pathways in data set (Table 1 and Supplemental Figure 2A in the publication by M. Li et al., Circulation, 2016, Appendix 1). We identified upregulation of gene coding for enzymes and transporters involved in glucose lactate catabolism in PH-Fibs (Table 2, M. Li et al., Circulation, 2016). Validation by RT-PCR analysis confirmed increased gene expression of the glycolytic genes in both human and PH-Fibs relative to control fibroblasts. Upregulation of the GLUT1 protein was observed in situ the adventitia of hypoxic hypertensive calves by immunofluorescence (Fig. 1C, Li et al., Circulation, 2016, Appendix 2).

To extensively corroborate the transcriptomic results, steady state and flux tracing experiments were performed via Ultra-High Pressure Liquid Chromatography-Mass Spectrometry (UHPLC-MS) by incubating CO and PH-Fibs with U-13C-glucose. Principal component analysis of metabolomics data revealed distinct metabolic phenotypes (metabotypes) for PH-fibroblasts and controls. Metabotypes of bovine PH-fibroblasts overlapped with the human counterparts, underpinning the validity of the animal model.

PH-fibroblasts were characterized by increased glucose uptake and lactate generation, and accumulation of glycolytic intermediates (Fig. 1). Decreased pyruvate export to the mitochondria and accumulation of metabolites of the pentose phosphate pathway were observed, consistent with the necessity to generate reducing equivalents (NADPH) to recycle oxidized glutathione. Indeed, increased levels of oxidized glutathione, impaired GSH/GSSG ratios, increased ROS levels (DCF and HSP33-FRET imaging) were observed in PH-fibroblasts. Increased fluxes through the non-oxidative phase of the pentose phosphate pathway and accumulation of products of lipid anabolism are consistent with the necessity to synthesize new DNA and cell membrane in proliferating PH-fibroblasts (Fig. 1).

Glutamine uptake was more sustained in PH fibroblasts, as determined by the ratios of steady state levels of the amino acid in the supernatants of cultured cells vs. controls. PH-fibroblasts mostly used glutamine to generate glutamate, both to synthesize reduced glutathione (to partially counteract oxidative stress) and fuel the Krebs cycle through the generation of alpha-ketoglutarate. However, increased oxidative stress affected oxygen consumption rates at the Complex I level, resulting in a metabolic blockade in late Krebs cycle reactions. On the other hand, alpha-ketoglutarate/citrate ratios could be interpreted on the basis of the mass action law, which suggests, together with the accumulation in 2-hydroxyglutarate, potential reductive carboxylation fluxes from glutamine in mitochondria. Data also suggest redox-dependent regulation of oxoglutarate dehydrogenase activity and ongoing substrate level phosphorylation to generate minimum levels of nucleoside triphosphates in mitochondria independently from the electron transport chain (Figure B). These results were published in two recent papers) L. Plecita´-Hlavata et al., Am. J. Resp. Cell Mol. Biol., Dec. 2015 (appendix reference 2) and M. Li et al., Circulation, Sept. 2016 (appendix reference 1).

Figure 1

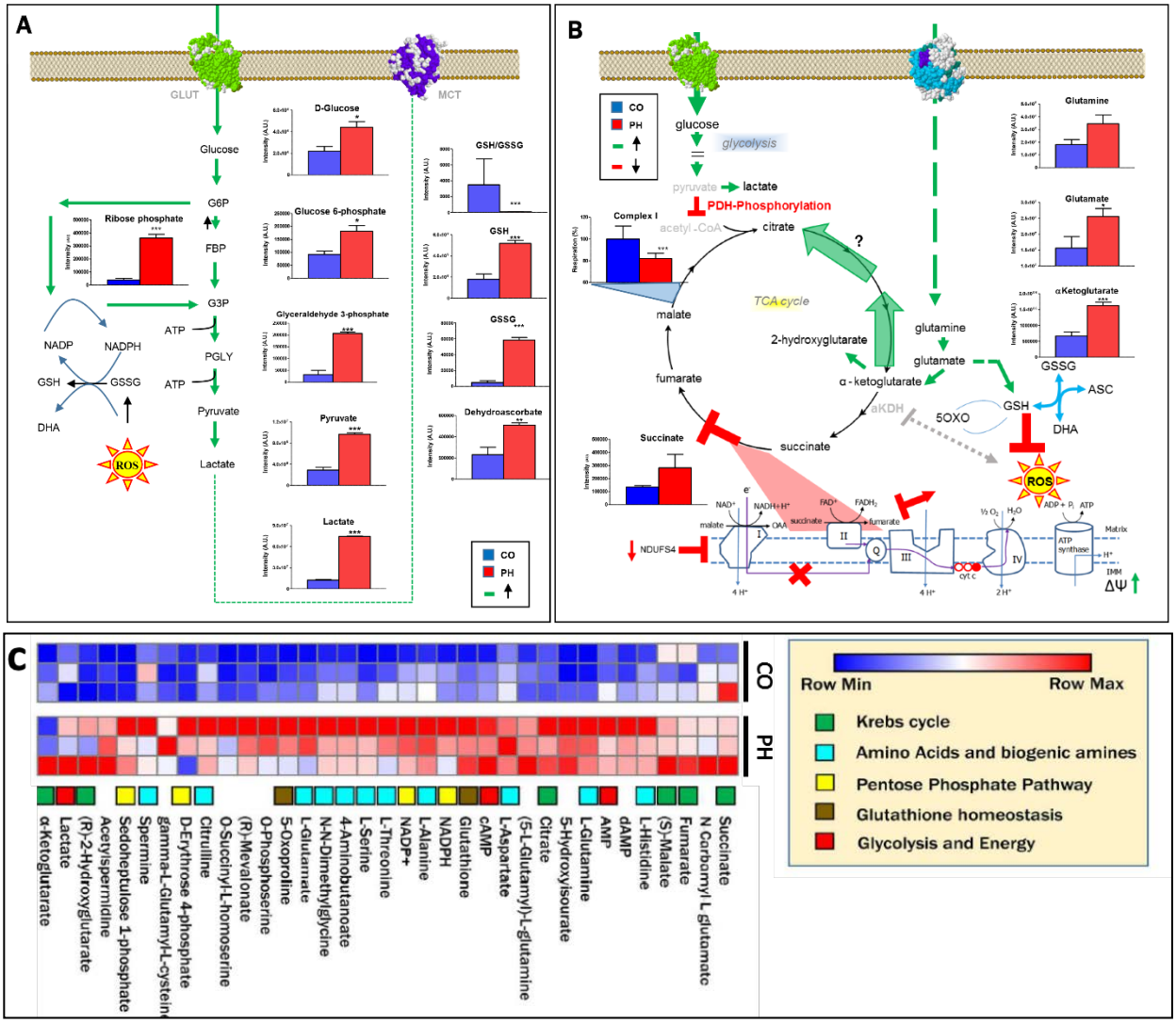

Fig. 1: Metabolic reprogramming in human PH-fibroblast (red) versus control (CO - blue), as determined through UHPLC-MS. An overview of glycolysis and pentose phosphate pathway (A) and glutaminolysis and Krebs cycle (B) is provided. (C) Heat-map generated from UHPLC-showed the levels of metabolites involved in different metabolic pathway. (n=6, * P <0.05; ** P<0.001).

Major Goal 2: **Define the signaling pathways through which metabolic dysregulation and pro-inflammatory activation of PH-Fibs contributes to the recruitment, retention, and activation of macrophages**.

What was accomplished under this goal?

Our findings of glycolytic programming and consistently increased free NADH in PH-Fibs were consistent with observations in cancer cells where C-terminal binding protein 1 (CtBP1), a transcriptional co-repressor, which specifically binds genes involved in regulating proliferation, apoptosis, and inflammation is increased and contributes to their hyperproliferative apoptosis resistant phenotype. Our studies show, for the first time, upregulation in vivo in cells of the adventitia and in cultured adventitial fibroblasts of CtBP1 in a non-cancerous disease condition. We performed extensive studies using both siCtBP1 and a novel pharmacologic inhibitor of CtBP1, 4-Methylthio-2-oxobuteric acid (MTOB) and demonstrated that CtBP1 controlled expression of the cyclin-dependent genes p15, p21, the pro-apoptotic regulators NOXA and PERP, and also attenuated proliferation, corrected the glycolytic reprogramming of PH-Fibs and augmented transcription of the anti-inflammatory gene HMOX1 (Fig. 2).

Figure 2

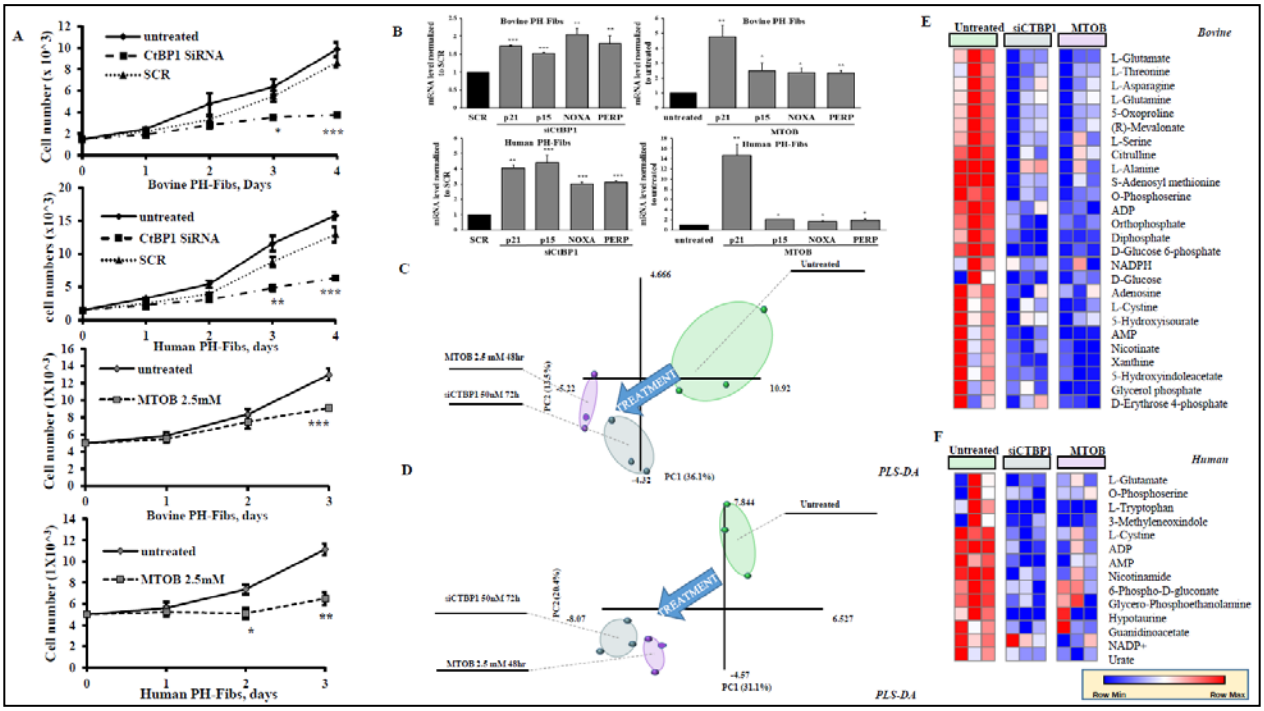

Fig. 2: CtBP1 regulates the expression of genes involved in proliferation, cell survival and metabolic state in adventitial fibroblasts. Inhibition of CtBP1 by siRNA (50nM, 72hrs) or by MTOB (2.5mM, 48hrs) (A) significantly attenuated proliferation of both bovine and human PH-Fibs (n=3-6. SCR=scrambled. *, P <0.05; **, P <0.01; ***, P <0.001, compared to scrambled siRNA treated PH-Fibs-repeated measures ANOVA), (B) restored anti-proliferative gene (p21, p15) and pro-apoptosis gene (NOXA, PERP) expression. (n=3-6. *, P <0.05; **, P <0.01; ***, P <0.001, compared to scrambled siRNA treated or untreated PH-Fibs). MS metabolomic analysis (n=3) revealed that siCtBP1 and MTOB (C, D) altered the overall metabolic status of both bovine and human PH-Fibs and (E, F) showed the tendency to decrease the levels of metabolites involved in proliferative anabolic pathways (e.g. energy metabolism – AMP, ADP, orthophosphate and diphosphate; nucleotide biosynthesis, and antioxidant reactions – amino acids, glutamine/ glutamate, and pentose phosphate pathway intermediates), consistent with a less proliferative phenotype.

In addition, using Chip analysis we demonstrated for the first time that CtBP1 directly binds the HMOX1 promoter thus explaining, in part, how changes in metabolism can directly regulate the inflammatory state of the cell. Most intriguingly we found that treatment of hypoxic mice with MTOB decreased glycolysis and expression of inflammatory genes, attenuated proliferation, and suppressed macrophage numbers in remodeling in the distal pulmonary vasculature (Fig. 3).

Figure 3

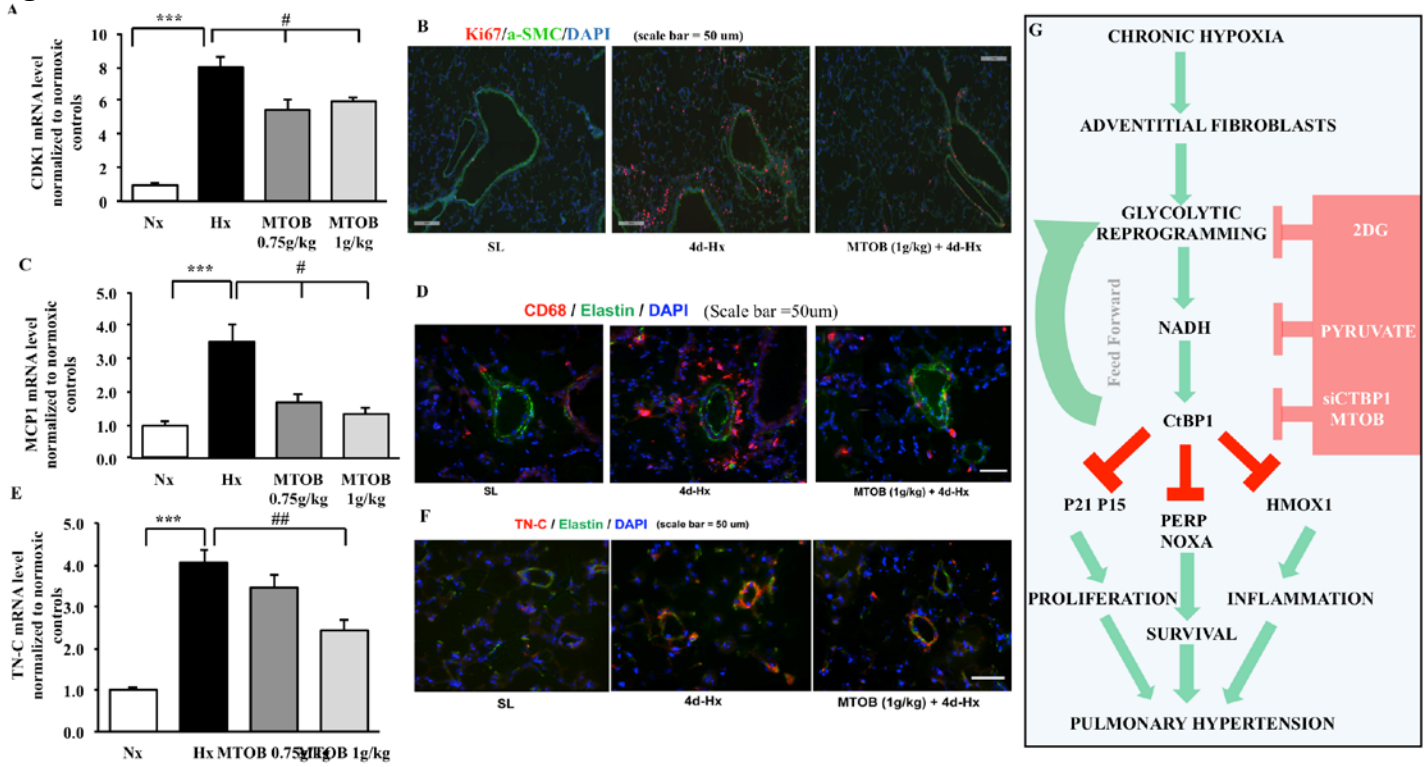

Figure 3: Hypoxia exposure induced and MTOB treatment inhibited proliferation, inflammation and vascular remodeling in mouse lung. (A) Four day hypoxia exposure significantly increased cyclin-dependet kinase 1 (CDK1) mRNA expression in mouse whole lung tissues compared to their normoxic contols; MTOB treatment significantly decreased CDK1 levels. (B) Ki67 immunoflurescent staning (red=ki67, green= ŧSMC, blue=DAPI, scale bar=50um) demonstrated that hypoxia increased and MTOB decreased cell proliferation in mouse lung tissue. (C) Four day hypoxia exposure significantly increased MCP1 mRNA expression in mouse whole lung tissues compared to their normoxic contols, and MTOB treatment significantly decreased the MCP1 level. (D) Consistent with qPCR data for MCP1, staining of the monocyte/ macrophage marker, CD68, showed hypoxia increased, and MTOB decreased, recruitment of monocytes/macrophage (red=CD68, green=elastin, blue=DAPI, scale bar=50um). (E) Four day hypoxia exposure significantly increased tenascin C (TN-C), an extra-cellular matrix marker, mRNA expression in mouse whole lung tissues compared to their normoxic contols, and MTOB treatment significantly decreased the TN-C level. (F) Accordingly, TN-C staining demonstrated MTOB attenuated vascular remodeling induced by hypoxia exposure (red=TN-C, green=elastin, blue=DAPI, scale bar=50um) (n=5, ***, $P<0.001$, compared to normoxic controls. #, $P<0.05$; ##, $P < 0.01$ compared to hypoxic mouse lungs). (G) CtBP1 links metabolic changes to gene expression and contributes to the development of pulmonary hypertension: pulmonary artery adventitial fibroblast cells isolated from chronic hypoxia induced pulmonary hypertensive cow model and patients with pulmonary hypertension (PH-Fibs) and maintained under normoxic conditions demonstrated a perpetuated pro-inflammatory and hyper-proliferative phenotype, as well as a metabolic reprograming towards aerobic glycolysis and subsequently increased NADH levels. The transcriptional co-repressor activity of CtBP1 is stimulated as a result of elevated NADH level. CtBP1 then enhances cell proliferation via transcriptional repression of cell cycle inhibitors *P21, P15*, and promotes cell survival through repression of pro-apoptotic genes (*NOXA* and *PERP*). CtBP1 also induces inflammation through the repression of anti-inflammatory gene *HMOX1*. Reducing NADHs level by 2DG or pyruvate can inhibit proliferation in PH-Fibs and augment the anti-inflammatory phenotype of PH-Fibs. Targeting CtBP1 at the RNA level via siRNA or at the protein level by MTOB can not only inhibit proliferation and augment anti-inflammatory phenotype of PH-Fibs, but can also rescue cell metabolic state.

The entirety of this data was recently published in Circulation (appendix 1).

Major Goal 3: Define the mechanisms by which the transcriptional splicing factor PTBP1 regulates PKM1 to PKM2 switching and thus the metabolic status of pulmonary hypertensive fibroblasts and further to determine whether restoring PTBP1 to normal would abrogate metabolic dysfunction and normalize the proliferative and inflammatory characteristics of PH-Fibs.

What was accomplished under this goal?

In previous experiments we have shown that in the PH-Fibs described above that there is a significant decrease in miR124 expression (D. Wang et al., *MicroRNA-124 controls the proliferative, migratory, and*

inflammatory phenotypes of pulmonary vascular fibroblasts. Circ. Res., 2014, p67-78). We further showed that miR124 regulates PTBP1 expression. Furthermore, we previously established that PH-Fibs (both bovine and human) have increased Class 1 HDAC expression and that HDAC inhibitors (HDACi) restore miR124 and decrease PTBP1 expression. In cancer cells it has been established that increases in the expression of PTBP1 promotes switching of pyruvate kinase isozyme expression from M1(PKM1) to (PKM2), which favors aerobic glycolysis. We have now performed extensive experiments testing the hypothesis that 1) high PTBP1 expression, as a result of decreased miR124 expression, mechanistically underlies the elevated PKM2 to PKM1 ratio and thus aerobic glycolysis and that normalizing PTBP1 or miR124 or treating cells with HDAC inhibitors would abrogate the metabolic and functional changes.

Hyper-proliferative, apoptosis-resistant, pro-inflammatory PH-Fibs exhibit an altered metabolic status that favors aerobic glycolysis (high glucose uptake, increased PDH phosphorylation and increased lactate production) and constitutive mitochondrial alterations (mitochondrial hyperpolarization, retarded oxidative phosphorylation, and increased ROS production). In PH-Fibs, PTBP1 knockdown, restoration of miR124 or treatment with HDACi – all resulted in: 1) Reversed glycolysis reprogramming to normal (decreased metabolites, α-Ketoglutarate, GSH, Glutamine…and decreased lactate production); 2) rescued mitochondria abnormalities towards to normal (enhanced maximal respiratory capacity, decreased mitochondrial membrane potential and decreased ROS production); 3) significantly reduced cell proliferation. A small molecule, PKM2 activator inhibited lactate production and cell proliferation by promoting PKM2 tetramer formation (Fig. 4).

Figure 4

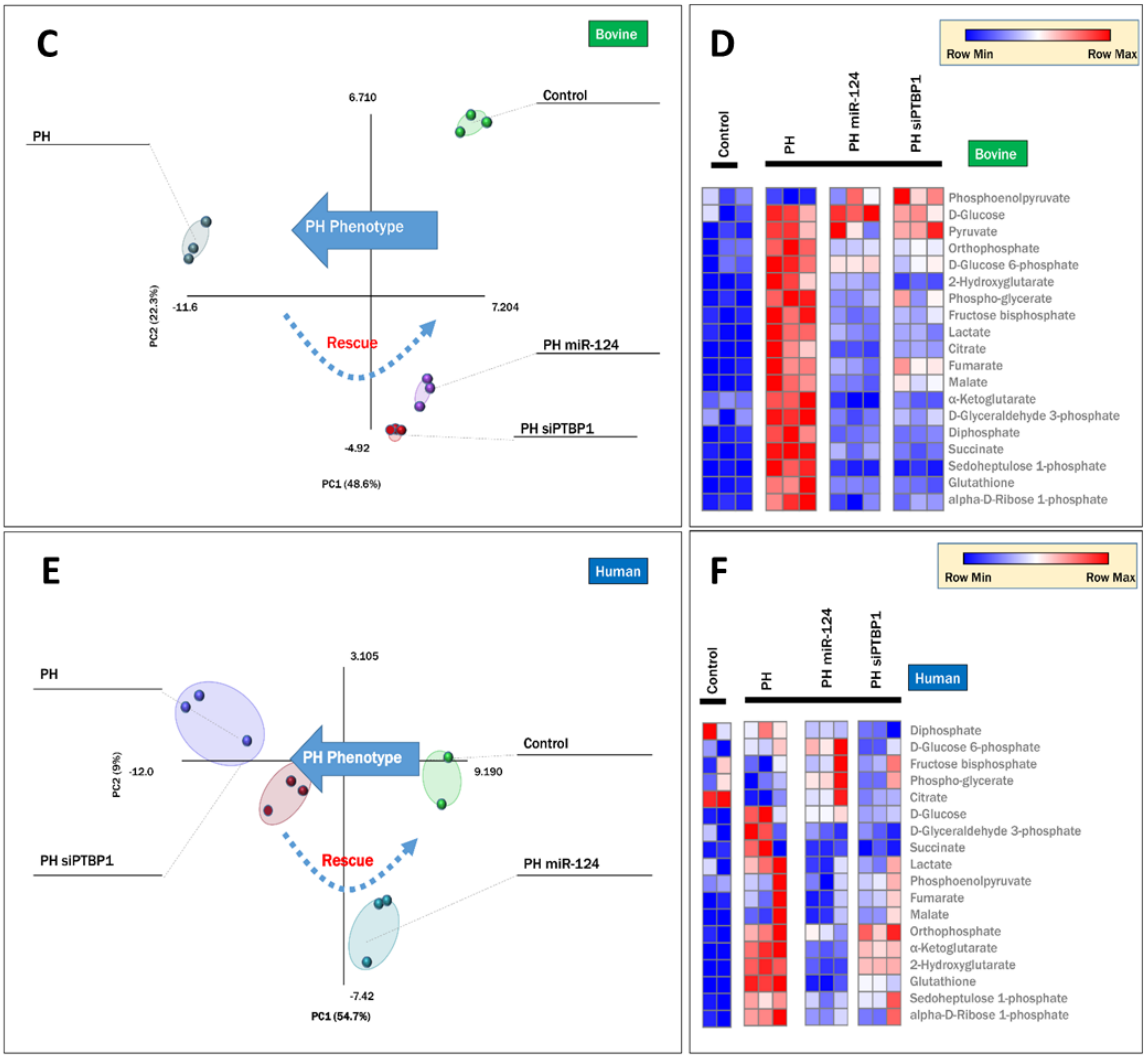

Fig. 4: MiR-124 overexpression and PTBP1 silencing regulate the metabolic phenotype in PH-Fibs. Steady state UHPLC- MS demonstrated decreased glucose uptake and lactate production 48hrs post-transfection of miR-124 mimic and siPTBP1 in PH-Fibs (A, bovine; B, human). MS metabolomic analysis revealed that miR-124 mimic and siPTBP1 altered the overall metabolic status of both

bovine (C) and human (E) toward to CO-Fibs. Heat-map generated from MS showed the tendency to decrease the levels of metabolites involved in glycolysis and mitochondrial oxidative phosphorylation 48hrs post-transfection with miR-124 mimic and siPTBP1. Each column represents an individual samples from each group (D, bovine; F, human). (n=3, *P<0.05, **P<0.01, ***P<0.001, compared to scrambled siRNA).

At present, we can conclude that in PH-Fibs, PTBP1 silencing, miR-124 restoration, or treatment with HDAC*i* can reverse the overall metabolic state of the cells and result in normalization of proliferative and inflammatory capabilities. These data have been presented in abstract form (appendix #3) and will be submitted for publication by November 1, 2016.

What opportunity for training and professional development has the project provided?

Nothing to report

How were the results disseminated to communities of interest?

1. Kurt R. Stenmark. *Metabolic Reprograming and Hypoxia in Pulmonary Arterial Hypertension*, Basic Translational Scientific Symposium, American Thoracic Society (ATS), San Francisco, CA.
2. Hui Zhang, Daren Wang, Min Li, Lydie Plecitá, Angelo D'alessandro, Suzette Riddle, B. Alexandre McKeon, Amanda Flockton, Maria Frid, Petr Ježek, Karim El Kasmi, Kurt Stenmark. *Using Genetics, Epigenetics and Small Molecules to Reverse Metabolic Reprogramming in Adventitia Fibroblasts for Pulmonary Hypertension Therapy.* American Thoracic Society (ATS), San Francisco, CA.
3. Angelo D'Alessandro, Suzette Riddle, Hui Zhang, Min Li, Amanda Flockton, Natalie J. Serkova, Kirk C. Hansen, Radu Moldvan, Jens Poth, B. Alexandre McKeon, Maria Frid, Hong Li, Hongbin Liu, Angela Canovas, Juan Medrano, Dijana Illoska, Lydie Plecita-Hlavata, Petr Ježek, Mehdi A. Fini, Soni Pullamsetti, Karim C. El Kasmi, Qinghong Zhang, Kurt R. Stenmark. *Metabolic Reprogramming in Pulmonary Hypertension as gleaned through Mass Spectrometry-Based Metabolomics.* American Thoracic Society (ATS), San Francisco, CA.
4. Hui Zhang, Min Li, Daren Wang, Lydie Plecitá, Suzette Riddle, B. Alexandre McKeon, Amanda Flockton, Maria Frid, Petr Ježek, and Kurt Stenmark. *Epigenetic Regulation of the Metabolic State of Vascular Adventitial Fibroblasts in Pulmonary Hypertension.* American Thoracic Society (ATS), San Francisco, CA.

What do you plan to do during the next reporting period to accomplish the goals?

We will finish the experiments needed to submit a manuscript on Major Goal 3, described above. We will also begin working on our next major goal, which is to identify specific epigenetic changes in the histone acetylation status of miR-124 and/or miR processing genes in PH-Fibs that lead to decreased expression of miR-124. Lastly, we will obtain IRB approval to obtain blood from human subjects to identify glycolytic metabolites (biomarkers and serum) that will aid in the diagnosis portion of disease severity in responses to therapy.

4. IMPACT

The impact on the development of the principal discipline(s) of the project:

In pulmonary hypertension, little is known about the molecular mechanisms that link the metabolic state of cells to gene transcription and functional changes in their phenotype. We show that CtBP1, a transcription factor that is activated by increased free NADH, acts as a molecular linker to drive the proliferative and pro-inflammatory phenotype of adventitial fibroblasts within the hypertensive vessel wall.

This work supports the novel hypothesis that at least some forms or stage of pulmonary hypertension are associated with the rewiring of cellular metabolic programs that use alterations in the cellular redox state to control the activity of CtBP1, which then coordinates expression of a network of genes implicated in cell proliferation, apoptosis resistance, and inflammation. This changes the way we think about how functional changes in cells are initiated and maintained.

We also found that treatment of fibroblasts from the pulmonary hypertensive vessel and of hypoxic mice with a pharmacological inhibitor of CtBP1, MTOB, leads to a normalization of proliferation, inflammation, and the aberrant metabolic signaling. Our results suggest that targeting this metabolic sensor may be a more specific approach to treating metabolic abnormalities in pulmonary hypertension than use of more global metabolic inhibitors.

It will be important in future studies to determine whether inhibition of CyBP1 can be combined with other vasodilating drugs to effect reversal of established severe forms of pulmonary hypertension.

What was the impact on other disciplines?

Our findings regarding miR-124 and its regulation of the glycolytic phenotype of cells has now been extended by collaborative investigators of ours who show that similar abnormalities in miR-124 processing and in targets (PTBP1 an subsequently PKM2) contribute to dysregulation of circulating endothelial progenitor cells in patients with idiopathic or hereditary PAH. These abnormalities in the behavior of endothelial cells have been shown not only in PH but also in other lung and cardiac fibrotic conditions. Thus, the impact of the original work proposed is having far reaching effects on the understanding of PH and lung fibrotic conditions that were not predicted at the time the experiments were proposed.

What was the impact on technology transfer?

Nothing to report

What was the impact on society beyond science and technology?

Nothing to report

5. CHANGES / PROBLEMS

Nothing to report

6. PRODUCTS

Publications, conference papers, and presentation

1. Plecita-Hlavata L, Tauber J, Li M, Zhang H, Flockton AR, Pullamsetti S, Chelladurai P, D'alessandro A, El Kasmi KC, Jezek P, and Stenmark KR. *Constitutive Reprogramming of Fibroblast Mitochondrial Metabolism in Pulmonary Hypertension.* Am. J. Resp. Cell. Molec. Biol. 55(1):47-57, 2016. (PMID: 26699943).
2. Li M, Riddle SR, Zhang H, D'Alessandro A, Flockton AR, Serkova NJ, Hansen KC, Moldovan R, McKeon BA, Frid MG, Kumar S, Li H, Liu H, Canovas A, Medrano JF, Thomas MG, Iloska D, Plecita-Hlavata L, Ježek P, Pullamsetti S, Fini M, El Kasmi KC, Zhang Q, and Stenmark KR. *Metabolic Reprogramming Regulates the Proliferative and Inflammatory Phenotype of Adventitial Fibroblasts in Pulmonary Hypertension through the Transcriptional Co-Repressor C-terminal Binding Protein-1*. Circulation. 2016; CIRCULATIONAHA.116.023171 [Epub ahead of print, Aug. 25 2016]. http://dx.doi.org/10.1161/CIRCULATIONAHA.116.023171
3. Stenmark KR, Tuder RM, and El Kasmi KC. *Metabolic Reprogramming and Inflammation Act in Concert to Control Vascular Remodeling in Hypoxic Pulmonary Hypertension*. J. Appl. Physiol. 119(10:1164-1172, 2015. (PMID: 25930027).
4. El Kasmi KC and Stenmark KR. *Contribution of Metabolic Reprogramming to Macrophage Plasticity and Function*. Semin. Immunol. S1044-S5323, 2015. (PMID: 26454572).

7. PARTICIPANTS / COLLABORATING ORGANIZATIONS

What individuals have worked on the project?

Kurt R. Stenmark, MD

Identifier: 125823

Nearest person month worked: 3

Contributions to the project

Stenmark oversaw experimental design, data collection, and data interpretation.

Funding support

P01 HL014985 - NHLBI
1R01HL114887 - NHLBI
1R01HL125642 - NHLBI

Hui Zhang, PhD

Identifier: 245717

Nearest person month worked: 8

Contributions to the project

Did all cell and molecular experiments provided in the report.

Funding support

NIH/NHLBI PPG – 5 P01 HL014985-40A1

Angelo D'alessandro, PhD

Identifier: 264840

Nearest person month worked: 2

Contributions to the project

Performed all ultra-high pressure liquid chromatography mass spectrometry analysis in human and bovine cells.

Funding support

No change

Mehdi Fini, MD

Identifier:

Nearest person month worked: 1

Contributions to the project

Consulting on the project and preparing regulatory documents for human tissue studies

Funding support

No change

CHENG JUN HU, PhD

Identifier: 184956

Nearest person month worked: 3

Contributions to the project

Worked with Hui Zhang to perform experiments aimed at understanding regulation of PCAM1/2 ratio changes and participated in experiments aimed at understanding miR-124 control of PTBP1 and PCAM1/2 splicing.

Funding support

No change

Flockton Amanda

Identifier: 141862

Nearest person month worked: 3

Contributions to the project

Technician – helped to perform all cell experiments

Funding support

No change

Brittany McKeon

Identifier: 211509

Nearest person month worked: 2

Contributions to the project

Technician – helped to perform all cell experiments

Funding support

No change

Min Li

Identifier: 184463

Nearest person month worked: 4

Contributions to the project

Technician – helped to perform cells characterization experiments

Funding support

none

Maria Frid

Identifier: 125931

Nearest person month worked: 1

Contributions to the project

Technician – helped to prepare ACURO and IACUC documentation

Funding support

none

Has there been a change in the active other support of the PD/PI(s) or senior/key personnel since the last reporting period?

No changes

What other organizations were involved as partners?

Nothing to report

8. SPECIAL REPORTING REQUIREMENTS

N/A

9. APPENDICES

ORIGINAL RESEARCH

Constitutive Reprogramming of Fibroblast Mitochondrial Metabolism in Pulmonary Hypertension

Lydie Plecitá-Hlavatá[1], Jan Tauber[1], Min Li[2], Hui Zhang[2,3], Amanda R. Flockton[2], Soni Savai Pullamsetti[4], Prakash Chelladurai[4], Angelo D'Alessandro[5], Karim C. El Kasmi[6], Petr Ježek[1], and Kurt R. Stenmark[2]

[1]Department of Membrane Transport Biophysics, Institute of Physiology, Czech Academy of Sciences, Prague, Czech Republic; [2]Developmental Lung Biology and Cardiovascular Pulmonary Research Laboratory, University of Colorado, Denver, Colorado; [3]Department of Pediatrics, Shengjing Hospital of China Medical, University, Shenyang, China; [4]Department of Lung Development and Remodeling, University of Giessen and Marburg Lung Center, Bad Nauheim, Germany; and Department of [5]Biochemistry and Molecular Genetics, and [6]Pediatric Gastroenterology, University of Colorado, Denver, Colorado

Abstract

Remodeling of the distal pulmonary artery wall is a characteristic feature of pulmonary hypertension (PH). In hypoxic PH, the most substantial pathologic changes occur in the adventitia. Here, there is marked fibroblast proliferation and profound macrophage accumulation. These PH fibroblasts (PH-Fibs) maintain a hyperproliferative, apoptotic-resistant, and proinflammatory phenotype in *ex vivo* culture. Considering that a similar phenotype is observed in cancer cells, where it has been associated, at least in part, with specific alterations in mitochondrial metabolism, we sought to define the state of mitochondrial metabolism in PH-Fibs. In PH-Fibs, pyruvate dehydrogenase was markedly inhibited, resulting in metabolism of pyruvate to lactate, thus consistent with a Warburg-like phenotype. In addition, mitochondrial bioenergetics were suppressed and mitochondrial fragmentation was increased in PH-Fibs. Most importantly, complex I activity was substantially decreased, which was associated with down-regulation of the accessory subunit nicotinamide adenine dinucleotide reduced dehydrogenase (ubiquinone) Fe-S protein 4 (NDUFS4). Owing to less-efficient ATP synthesis, mitochondria were hyperpolarized and mitochondrial superoxide production was increased. This pro-oxidative status was further augmented by simultaneous induction of cytosolic nicotinamide adenine dinucleotide phosphate reduced oxidase 4. Although acute and chronic exposure to hypoxia of adventitial fibroblasts from healthy control vessels induced increased glycolysis, it did not induce complex I deficiency as observed in PH-Fibs. This suggests that hypoxia alone is insufficient to induce NDUFS4 down-regulation and constitutive abnormalities in complex I. In conclusion, our study provides evidence that, in the pathogenesis of vascular remodeling in PH, alterations in fibroblast mitochondrial metabolism drive distinct changes in cellular behavior, which potentially occur independently of hypoxia.

Keywords: mitochondria; complex I; oxidative metabolism; pulmonary hypertension; adventitial fibroblasts

Chronic pulmonary hypertension (PH) is a complex disease characterized by sustained increases in pulmonary vascular resistance, severe obliterative remodeling of the pulmonary arteries, right ventricular dysfunction, and premature death (1). The vascular remodeling observed in PH involves an imbalance of cell proliferation versus cell death and, almost uniformly, persistent inflammation. These observations have led to the hypothesis that the cellular and molecular features of PH resemble hallmark characteristics of cancer (1–6). It is increasingly recognized that changes in cell metabolism in cancer cells, as well as in cells in the surrounding stroma, are essential for cancer cells to proliferate, migrate, and exhibit proinflammatory characteristics. As such, there is an intense effort in the cancer field to define the mechanisms regulating the links between changes in metabolism, growth, and inflammation, as they may offer new opportunities for therapy.

(Received in original form April 30, 2015; accepted in final form December 8, 2015)

This work was supported by National Institutes of Health (NIH) program project grant 5 P01 HL014985-40A1, NIH R01 grant 1 R01 HL125827-01, and Department of Defense grant PR140977 (K.R.S.), and by Czech Ministry of Education KONTAKT grants LH 11055 and LH 15071 (L.P.-H.).

Author Contributions: Conception and design—L.P.-H. and K.R.S.; analysis and interpretation—L.P.-H., J.T., M.L., A.D'A., K.C.E.K., P.J., and K.R.S.; performance of experiments—L.P.-H., J.T., M.L., H.Z., A.R.F., S.S.P., P.C., A.D'A., and K.C.E.K.

Correspondence and requests for reprints should be addressed to Lydie Plecitá-Hlavatá, Ph.D., Institute of Physiology, Czech Academy of Sciences, Vídeňská 1083, 14220 Prague, Czech Republic. E-mail: plecita@biomed.cas.cz

This article has an online supplement, which is accessible from this issue's table of contents at www.atsjournals.org

Am J Respir Cell Mol Biol Vol 55, Iss 1, pp 47–57, Jul 2016

Originally Published in Press as DOI: 10.1165/rcmb.2015-0142OC on December 23, 2015
Internet address: www.atsjournals.org

Clinical Relevance

Our study provides evidence that, in the pathogenesis of vascular remodeling in pulmonary hypertension (PH), alterations in fibroblast mitochondrial metabolism drive distinct changes in cellular behavior, which potentially occur independently of hypoxia. This brings new knowledge to the field of PH and its metabolic theory.

Strikingly, metabolic changes, resembling those observed in cancer, have also recently been reported in PH (1, 2, 4, 6, 7). These changes have been described to occur in smooth muscle cells (SMCs) (8), endothelial cells (7), and, recently, in fibroblasts (9). These observations support a metabolic hypothesis of PH whereby mitochondrial and cytosolic alterations drive a metabolic adaptation similar to that observed in cancer cells and referred to as Warburg metabolism (described originally for cancer cells, which reprogram metabolic pathways toward aerobic glycolysis to support high proliferation). Recent studies provide evidence that inflammatory activation of immune cells also involves metabolic adaptations that closely resemble those observed by Warburg (6). Therefore, the molecular and functional abnormalities seen in PH cells, including excessive proliferation, apoptosis resistance, and inflammation, might be closely linked to cellular reprogramming of metabolism (7).

Fibroblasts have been recognized to play a critical role within the microenvironment of the vasculature, where they detect and respond to a variety of local environmental stresses, and thereby initiate and coordinate pathophysiological tissue responses, including innate immune/proinflammatory functions (10–14). We have documented that, in both experimental hypoxic PH and human PH, the pulmonary artery adventitia harbors activated fibroblasts (hereafter termed PH-Fibs) with a hyperproliferative, apoptosis-resistant, and proinflammatory phenotype, which persists *ex vivo* over numerous passages in culture (15–19). Furthermore, in line with the paradigm that stromal cells play a critical role in initiation and perpetuation of vascular inflammation (14, 20–22), we have recently shown that PH-Fibs potently recruit, retain, and activate naive macrophages through paracrine signaling (17, 23). However, at present, no studies have tested the hypothesis that abnormalities in mitochondrial metabolism drive the dramatic phenotypic changes observed in adventitial fibroblasts in PH, and even more importantly, if metabolic alterations can become imprinted and persist *ex vivo*.

Here, we sought to delineate mitochondrial metabolism in adventitial fibroblasts from chronically hypoxic hypertensive calves and humans with idiopathic pulmonary arterial hypertension (IPAH) demonstrating a hyperproliferative, apoptotic-resistant, and proinflammatory phenotype. We focused our studies on the role of mitochondria in the cellular redox status, as numerous studies have implicated heightened reactive oxygen species (ROS) production as playing a key role in driving the altered phenotype of cells, especially in hypoxic forms of PH (24–26). We studied respiratory parameters of fibroblasts, focusing on intensity and capacity of oxidative phosphorylation along with the activity of respiratory chain complexes, with emphasis on complex I. Employing a variety of redox-sensitive probes, we determined redox status in both the mitochondria and cytosol. We demonstrate the emergence of fibroblast-like cells in both a human and a bovine model of PH, with markedly heightened ROS production secondary to an acquired and persistent defect in complex I that is not simply secondary to hypoxia-induced changes in metabolism.

Materials and Methods

Unless specified otherwise, chemicals were purchased from Sigma (St. Louis, MO).

Cell Cultures

Bovine/human pulmonary artery adventitial fibroblasts were isolated from control/donor (CO-Fibs/hCO-Fibs) and hypoxic hypertensive/IPAH (PH-Fibs/hPH-Fibs) calves/humans, as described in the online supplement.

Isolated calf fibroblasts were cultivated at 37°C in humidified air with 5% CO_2 in Dulbecco's modified Eagle's medium (Life Technologies, Carlsbad, CA) without glucose supplemented with 4 mM glutamine, 1 mM sodium pyruvate, 25 mM HEPES, 10% bovine calf serum, nonessential amino acids, and 25 mM glucose. The experiments were performed between four and eight passages. For hypoxic cultivation (5%/38 or 3%/23 mm Hg O_2, besides 5% CO_2), Scitive N workstation (Ruskinn, Pencoed, UK) was employed.

Immunochemical Semiquantification

Protein detection was performed as described previously (27). Primary antibodies (i.e., translocase of inner mitochondrial membrane 23 [Tim23], pyruvate dehydrogenase [PDH], phosphorylated PDH, nicotinamide adenine dinucleotide reduced dehydrogenase [ubiquinone] Fe-S protein 4 [NDUFS4], nicotinamide adenine dinucleotide phosphate reduced oxidase isoform 4 [NOX4], hypoxia-inducible factor [HIF] 1α, oxidative phosphorylation [OXPHOS] cocktail, optic atrophy 1 [autosomal dominant] [OPA1], and mitofusin 2 [MFN2]) all were purchased from Abcam (Cambridge, MA). Quantitative analysis was performed with Image J software (ImageJ, U.S. National Institutes of Health, Bethesda, MD) densitometry.

Conventional Confocal Microscopy

Fibroblasts were cultured on poly-L-lysine–coated glass coverslips. A TCS SP2/SP8 AOBS microscope (Leica Microsystems, Mannheim, Germany) was employed, using a PL APO 100×/1.4–0.7 oil immersion objective (a pinhole 1 Airy unit). The samples were placed into a thermostable, gas-controlled chamber. LCS software (Leica Microsystems) was used for quantification.

Semiquantification of Matrix Superoxide Release Rate Using Confocal Microscopy

MitoSOX Red (Life Technologies) was used to detect *in situ* surplus $O_2^{\bullet -}$ release to the matrix rate of mitochondrial superoxide production (J_m), as described previously (28).

Semiquantification of Cytosolic ROS Levels Using Confocal Microscopy and Spectrofluorometry

For microscopic ROS detection, the cells attached on coverslips were transiently transfected with a plasmid expressing the

redox-sensitive heat shock protein 33 (HSP33) protein targeted to FRET probe (29) by Lipofectamine 2,000 (Life Technologies). After 24-hour incubation, the Forster resonance energy transfer (FRET) emission was recorded in time. Alternatively, carboxy-2′,7′dichlorodihydro fluorescein diacetate (H_2DCFDA) (Life Technologies) was used according to the manual, and fluorescence emission was recorded on an RF PC fluorometer (Shimadzu, Tokyo, Japan).

Semiquantification of mitochondrial membrane potential using confocal microscopy was assessed using mitochondrial membrane potential probe (JC1) probe (Life Technologies) (*see* the online supplement).

Lactate Quantification

Determination of lactate content was based on nicotinamide adenine dinucleotide$^+$ reduced (NADH) absorption, as described previously (30).

Isolation of Mitochondria

Mitochondria were isolated using a standard procedure (31).

High-Resolution Respirometry

O_2 consumption was measured using an Oxygraph 2k (Oroboros, Innsbruck, Austria) after the air calibration and background correction in cultivation medium (for trypsinized cells) or in respiratory buffer (125 mM sucrose, 65 mM KCl, 10 mM HEPES, 1 mM Tris-EGTA, 0.5 mM KPi, 100 μM $MgCl_2$, pH 7,2; for isolated mitochondria). Endogenous respiration was followed by oligomycin (ATP synthase inhibitor), trifluoromethoxy carbonylcyanide phenylhydrazone (FCCP) (uncoupler of electron transport chain and ATP synthase), and potassium cyanide (KCN) (cytochrome c oxidase inhibitor) addition, respectively, or in combination. Rotenone/piericidine stepwise titration was used to inhibit respiration from complex I. Mitochondrial respiration was established by 1 mM malate, 5 mM glutamate and pyruvate, and 1 mM ADP.

Statistical Analysis

All experiments were repeated at least three times. The average values (±SD) was plotted. Student's *t* test was employed.

Results

Pulmonary Adventitial Fibroblasts from Chronically Hypoxic Hypertensive Calves and Humans (PH-Fibs) Exhibit Decreased Pyruvate Entry to the Krebs Cycle

Similar to our previous findings (15–19, 32), all PH-Fibs (both bovine and human) used in these studies demonstrated a significantly higher growth rate than CO-Fibs (data not shown). This raised the possibility that the glycolytic state of these cells would be altered. The glycolytic pathway gives rise to pyruvate as the final product. The pyruvate can then either be converted by PDH to acetyl–coenzyme A (CoA) in mitochondria or by lactate dehydrogenase to lactate in cytoplasm according to PDH phosphorylation status. The latter reaction is typical for fast-proliferating cells, such as cancer cells. Lactate production was found to be increased in PH-Fibs (Figure 1A). Thus, we determined the portion of phosphorylated PDH, which leads to the inhibition of its activity. We found a roughly 30% increase in phosphorylated:nonphosphorylated PDH ratio in both bovine and human PH-Fibs (Figure 1B). Increased PDH phosphorylation restricts influx of pyruvate into the mitochondria of PH-Fibs.

Oxidative Phosphorylation of PH-Fibs Is Diminished and the Mitochondrial Network Is Fragmented

The finding of suppressed pyruvate processing to acetyl-CoA, necessary for feeding the Krebs cycle, prompted us to characterize mitochondrial energy production machinery and respiration in PH-Fibs. The difference in endogenous respiration, (i.e., oxygen consumption) was not statistically different compared with CO-Fibs (Figure 2A). However, the respiratory control ratio, which assesses the potential of ATP synthesis (i.e., mitochondrial oxidative phosphorylation, within endogenous respiration, showed significant suppression in PH-Fibs; (Figure 2B). An even greater suppression (~35%) in the maximal respiratory capacity was observed in PH-Fibs (Figure 2C). As these findings might result from a lower mitochondrial mass in PH-Fibs versus CO-Fibs, we quantified the mitochondrial mass by immunocytochemistry with Tim23

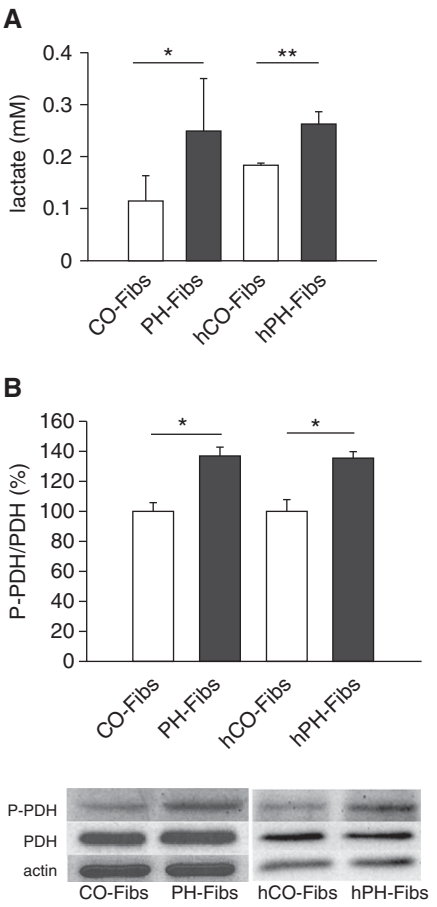

Figure 1. Warburg phenotype of bovine pulmonary hypertension (PH) and human pulmonary hypertension (hPH) fibroblasts (PH-Fibs/hPH-Fibs). (*A*) Lactate production in PH-Fibs/hPH-Fibs and control/donor fibroblasts (CO-Fibs/hCO-Fibs) ($n = 5/3$ for CO-Fibs/hCO-Fibs, $n = 7/4$ for PH-Fibs/hPH-Fibs). (*B*) Phosphorylation of pyruvate dehydrogenase (PDH) in PH-Fibs/hPH-Fibs and CO-Fibs/hCO-Fibs expressed as phosphorylated PDH (P-PDH)/total PDH protein ratio ($n = 7$ and 3 for hFibs). It was quantified by Western blot analysis using specific P-PDH and PDH antibodies. Representative Western blots are shown at the *bottom*, including control of protein loading (actin quantification). Values are expressed as percentages of the CO-Fibs/hCO-Fibs values. Average values (±SD) are shown. $^*P < 0.05$; $^{**}P < 0.01$.

antibodies along with mitochondrial green fluorescent protein (GFP) signal quantification using fluorescent confocal microscopy (Figure 2D). We did not detect a significant difference in mitochondrial mass between the two cell populations. Although differences in the amount of respiratory chain complexes in PH-Fibs could also explain the repressed respiratory parameters in PH-Fibs, the total amount of

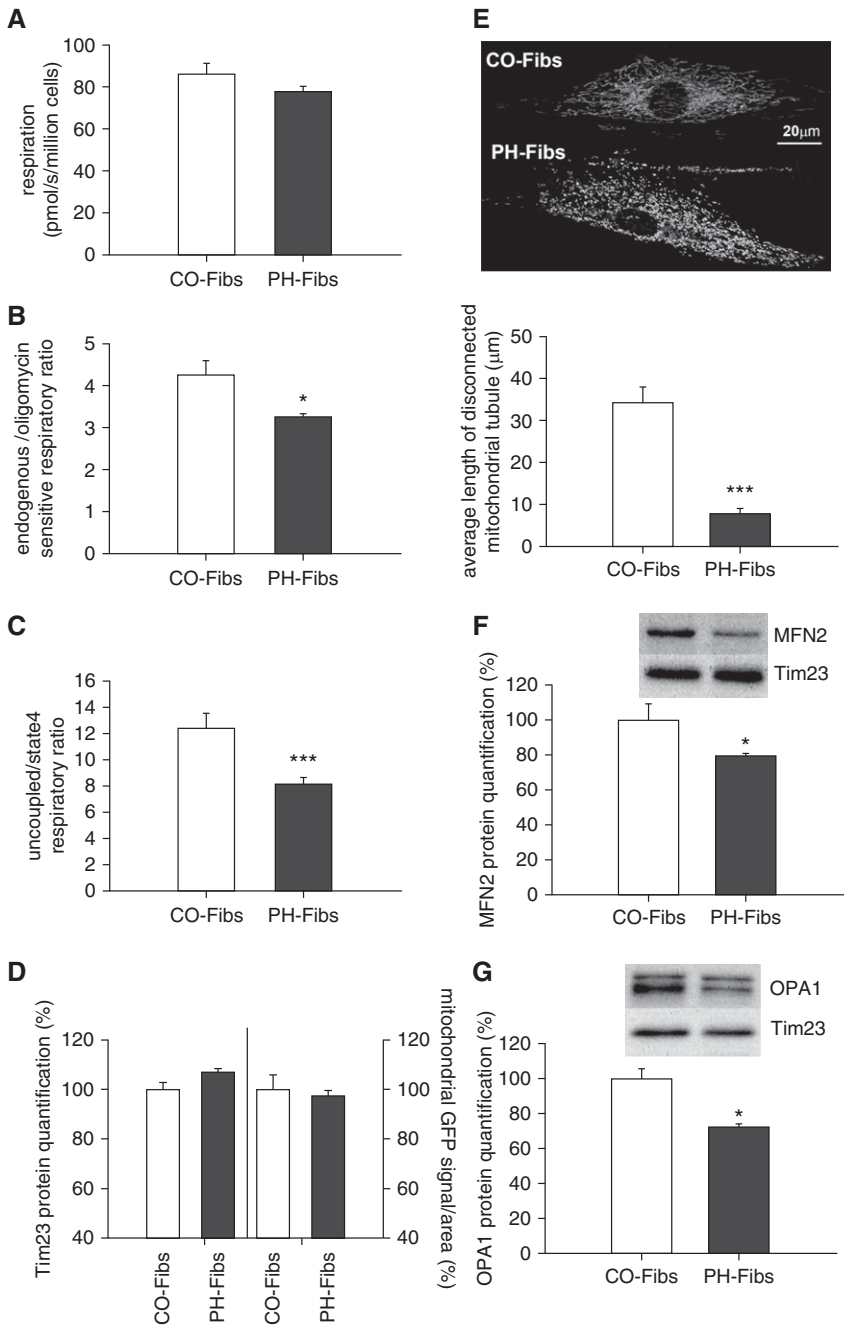

Figure 2. Mitochondrial respiratory activity, mass quantification, and mitochondrial morphology of PH-Fibs and CO-Fibs. (*A*) Endogenous respiration (pmol/s/million cells) of Fibs. (*B*) Respiratory control ratio expressed as endogenous (state 3)/ATP synthase–inhibited (oligomycin, state 4) respiratory ratio. (*C*) Maximal respiratory capacity expressed as uncoupled trifluoromethoxy carbonylcyanide phenylhydrazone (FCCP)/ATP synthase–inhibited (oligomycin, state4) respiratory ratio. (*D*) Quantification of mitochondrial mass by translocase of inner mitochondrial membrane 23 (Tim23) protein quantification determined by Western blot analysis using specific Tim23 antibodies and by mitochondria-tagged green fluorescent protein (GFP) signal determination per cell area. (*E*) Visualization and quantification of mitochondrial fragmentation in PH-Fibs. It was performed by mitochondria-targeted GFP using confocal microscopy. The analysis was done using Amira software (FEI, Hillsboro, Oregon). (*F*) Quantification of mitofusin 2 (MFN2) fusion protein levels in CO/PH-Fibs. (*G*) Quantification of optic atrophy 1 (autosomal dominant) (OPA1) fusion protein levels in CO/PH-Fibs. (*F* and *G*) Quantification by Western blot analysis using specific MFN2 and OPA1 antibodies. Representative Western blots are shown at the *top*, including control of protein loading (Tim23 quantification). Values are expressed as percentage of the CO-Fibs values. Average values (±SD) are shown. $^{*}P < 0.05$; $^{***}P < 0.001$.

respiratory complexes, represented by specific subunits, was determined, but was not statistically different in PH-Fibs versus CO-Fibs (Figure E2). Moreover, we observed that the mitochondrial network was significantly fragmented in PH-Fibs (Figure 2E). Decreased expression of the fusion proteins, Opa1 and Mfn2, was also found (Figures 2F and 2G).

Mitochondrial Complex I is Down-Regulated in PH-Fibs, Leading to Mitochondrial Superoxide Production

A detailed quantification of each protein complex of respiratory chain separately showed a significant down-regulation of the accessory protein subunit of complex I–NDUFS4 in PH-Fibs (bovine and human) versus CO-Fibs (both bovine and human) (Figure 3A). Deficiencies in this subunit have been shown to be associated with certain neurodegenerative pathologies, excessive inflammation, and cardiomyopathy (33). We investigated the impact of complex I deficiency on respiratory activity in PH-Fibs. We examined complex I activity using both rotenone and piericidine (complex I inhibitors) to evaluate the extent of inhibition of respiration. We found that respiration was decreased in PH-Fibs to a much greater extent compared with CO-Fibs when the same amount of rotenone or piericidine was applied (Figure 3B).

To directly determine complex I activity *in situ*, we isolated mitochondria from CO-Fibs and PH-Fibs and performed respiratory measurements using substrates for complex I (glutamate plus malate and pyruvate) and ADP to determine the capacity of oxidative phosphorylation driven through complex I. We found a roughly17% drop in oxygen consumption in PH-Fibs versus Co-Fibs (Figure 3C), which corresponded to the down-regulation of complex I documented in Figure 3A.

Complex I belongs to the proton pumping complexes of the respiratory chain; thus, its decreased activity, in the absence of compensation, must influence proton-motive force and its component, mitochondrial membrane potential. Indeed, we found an approximate twofold increase in fluorescence, reflecting mitochondrial membrane potential, indicating that mitochondria were hyperpolarized in PH-Fibs (Figure 3D).

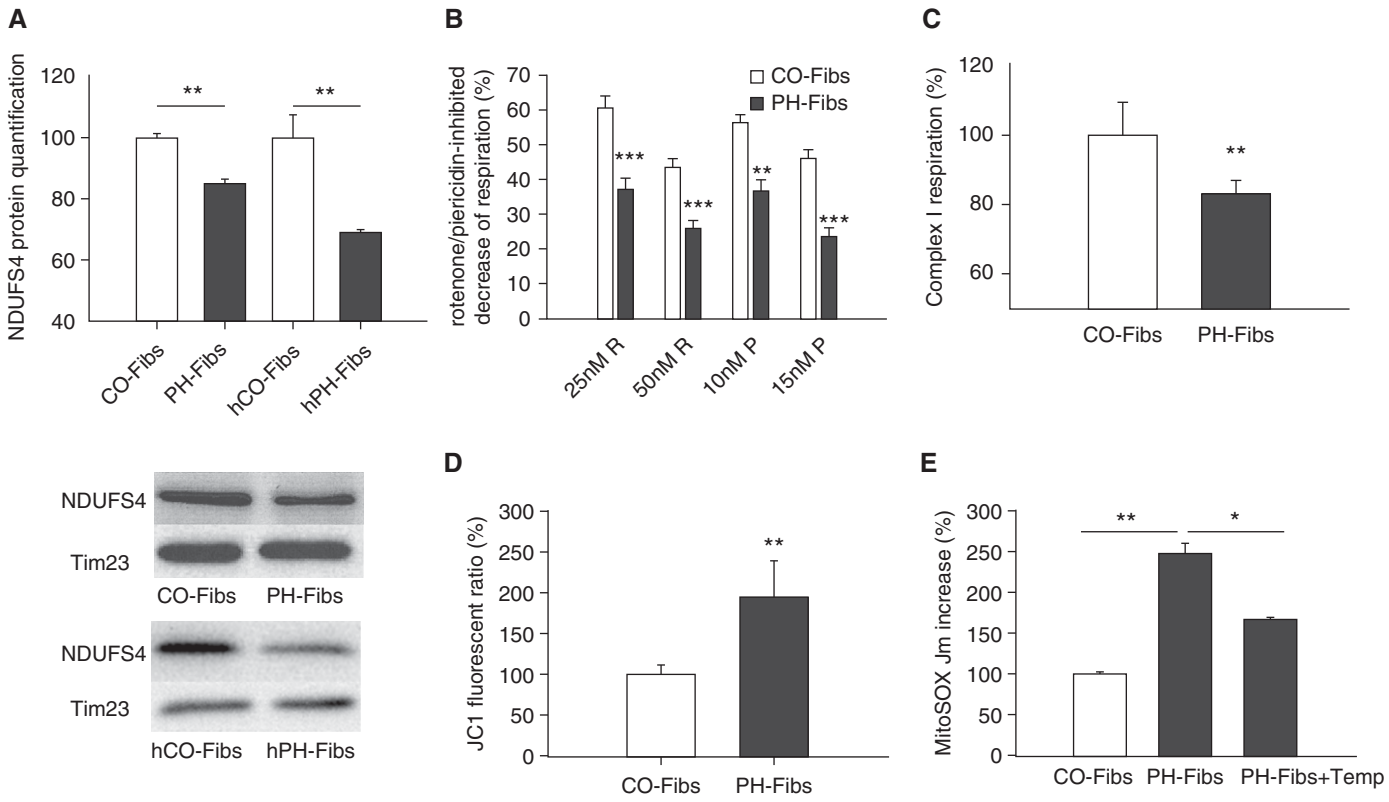

Figure 3. Complex I deficiency in PH-Fibs/h PH-Fibs and mitochondrial oxidative status of PH-Fibs. (*A*) Quantification of nicotinamide adenine dinucleotide reduced dehydrogenase (ubiquinone) Fe-S protein 4 (NDUFS4) subunit of complex I in PH-Fibs/hPH-Fibs and CO-Fibs/hCO-Fibs by Western blot analysis using specific NDUFS4 antibodies. Representative Western blot is shown at the *bottom*, including control of protein loading (Tim23 quantification). (*B*) *In situ* quantification of complex I activity in PH-Fibs and CO-Fibs determined by rotenone (R)/piericidine (P)–inhibited decrease of respiration (100% represents nontreated samples). (*C*) *In vitro* quantification of complex I–derived respiratory activity in mitochondria of PH-Fibs and CO-Fibs. (*D*) Determination of mitochondrial membrane potential in CO-Fibs and PH-Fibs expressed by mitochondrial membrane potential probe (JC1) ratio. The values are expressed as percentage of the CO-Fibs values. (*E*) Quantification of mitochondrial superoxide in CO-Fibs, PH-Fibs, and PH-Fibs treated with 1 mM tempol for 3 days by MitoSOX fluorescence increase rate, Jm. Values are expressed as percentage of the CO-Fibs values. Average values (±SD) are shown. $^{*}P < 0.05$; $^{**}P < 0.01$; $^{***}P < 0.001$.

Complex I is also known to comprise one of the major sites of superoxide production within mitochondria. We found an approximate 2.5-fold increase of matrix superoxide release rate of J_m rates in PH-Fibs versus CO-Fibs (Figure 3E).

PH-Fibs Exhibit Pro-Oxidative Cellular Status

To elucidate cytosolic redox status in addition to the mitochondrial redox state, we employed both a redox-sensitive HSP33-FRET probe (containing redox-sensitive cysteines) and a nonspecific cell-permeable difluorescein (DCF) probe. Both approaches showed elevation in cytosolic oxidation in PH-Fibs (Figure 4A). As NOX4 has been shown previously to be up-regulated in adventitial fibroblasts in various models of PH (24, 34), we quantified NOX4 protein levels. We observed marked increases in NOX4 expression in PH-Fibs (Figure 4B). The importance of this pro-oxidative status for the hyperproliferative phenotype of PH-Fibs was highlighted by experiments in which PH-Fibs were exposed to antioxidant, tempol. Tempol reduced the proliferative potential of PH-Fibs (Figure 4C) while also decreasing mitochondrial and cytosolic ROS production (Figures 3E and 4A).

Hypoxia Alone Is Not Sufficient to Induce Complex I Deficiency

To investigate potential mechanisms responsible for the mitochondrial changes observed in PH-Fibs *in vivo*, we used an *in vitro* approach and exposed CO-Fibs to hypoxic conditions (3 and 5% O_2) for a minimum of 24 hours, up to 10 days. Metabolic phenotypes of PH and CO-Fibs were assayed through UHPLC–mass spectrometry–based metabolomics, confirming increased levels of lactate, impaired redox homeostasis, and accumulation of Krebs cycle intermediates (Figure 5). Exposure to 3% hypoxia for 24 hours promoted transient alterations of the metabolic phenotype of CO-Fibs, which were restored by subsequent exposure to normoxia for 24 hours (Figure 5). We then detected a large (three- to eightfold) increase of the master regulatory transcription factor, HIF1α, in human Fibs (Figure E2). We found an increased phosphorylation of PDH in CO-Fibs exposed to 3 or 5% O_2 at all time points examined (Figure 6A). Concurrently, we also observed increased lactate production (Figure 5). We next investigated the effects of hypoxic exposure on mitochondrial energy metabolism. We observed a significant (~30%) decrease of endogenous respiration of hypoxic

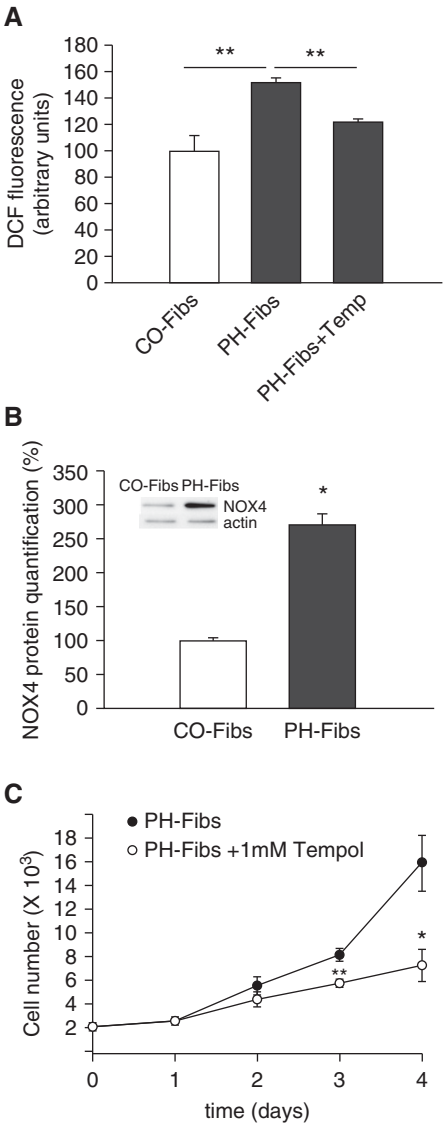

Figure 4. Redox status of cytoplasm in CO-Fibs, PH-Fibs, and PH-Fibs treated with 1 mM tempol for 3 days. (*A*) Detection of cytosolic oxidation in CO-Fibs, PH-Fibs, and PH-Fibs treated with 1 mM tempol for 3 days using difluorescein (DCF) probe. (*B*) Nicotinamide adenine dinucleotide phosphate reduced (NADPH) oxidase (NOX) 4 protein quantification in CO-Fibs and PH-Fibs by protein-normalized Western blot analysis using NOX4-specific antibodies. Values are expressed as percentage of the CO-Fibs values. A representative Western blot is shown at the *top*. (*C*) PH-Fibs and CO-Fibs cell proliferation after tempol (1 mM) treatment. Average values (±SD) are shown. $^{*}P < 0.05$; $^{**}P < 0.01$.

CO-Fibs (Figure 6B, *a*). Similarly, the respiratory control ratio (involvement of oxidative phosphorylation) and maximal respiratory capacity of CO-Fibs were down-regulated in hypoxic conditions (Figure 6B, *b* and *c*). To determine whether this was due to down-regulation of mitochondrial mass, we quantified mitochondrial protein by Tim23 immunochemistry. We did not observe significant changes in mitochondrial mass (data not shown) in response to hypoxic conditions. We examined the effect of hypoxia on complex I of the electron transport chain in CO-Fibs, first performing a rotenone inhibitory assay along with quantification of complex I NDUFS4 subunit. We did not find any effect of 3 or 5% O_2 exposure for up to 10 days on complex I activity or NDUFS4 protein levels (Figure 6C, *a* and *b*). Furthermore, no effects of hypoxia on mitochondrial superoxide production or membrane potential were observed (Figure 6D, *a* and *b*). Thus, *ex vivo* exposure of control fibroblasts to hypoxia alone induced predictable changes toward increased glycolysis and reduced mitochondrial metabolism, but did not cause complex I down-regulation or significant increases in ROS production. Importantly, hypoxia alone was insufficient to have any further effect on PH-Fib mitochondrial metabolism (data not shown). These data suggest that hypoxia alone and hypoxia-induced HIF1 signaling is insufficient to induce the complex I alterations observed in PH-Fibs, and that metabolic reprogramming observed in PH-Fibs is not explained by the effect of hypoxia alone.

Paracrine Signaling by PH-Fib–Activated Macrophages Does Not Induce Mitochondrial Dysfunction of CO-Fibs *Ex Vivo*

We previously reported that PH-Fibs induce a distinct proinflammatory, profibrotic phenotype in macrophages. These fibroblast-activated macrophages, in turn, can stimulate proliferation of control fibroblasts and SMCs. To determine whether fibroblast-activated macrophages can contribute to complex I suppression in control fibroblasts *ex vivo*, we cocultured CO-Fibs with supernatant from PH-Fib–activated macrophages under normoxic conditions. Within the experimental time frame, we did not observe any changes in complex I subunit protein amount (data not shown) compared with untreated CO-Fibs.

Suppression of PDH Inhibition in PH-Fibs Does Not Correct Energy and Redox Metabolism

PH-Fibs exhibit suppressed influx of pyruvate to mitochondria due to inhibition of PDH compared with CO-Fibs. As dichloroacetate (DCA) is a widely used pyruvate dehydrogenase kinase (PDK) inhibitor, and has even been proposed as a treatment for patients with PAH (6), we wanted to determine if DCA could restore mitochondrial bioenergetics and redox homeostasis in PH-Fibs. We found that, although DCA treatment of PH-Fibs decreased inhibition of PDH and suppressed cell proliferation, mitochondrial endogenous respiration did not show any increase in oxygen consumption, indicating continued complex I dysfunction and persistent mitochondrial and cytosolic ROS production (Figure E1).

Discussion

Here, we show that persistent alterations in mitochondrial metabolism, specifically in complex I, characterize the hyperproliferative, apoptotic-resistant, and proinflammatory adventitial fibroblasts derived from the remodeled pulmonary arteries of hypoxic calves and humans with IPAH. Mitochondrial energy metabolism of PH-Fibs is also decreased, which, together with down-regulation of complex I, leads to increased mitochondrial superoxide production. Furthermore, this pro-oxidative mitochondrial metabolism is accompanied by increased cytosolic ROS production, which our data suggest is most probably due to NOX4. Importantly, our data functionally link these metabolic changes to cellular function, as we show markedly decreased proliferation of PH-Fibs upon treatment with the ROS scavenger, tempol.

An additional important observation of our studies is that mitochondrial respiratory parameters were decreased in PH-Fibs, even under normoxic conditions. Mechanistically, decreased mitochondrial respiration can potentially be attributed to enhanced phosphorylation of PDH, resulting in its inhibition. PDH acts as a gatekeeper enzyme for the entry of pyruvate produced by glycolysis into the mitochondrial tricarboxylic acid cycle by converting it to acetyl-CoA and thus

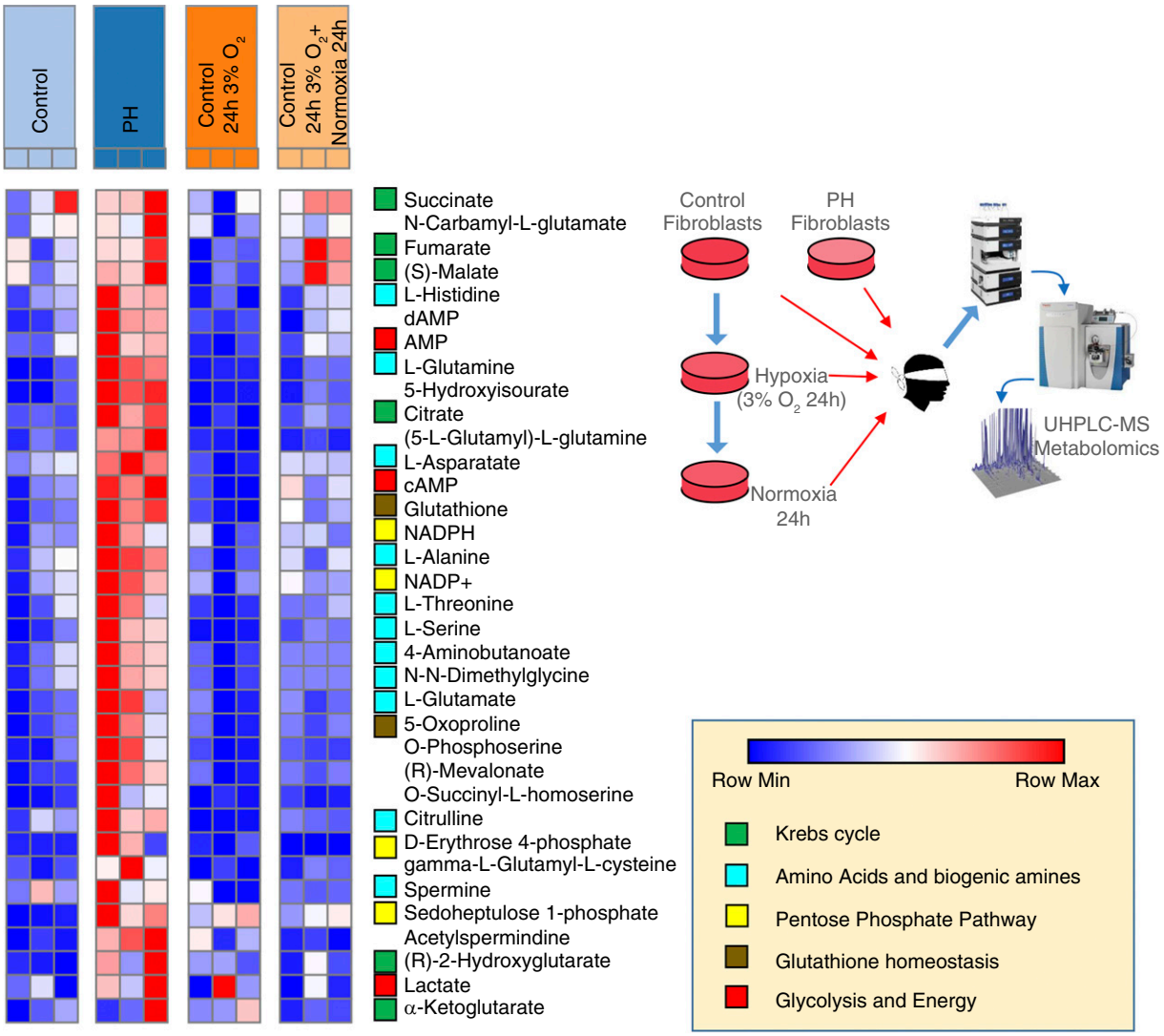

Figure 5. PH-Fibs are characterized by distinct metabolic phenotypes in comparison to CO-Fibs, hypoxic CO-Fibs, and transiently hypoxic CO-Fibs. Ultra-high performance liquid chromatography (UHPLC)–mass spectrometry (MS) metabolomics analyses were performed on CO-Fibs and PH-Fibs. Relative metabolite quantities were graphed through heat maps, upon Z score normalization of values determined across samples (*blue*, lowest values; *red*, highest values). In agreement with the other measurements, metabolomics analyses confirmed that PH-Fibs were characterized by significant alterations of glycolysis, Krebs cycle, redox homeostasis (glutathione homeostasis and pentose phosphate pathway), and amino acid metabolism. Hypoxia (3% O_2 for 24 h) or reoxygenation of hypoxic CO-Fibs were not sufficient to mimic the extreme metabolic derangement observed in PH-Fibs in the tested time window. Metabolic pathways were color coded, as detailed in the *bottom right chart*. Each sample is represented by three independent experiments depicted in columns.

regulating mitochondrial metabolism. PDH phosphorylation has been shown to be regulated by hypoxia, as HIF1 increases the expression and activity of PDH kinase, which increases PDH phosphorylation (35). Interestingly, our studies suggest that hypoxia alone, and HIF1 signaling in response to hypoxia, likely do not contribute to this metabolic alteration in PH-Fibs. In contrast, we observed a critical role for HIF1 and hypoxia in controlling PDK, and thus pyruvate flux, in fibroblasts exposed to hypoxia. Exposing CO-Fibs to hypoxia *ex vivo* was sufficient to decrease mitochondrial respiratory parameters through enhancement of PDH phosphorylation, but did not promote the extreme metabolic reprogramming observed in normoxic PH-Fibs, nor did it lead to a complex I deficiency in a 24-hour to 10-day time window, respectively. These data suggest that *in vivo* hypoxia alone and increased HIF1 signaling in response to hypoxia are insufficient to promote the activated PH-Fib phenotype. These findings are consistent with the hypothesis regarding cellular activation of inflammatory macrophages exhibiting similar metabolic alterations (36). Current data suggest that signals within the microenvironment, such as lactate, cytokines, and danger signals alone or in combination with hypoxia, but likely not hypoxia alone, are important regulators of cellular metabolic programs that allow inflammatory activation. Thus, microenvironmental signals within the adventitia, in addition to hypoxia, are likely driving the PH-Fib phenotype. In

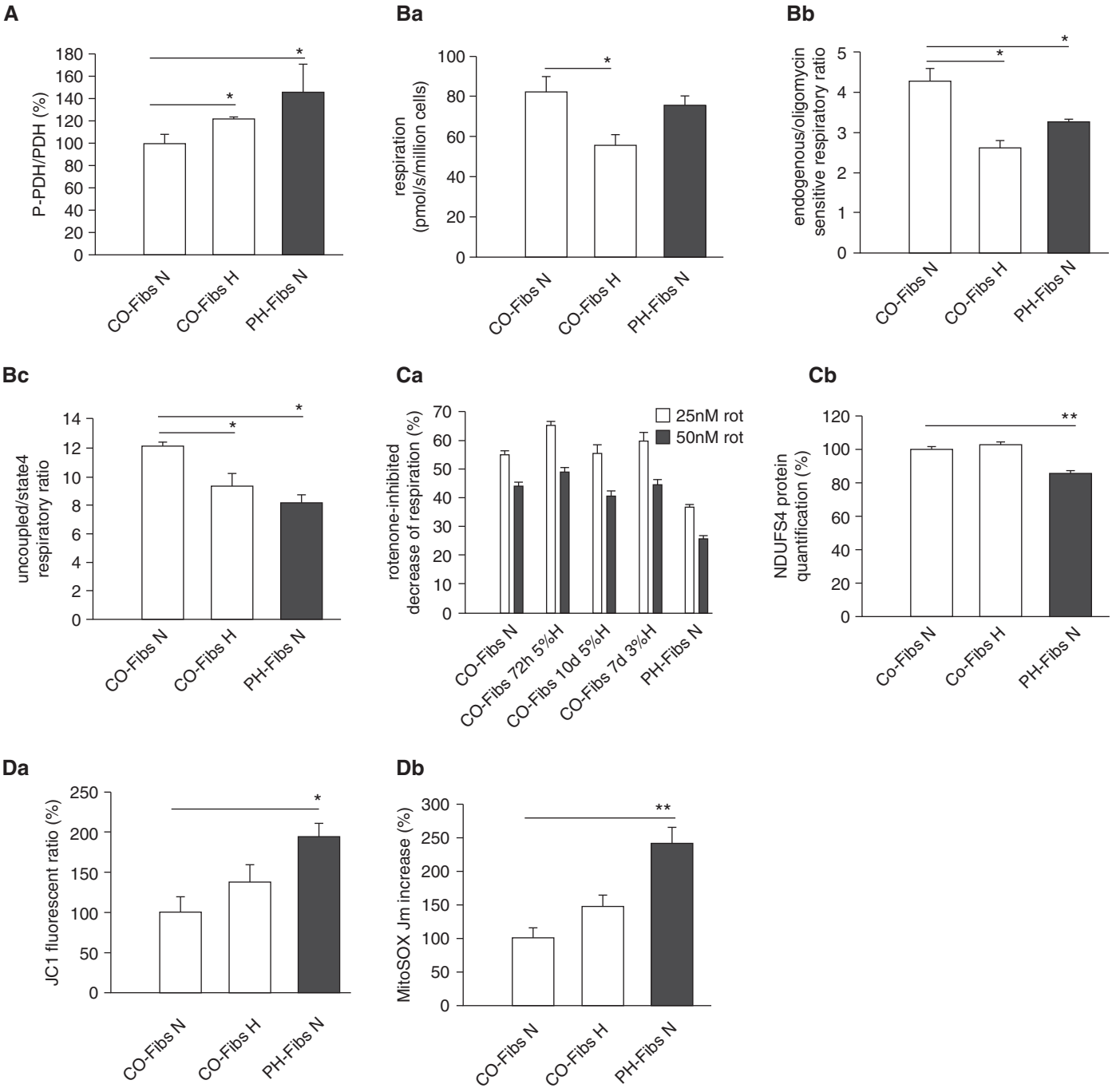

Figure 6. State of glycolytic switch, mitochondrial parameters, complex I, and mitochondrial oxidation in normoxic CO/PH-Fibs and CO-Fibs kept in 3 or 5% hypoxia for up to 10 days. (*A*) Phosphorylation of PDH in normoxic CO/PH-Fibs and CO-Fibs kept in 72-hour hypoxia (5% O_2) expressed as P-PDH: PDH protein ratio. It was quantified by protein-normalized Western blot analysis using specific P-PDH and PDH antibodies. (*B*) Respiratory parameters under 72-hour hypoxia (5% O_2). (*Ba*) Endogenous respiration (pmol/s/million cells) of normoxic CO/PH-Fibs and CO-FIBs in 72-hour hypoxia (5% O_2). (*Bb*) Respiratory control ratio expressed as endogenous (state 3)/ATP synthase–inhibited (oligomycin, state 4) respiratory ratio. (*Bc*) Maximal respiratory capacity expressed as uncoupled (FCCP)/ATP synthase–inhibited (oligomycin, state 4) respiratory ratio. (*C*) Complex I state under hypoxia. (*Ca*) *In situ* quantification of complex I activity in normoxic CO/PH-Fibs and CO-Fibs kept in 72-hour/10-day hypoxia (5% O_2) or 7-day hypoxia (3% O_2) determined by rotenone-inhibited decrease of respiration. (*Cb*) Quantification of NDUFS4 subunit of complex I in normoxic CO/PH-Fibs and CO-Fibs kept in 72-hour hypoxia (5% O_2) by Western blot analysis using specific NDUFS4 antibodies. (*D*) Mitochondrial redox state under hypoxia. (*Da*) Determination of mitochondrial membrane potential in normoxic CO/PH-Fibs and CO-Fibs kept in 72-hour hypoxia (5% O_2) expressed by JC1 ratio. (*Db*) Quantification of mitochondrial superoxide in normoxic CO/PH-Fibs and CO-Fibs kept in 72-hour hypoxia (5% O_2) by MitoSOX fluorescence increase rate, Jm. (*A*, *C*, and *D*) Values are expressed as percentage of the normoxic CO-Fibs values. Average values (±SD) are shown. $^*P < 0.05$; $^{**}P < 0.01$.

addition, as we have previously shown for inflammatory macrophages, HIF1 signaling can be increased by a variety of factors (e.g., lactate, IL-6 [6, 23, 36]). However, the exact microenvironmental signals that induce and maintain cellular changes in metabolism remain elusive. We have therefore begun to address this question in part in the present study by exposing control fibroblasts to soluble factors derived from fibroblast-activated macrophages. Unfortunately, these experiments did not induce metabolic alterations in control fibroblasts that would recapitulate the PH-Fib metabolic phenotype. Therefore, future studies are required to define the local adventitial microenvironment *in situ* to find potential molecular mediators that induce PH-Fib metabolic changes.

Furthermore, the induction of pyruvate entry to mitochondria by DCA treatment of PH-Fibs did not correct either mitochondrial metabolism or complex I alterations, although it significantly decreased the proliferative potential of PH-Fibs. This indicates that DCA treatment is not able to correct all of the cell phenotypes that emerge and are associated with PH development. Thus, the decrease in complex I activity in PH-Fibs cannot be explained simply by a hypoxia-induced decrease of pyruvate entry into the mitochondria. Rather, we found that the reduced activity of complex I was caused by down-regulation of one of its accessory subunits, NDUFS4, which might then affect the complex assembly.

In the bovine species, complex I consists of 45 different subunits that combine into the complex I holo-complex to form an approximately 1 megadaltons MD assembly. Seven complex I subunits originate from mitochondrial DNA, and the rest from the nuclear DNA. NDUFS4 is a nuclear-encoded subunit, which, once phosphorylated by cAMP/protein kinase A (PKA) in the cytosol on its C-terminal end of the protein (37), promotes import and maturation of the precursor protein, which then incorporates into the core complex of complex I and enables its proper activity. Pathological mutations in the human NDUFS4 gene result in the disappearance of the protein encoded by the gene, failure of the final step of complex I assembly, and suppression of the NADH ubiquinone oxidoreductase activity (38). Complex I dysfunction is frequently associated with abnormalities of inflammation and cardiac dysfunction (39, 40). Thus, we suggest that NDUFS4 might be a significant player in the mitochondrial abnormalities observed in cells that are important in PH development.

In PH-Fibs, the activity of complex I is decreased, leading to an increase in the proton-motive force. The proton pumping in complexes III and IV must then substitute for the deficiency in complex I, leading to increased proton-motive force and its mitochondrial membrane potential component. Note also that less-efficient ATP synthesis giving the lower H^+ backflow via the ATP-synthase F_0 moiety also leads to the observed increase in membrane potential. The elevated leak of electrons from the mitochondrial respiratory chain at $NADH >> NAD^+$ and the reaction of these electrons with molecular oxygen lead to increased superoxide production. Of note, complex I is one of the major superoxide-producing sites in the mitochondria (41), with the resultant ROS production localized to the mitochondrial matrix. These observations thus establish the increased pro-oxidative features of mitochondria in PH-Fibs. In addition, the complex I malfunction in humans derived from a reduced level or a complete absence of fully assembled complex I has been shown to induce mitochondrial ROS formation (42).

We also found that NOX4, the only constitutively active NOX isoform, is increased in PH-Fibs. In parallel, the increased oxidative status in the cytosol can be linked to NOX4 activity in PH-Fibs. Recently, this isoform was expressed in endothelium and adventitia during development of PH in rat models of PAH (34). That study showed that increased expression of NOX4 in the absence of other stimuli was sufficient to increase fibroblast migration and proliferation; and inhibition of NOX4 activity reduced cellular proliferation. Similarly, we observed that suppressing the pro-oxidative status in PH-Fibs using the antioxidant, tempol, a superoxide dismutase mimetic and pleiotropic intracellular antioxidant, decreased their proliferative potential. Thus, pro-oxidative metabolism of PH-Fibs comprising mitochondrial and/or cytosolic sources might be crucial for proliferation and thus remodeling of the artery. However, the exact contribution of either ROS sources to PH development remains to be elucidated. The importance of pro-oxidative metabolism in PH is supported by studies where suppression of oxidative metabolism, including the use of tempol, leads to the reduction of PH development (24–26, 43–45).

We also show that the mitochondrial network of PH-Fibs is significantly fragmented, with associated changes in the expression of the mitochondrial fusion proteins, OPA1 and MFN2. The fragmentation of mitochondria in PH-Fibs corresponds with observations in other cells from the pulmonary hypertensive vessel wall (46). However, in addition to the altered expression levels of these proteins, the fusion/fission of mitochondria is also regulated by post-translational modifications of the proteins mentioned previously here, their mitochondrial recruitment, presence of cofactors, and membrane lipid composition (47). The significance of a fragmented mitochondrial network in PH-Fibs with mitochondrial suppressed oxidative phosphorylation and pro-oxidative metabolism remains to be investigated.

The adventitia comprises a loosely defined array of cells, including fibroblasts, collagen, and elastic fibers and immune cells that encircle the tunica media and intima layers of the blood vessel. The adventitia, thus, is capable of orchestrating inflammation and vascular proliferation in response to any incoming insult, such as chronic hypoxia, and therefore playing an important role in the induction of PH. In response to many stimuli, fibroblasts, likely specific subpopulations, secrete growth factors, chemokines, and inflammatory cytokines (16). The precise mechanisms controlling such secretion have not been well defined. However, the secretion of soluble factors could be regulated by the pro-oxidative status of the PH-Fibs represented by hydrogen peroxide as a mediator of signaling or deficiency of complex I alone (40–42). Interestingly, complex I deficiency has been found to be the most common disorder of the mitochondrial oxidative phosphorylation system in human pathologies (48). However, complex I defects have not yet been described in other cell types involved in the remodeling of the pulmonary artery wall during PH development, such as SMCs and endothelial cells. In these cells,

mitochondria were shown to be hyperpolarized, with a restricted influx of carbohydrates, and thus mitochondrial energy metabolism is suppressed and cells are apoptosis resistant (4). Further studies need to be directed at investigating the relevance of complex I disorders in PH. Do complex I defects simply initiate a pro-oxidative signaling through mitochondria (e.g., for regulation of inflammation and/or proliferation), or does complex I deficiency regulate further signaling through decreased oxidative phosphorylation? The oxidative signaling derived from complex I deficiency was shown to be relevant in studies with stable down-regulation of a single subunit of complex I (NADH: ubiquinone oxidoreductase subunit A13 [GRIM-19] or NDUFS3) in HeLa cells, decreasing its activity, leading to enhanced cell adhesion, migration, and invasion, and thus influencing the expression of extracellular matrix molecules and playing a role in cancer metastasis (49). It is possible that cells exhibiting a variety of mitochondrial abnormalities will exist during the development of PH. It will be important to ultimately determine whether and if these abnormalities can or should be targeted therapeutically. ■

Author disclosures are available with the text of this article at www.atsjournals.org.

Acknowledgments: The help of Jana Vaicova with Western blotting, Hana Engstová with Amira software (FEI, Hillsboro, OR), and Marcia McGowan with EndNote software are gratefully acknowledged. The collaboration between the U.S. and Czech partners was initiated by Petr Paucek (University of Colorado, Boulder, CO).

References

1. Tuder RM, Archer SL, Dorfmüller P, Erzurum SC, Guignabert C, Michelakis E, Rabinovitch M, Schermuly R, Stenmark KR, Morrell NW. Relevant issues in the pathology and pathobiology of pulmonary hypertension. *J Am Coll Cardiol* 2013;62(25 suppl):D4–D12.
2. Cottrill KA, Chan SY. Metabolic dysfunction in pulmonary hypertension: the expanding relevance of the Warburg effect. *Eur J Clin Invest* 2013; 43:855–865.
3. Hanahan D, Weinberg RA. Hallmarks of cancer: the next generation. *Cell* 2011;144:646–674.
4. Paulin R, Michelakis ED. The metabolic theory of pulmonary arterial hypertension. *Circ Res* 2014;115:148–164.
5. Tuder RM, Davis LA, Graham BB. Targeting energetic metabolism: a new frontier in the pathogenesis and treatment of pulmonary hypertension. *Am J Respir Crit Care Med* 2012;185:260–266.
6. Stenmark KR, Tuder RM, El Kasmi KC. Metabolic reprogramming and inflammation act in concert to control vascular remodeling in hypoxic pulmonary hypertension. *J Appl Physiol (1985)* 2015;119:1164–1172.
7. Fijalkowska I, Xu W, Comhair SA, Janocha AJ, Mavrakis LA, Krishnamachary B, Zhen L, Mao T, Richter A, Erzurum SC, *et al*. Hypoxia inducible-factor1α regulates the metabolic shift of pulmonary hypertensive endothelial cells. *Am J Pathol* 2010;176:1130–1138.
8. McMurtry MS, Bonnet S, Wu X, Dyck JR, Haromy A, Hashimoto K, Michelakis ED. Dichloroacetate prevents and reverses pulmonary hypertension by inducing pulmonary artery smooth muscle cell apoptosis. *Circ Res* 2004;95:830–840.
9. Zhao L, Chen CN, Hajji N, Oliver E, Cotroneo E, Wharton J, Wang D, Li M, McKinsey TA, Stenmark KR, *et al*. Histone deacetylation inhibition in pulmonary hypertension: therapeutic potential of valproic acid and suberoylanilide hydroxamic acid. *Circulation* 2012;126:455–467.
10. Baglole CJ, Ray DM, Bernstein SH, Feldon SE, Smith TJ, Sime PJ, Phipps RP. More than structural cells, fibroblasts create and orchestrate the tumor microenvironment. *Immunol Invest* 2006;35: 297–325.
11. Barone F, Nayar S, Buckley CD. The role of non-hematopoietic stromal cells in the persistence of inflammation. *Front Immunol* 2012;3:416.
12. Flavell SJ, Hou TZ, Lax S, Filer AD, Salmon M, Buckley CD. Fibroblasts as novel therapeutic targets in chronic inflammation. *Br J Pharmacol* 2008;153:S241–S246.
13. Smith RS, Smith TJ, Blieden TM, Phipps RP. Fibroblasts as sentinel cells: synthesis of chemokines and regulation of inflammation. *Am J Pathol* 1997;151:317–322.
14. Stenmark KR, Yeager ME, El Kasmi KC, Nozik-Grayck E, Gerasimovskaya EV, Li M, Riddle SR, Frid MG. The adventitia: essential regulator of vascular wall structure and function. *Annu Rev Physiol* 2013;75:23–47.
15. Anwar A, Li M, Frid MG, Kumar B, Gerasimovskaya EV, Riddle SR, McKeon BA, Thukaram R, Meyrick BO, Fini MA, *et al*. Osteopontin is an endogenous modulator of the constitutively activated phenotype of pulmonary adventitial fibroblasts in hypoxic pulmonary hypertension. *Am J Physiol Lung Cell Mol Physiol* 2012;303:L1–L11.
16. Das M, Burns N, Wilson SJ, Zawada WM, Stenmark KR. Hypoxia exposure induces the emergence of fibroblasts lacking replication repressor signals of PKCzeta in the pulmonary artery adventitia. *Cardiovasc Res* 2008;78:440–448.
17. Li M, Riddle SR, Frid MG, El Kasmi KC, McKinsey TA, Sokol RJ, Strassheim D, Meyrick B, Yeager ME, Flockton AR, *et al*. Emergence of fibroblasts with a proinflammatory epigenetically altered phenotype in severe hypoxic pulmonary hypertension. *J Immunol* 2011;187:2711–2722.
18. Panzhinskiy E, Zawada WM, Stenmark KR, Das M. Hypoxia induces unique proliferative response in adventitial fibroblasts by activating PDGFβ receptor-JNK1 signalling. *Cardiovasc Res* 2012;95: 356–365.
19. Wang D, Zhang H, Li M, Frid MG, Flockton AR, McKeon BA, Yeager ME, Fini MA, Morrell NW, Pullamsetti SS, *et al*. MicroRNA-124 controls the proliferative, migratory, and inflammatory phenotype of pulmonary vascular fibroblasts. *Circ Res* 2014;114:67–78.
20. Barron L, Smith AM, El Kasmi KC, Qualls JE, Huang X, Cheever A, Borthwick LA, Wilson MS, Murray PJ, Wynn TA. Role of arginase 1 from myeloid cells in Th2-dominated lung inflammation. *PLoS One* 2013;8:e61961.
21. Hassoun PM, Mouthon L, Barberà JA, Eddahibi S, Flores SC, Grimminger F, Jones PL, Maitland ML, Michelakis ED, Morrell NW, *et al*. Inflammation, growth factors, and pulmonary vascular remodeling. *J Am Coll Cardiol* 2009;54(1suppl): S10–S19.
22. Stenmark KR, Frid MG, Yeager M, Li M, Riddle S, McKinsey T, El Kasmi KC. Targeting the adventitial microenvironment in pulmonary hypertension: a potential approach to therapy that considers epigenetic change. *Pulm Circ* 2012;2:3–14.
23. El Kasmi KC, Pugliese SC, Riddle SR, Poth JM, Anderson AL, Frid MG, Li M, Pullamsetti SS, Savai R, Nagel MA, *et al*. Adventitial fibroblasts induce a distinct proinflammatory/profibrotic macrophage phenotype in pulmonary hypertension. *J Immunol* 2014;193: 597–609.
24. Adesina SE, Kang BY, Bijli KM, Ma J, Cheng J, Murphy TC, Michael Hart C, Sutliff RL. Targeting mitochondrial reactive oxygen species to modulate hypoxia-induced pulmonary hypertension. *Free Radic Biol Med* 2015;87:36–47.
25. Mittal M, Roth M, König P, Hofmann S, Dony E, Goyal P, Selbitz AC, Schermuly RT, Ghofrani HA, Kwapiszewska G, *et al*. Hypoxia-dependent regulation of nonphagocytic NADPH oxidase subunit NOX4 in the pulmonary vasculature. *Circ Res* 2007;101:258–267.
26. Waypa GB, Marks JD, Guzy R, Mungai PT, Schriewer J, Dokic D, Schumacker PT. Hypoxia triggers subcellular compartmental redox signaling in vascular smooth muscle cells. *Circ Res* 2010;106: 526–535.
27. Assay-Protocol. Western-blot protocol. Biology Assays & Protocols. Available from: www.assay-protocol.com

28. Dlasková A, Hlavatá L, Jezek J, Jezek P. Mitochondrial complex I superoxide production is attenuated by uncoupling. *Int J Biochem Cell Biol* 2008;40:2098–2109.
29. Guzy RD, Hoyos B, Robin E, Chen H, Liu L, Mansfield KD, Simon MC, Hammerling U, Schumacker PT. Mitochondrial complex III is required for hypoxia-induced ROS production and cellular oxygen sensing. *Cell Metab* 2005;1:401–408.
30. Williamson DH, Lund P, Krebs HA. The redox state of free nicotinamide-adenine dinucleotide in the cytoplasm and mitochondria of rat liver. *Biochem J* 1967;103:514–527.
31. Frezza C, Cipolat S, Scorrano L. Organelle isolation: functional mitochondria from mouse liver, muscle and cultured fibroblasts. *Nat Protoc* 2007;2:287–295.
32. Frid MG, Li M, Gnanasekharan M, Burke DL, Fragoso M, Strassheim D, Sylman JL, Stenmark KR. Sustained hypoxia leads to the emergence of cells with enhanced growth, migratory, and promitogenic potentials within the distal pulmonary artery wall. *Am J Physiol Lung Cell Mol Physiol* 2009;297:L1059–L1072.
33. Koene S, Rodenburg RJ, van der Knaap MS, Willemsen MA, Sperl W, Laugel V, Ostergaard E, Tarnopolsky M, Martin MA, Nesbitt V, *et al*. Natural disease course and genotype–phenotype correlations in complex I deficiency caused by nuclear gene defects: what we learned from 130 cases. *J Inherit Metab Dis* 2012;35:737–747.
34. Barman SA, Chen F, Su Y, Dimitropoulou C, Wang Y, Catravas JD, Han W, Orfi L, Szantai-Kis C, Keri G, *et al*. NADPH oxidase 4 is expressed in pulmonary artery adventitia and contributes to hypertensive vascular remodeling. *Arterioscler Thromb Vasc Biol* 2014;34: 1704–1715.
35. Kim JW, Tchernyshyov I, Semenza GL, Dang CV. HIF-1–mediated expression of pyruvate dehydrogenase kinase: a metabolic switch required for cellular adaptation to hypoxia. *Cell Metab* 2006;3: 177–185.
36. O'Neill LA, Hardie DG. Metabolism of inflammation limited by AMPK and pseudo-starvation. *Nature* 2013;493:346–355.
37. De Rasmo D, Signorile A, Larizza M, Pacelli C, Cocco T, Papa S. Activation of the cAMP cascade in human fibroblast cultures rescues the activity of oxidatively damaged complex I. *Free Radic Biol Med* 2012;52:757–764.
38. Scacco S, Petruzzella V, Budde S, Vergari R, Tamborra R, Panelli D, van den Heuvel LP, Smeitink JA, Papa S. Pathological mutations of the human NDUFS4 gene of the 18-kDa (AQDQ) subunit of complex I affect the expression of the protein and the assembly and function of the complex. *J Biol Chem* 2003;278:44161–44167.
39. Chouchani ET, Methner C, Buonincontri G, Hu CH, Logan A, Sawiak SJ, Murphy MP, Krieg T. Complex I deficiency due to selective loss of Ndufs4 in the mouse heart results in severe hypertrophic cardiomyopathy. *PLoS One* 2014;9:e94157.
40. Jin Z, Wei W, Yang M, Du Y, Wan Y. Mitochondrial complex I activity suppresses inflammation and enhances bone resorption by shifting macrophage–osteoclast polarization. *Cell Metab* 2014;20: 483–498.
41. Brand MD. The sites and topology of mitochondrial superoxide production. *Exp Gerontol* 2010;45:466–472.
42. Roestenberg P, Manjeri GR, Valsecchi F, Smeitink JA, Willems PH, Koopman WJ. Pharmacological targeting of mitochondrial complex I deficiency: the cellular level and beyond. *Mitochondrion* 2012;12: 57–65.
43. Kamezaki F, Tasaki H, Yamashita K, Tsutsui M, Koide S, Nakata S, Tanimoto A, Okazaki M, Sasaguri Y, Adachi T, *et al*. Gene transfer of extracellular superoxide dismutase ameliorates pulmonary hypertension in rats. *Am J Respir Crit Care Med* 2008;177:219–226.
44. Lachmanová V, Hnilicková O, Povýsilová V, Hampl V, Herget J. N-acetylcysteine inhibits hypoxic pulmonary hypertension most effectively in the initial phase of chronic hypoxia. *Life Sci* 2005;77: 175–182.
45. Soon E, Crosby A, Southwood M, Yang P, Tajsic T, Toshner M, Appleby S, Shanahan CM, Bloch KD, Pepke-Zaba J, *et al*. Bone morphogenetic protein receptor type II deficiency and increased inflammatory cytokine production: a gateway to pulmonary arterial hypertension. *Am J Respir Crit Care Med* 2015;192: 859–872.
46. Ryan J, Dasgupta A, Huston J, Chen KH, Archer SL. Mitochondrial dynamics in pulmonary arterial hypertension. *J Mol Med (Berl)* 2015; 93:229–242.
47. Kasahara A, Scorrano L. Mitochondria: from cell death executioners to regulators of cell differentiation. *Trends Cell Biol* 2014;24:761–770.
48. Smeitink J, van den Heuvel L, DiMauro S. The genetics and pathology of oxidative phosphorylation. *Nat Rev Genet* 2001;2:342–352.
49. He X, Zhou A, Lu H, Chen Y, Huang G, Yue X, Zhao P, Wu Y. Suppression of mitochondrial complex I influences cell metastatic properties. *PLoS One* 2013;8:e61677.

Metabolic Reprogramming Regulates the Proliferative and Inflammatory Phenotype of Adventitial Fibroblasts in Pulmonary Hypertension Through the Transcriptional Corepressor C-Terminal Binding Protein-1

BACKGROUND: Changes in metabolism have been suggested to contribute to the aberrant phenotype of vascular wall cells, including fibroblasts, in pulmonary hypertension (PH). Here, we test the hypothesis that metabolic reprogramming to aerobic glycolysis is a critical adaptation of fibroblasts in the hypertensive vessel wall that drives proliferative and proinflammatory activation through a mechanism involving increased activity of the NADH-sensitive transcriptional corepressor C-terminal binding protein 1 (CtBP1).

METHODS: RNA sequencing, quantitative polymerase chain reaction, ^{13}C–nuclear magnetic resonance, fluorescence-lifetime imaging, mass spectrometry–based metabolomics, and tracing experiments with U-^{13}C-glucose were used to assess glycolytic reprogramming and to measure the NADH/NAD^+ ratio in bovine and human adventitial fibroblasts and mouse lung tissues. Immunohistochemistry was used to assess CtBP1 expression in the whole-lung tissues. CtBP1 siRNA and the pharmacological inhibitor 4-methylthio-2-oxobutyric acid (MTOB) were used to abrogate CtBP1 activity in cells and hypoxic mice.

RESULTS: We found that adventitial fibroblasts from calves with severe hypoxia-induced PH and humans with idiopathic pulmonary arterial hypertension (PH-Fibs) displayed aerobic glycolysis when cultured under normoxia, accompanied by increased free NADH and NADH/NAD^+ ratios. Expression of the NADH sensor CtBP1 was increased in vivo and in vitro in fibroblasts within the pulmonary adventitia of humans with idiopathic pulmonary arterial hypertension and animals with PH and cultured PH-Fibs, respectively. Decreasing NADH pharmacologically with MTOB or genetically blocking CtBP1 with siRNA upregulated the cyclin-dependent genes (p15 and p21) and proapoptotic regulators (NOXA and PERP), attenuated proliferation, corrected the glycolytic reprogramming phenotype of PH-Fibs, and augmented transcription of the anti-inflammatory gene *HMOX1*. Chromatin immunoprecipitation analysis demonstrated that CtBP1 directly binds the *HMOX1* promoter. Treatment of hypoxic mice with MTOB decreased glycolysis and expression of inflammatory genes, attenuated proliferation, and suppressed macrophage numbers and remodeling in the distal pulmonary vasculature.

CONCLUSIONS: CtBP1 is a critical factor linking changes in cell metabolism to cell phenotype in hypoxic and other forms of PH and a therapeutic target.

Min Li, PhD
Suzette Riddle, PhD
Hui Zhang, MD, PhD
Angelo D'Alessandro, PhD
Amanda Flockton, BS
Natalie J. Serkova, MD
Kirk C. Hansen, PhD
Radu Moldvan, PhD
B. Alexandre McKeon, MS
Maria Frid, PhD
Sushil Kumar, PhD
Hong Li, PhD
Hongbing Liu, MD, PhD
Angela Cánovas, PhD
Juan F. Medrano, PhD
Milton G. Thomas, PhD
Dijana Iloska, MSc
Lydie Plecitá-Hlavatá, PhD
Petr Ježek, PhD
Soni Pullamsetti, PhD
Mehdi A. Fini, PhD
Karim C. El Kasmi, MD, PhD
QingHong Zhang, PhD†
Kurt R. Stenmark, MD

†Deceased.

Correspondence to: Kurt R. Stenmark, MD, Pediatric Critical Care Medicine/CVP Research, University of Colorado Denver, 12700 E 19th Ave, RC2, B131, Aurora, CO 80045. E-mail kurt.stenmark@ucdenver.edu

Sources of Funding, see page 1119

Key Words: cell proliferation ■ fibroblasts ■ glycolysis ■ hypertension, pulmonary ■ metabolism

Clinical Perspective

What Is New?

- In pulmonary hypertension, little is known about the molecular mechanisms that link the metabolic state of cells to gene transcription and functional changes in their phenotype. We show that C-terminal binding protein-1, a transcription factor that is activated by increased free NADH, acts as a molecular linker to drive the proliferative and proinflammatory phenotype of adventitial fibroblasts within the hypertensive vessel wall.
- This work supports the novel hypothesis that some forms of pulmonary hypertension lead to the rewiring of cellular metabolic programs that use alterations in the cellular redox state to control the activity of C-terminal binding protein-1, which then coordinates expression of a network of genes implicated in cell proliferation, apoptosis resistance, and inflammation.

What Are the Clinical Implications?

- We also found that treatment of fibroblasts from the pulmonary hypertensive vessel and of hypoxic mice with a pharmacological inhibitor of C-terminal binding protein-1, 4-methylthio-2-oxobutyric acid, leads to a normalization of proliferation, inflammation, and the aberrant metabolic signaling.
- Our results suggest that targeting this metabolic sensor may be a more specific approach to treating metabolic abnormalities in pulmonary hypertension than use of more global metabolic inhibitors.
- It will be important in future studies to determine whether inhibition of C-terminal binding protein-1 can be combined with other vasodilating drugs to effect reversal of established severe forms of pulmonary hypertension.

Pulmonary hypertension (PH) is a devastating syndrome with high mortality, affecting both pediatric and adult patients with a wide variety of disorders.[1] The pulmonary vasculature in these patients exhibits significant cellular and structural changes within the intima, media, and adventitia that include augmented proliferation, resistance to apoptosis, and increased production of inflammatory mediators and extracellular matrix proteins.[2] These cellular changes are recapitulated, at least in part, in various animal models of PH.[3] Notably, some of the earliest pathophysiological changes are observed in the pulmonary artery adventitia and include robust proliferation of fibroblasts and accumulation of macrophages.[4–7] These phenotypic changes in adventitial fibroblasts are maintained ex vivo over multiple passages in culture and are regulated, in part, through epigenetic mechanisms.[4,5,7–9] Collectively, these observations are consistent with the hypothesis that many of the cellular and molecular features of PH resemble hallmark characteristics of cancer.[10,11]

It is increasingly recognized that increased proliferation and inflammatory activation can occur in the context of changes in cellular metabolism toward aerobic glycolysis (the Warburg effect) and that there is an intimate link between metabolic adaptation and functional cellular phenotype.[12,13] It is important to note that metabolic changes closely resembling those of cancer cells have been reported in PH in endothelial cells, smooth muscle cells, and most recently fibroblasts and have formed the basis for a metabolic theory of PH.[12,14] Furthermore, findings using in-vivo noninvasive imaging approaches support the hypothesis that the fludeoxyglucose positron emission tomography signal originated in the adventitia where activated fibroblasts and macrophages are observed.[14] However, the mechanisms that link metabolic reprogramming to inflammatory and proliferative pathways in PH remain largely unknown.

C-terminal binding protein (CtBP) comprises a dimeric family of transcriptional repressors encoded by 2 paralogous genes (*CTBP1* and *CTBP2*) that have major roles in animal cell development and cancer and have been suggested to be sensors of the metabolic state of cells that can modulate many aspects of cell phenotype.[15] Overexpression of CtBP is observed in a number of cancers, including prostate, ovarian, colon, and breast.[16–18] Studies in cancer and nervous system revealed that CtBPs promote cellular survival primarily through repression of Bcl-2 family members and other proapoptotic molecules (PERP, Bax, Bik, Puma, p21, and Noxa), as well as tumor suppressors (eg, p16INK4a and p15 INK4b).[15,18,19] Importantly, there is emerging evidence that CtBPs may also function to modulate the inflammatory response.[20] Furthermore, a recent genome-wide analysis in breast cancer provided a more comprehensive description of CtBP repression targets.[18,21] CtBP targets were categorized into 3 main categories: genes that regulate cell renewal and pluripotency, genes that control genome stability, and genes that regulate epithelial differentiation and prevent epithelial-to-mesenchymal transition, all processes of potential importance in PH pathogenesis.[18,21]

CtBP is unique among transcription factors in the incorporation of a D-isomer– specific 2-hydroxyacid dehydrogenase domain, which reduces or oxidizes substrates using the coenzyme NADH.[15,18] CtBP recruitment of coenzyme NAD^+ or NADH induces dimerization, an event necessary for transcriptional repressor activity, linking enzymatic function and transcriptional activity. Although both forms of this dinucleotide are capable of inducing CtBP dimerization, CtBPs bind NADH with up to 100-fold higher affinity than NAD^+, suggesting that these proteins are in fact sensitive to the ratio of NADH to NAD^+ within the nucleus.[22,23] Thus, metabolic changes in cells that favor increases in free NADH (eg, hypoxia or aerobic glycolysis) activate CtBPs and lead to transcrip-

Circulation. 2016;134:1105–1121. DOI: 10.1161/CIRCULATIONAHA.116.023171

tional repressor activity. CtBPs may thus be an example of how cellular metabolic status can influence epigenetic control of cell function and fate.

Here, we sought to test a novel hypothesis that in PH the metabolic/redox sensor CtBP1 drives persistent proproliferative, antiapoptotic and proinflammatory activation of pulmonary adventitial fibroblasts by linking metabolic reprogramming (aerobic glycolysis and subsequently increased NADH) to gene transcription. Our approach was first to use RNA sequencing (RNA-Seq) to determine whether metabolic pathways differ between control (CO-Fibs) and pulmonary hypertensive (PH-Fibs). We then performed a detailed metabolic evaluation of both CO-Fibs and PH-Fibs cultured under normoxic conditions using nuclear magnetic resonance (NMR) and mass spectrometry (MS; steady-state and tracing experiments with ^{13}C-glucose). We assessed NADH directly using MS and fluorescence lifetime imaging (FLIM) in cultured fibroblasts. CtBP1 expression was also evaluated by quantitative polymerase chain reaction (qPCR) and immunostaining approaches. We assessed the functional role of CtBP1 in controlling cell phenotype using both genetic (siRNA) and a novel pharmacological inhibitor of CtBP1, 4-methylthio-2-oxobutyric acid (MTOB), a substrate of CtBP dehydrogenase that has recently been shown to antagonize CtBP transcriptional regulation.[18,24] Finally, using a hypoxic mouse model of PH, we treated mice with MTOB to prove the concept that CtBP1 could serve as a therapeutic target to inhibit hypoxia-induced cell proliferation and inflammation.

METHODS

A detailed Methods section is provided in the online-only Data Supplement.

Animals

Neonatal calves and C57BL/6 mice exposed to chronic hypoxia were used in this study. All animal procedures were performed in accordance with the Guidelines for Animal Experimentation established and approved by the University of Colorado Anschutz Medical Campus and Colorado State University Institutional Review boards.

Tissue Specimen

Lung tissues from hypertensive and control calves (n= 5–7 for each group) and mice (n= 5 for each group) were used for reverse transcription–PCR and immunohistochemical/immunofluorescent staining analyses. Human lung tissue specimens from subjects with idiopathic pulmonary arterial hypertension (IPAH; n=7) or donor control subjects (n=8) were obtained during lung transplantation and used for qPCR and immunohistochemical staining analysis. The study protocol for tissue donation was approved by the ethics committee (Ethik Kommission am Fachbereich Humanmedizin der Justus Liebig Universität Giessen) of the University Hospital Giessen (Giessen, Germany) in accordance with national law and with Good Clinical Practice/International Conference on Harmonization guidelines. Written informed consent was obtained from each individual patient or the patient's next of kin (AZ 31/93).

Cell Culture

Isolation of adventitial fibroblasts from distal pulmonary arteries of hypertensive and control calves was performed as described in Methods in the online-only Data Supplement. Human pulmonary artery fibroblasts were derived from patients with IPAH or from control donors undergoing lobectomy or pneumonectomy. All cells were cultured under normoxic conditions. Experiments were performed on cells at passages 5 to 10.

RNA Sequencing

RNA from bovine CO-Fibs and PH-Fibs (n=6 for each group) was used to perform RNA-Seq analysis. Total RNA was purified, fragmented, and converted to cDNA. Sequencing libraries were made with the TruSeq RNA Sample Preparation kit (Illumina, San Diego, CA). RNA-Seq was performed on a HiSeq2000 sequencer analyzer. Sequence reads were assembled to the annotated UMD3.1 bovine reference genome.[25] Quality control analysis was performed with the CLC Genomics workbench software (CLC Bio, Aarhus, Denmark). All the samples analyzed passed all the quality control parameters, indicating a very good quality.

Data were normalized by calculating the reads per kilobase per million mapped reads for each gene. Statistical analysis was performed with the total exon reads used as expression values by the empirical analysis of differential gene expression tool of CLC Bio Genomic workbench software. This tool is based on the EdgeR Bioconductor package and uses count data (ie, total exon reads) for the statistical analysis. Genes were filtered on the basis of minimum expression >0.2 reads per kilobase per million mapped reads. False discovery rate (FDR) was used for multiple testing corrections. Finally, differentially expressed genes were selected based on fold change (≥2), P value (P<0.01), and FDR value (q<0.1). Detailed methods are provided in the online-only Data Supplement.

Real-Time Reverse Transcription–PCR

Total RNA from cultured cells was isolated using Qiagen Mini Kit (Qiagen, Valencia, CA). Total RNA from tissues was isolated with Trizol. The sequences for all primers are listed in Table I in the online-only Data Supplement. Results are presented as fold change using the Δ-ΔCt method.

Quantitative Multi-NMR Metabolomics and ^{13}C-Glucose Fluxes

Fibroblasts were incubated with 10 mmol/L $^{13}C_1$-glucose (glucose with ^{13}C at C_1 position, Cambridge Isotope Laboratories, Tewksbury, MA) as the exclusive glucose source (and otherwise under standard growth conditions). After 24 hours, cells were extracted with perchloric acid and used for NMR analysis. High-resolution ^{1}H-, ^{31}P-, and ^{13}C-NMR experiments were performed with a Bruker 400-MHz Avance III spectrometer (Bruker BioSpin, Fremont, CA). In cell extracts, intracellular ^{13}C-glucose and its ^{13}C-labeled products from glycolysis and the tricarboxylic acid cycle were calculated from ^{13}C-NMR spectra. Spectra

acquisition and metabolite integration were performed with Bruker TopSpin software. Metabolite identification and multivariate partial least squares–discriminant analysis were performed using the Human Metabolome Database. Data were normalized to cell mass.

Ultrahigh-Performance Liquid Chromatography–MS–Based Direct NADH Measurements and Metabolomics Analyses: Steady State and U-^{13}C-Glucose Tracing Experiments

CO-Fibs and PH-Fibs (n=3 for each group), cultured in normal media or in media supplemented with 10 mmol/L U-^{13}C-glucose (Cambridge Isotope Laboratories) for 5 minutes and 1, 8, and 24 hours were extracted (2×10^6 cells/mL buffer) and run through a C18 reversed-phase column (Phenomenex, Torrance, CA) through an ultrahigh-performance liquid chromatography (UHPLC) system (Vanquish, Themo Fisher). Metabolite assignment, peak integration for relative quantification, and isotopologue distributions in tracing experiments were calculated through the software Maven (Princeton), against the KEGG pathway database and an in-house validated standard library (>650 compounds, also including NADH; product No. N8129, Sigma Aldrich, IROATech). To determine linearity (r^2 >0.99) and sensitivity of the approach (limit of detection and limit of quantification), NADH was weighed and progressively diluted (from 0.5–5000 injected pmol range; 4 orders of magnitude) before injection through UHPLC-MS. Integrated peak areas were exported into Excel (Microsoft, Redmond, CA) for statistical analysis (*t* test, ANOVA through the software GraphPad Prism).

Frozen mouse whole-lung tissues were snap-frozen, powered, and weighed in the presence of liquid nitrogen and dry ice, and cold lysis buffer (10 mg tissue/mL buffer) was added. Samples were extracted at 4°C for 30 minutes and centrifuged, and the supernatants were used for metabolomics analysis as described above. Data were normalized by tissue mass.

Assessment of NADH/NAD$^+$ Ratio

NADH/NAD$^+$ ratio was determined with an enzymatic cycling reaction using modified methods by Williamson et al[26] as described in Methods in the online-only Data Supplement.

Fluorescence Lifetime Imaging

To directly visualize NADH level in cells, FLIM of 2-photon–excited NADH was performed at the University of California-Davis Advanced Light Microscopy Core.

Inhibition of CtBP1

CtBP1 was inhibited either genetically by siRNA or pharmaceutically by MTOB. Transfection efficiencies are shown in Figure I in the online-only Data Supplement.

Cell Proliferation Assay

An equal number of cells were plated onto 24-well plates in full DMEM supplemented with 10% bovine calf serum for bovine cells or with 10% fetal bovine serum for human cells and then treated with 2-deoxy-glucose (2-DG; 10 mmol/L), pyruvate (20 mmol/L), MTOB (2.5 mmol/L), CtBP1 siRNA (50 nmol/L), or scrambled siRNA or were left untreated. Cell numbers were counted in triplicate wells on days 1, 2, and 3. In parallel, cells with each type of treatment were collected for reverse transcription–PCR.

Chromatin Immunoprecipitation Assay

Chromatin immunoprecipitation assay was used to study CtBP1 protein interaction with its target gene. Human fibroblasts were cross-linked with ice-cold 1% formaldehyde for 15 minutes, and the reaction was stopped by adding 0.125 mol/L glycine. Cell lysates were centrifuged, and the pellet was sonicated in lysis buffer to shear DNA. Fragmented DNA was precipitated with CtBP1 antibody (EMD Millipore, Billerica, MA) with the use of immobilized recombinant protein A affinity resins (RepliGen, Waltham, MA). Unbound DNA fragments were washed off, and beads were removed with elution buffer. Precipitated protein/DNA complexes were reverse cross-linked by adding 350 mmol/L NaCl and incubated for 6 hours at 65°C. DNA was then purified and used for PCR analysis.

Statistical Analysis

Prism software version 5 (GraphPad, Software, Inc[27]) was used for *t* test or ANOVA followed by Bonferroni posttest analysis.

Values were expressed as mean±SEM. For basic comparisons of 2 gaussian-distributed sample sets, we used Student *t* tests. In comparisons of multiple groups, the respective ANOVA (1 way when comparing 1 characteristic, or 2 way if 2 dependent variables were involved) was performed. *P* values were subject to multiple testing adjustment with Bonferroni correction. Supervised partial least squares–discriminant analysis (Simca, Umetrics, San Jose, CA) was used to determine the variance of metabolic phenotypes in CO-Fibs and PH-Fibs as determined via NMR and MS analyses and were sufficient to discriminate biological samples. To validate partial least squares–discriminant analysis, random permutations were performed through MetaboAnalyst and Multibase (20 random permutations were selected; significance threshold, 0.05; <100 variables tested). FDR (Benjamini Hochberg) was <0.1 for all significant metabolites. Power analysis was performed to ensure that the number of replicates was sufficient to ensure >80% probability to have an FDR<0.1 for all the significant observations (tested through MetaboAnalyst 3.0). Differences with values of $P<0.05$ were considered statistically significant.

RESULTS

PH-Fibs Are Metabolically Reprogrammed to Aerobic Glycolysis

RNA-Seq analysis elucidated >1000 differentially regulated genes in bovine PH-Fibs compared with CO-Fibs (n=6 for each group; $P<0.01$; fold change >2). Glycolysis/gluconeogenesis and pyruvate metabolism were identified as 2 of the most significantly upregulated pathways (Table 1 and Figure IIA in the online-only Data Supplement). In particular, 9 genes that code for enzymes and transporters involved in glucose-to-lactate catabolism were upregulated in PH-Fibs (Table 2).

Table 1. Most Significant Pathways Identified in the List of 1012 Differentially Expressed Genes (P<0.01 and Fold Change >2) Between Control and Hypertensive Calves by Blast2GO

Pathway	Sequences, n	Enzymes, n	*P* Value (Fisher Exact Test)	*P* Value (Bonferroni)	Pathway	Sequences, n	Enzymes, n	*P* Value (Fisher Exact Test)	*P* Value (Bonferroni)
Purine metabolism	27	17	3.06E–07	5.84E–05	Phenylalanine metabolism	4	3	0.002	0.251
Phosphatidylinositol signaling system	11	5	5.33E–07	1.02E–04	Tyrosine metabolism	4	3	0.002	0.270
Glycolysis/ gluconeogenesis	9	10	2.10E–06	4.02E–04	Propanoate metabolism	4	3	0.002	0.310
Inositol phosphate metabolism	9	4	1.02E–05	0.002	Glycosaminoglycan biosynthesis, chondroitin sulfate/dermatan sulfate	4	5	0.002	0.328
Glycerolipid metabolism	7	6	1.04E–05	0.002	Glycosaminoglycan degradation	4	2	0.002	0.367
Pyrimidine metabolism	7	6	2.68E–05	0.005	Pentose and glucuronate interconversions	4	4	0.003	0.384
β-Alanine metabolism	6	5	2.76E–05	0.005	Biosynthesis of unsaturated fatty acids	3	2	0.003	0.393
Galactose metabolism	6	5	3.46E–05	0.007	Metabolism of xenobiotics by cytochrome P450	3	3	0.004	0.521
Nitrogen metabolism	5	3	6.44E–05	0.012	Chloroalkane and chloroalkene degradation	3	2	0.005	0.579
Glycerophospholipid metabolism	5	4	1.33E–04	0.020	Streptomycin biosynthesis	3	2	0.005	0.582
Fructose and mannose metabolism	5	5	2.12E–04	0.040	Valine, leucine, and isoleucine degradation	3	2	0.005	0.625
Steroid hormone biosynthesis	5	4	2.42E–04	0.045	Lysine degradation	3	2	0.005	0.630
Arachidonic acid metabolism	4	5	3.81E–04	0.070	Starch and sucrose metabolism	3	2	0.005	0.540
Sulfur metabolism	4	4	4.46E–04	0.082	Fatty acid metabolism	3	2	0.005	0.640
Drug metabolism, other enzymes	4	3	4.53E–04	0.065	Glycine, serine, and threonine metabolism	3	2	0.005	0.554
Pyruvate metabolism	4	3	6.05E–04	0.109	Ascorbate and aldarate metabolism	3	2	0.006	0.506
Methane metabolism	4	4	0.001	0.206	Histidine metabolism	3	3	0.008	0.691
Amino sugar and nucleotide sugar metabolism	4	3	0.001	0.195	mTOR signaling pathway	3	2	0.009	0.666

mTOR indicates mammalian target of rapamycin.

Validation by reverse transcription–PCR analysis confirmed increased gene expression of the glycolytic genes *GLUT1*, *HK2*, and *LDHA* in both bovine and human PH-Fibs relative to CO-Fibs (Figure 1A). In addition, upregulation of *GLUT1*, *GLUT4*, and *G6PD* genes (as well as *HK2* and *LDHA*, which are submitted as part of another manuscript) was observed in vessels isolated by laser capture microdissection of IPAH patients compared with control subjects (Figure 1B). Furthermore, upregulation of GLUT1 protein expression was observed in situ in the adventitia of hypoxic hypertensive calves by immunofluorescence (Figure 1C) and in vitro in cultured bovine and human PH-Fibs by Western blot (Figure 1D).

NMR- and MS-based metabolomics analyses confirmed transcriptomics results, showing that significantly different metabolic phenotypes exist between CO-Fibs and PH-Fibs (Figures IIB, IIC, IIIA, and IIIB in the online-only Data Supplement), as well as metabolic reprogramming to aerobic glycolysis in PH-Fibs (Figure 2 and Figures II and III in the online-only Data Supplement). Glycolytic changes included increased glucose uptake; generation of sugar phosphates, ^{13}C-glycolytic signature, and ^{13}C-lactate (from $^{13}C_1$-glucose steady-state NMR analyses; Figures IIC, IIIC, and IIID in the online-only Data Supplement); and increased D-glucose, glyceraldehyde 3-phosphate, pyruvate, and lactate production (from steady-state MS analyses Figure 2A and 2B).

Finally, PH-Fibs displayed alterations in redox homeostasis as indicated by increased amounts of reduced (GSH) and oxidized (glutathione disulfide, GSSG) glutathione, evidence of use of the NADPH-generating pentose phosphate pathway, and increased phosphogluconate and ribose phosphate (Figure 2B and Figure IIB in the online-only Data Supplement). These findings are consistent with our recent observations of oxygen-independent increased mitochon-

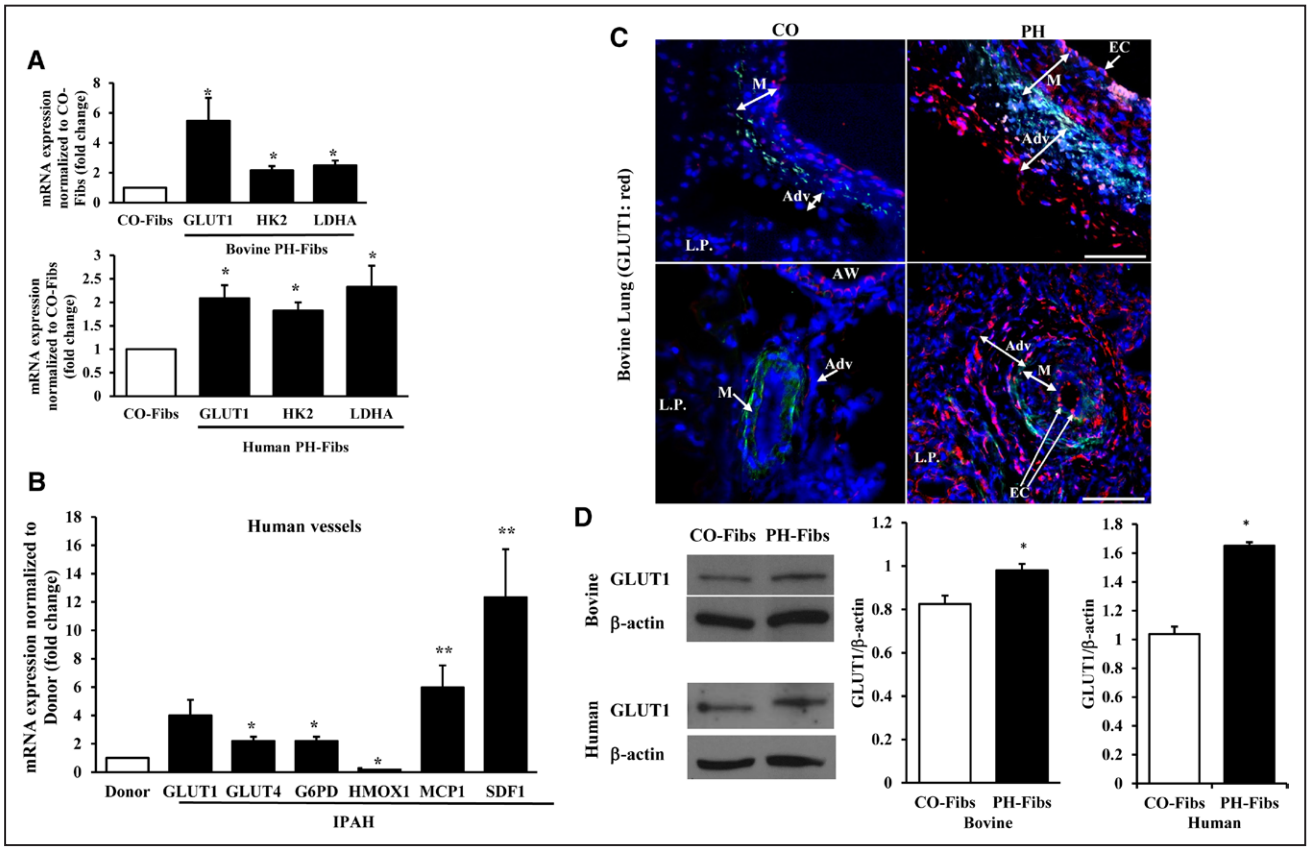

Figure 1. Bovine and human hypoxic-induced hypertensive pulmonary artery adventitial fibroblast cells (PH-Fibs) exhibit differences in mRNA and protein expression of genes involved in glucose metabolism compared with control fibroblasts (CO-Fibs).

A, Quantitative polymerase chain reaction showed significantly higher expression of glucose transporter 1 (*GLUT1*), hexokinase 2 (*HK2*), and lactate dehydrogenase A (*LDHA*) mRNA levels in both bovine and human PH-Fibs compared with CO-Fibs. **B**, Upregulation of *GLUT1*, *GLUT4*, *glucose-6-phosphate dehydrogenase* (*G6PD*), *monocyte chemotactic protein-1* (*MCP1*), and *stromal cell–derived factor-1* (*SDF1*) and downregulation of *heme oxygenase-1 (HMOX1)* were observed in vessels isolated by laser capture microdissection of IPAH patients compared with controls. **C**, Immunofluorescent staining showed higher expression of GLUT1 (red) in the adventitia (Adv) of chronic hypoxia-induced pulmonary hypertensive bovine lung section compared with control lungs. AW indicates airway; EC, endothelium; L.P., lung parenchyma; and M, media. Scale bar=100 μm. **D**, Western blot confirmed higher protein expression of *GLUT1* in both bovine and human PH-Fibs. Data are presented as mean±SEM; n=3–9. **P*<0.05, ***P*<0.01 vs CO-Fibs or vessels from human donors.

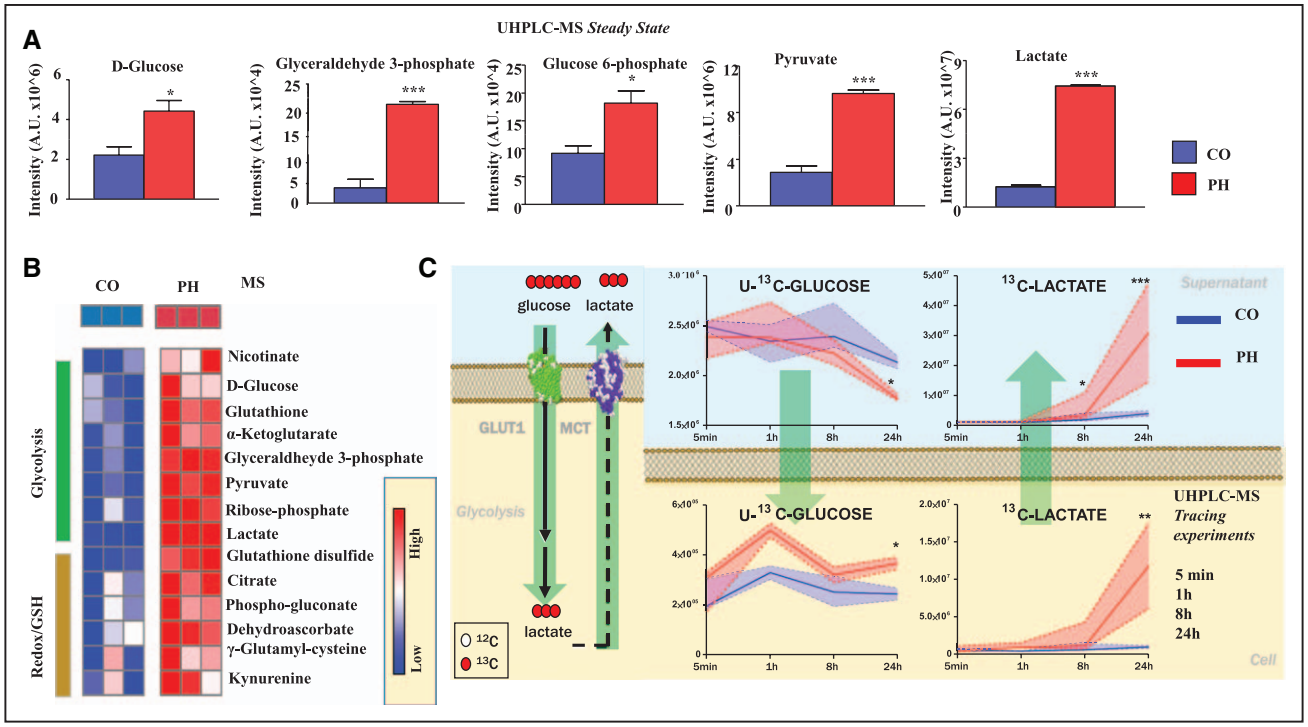

Figure 2. Metabolomics evidence for aerobic glycolysis in pulmonary hypertension fibroblasts (PH-Fibs). Steady-state and flux tracing experiments were performed via ultrahigh-performance liquid chromatography–mass spectrometry (UHPLC-MS) by incubating bovine control fibroblasts (CO-Fibs) and PH-Fibs with U-^{13}C-glucose. **A**, Steady-state UHPLC-MS demonstrated increased glucose content, utilization through glycolysis, and increased lactate production in PH-Fibs compared with CO-Fibs (n=3; **P*<0.05, ****P*<0.001 vs CO-Fibs). **B**, Heat map generated from MS showed differences in metabolite production between CO-Fibs and PH-Fibs. Each column represents an individual samples from each group, and the differences between each groups are significantly different (*P*<0.05). **C**, Tracing experiments were performed by incubating CO-Fibs and PH-Fibs (n=3) for 5 minutes or 1, 8, or 24 hours with U-^{13}C-glucose to confirm increased uptake and catabolism of glucose through aerobic glycolysis in PH-Fibs cultured in normoxia. Median (continuous line) and interquartile ranges (dashed lines) are shown for CO-Fibs (blue) and PH-Fibs (red). **P*<0.05, ***P*<0.01, ****P*<0.001 vs CO-Fibs, repeated measures ANOVA.

drial and cytoplasmic (NOX4-generated) reactive oxygen species production in both human and bovine PH-Fibs.[28]

To validate steady-state observations suggesting increased uptake and oxidation of glucose through glycolysis, CO-Fibs and PH-Fibs were cultured under normoxia in the presence of U-^{13}C-glucose for 5 minutes and 1, 8, and 24 hours. Tracing experiments via UHPLC-MS confirmed significantly increased (*P*<0.05, ANOVA) glucose uptake and intracellular and supernatant $^{13}C_{1\text{-}3}$-lactate generation in PH-Fibs as early as 8 hours from normoxic incubation with heavy glucose (Figure 2C).

NADH Concentrations Are Increased in PH-Fibs

To determine whether aerobic glycolysis in PH-Fibs formed the basis of increased concentrations of NADH (reflecting changes in the cellular redox status), FLIM (Figure 3A, red) and UHPLC-MS–based measurements (Figure 3B) were used to visualize free NADH and to directly measure NADH and NAD$^+$. Free NADH was markedly higher in bovine and human PH-Fibs relative to CO-Fibs (Figure 3A). Direct measurements of total NADH and NAD$^+$ were performed through a targeted UHPLC-MS method, after determining linearity (Figure IVA in the online-only Data Supplement) of the NADH detection down to a limit of quantification of 500 fmol injected, over 4 orders of magnitude. The results showed significant increased NADH in both bovine and human PH-Fibs compared with CO-Fibs (Figure 3B). The NADH/NAD$^+$ ratio was also significantly increased in bovine PH-Fibs. The NADH/NAD$^+$ ratio was remarkably higher in each human PH-Fib population, but because of the extremely low NAD$^+$ value found in 1 human PH-Fib, the overall variability is high, and *P*=0.07 (Figure IVB in the online-only Data Supplement). To further validate these observations, we performed an orthogonal and frequently used measure of the NADH/NAD$^+$ ratio based on an enzymatic cycling reaction and represented by lactate/pyruvate ratio[26,29] (Figure IVC in the online-only Data Supplement).

Aerobic Glycolysis and Free NADH Are Critical in PH-Fib Proliferation

We next determined whether metabolic reprogramming and increased NADH concentrations were critical for promoting proliferation in PH-Fibs. Bovine and human PH-Fibs

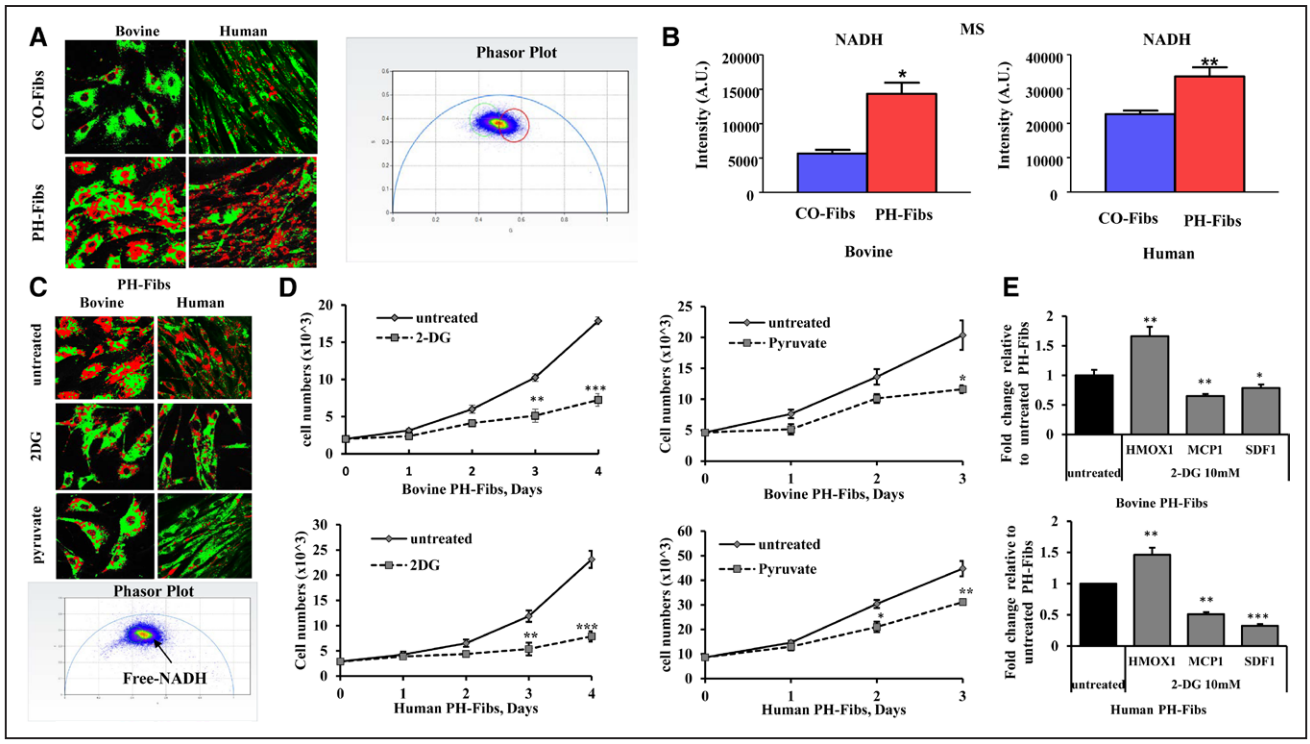

Figure 3. Pulmonary hypertension fibroblasts (PH-Fibs) exhibit increased NADH levels compared with control fibroblasts (CO-Fibs).

2-Deoxy-glucose (2-DG) and pyruvate inhibited proliferation and attenuated the inflammatory phenotype of PH-Fibs by decreasing NADH levels and thus decreasing C-terminal binding protein 1 (CtBP1) activity. **A**, Fluorescence lifetime imaging (FLIM) of 2-photon–excited NADH was performed to directly visualize free NADH (shorter lifetime, red). Phasor plot showed free NADH collection localization (red circle). A remarkably increased detection of free NADH was seen in PH-Fibs compared with CO-Fibs. **B**, Direct NADH measurements were performed through a targeted ultrahigh-performance liquid chromatography–mass spectrometry (UHPLC-MS) method after determination of the linearity of the NADH detection down to a limit of quantification of 500 fmol injected over 4 orders of magnitude. NADH analysis of bovine and human via UHPLC-MS confirmed the results obtained with FLIM and showed a significant increase in NADH in PH-Fibs compared with CO-Fibs (n=3; $*P<0.05$, $**P<0.01$ vs CO-Fibs). **C**, Treatment with 2-DG (10 mmol/L) and pyruvate (20 mmol/L) for 48 hours decreased free NADH (red color) detection (FLIM) in PH-Fibs. **D**, 2-DG and pyruvate significantly inhibited the proliferation of PH-Fibs (n=3; $*P<0.05$, $**P<0.01$, $***P<0.001$ vs untreated PH-Fibs, repeated measures ANOVA). **E**, 2-DG decreased proinflammatory factors (monocyte chemotactic protein-1 [*MCP1*] and stromal cell–derived factor-1 [*SDF1*]) and increased anti-inflammatory factor (*HMOX1*) expression in PH-Fibs (n=3–8; $*P<0.05$, $**P<0.01$, $***P<0.001$ vs untreated PH-Fibs).

were treated with 2-DG (10 mmol/L) to block glucose metabolism or with pyruvate (20 mmol/L) to directly decrease NADH by providing a substrate for NADH recycling to NAD^+ by lactate dehydrogenase. FLIM analysis showed the both 2-DG and pyruvate decreased free NADH in bovine and human PH-Fibs (Figure 3C). Enzymatic cycling reaction measurement also demonstrated that 2-DG significantly decreased the NADH/NAD^+ ratio in bovine and human cells (Figure IVD in the online-only Data Supplement). These decreases in free NADH resulted in a significant reduction in proliferation of both bovine and human PH-Fibs (Figure 3D).

Aerobic Glycolysis Is Critical for the Proinflammatory PH-Fib Phenotype

Recent reports demonstrate that proinflammatory activation of macrophages depends on metabolic reprogramming to aerobic glycolysis.[30,31] Similar to observations in activated macrophages, we have previously reported that PH-Fibs express high amounts of proinflammatory mediators.[5,7] Confirming our previous report of increased *MCP1* and *SDF1* gene and protein expression in PH-Fibs[7] we detected increased expression of monocyte chemotactic protein-1 and stromal cell–derived factor-1 in vessels isolated by laser capture microdissection of IPAH patients compared with control subjects (Figure 1B). Importantly, inhibition of aerobic glycolysis with 2-DG resulted in significantly attenuated transcription of monocyte chemotactic protein-1 and stromal cell–derived factor-1 (Figure 3E). Interestingly, recent reports have suggested that metabolic reprogramming to aerobic glycolysis prevents transcription of anti-inflammatory genes.[30] *HOMX1* has been regarded as an important anti-inflammatory gene in PH.[32,33] qPCR analysis from vessels isolated by

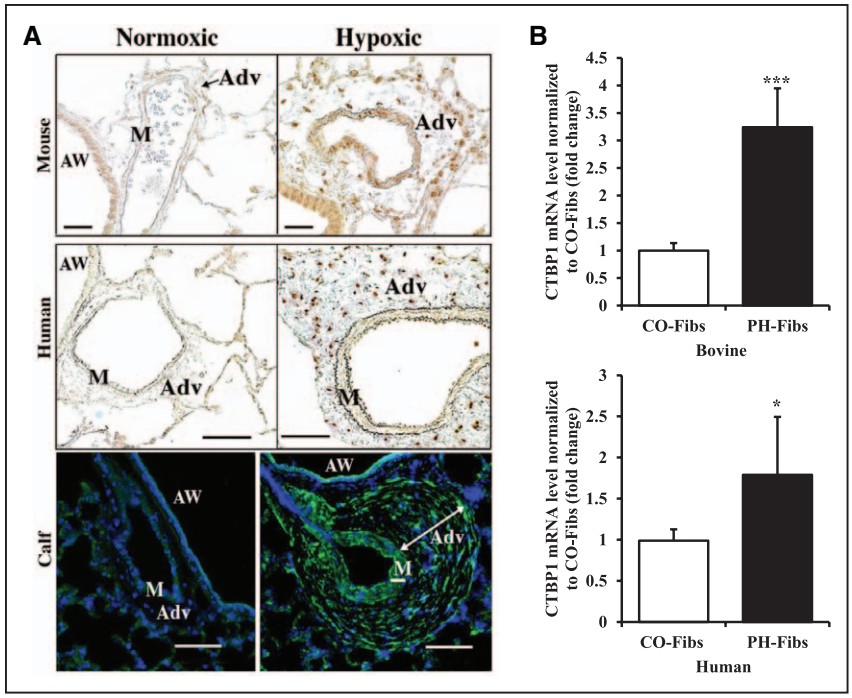

Figure 4. C-terminal binding protein 1 (CtBP1) expression is increased in the adventitia of hypertensive pulmonary arteries (PAs) and in isolated hypertensive adventitial fibroblast cells.
A, Immunohistochemistry (dark brown staining) and immunofluorescent staining (green staining; space bar=100 μm) showed that CtBP1 protein is overexpressed in the adventitia (Adv) of chronic hypoxia-induced pulmonary hypertensive (PH) but not control (CO), mouse, human, and bovine PA. AW indicates airway; and M, media. **B**, Real-time polymerase chain reaction data showed that high CtBP1 expression is maintained under normoxia conditions in fibroblasts cultured from both hypertensive calves and humans with idiopathic pulmonary arterial hypertension (n=4–15; **P*<0.05, ****P*<0.001 vs CO-Fibs).

laser capture microdissection of IPAH patients showed decreased expression of the *HMOX1* relative to control subjects (Figure 1B). Inhibition of aerobic glycolysis with 2-DG resulted in increased expression of *HMOX1* in both bovine and human PH-Fibs (Figure 3E).

CtBP1 Expression Is Increased in Adventitial Fibroblasts in PH

Considering that aerobic glycolysis promotes increases in free NADH concentrations that in turn increase CtBP1 activity, we questioned whether CtBP1 expression was simultaneously increased in PH-Fibs. Notably, immunofluorescence and immunohistochemical staining demonstrated that CtBP1 protein expression was increased in situ in the mouse and bovine hypoxic PH models and in pulmonary arteries from humans with IPAH relative to control subjects (Figure 4A). Importantly, CtBP1 expression was localized primarily to the pulmonary arterial adventitia of hypoxic hypertensive subjects (Figure 4A). Consistent with increased expression of CtBP1 in PH-Fibs observed in RNA-Seq analysis (*P*=0.033, FDR), expression of CtBP1 was increased in both cultured bovine and human PH-Fibs relative to CO-Fibs (Figure 4B).

CtBP1 Links Aerobic Glycolysis With Proliferation in PH-Fibs

Simultaneous increases in CtBP1 expression and NADH accumulation suggest a functional role for CtBP1 in PH-Fibs. Therefore, we next determined the role of CtBP1 in PH-Fib proliferation using siRNA to knock down *CTBP1* expression and MTOB (2.5 mmol/L) to inhibit CtBP1 activity. Both siCTBP1 and MTOB significantly inhibited PH-Fib proliferation (Figure 5A). We also determined the effects of these agents on the expression of genes involved in cell proliferation and cell survival that had previously been shown to be direct targets of CtBP1 in cancer cells.[15,18,24] siCTBP1 and MTOB treatment resulted in significant upregulation of genes that promote growth arrest (eg, cyclin-dependent kinase inhibitors genes *P21* and *P15*) and apoptosis (eg, *NOXA* and *PERP*; Figure 5B and Figure V in the online-only Data Supplement).

The antiproliferative effect induced by genetic or pharmacological inhibition of CtBP1 was accompanied by a correction of the main metabolic aberrations of bovine and human PH-Fibs. Silencing of CTBP1 or treatment with MTOB resulted in a significant decrease in relative levels of metabolites involved in proliferative anabolic pathways (eg, energy metabolism, nucleotide biosynthesis, and antioxidant reactions; Figure 5C and 5E) and human PH-Fibs (Figure 5D and 5F).

CtBP1 Suppresses Anti-Inflammatory *HMOX1* Expression in PH-Fibs

Because metabolic reprogramming to aerobic glycolysis has been shown to suppress anti-inflammatory genes in macrophages,[34] we hypothesized that disruption of CtBP1 signaling would increase transcription of anti-inflammatory genes in PH-Fibs. As mentioned above, the important anti-inflammatory gene implicated in the pathogenesis of PH, *HMOX1*,[35–38] was decreased in IPAH vessels (Figure 1B) and in PH-Fibs relative to controls (Figure 6A). Consistent with the proposed repressive activity of CtBP1, siRNA knockdown or pharmacological

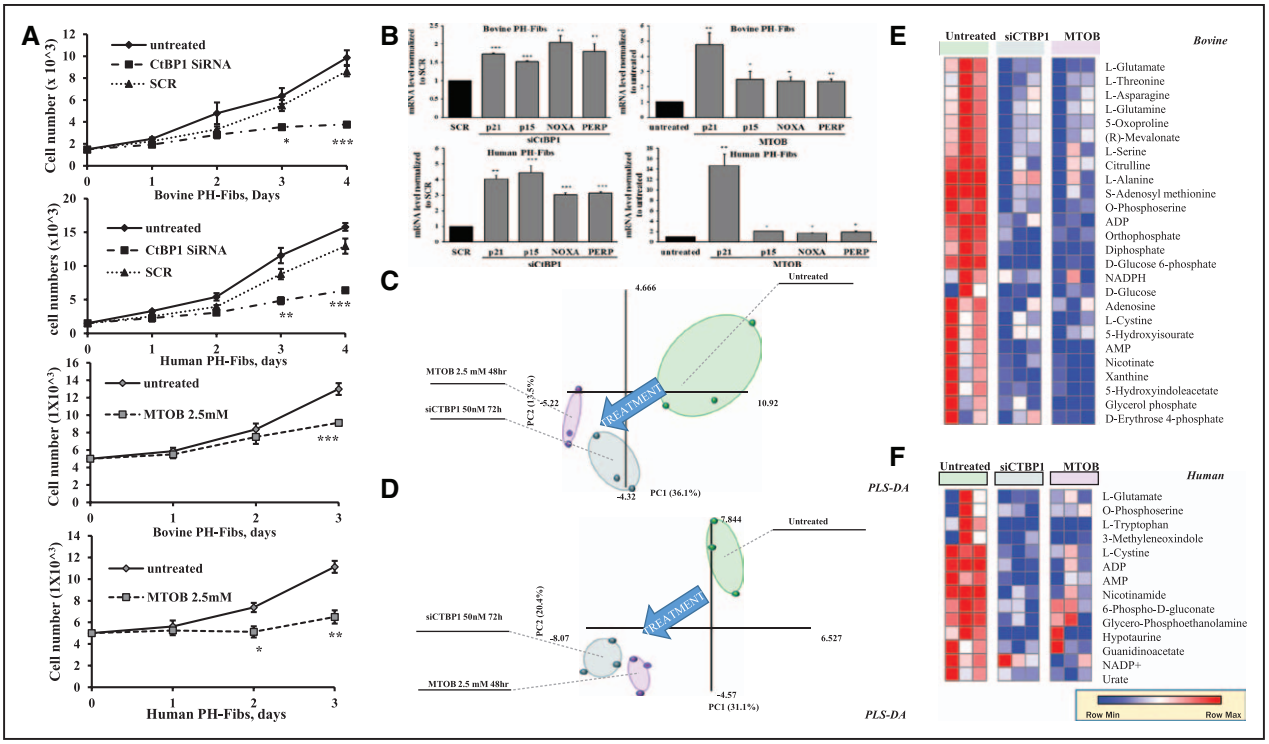

Figure 5. C-terminal binding protein 1 (CtBP1) regulates the expression of genes involved in proliferation, cell survival, and metabolic state in adventitial fibroblasts.

Inhibition of CtBP1 by siRNA (50 nmol/L, 72 hours) or by 4-methylthio-2-oxobutyric acid (MTOB; 2.5 mmol/L, 48 hours; **A**) significantly attenuated proliferation of both bovine and human pulmonary hypertension fibroblasts (PH-Fibs; n=3–6). **P*<0.05, ***P*<0.01, ****P*<0.001 vs scrambled (SCR) siRNA–treated PH-Fibs, repeated measures ANOVA. **B**, Restored antiproliferative gene (p21, p15) and proapoptosis gene (*NOXA*, *PERP*) expression (n=3–6; **P*<0.05, ***P*<0.01, ****P*<0.001 vs scrambled siRNA–treated or untreated PH-Fibs). Mass spectrometry metabolomic analysis (n=3) revealed that siCtBP1 and MTOB (**C** and **D**) altered the overall metabolic status of both bovine and human PH-Fibs and (**E** and **F**) showed the tendency to decrease the levels of metabolites involved in proliferative anabolic pathways (eg, energy metabolism: AMP, ADP, orthophosphate, and diphosphate; nucleotide biosynthesis; and antioxidant reactions: amino acids, glutamine/glutamate, and pentose phosphate pathway intermediates), consistent with a less proliferative phenotype. PLS-DA partial least squares–discriminant analysis.

inhibition of CtBP1 by MTOB resulted in significantly increased *HMOX1* transcription (Figure 6A).

These findings suggested that *HMOX1* was a direct target of the repressive activity of CtBP1, which, to the best of our knowledge, has not been previously reported. We therefore used chromatin immunoprecipitation assay to determine direct binding of CtBP1 to the *HMOX1* promoter in human PH-Fibs. We also examined whether 2-DG, pyruvate, or MTOB would decrease recruitment of CtBP1 to the *HMOX1* promoter. *HMOX1* promoter binding was significantly higher in PH-Fibs compared with CO-Fibs. Knockdown of *CTBP1* by siRNA decreased binding of CtBP1 to the *HMOX1* promoter. 2-DG, pyruvate, and MTOB also suppressed binding of CtBP1 to the *HMOX1* promoter region (Figure 6B).

MTOB Inhibits Proliferation and Inflammation In Vivo in a Mouse Model of Hypoxic PH

In light of the ability of MTOB to attenuate proliferation, correct metabolism, and reduce inflammation of cultured PH-Fibs, we next sought to determine the therapeutic potential of MTOB in vivo in a mouse model of hypoxic PH (mice were chosen because the extremely high cost of the compound; eg, the cost of similar experiments in rats was calculated to exceed $35 000). Initial time course experiments using different time points of hypoxic exposure (4, 14, and 28 days) performed to determine longitudinal expression of known genes involved in cellular proliferation and inflammatory activation demonstrated that expression of most of these genes peaked at day 4 (Figure VIA in the online-only Data Supplement), which is consistent with previous studies in hypoxic mice.[38,39] Hypoxic (4 days) whole mouse lung tissue exhibited increased glycolysis compared with normoxia as evidenced by the accumulation of lactate and increased NADH/NAD^+ ratios (Figure 7A and 7B). Metabolomics analyses by MS indicated a progressive alteration of lung normoxic metabolic phenotype during prolonged exposure to hypoxia, alterations that were corrected by the MTOB treatment (Figure 7C). Specifically, MTOB corrected the hypoxia-induced increase in

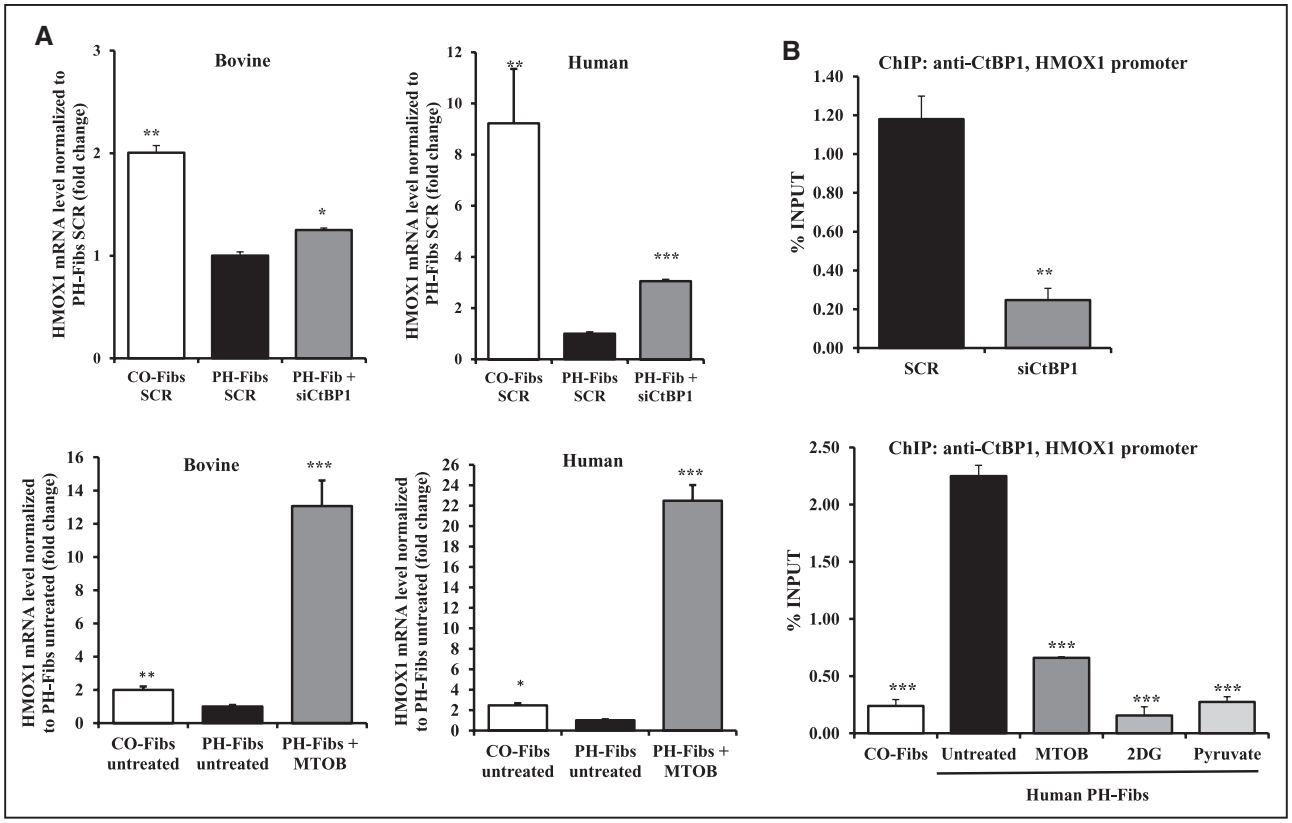

Figure 6. C-terminal binding protein 1 (CtBP1) directly regulates *HMOX1* gene expression in pulmonary artery adventitial fibroblasts.

A, Inhibition of CtBP1 by siRNA (50 nmol/L, 72 hours) or 4-methylthio-2-oxobutyric acid (MTOB; 2.5 mmol/L, 48 hours) significantly increased anti-inflammatory gene *HMOX1* expression in bovine and human pulmonary hypertension fibroblasts (PH-Fibs; n=3–6; **P*<0.05, ***P*<0.01, ****P*<0.001 vs scrambled [SCR] siRNA–treated PH-Fibs). **B**, Chromatin immunoprecipitation (ChIP) assay confirmed increased recruitment of CtBP1 to the promoter region of *HMOX1* in PH-Fibs compared with control fibroblasts (CO-Fibs). *CTBP1* siRNA attenuated precipitation of CtBP1 with *HMOX1*. 2-Deoxy-glucose (2-DG), pyruvate, and MTOB also suppressed binding of CtBP1 with *HMOX1* (n=3; **P*<0.05, ****P*<0.001 vs scrambled siRNA–treated PH-Fibs or untreated PH-Fibs).

glucose consumption and prevented the accumulation of glycolytic intermediates (glyceraldehyde 3-phosphate) and products (NADH/NAD^+ ratios [Figure 7B] and lactate [Figure 7A and 7D]). At day 4 of hypoxia, qPCR data demonstrated an 8-fold increase in the expression of the proproliferative gene *CDK1* (cyclin-dependent kinase 1), which was inhibited by MTOB treatment (Figure 8A). Immunostaining for Ki67 nuclear proliferation–associated antigen revealed that at 4 days of hypoxia, the number of proliferating lung cells was significantly increased and that MTOB treatment markedly decreased the number of proliferating cells (Figure 8B). These changes were especially prominent in the distal pulmonary vasculature and in lung parenchyma. Furthermore, qPCR analysis of the whole-lung tissue demonstrated that hypoxia promoted monocyte chemotactic protein-1 (*Mcp1/Ccl2*) mRNA expression and that MTOB treatment attenuated it (Figure 8C). Correspondingly, we demonstrated an influx of monocytes/macrophages (expressing the macrophage marker CD68) into pulmonary vascular adventitia of hypoxic hypertensive mice, and this proinflammatory response was markedly attenuated in distal pulmonary vasculature by MTOB treatment (Figure 8D). Last, to assess early pulmonary vascular remodeling (at day 4 of hypoxic exposure, before any significant deposition of collagen can be identified), we determined mRNA and protein expression of tenascin-C (TN-C), a matricellular protein with an expression that is sharply upregulated in tissues undergoing remodeling, neovascularization, inflammation, or tumorigenesis.[40] At day 4 of hypoxic exposure, TN-C mRNA expression in lung tissues was upregulated 4-fold compared with normoxic controls, and TN-C protein was prominent in distal pulmonary vasculature (Figure 8E and 8F). MTOB treatment attenuated TN-C expression at mRNA and protein levels (Figure 8E and 8F). We did not observe significant differences in CDK1, TN-C, and monocyte chemotactic protein-1 mRNA levels between untreated and MTOB- (1g/kg) treated normoxic mice (online-only Data Supplement Figure VIB). Hematoxylin and eosin staining and α-smooth muscle actin staining also showed perivascular inflammation and vascular remodeling, respectively, in hypoxic mice lung

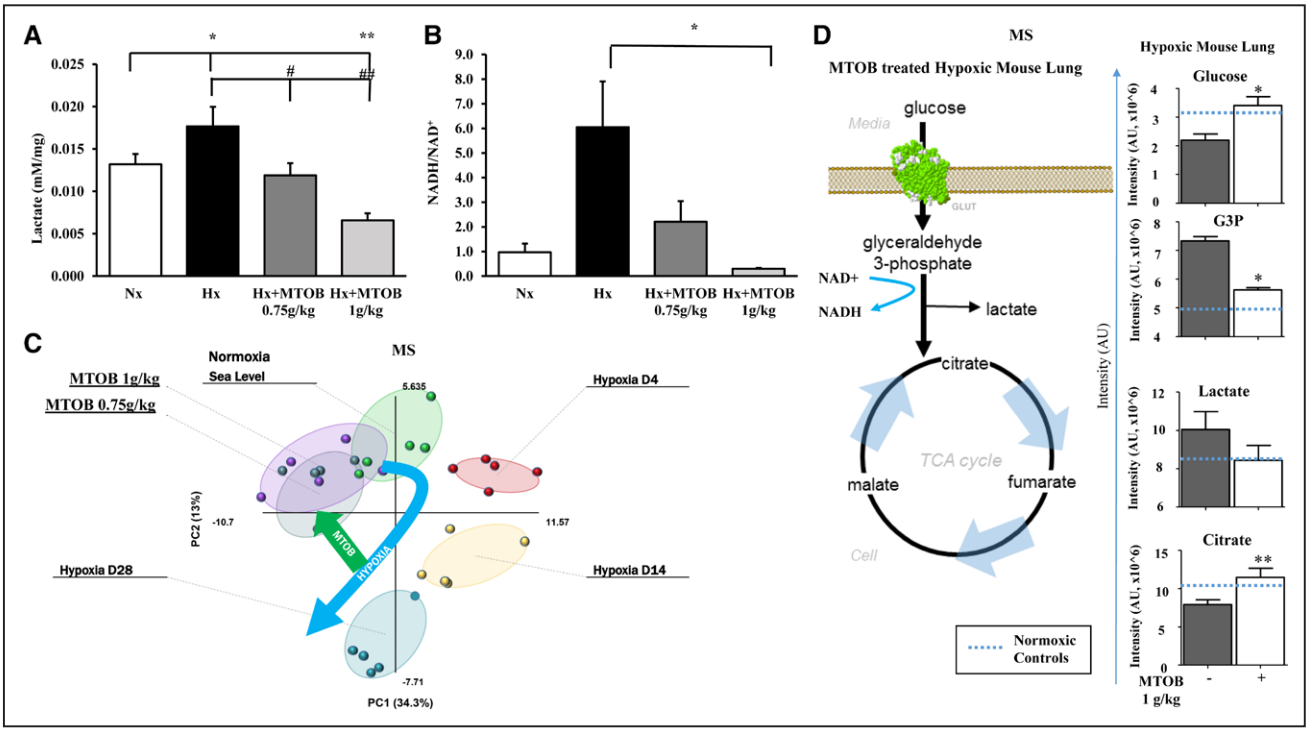

Figure 7. Hypoxia (Hx)-induced glycolysis reprogramming and increased NADH level in mouse lung tissue, and 4-methylthio-2-oxobutyric acid (MTOB) rescued the metabolic phenotype back to normoxic (Nx) controls.
A and **B**, Hypoxic exposure of mice (4 days) increased lactate production and the NADH/NAD+ ratio in whole-lung tissues compared with their normoxic controls. Animals were pretreated with MTOB for a week (3 times a week; intraperitoneal injection with 2 different doses: 0.75 or 1 g/kg) and received 2 more injections after being put into hypoxia chamber. MTOB decreased the lactate level and NADH/NAD+ ratio in hypoxia-exposed lungs (determined by enzymatic cycling reaction; n=3–5; **P*<0.05, ***P*<0.01 vs normoxic lungs; #*P*<0.05, ##*P*<0.01 vs hypoxic lungs). Mass spectrometry (MS) metabolomic analysis discovered that (**C**) the overall metabolic profile of mouse lung tissue becomes increasingly altered from its normoxic state as hypoxia exposure continues, yet MTOB was able to recover the metabolic state of lung tissue back to normoxic control levels (n=5 in each group) and that (**D**) MTOB decreased glucose consumption, glyceraldehyde-3-phosphate production, a substrate for GAPDH to generate NADH, and lactate production (n=5; **P*<0.05, ***P*<0.01 vs mouse whole-lung tissue not treated with MTOB).

tissue, and both were attenuated by MTOB treatment (online-only Data Supplement Figure VII).

Taken together, MTOB treatment of hypoxic hypertensive mice successfully attenuated pulmonary vascular cell proliferation, inflammation (as seen by the reduction in *Ccl2/Mcp1* expression and decreased recruitment of CD68-expressing macrophages), and vascular remodeling (TN-C, α-smooth muscle actin, and hematoxylin and eosin staining).

DISCUSSION

In the present study, we have demonstrated that in the pathogenesis of PH, adventitial fibroblasts undergo metabolic reprogramming with increased aerobic glycolysis relative to oxidative phosphorylation. Our findings expand on our previous observations of anomalous mitochondrial metabolism in PH and highlight the critical function of metabolic adaptations in supporting fibroblast proliferation and inflammatory activation.[28] We have also demonstrated increased expression of CtBP1 in the lungs of hypoxia-induced experimental PH in the cow and mouse model and in patients with IPAH patients and linked that expression to disease pathogenesis. It is important to note that we identified CtBP1, a transcriptional corepressor that is activated by increased free NADH secondary to glycolytic reprogramming, as a molecular link and potential therapeutic target to correct the aberrant metabolic, hyperproliferative, and inflammatory phenotype of bovine and human PH-Fibs in vitro and in hypoxic mice in vivo. Our study thus supports the novel hypothesis that chronic hypoxic PH and seemingly IPAH or familial pulmonary arterial hypertension lead to the rewiring of cellular metabolic programs that use alterations in the cellular redox state (ie, available NADH) to control activity of CtBP1 and thus coordinate expression of a network of genes implicated in cell proliferation, apoptosis resistance, and inflammation (Figure 8G).

PH pathology often involves an imbalance of cell proliferation versus cell death; thus, the hypothesis has been put forth that the cellular and molecular features seen in PH resemble hallmark characteristics described

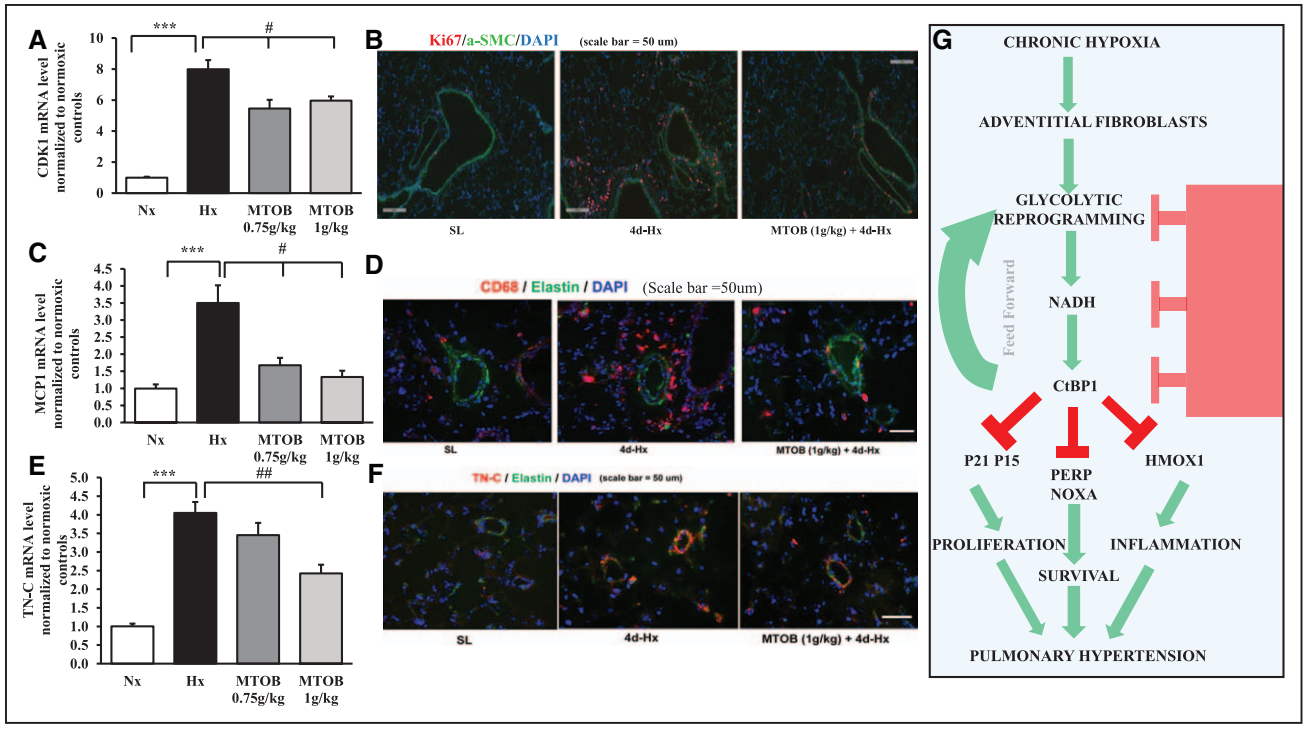

Figure 8. Hypoxia (Hx) exposure induced and 4-methylthio-2-oxobutyric acid (MTOB) treatment inhibited proliferation, inflammation, and vascular remodeling in mouse lung.

A, A 4-day hypoxia exposure significantly increased cyclin-dependent kinase 1 (CDK1) mRNA expression in mouse whole-lung tissues compared with their normoxic (Nx) controls. MTOB treatment significantly decreased CDK1 levels. **B**, Ki67 immunofluorescent staining (red, ki67; green, α-smooth muscle cell; blue, DAPI; scale bar=50 μm) demonstrated that hypoxia increased and MTOB decreased cell proliferation in mouse lung tissue. **C**, A 4-day hypoxia exposure significantly increased monocyte chemotactic protein-1 (MCP1) mRNA expression in mouse whole-lung tissues compared with their normoxic controls, and MTOB treatment significantly decreased the MCP1 level. **D**, Consistent with quantitative polymerase chain reaction data for MCP1, staining of the monocyte/macrophage marker CD68 showed that hypoxia increased and MTOB decreased the recruitment of monocytes/macrophage (red, CD68; green, elastin; blue, DAPI; scale bar=50 μm). **E**, A 4-day hypoxia exposure significantly increased tenascin-C (TN-C), an extracellular matrix marker, mRNA expression in mouse whole-lung tissues compared with their normoxic controls, and MTOB treatment significantly decreased the TN-C level. **F**, Accordingly, TN-C staining demonstrated that MTOB attenuated vascular remodeling induced by hypoxia exposure (red, TN-C; green, elastin; blue, DAPI; scale bar=50 μm; n=5; ***P<0.001 vs normoxic controls; #P<0.05, ##P<0.01 vs hypoxic mouse lungs). **G**, CtBP1 links metabolic changes to gene expression and contributes to the development of pulmonary hypertension. Pulmonary artery adventitial fibroblast cells isolated from chronic hypoxia-induced pulmonary hypertensive cow model and patients with pulmonary hypertension (PH-Fibs) and maintained under normoxic conditions demonstrated a perpetuated proinflammatory and hyperproliferative phenotype, as well as a metabolic reprogramming toward aerobic glycolysis and subsequently increased NADH levels. The transcriptional corepressor activity of CtBP1 is stimulated as a result of elevated NADH level. CtBP1 then enhances cell proliferation via transcriptional repression of the cell cycle inhibitors *P21* and *P15* and promotes cell survival through repression of proapoptotic genes (*NOXA* and *PERP*). CtBP1 also induces inflammation through the repression of the anti-inflammatory gene *HMOX1*. Reducing NADHs level by 2-deoxy-glucose (2DG) or pyruvate can inhibit proliferation in PH-Fibs and augment the anti-inflammatory phenotype of PH-Fibs. Targeting CtBP1 at the RNA level via siRNA or at the protein level by MTOB not only can inhibit proliferation and augment the anti-inflammatory phenotype of PH-Fibs but also can rescue cell metabolic state.

for cancer.[11,12,41] Changes in metabolism have emerged as key contributors to cancer pathophysiology and inflammation and thus have become emerging targets for novel diagnostic and therapeutic approaches that may have relevance to PH.[11,41,42] Our study provides strong evidence that in vivo and in vitro aerobic glycolysis is a metabolic adaptation in pulmonary artery adventitial fibroblasts in the setting of chronic hypoxia and in IPAH. Metabolic data here suggest that, akin to Warburg metabolism in cancer cells and inflammatory macrophages, incomplete glucose oxidation provides PH-Fibs with building blocks to support anabolic reactions (amino acid anabolism, fatty acid synthesis, urea cycle, gluconeogenesis) necessary to sustain proliferation and inflammatory activation, counteract oxidative stress, and promote resistance to apoptosis.

Unlike other transcriptional corepressors, CtBP1 is uniquely structured to sense increases in free NADH

Table 2. Genes From RNA-Seq Data Showing Significant Changes in Bovine PH-Fibs Compared With CO-Fibs

Gene Name	Ensembl Identification	Gene Description	Fold Change	*P* Value*
PFKFB 3	ENSBTAG00000008401	6-Phosphofructo-2-kinase/fructose-2,6-biphosphatase 3	6	1.25E–05
PGM5	ENSBTAG00000033190	Phosphoglucomutase-like protein 5	3.9	2.16E–06
GLUT1/SLC2A1	ENSBTAG00000009617	Solute carrier family 2, facilitated glucose transporter member 1	2.4	7.03E–03
HK1	ENSBTAG00000012380	Hexokinase 1	2.6	4.21E–03
PFKM	ENSBTAG00000000286	6-Phosphofructokinase, muscle type	2.1	2.30E–05
GPI	ENSBTAG00000006396	Glucose-6-phosphate isomerase	1.6†	2.10E–03
PFKFB 4	ENSBTAG00000006752	6-Phosphofructo-2-kinase/ fructose-2,6-biphosphatase 4	1.5†	1.32E–03
PGM1	ENSBTAG00000019011	Phosphoglycerate mutase 1	1.4†	6.40E–03
PGM2	ENSBTAG00000005773	Phosphoglycerate mutase 2	1.3†	8.04E–03
ID1	ENSBTAG00000016169	DNA-binding protein inhibitor ID-1	–5.78	9.35E–04
ID2	ENSBTAG00000021187	DNA-binding protein inhibitor ID-2	–4.25	4.92E–04
SIRT4	ENSBTAG00000021168	NAD-dependent protein deacetylase sirtuin-4	–1.3†	4.80E–03
RGS5	ENSBTAG00000016341	Regulator of G-protein signaling 5	551.37	1.56E–04

CO-Fibs indicates control fibroblasts; PH-Fibs, pulmonary hypertension fibroblasts; and RNA-Seq, RNA sequencing.

*The presented *P* values have a q value <0.1 (false discovery rate).

†These genes are related to the function of C-terminal binding protein 1, the phenotype of fibroblast cells, or are also important genes involved in glycolysis, even with a fold change of <2.

concentrations that typically occur secondary to glycolytic reprogramming.[22,23] Studies by our group and others have demonstrated that changes in the cellular reducing environment alter the interaction of CtBP1 with DNA-binding transcriptional repressors.[23,29,43,44] As a foe of multiple tumor suppressors, CtBP1 also provides a link between transcriptional regulation and the metabolic status of the cell.[15] In line with the hypothesis that free NADH concentrations increased CtBP activity, treatment of PH-Fibs with 2-DG or pyruvate to interfere with aerobic glycolysis or promote NADH oxidation to NAD^+ in PH-Fibs, respectively, was associated with attenuation of activity of CtBP1. Decreased CtBP1 activity translated to reduced PH-Fib proliferation and attenuated inflammatory activation, normalization of aberrant metabolic phenotypes, and increased expression of anti-inflammatory *HMOX1*. In PH-Fibs (both bovine and human), this increase in CtBP1 activity was maintained in the absence of a hypoxic stimulus, indicating that, akin to what has been described in cancer cells, stable rewiring or reprogramming of metabolism occurs in PH-Fibs and drives activity of transcriptional repressors such as CtBP1. It is striking that knockdown of *CTBP1* by siRNA or inhibition of CtBP1 dehydrogenase activity by MTOB treatment attenuated the proliferation of PH-Fibs (Figure 5A). Similar to cancer cells, inhibition of CtBP1 increased expression of cyclin-dependent kinase inhibitors (p15 and p21) and proapoptotic genes (*NOXA* and *PERP*).[18,23]

Our findings of an important role for CtBP1-mediated change in cell phenotype in PH are consistent with previous findings in PH. It was recently reported that hypoxia, a paramount stimulus for the development of PH, suppresses the expression of inhibitor of differentiation 1, a downstream target of the bone morphogenetic protein receptor type II pathway, in human pulmonary artery smooth muscle cells.[45] Hypoxia-induced changes in the $NADH/NAD^+$ ratio and histone deacetylases upregulated transcriptional corepressor CtBP-1 activity and subsequently attenuated bone morphogenetic protein signaling.[45] As a result of the near-universal association between metabolic reprogramming and an activated cell phenotype in both cancer and PH, there has been great interest in identifying factors that might link these changes. CtBPs have emerged as candidates in this regard. It is important to note that we also observed significantly reduced levels of inhibitor of differentiation 1 and 2 in PH-Fibs with high CtBP1 expression (Table 2). These findings are furthermore consistent with the proposed role of CtBPs in tumor genesis and tumor progression as we observed similar CtBP1 targets, including p15, p21, *NOXA*, and *PERP*.[15,18,24]

Inflammation is critically involved in the pathogenesis of PH, although how this is related to or regulated by metabolic reprogramming is unclear.[41] Because of its prominent role in the pathogenesis of PH, we focused attention on the anti-inflammatory gene *HMOX1* and demonstrat-

ed that inhibition of aerobic glycolysis was associated with robust increases in *HMOX1* expression. The results showed that *HMOX1* is a direct target of CtBP1, which has not previously been reported. Heme oxygenase (HO) catalyzes the oxidation of heme to carbon monoxide and biliverdin, which is then converted to bilirubin by biliverdin reductase.[46] Carbon monoxide released by HO-1 confers protection against vasoconstriction and vascular remodeling induced by hypoxia in vitro.[47,48] Studies using an HO-1–null mouse model suggest that HO-1 plays a central role in protecting the right ventricle from hypoxic pulmonary pressure–induced injury.[49] In contrast, transgenic mice with constitutive, lung-specific overexpression of HO-1 do not manifest the early inflammatory changes and are protected against PH on continued exposure to hypoxia,[32] suggesting that increasing HO-1 can serve as a prevention or therapeutic intervention for PH. In all, our findings suggest that it is possible that targeting CtBP1 has the potential to convert proinflammatory activation to an anti-inflammatory phenotype and thus to suppress inflammation and vascular remodeling, as was observed in our MTOB-treated hypoxic mice.

Until recently, CtBP1 had been implicated in responding to the metabolic status of the cell rather than regulating the cellular metabolic pathways.[18,50] It is interesting to note that a recent study demonstrated that CtBP promotes glutaminolysis in cancer cells by directly decreasing SIRT4 gene expression, a mitochondrial repressor of glutamate dehydrogenase and thus glutaminolysis. Therefore, increased CtBP levels in cancer cells repress SIRT4, which in turn leads to an increase in glutamine supply that promotes ammonia production to neutralize the acidification associated with increased glycolytic fluxes.[51] Because glycolytic rate drops as pH falls, the role of CtBP1 in preventing intracellular acidification sustains glycolysis and, in turn, cancer cell growth. RNA-Seq and metabolomic analysis from our study are consistent with these findings, showing higher level of glutamate dehydrogenase (P=0.02, FDR) together with significantly decreased SIRT4 level (Table 2) in PH-Fibs with concomitant increases in the expression and activation of CtBP1. Consistently, inhibition of CtBP1 by siRNA or MTOB corrected the metabolic phenotype of PH-Fibs and mouse lung tissue (Figures 5C–5F, 7C, and 7C). In particular, MTOB treatment prevented the accumulation of glycolytic reprogramming induced by prolonged exposure to hypoxia in mouse lungs (Figure 7C). Indeed, although prolonged hypoxia promoted increases in glycolysis in mice lungs, MTOB treatment resulted in normoxic-like levels of glyceraldehyde 3-phosphate, lactate, and NADH/NAD^+ ratios (Figure 7). Thus, similar to cancer, the proliferation-promoting function of CtBP1 in PH-Fibs requires its involvement in metabolic control. We have previously reported that the PH-Fibs described in this study fail to exhibit high expression levels of α-smooth muscle actin and Col1 and in fact continue to express markers of mesenchymal progenitors such as RGS5 (Table 2). CtBP1 could thus be an essential regulator to support self-renewal and expansion, particularly in hypoxic environments as might be observed at the medial-adventitial border of inflamed vessels. Of note, metabolic reprogramming toward aerobic glycolysis was observed in PH-Fibs cultured under normoxia, suggesting that whether hypoxia represents a key trigger to promote metabolic reprogramming and CtBP1 activation, hypoxia-independent perpetuation of the metabolic reprogramming-CtBP1 activity axis results in a feed-forward mechanism that can be disrupted by pharmacological or genetic ablation of either component of the axis in vitro and in vivo.

Last, our ex-vivo data demonstrate that targeting CtBP1 at the RNA level via siRNA or at the activity level by MTOB or reducing NADH level by 2-DG or pyruvate can inhibit the proliferative and augment the anti-inflammatory phenotype of PH-Fibs. These results provide evidence that small molecules such as MTOB or NSC9539 (a CDC25 inhibitor that inhibits the CtBP1-adenovirus E1A protein interaction) that demonstrate anticancer properties may be used as tools to treat hypoxia-induced PH.[52,53] As a first step in examining this hypothesis, we treated mice made hypoxic with MTOB (at present a prohibitively expensive drug). We found that MTOB successfully attenuated vascular remodeling (cell proliferation, glycolytic and overall metabolic reprogramming, macrophage accumulation, and extracellular matrix production) induced by hypoxia. Thus, it is tempting to speculate that in certain forms or stages of PH, including hypoxia (group 3), targeting the transcriptional repressor CtBP1, which links changes in metabolism to an activated cell phenotype, may have beneficial effects.

ACKNOWLEDGMENTS

The authors dedicate this work to the memory of their colleague, Dr QingHong Zhang, an inquisitive scientist and joyful spirit who initiated their work with CtBP1 but who passed away before the publication of this article. Dr Zhang leaves behind an excellent body of scholarship focusing on the role of CtBP1 in the cancer field. The authors are deeply saddened by her loss. The authors are thankful to Marcia McGowan for her outstanding help in preparing the manuscript, Dr Dale Brown and Andy Poczobutt for coordinating the calf studies, and Alma Islas-Trejo for making the libraries for RNA-Seq.

SOURCES OF FUNDING

This manuscript was supported by National Institutes of Health grants NIH HL084923, HL014985, and HL114887; Department of Defense grant W81XWH-15-1-0280; KONTAKT grants LH 11055 and LH 15071; and John E. Rouse Endowment for Animal Breeding Research, Colorado State University.

DISCLOSURES

None.

AFFILIATIONS

From Cardiovascular Pulmonary Research Laboratories, Department of Pediatrics and Medicine, University of Colorado Anschutz Medical Campus, Aurora, CO (M.L., S.R., H.Z., A.F., B.A.M., M.F., S.K., M.A.F., K.R.S.); Department of Biochemistry and Molecular Genetics and Biological Mass Spectrometry Shared Resource (A.D., K.C.H.), Department of Anesthesiology (N.J.S.), Advanced Light Microscopy Core Facility (R.M.), Department of Dermatology (H.L., H.L., Q.Z.), and Department of Pediatrics, Division of Gastroenterology, Hepatology, and Nutrition (K.C.E.K.), University of Colorado, Denver; Department of Mitochondrial Physiology, Institute of Physiology, Czech Academy of Sciences, Prague, Czech Republic (L.P.-H., P.J.); Department of Lung Development and Remodeling, Max-Planck-Institute for Heart and Lung Research, Bad Nauheim, Germany (D.I., S.P.); Center for Genetic Improvement of Livestock, Department of Animal Bioscience, University of Guelph, Guelph, ON, Canada (A.C.); Department of Animal Science, University of California-Davis, Davis (J.F.M.); and Department of Animal Science, Colorado State University, Fort Collins (M.G.T.).

FOOTNOTES

Received February 25, 2016; accepted August 12, 2016.

The online-only Data Supplement is available with this article at http://circ.ahajournals.org/lookup/suppl/doi:10.1161/CIRCULATIONAHA.116.023171/-/DC1.

Circulation is available at http://circ.ahajournals.org.

REFERENCES

1. Simonneau G, Gatzoulis MA, Adatia I, Celermajer D, Denton C, Ghofrani A, Gomez Sanchez MA, Krishna Kumar R, Landzberg M, Machado RF, Olschewski H, Robbins IM, Souza R. Updated clinical classification of pulmonary hypertension. *J Am Coll Cardiol*. 2013;62(suppl):D34–D41. doi: 10.1016/j.jacc.2013.10.029.
2. Price LC, Wort SJ, Perros F, Dorfmüller P, Huertas A, Montani D, Cohen-Kaminsky S, Humbert M. Inflammation in pulmonary arterial hypertension. *Chest*. 2012;141:210–221. doi: 10.1378/chest.11-0793.
3. Stenmark KR, Meyrick B, Galie N, Mooi WJ, McMurtry IF. Animal models of pulmonary arterial hypertension: the hope for etiological discovery and pharmacological cure. *Am J Physiol Lung Cell Mol Physiol*. 2009;297:L1013–L1032. doi: 10.1152/ajplung.00217.2009.
4. Das M, Burns N, Wilson SJ, Zawada WM, Stenmark KR. Hypoxia exposure induces the emergence of fibroblasts lacking replication repressor signals of PKCzeta in the pulmonary artery adventitia. *Cardiovasc Res*. 2008;78:440–448. doi: 10.1093/cvr/cvn014.
5. El Kasmi KC, Pugliese SC, Riddle SR, Poth JM, Anderson AL, Frid MG, Li M, Pullamsetti SS, Savai R, Nagel MA, Fini MA, Graham BB, Tuder RM, Friedman JE, Eltzschig HK, Sokol RJ, Stenmark KR. Adventitial fibroblasts induce a distinct proinflammatory/profibrotic macrophage phenotype in pulmonary hypertension. *J Immunol*. 2014;193:597–609. doi: 10.4049/jimmunol.1303048.
6. Krick S, Hänze J, Eul B, Savai R, Seay U, Grimminger F, Lohmeyer J, Klepetko W, Seeger W, Rose F. Hypoxia-driven proliferation of human pulmonary artery fibroblasts: cross-talk between HIF-1alpha and an autocrine angiotensin system. *FASEB J*. 2005;19:857–859. doi: 10.1096/fj.04-2890fje.
7. Li M, Riddle SR, Frid MG, El Kasmi KC, McKinsey TA, Sokol RJ, Strassheim D, Meyrick B, Yeager ME, Flockton AR, McKeon BA, Lemon DD, Horn TR, Anwar A, Barajas C, Stenmark KR. Emergence of fibroblasts with a proinflammatory epigenetically altered phenotype in severe hypoxic pulmonary hypertension. *J Immunol*. 2011;187:2711–2722. doi: 10.4049/jimmunol.1100479.
8. Panzhinskiy E, Zawada WM, Stenmark KR, Das M. Hypoxia induces unique proliferative response in adventitial fibroblasts by activating PDGFβ receptor-JNK1 signalling. *Cardiovasc Res*. 2012;95:356–365. doi: 10.1093/cvr/cvs194.
9. Wang D, Zhang H, Li M, Frid MG, Flockton AR, McKeon BA, Yeager ME, Fini MA, Morrell NW, Pullamsetti SS, Velegala S, Seeger W, McKinsey TA, Sucharov CC, Stenmark KR. MicroRNA-124 controls the proliferative, migratory, and inflammatory phenotype of pulmonary vascular fibroblasts. *Circ Res*. 2014;114:67–78. doi: 10.1161/CIRCRESAHA.114.301633.
10. Guignabert C, Tu L, Le Hiress M, Ricard N, Sattler C, Seferian A, Huertas A, Humbert M, Montani D. Pathogenesis of pulmonary arterial hypertension: lessons from cancer. *Eur Respir Rev*. 2013;22:543–551. doi: 10.1183/09059180.00007513.
11. Hanahan D, Weinberg RA. Hallmarks of cancer: the next generation. *Cell*. 2011;144:646–674. doi: 10.1016/j.cell.2011.02.013.
12. Paulin R, Michelakis ED. The metabolic theory of pulmonary arterial hypertension. *Circ Res*. 2014;115:148–164. doi: 10.1161/CIRCRESAHA.115.301130.
13. Vander Heiden MG, Cantley LC, Thompson CB. Understanding the Warburg effect: the metabolic requirements of cell proliferation. *Science*. 2009;324:1029–1033. doi: 10.1126/science.1160809.
14. Zhao L, Ashek A, Wang L, Fang W, Dabral S, Dubois O, Cupitt J, Pullamsetti SS, Cotroneo E, Jones H, Tomasi G, Nguyen QD, Aboagye EO, El-Bahrawy MA, Barnes G, Howard LS, Gibbs JS, Gsell W, He JG, Wilkins MR. Heterogeneity in lung (18)FDG uptake in pulmonary arterial hypertension: potential of dynamic (18)FDG positron emission tomography with kinetic analysis as a bridging biomarker for pulmonary vascular remodeling targeted treatments. *Circulation*. 2013;128:1214–1224. doi: 10.1161/CIRCULATIONAHA.113.004136.
15. Chinnadurai G. The transcriptional corepressor CtBP: a foe of multiple tumor suppressors. *Cancer Res*. 2009;69:731–734. doi: 10.1158/0008-5472.CAN-08-3349.
16. Peña C, García JM, García V, Silva J, Domínguez G, Rodríguez R, Maximiano C, García de Herreros A, Muñoz A, Bonilla F. The expression levels of the transcriptional regulators p300 and CtBP modulate the correlations between SNAIL, ZEB1, E-cadherin and vitamin D receptor in human colon carcinomas. *Int J Cancer*. 2006;119:2098–2104. doi: 10.1002/ijc.22083.
17. Wang R, Asangani IA, Chakravarthi BV, Ateeq B, Lonigro RJ, Cao Q, Mani RS, Camacho DF, McGregor N, Schumann TE, Jing X, Menawat R, Tomlins SA, Zheng H, Otte AP, Mehra R, Siddiqui J, Dhanasekaran SM, Nyati MK, Pienta KJ, Palanisamy N, Kunju LP, Rubin MA, Chinnaiyan AM, Varambally S. Role of transcriptional corepressor CtBP1 in prostate cancer progression. *Neoplasia*. 2012;14:905–914.
18. Di LJ, Byun JS, Wong MM, Wakano C, Taylor T, Bilke S, Baek S, Hunter K, Yang H, Lee M, Zvosec C, Khramtsova G, Cheng F, Perou CM, Miller CR, Raab R, Olopade OI, Gardner K. Genome-wide profiles of CtBP link metabolism with genome stability and epithelial reprogramming in breast cancer. *Nat Commun*. 2013;4:1449. doi: 10.1038/ncomms2438.
19. Grooteclaes M, Deveraux Q, Hildebrand J, Zhang Q, Goodman RH, Frisch SM. C-terminal-binding protein corepresses epithelial and proapoptotic gene expression programs. *Proc Natl Acad Sci USA*. 2003;100:4568–4573. doi: 10.1073/pnas.0830998100.

20. Zhang G, Yan Y, Kang L, Cao Q, Ke K, Wu X, Gao Y, Hang Q, Li C, Zhu L, Yuan Q, Wu Q, Cheng C. Involvement of CtBP2 in LPS-induced microglial activation. *J Mol Histol*. 2012;43:327–334. doi: 10.1007/s10735-012-9399-x.
21. Byun JS, Gardner K. C-terminal binding protein: a molecular link between metabolic imbalance and epigenetic regulation in breast cancer. *Int J Cell Biol*. 2013;2013:647975. doi: 10.1155/2013/647975.
22. Fjeld CC, Birdsong WT, Goodman RH. Differential binding of NAD+ and NADH allows the transcriptional corepressor carboxyl-terminal binding protein to serve as a metabolic sensor. *Proc Natl Acad Sci USA*. 2003;100:9202–9207. doi: 10.1073/pnas.1633591100.
23. Zhang Q, Piston DW, Goodman RH. Regulation of corepressor function by nuclear NADH. *Science*. 2002;295:1895–1897. doi: 10.1126/science.1069300.
24. Straza MW, Paliwal S, Kovi RC, Rajeshkumar B, Trenh P, Parker D, Whalen GF, Lyle S, Schiffer CA, Grossman SR. Therapeutic targeting of C-terminal binding protein in human cancer. *Cell Cycle*. 2010;9:3740–3750. doi: 10.4161/cc.9.18.12936.
25. NCBI, Genomes & Maps, Genome. http://www.ncbi.nlm.nih.gov/genome/?term=bos+taurus. Accessed September 20, 2016.
26. Williamson DH, Lund P, Krebs HA. The redox state of free nicotinamide-adenine dinucleotide in the cytoplasm and mitochondria of rat liver. *Biochem J*. 1967;103:514–527.
27. GraphPad, Software, Inc. GraphPad Software. www.graphpad.com. Accessed September 20, 2016.
28. Plecitá-Hlavatá L, Tauber J, Li M, Zhang H, Flockton AR, Pullamsetti SS, Chelladurai P, D'Alessandro A, El Kasmi KC, Ježek P, Stenmark KR. Constitutive reprogramming of fibroblast mitochondrial metabolism in pulmonary hypertension. *Am J Respir Cell Mol Biol*. 2016;55:47–57. doi: 10.1165/rcmb.2015-0142OC.
29. Zhang Q, Yoshimatsu Y, Hildebrand J, Frisch SM, Goodman RH. Homeodomain interacting protein kinase 2 promotes apoptosis by downregulating the transcriptional corepressor CtBP. *Cell*. 2003;115:177–186.
30. Kelly B, O'Neill LA. Metabolic reprogramming in macrophages and dendritic cells in innate immunity. *Cell Res*. 2015;25:771–784. doi: 10.1038/cr.2015.68.
31. Stenmark KR, Tuder RM, El Kasmi KC. Metabolic reprogramming and inflammation act in concert to control vascular remodeling in hypoxic pulmonary hypertension. *J Appl Physiol (1985)*. 2015;119:1164–1172. doi: 10.1152/japplphysiol.00283.2015.
32. Minamino T, Christou H, Hsieh CM, Liu Y, Dhawan V, Abraham NG, Perrella MA, Mitsialis SA, Kourembanas S. Targeted expression of heme oxygenase-1 prevents the pulmonary inflammatory and vascular responses to hypoxia. *Proc Natl Acad Sci USA*. 2001;98:8798–8803. doi: 10.1073/pnas.161272598.
33. Palsson-McDermott EM, O'Neill LA. The Warburg effect then and now: from cancer to inflammatory diseases. *Bioessays*. 2013;35:965–973. doi: 10.1002/bies.201300084.
34. Palsson-McDermott EM, Curtis AM, Goel G, Lauterbach MA, Sheedy FJ, Gleeson LE, van den Bosch MW, Quinn SR, Domingo-Fernandez R, Johnston DG, Jiang JK, Jiang JK, Israelsen WJ, Keane J, Thomas C, Clish C, Vander Heiden M, Vanden Heiden M, Xavier RJ, O'Neill LA. Pyruvate kinase M2 regulates Hif-1α activity and IL-1β induction and is a critical determinant of the warburg effect in LPS-activated macrophages. *Cell Metab*. 2015;21:65–80. doi: 10.1016/j.cmet.2014.12.005.
35. Belhaj A, Dewachter L, Kerbaul F, Brimioulle S, Dewachter C, Naeije R, Rondelet B. Heme oxygenase-1 and inflammation in experimental right ventricular failure on prolonged overcirculation-induced pulmonary hypertension. *PLoS One*. 2013;8:e69470. doi: 10.1371/journal.pone.0069470.
36. Constantin M, Choi AJ, Cloonan SM, Ryter SW. Therapeutic potential of heme oxygenase-1/carbon monoxide in lung disease. *Int J Hypertens*. 2012;2012:859235. doi: 10.1155/2012/859235.
37. Liang OD, Mitsialis SA, Chang MS, Vergadi E, Lee C, Aslam M, Fernandez-Gonzalez A, Liu X, Baveja R, Kourembanas S. Mesenchymal stromal cells expressing heme oxygenase-1 reverse pulmonary hypertension. *Stem Cells*. 2011;29:99–107. doi: 10.1002/stem.548.
38. Vergadi E, Chang MS, Lee C, Liang OD, Liu X, Fernandez-Gonzalez A, Mitsialis SA, Kourembanas S. Early macrophage recruitment and alternative activation are critical for the later development of hypoxia-induced pulmonary hypertension. *Circulation*. 2011;123:1986–1995. doi: 10.1161/CIRCULATIONAHA.110.978627.
39. Paddenberg R, Stieger P, von Lilien AL, Faulhammer P, Goldenberg A, Tillmanns HH, Kummer W, Braun-Dullaeus RC. Rapamycin attenuates hypoxia-induced pulmonary vascular remodeling and right ventricular hypertrophy in mice. *Respir Res*. 2007;8:15. doi: 10.1186/1465-9921-8-15.
40. Hsia HC, Schwarzbauer JE. Meet the tenascins: multifunctional and mysterious. *J Biol Chem*. 2005;280:26641–26644. doi: 10.1074/jbc.R500005200.
41. Tuder RM, Archer SL, Dorfmüller P, Erzurum SC, Guignabert C, Michelakis E, Rabinovitch M, Schermuly R, Stenmark KR, Morrell NW. Relevant issues in the pathology and pathobiology of pulmonary hypertension. *J Am Coll Cardiol*. 2013;62(suppl):D4–12. doi: 10.1016/j.jacc.2013.10.025.
42. Tennant DA, Durán RV, Gottlieb E. Targeting metabolic transformation for cancer therapy. *Nat Rev Cancer*. 2010;10:267–277. doi: 10.1038/nrc2817.
43. Kim JH, Cho EJ, Kim ST, Youn HD. CtBP represses p300-mediated transcriptional activation by direct association with its bromodomain. *Nat Struct Mol Biol*. 2005;12:423–428. doi: 10.1038/nsmb924.
44. Mirnezami AH, Campbell SJ, Darley M, Primrose JN, Johnson PW, Blaydes JP. Hdm2 recruits a hypoxia-sensitive corepressor to negatively regulate p53-dependent transcription. *Curr Biol*. 2003;13:1234–1239.
45. Wu X, Chang MS, Mitsialis SA, Kourembanas S. Hypoxia regulates bone morphogenetic protein signaling through C-terminal-binding protein 1. *Circ Res*. 2006;99:240–247. doi: 10.1161/01.RES.0000237021.65103.24.
46. Abraham NG, Levere RD, Lin JH, Beru N, Hermine O, Goldwasser E. Co-regulation of heme oxygenase and erythropoietin genes. *J Cell Biochem*. 1991;47:43–48. doi: 10.1002/jcb.240470106.
47. Morita T, Mitsialis SA, Koike H, Liu Y, Kourembanas S. Carbon monoxide controls the proliferation of hypoxic vascular smooth muscle cells. *J Biol Chem*. 1997;272:32804–32809.
48. Morita T, Perrella MA, Lee ME, Kourembanas S. Smooth muscle cell-derived carbon monoxide is a regulator of vascular cGMP. *Proc Natl Acad Sci USA*. 1995;92:1475–1479.
49. Yet SF, Perrella MA, Layne MD, Hsieh CM, Maemura K, Kobzik L, Wiesel P, Christou H, Kourembanas S, Lee ME. Hypoxia induces severe right ventricular dilatation and infarction in heme oxygenase-1 null mice. *J Clin Invest*. 1999;103:R23–R29. doi: 10.1172/JCI6163.
50. Di LJ, Fernandez AG, De Siervi A, Longo DL, Gardner K. Transcriptional regulation of BRCA1 expression by a metabolic switch. *Nat Struct Mol Biol*. 2010;17:1406–1413. doi: 10.1038/nsmb.1941.
51. Wang L, Zhou H, Wang Y, Cui G, Di LJ. CtBP maintains cancer cell growth and metabolic homeostasis via regulating SIRT4. *Cell Death Dis*. 2015;6:e1620. doi: 10.1038/cddis.2014.587.
52. Blevins MA, Kouznetsova J, Krueger AB, King R, Griner LM, Hu X, Southall N, Marugan JJ, Zhang Q, Ferrer M, Zhao R. Small molecule, NSC95397, inhibits the CtBP1-protein partner interaction and CtBP1-mediated transcriptional repression. *J Biomol Screen*. 2015;20:663–672. doi: 10.1177/1087057114561400.
53. Yang Y, Yang WS, Yu T, Yi YS, Park JG, Jeong D, Kim JH, Oh JS, Yoon K, Kim JH, Cho JY. Novel anti-inflammatory function of NSC95397 by the suppression of multiple kinases. *Biochem Pharmacol*. 2014;88:201–215. doi: 10.1016/j.bcp.2014.01.022.

Metabolic Reprogramming Regulates the Proliferative and Inflammatory Phenotype of Adventitial Fibroblasts in Pulmonary Hypertension Through the Transcriptional Corepressor C-Terminal Binding Protein-1

Min Li, Suzette Riddle, Hui Zhang, Angelo D'Alessandro, Amanda Flockton, Natalie J. Serkova, Kirk C. Hansen, Radu Moldvan, B. Alexandre McKeon, Maria Frid, Sushil Kumar, Hong Li, Hongbing Liu, Angela Caánovas, Juan F. Medrano, Milton G. Thomas, Dijana Iloska, Lydie Plecitá-Hlavatá, Petr Jezek, Soni Pullamsetti, Mehdi A. Fini, Karim C. El Kasmi, QingHong Zhang and Kurt R. Stenmark

Circulation. 2016;134:1105-1121; originally published online August 25, 2016;
doi: 10.1161/CIRCULATIONAHA.116.023171
Circulation is published by the American Heart Association, 7272 Greenville Avenue, Dallas, TX 75231

Print ISSN: 0009-7322. Online ISSN: 1524-4539

SUPPLEMENTAL MATERIAL

METHODS

Animals (Bovine and Mouse)

All animal procedures were performed in accordance with the Guidelines for Animal Experimentation established and approved by the University of Colorado Anschutz Medical Campus and Colorado State University.

The neonatal calf model of severe chronic hypoxia-induced pulmonary hypertension (PH) has been described previously [1, 2]. Briefly, one day-old male Holstein calves were exposed to hypobaric hypoxia (P_B=445mmHg) for 2 weeks, while age-matched controls were kept at ambient altitude (P_B=640 mmHg). Standard veterinary care was used following institutional guidelines at the Department of Physiology, School of Veterinary Medicine, Colorado State University (Fort Collins, CO). Animals were euthanized by overdose of sodium pentobarbital (160 mg/kg body weight).

The hypoxic mouse model of PH is well established in our laboratory [3, 4]. Briefly, 8 weeks old male wild-type B6 mice (C57B6, Jackson Laboratories, Maine, USA) were kept at simulated sea level altitude for one week with controlled temperature (22–24 °C) under a 12-hour-light–dark cycle. Food and water were accessible ad libitum. After one week, they were randomly separated into four groups: 1) sea level normoxia, 2) sea level normoxia + MTOB, 3) hypoxia, 4) hypoxia + MTOB. Hypoxic groups were placed in hypobaric hypoxic chambers (0.5 atm) with simulated altitude of 18,000ft and in a ventilated chamber for 4, 14, or 28 days. The chamber was flushed with a mixture of room air and nitrogen and was opened on the alternate day during health check and feeding. The gas was re-circulated. The hypoxic condition was monitored using an oxygen monitor. Control mice (normoxia) were kept at sea level altitude under the same

light–dark cycle [3, 4]. MTOB groups were pre-treated for one week at sea level (I.P injection, 3 times per week, either 0.75g/kg or 1g/kg. Sigma-Aldrich, Saint Louis, MO). After pre-treatment, they were kept in either sea level or hypoxic chamber for 4 days with continued MTOB treatment. The I.P injection of MTOB was proved to be safe for mice [5].

Human, Bovine, and Mouse Tissues

For laser-capture microdissection, human lung tissue specimens from subjects with IPAH (n =7) or donor controls (n = 8), obtained during lung transplantation, were used as previously described [6]. Cryosections from lung tissues were mounted on polyethylene membrane-coated glass slides and 150–200 vessels per patient were collected. After briefly staining with hemalaun, intrapulmonary vessels (<100μm) were microdissected from the sections with the use of the LMD6000 (Leica, Wetzlar, Germany) as described [6]. Total cellular RNA from vessels was isolated with the micro RNeasy kit (Qiagen, Valencia, CA). The cDNA was synthesized using BioRad iScript cDNA synthesis kit (BioRad Laboratories, Reinach, Germany). The study protocol for tissue donation was approved by the ethics committee (Ethik Kommission am Fachbereich Humanmedizin der Justus Liebig Universität Giessen) of the University Hospital Giessen (Giessen, Germany) in accordance with national law and with Good Clinical Practice/International Conference on Harmonization guidelines. Written informed consent was obtained from each individual patient or the patient's next of kin (AZ 31/93). All lungs were reviewed for pathology, and the IPAH lungs were classified as grade III or IV according to Heath and Yacoub.

Frozen sections of lung tissue from human subjects with idiopathic pulmonary arterial hypertension (IPAH) were used for immunohistochemical analysis of CtBP1 as previously

described [1, 7-9]. Lung tissue sections from calves and mice described above were obtained and used for immunohistochemical or immunofluorescent analyses as previously described [3, 10, 11].

Cell Culture

Isolation of adventitial fibroblasts from distal pulmonary arteries of hypertensive and control calves was performed as described previously [1, 9, 11]. Human pulmonary artery fibroblasts were derived from patients with idiopathic PH or from control donors undergoing lobectomy or pneumonectomy. Cells were cultured under normoxic conditions. Experiments were performed on cells at passages 5-10.

Immunostaining

Mouse monoclonal antibody against CtBP1 was purchased from BD Biosciences (San Jose, CA), and used at 1:100 dilution. Mouse monoclonal antibody against GLUT1 was purchased from Novus Biologicals (Littleton, CO) and used at 1:1,000 dilution. Rabbit monoclonal antibody against Ki67 was purchased from Thermo Scientific (Waltham, MA), and used at 1:200 dilution. Rabbit polyclonal antibody against tenascin C (TN-C) was purchased from EMD Millipore (Billerica, MA. Brand Family: Chemicon), and used at 1:100 dilution [10 12]. Mouse monoclonal antibody against macrophage marker CD68 was purchased from AbD Serotec (Raleigh, NC) and used at 1:200 dilution. Indirect immunofluorescent (IF) staining was performed on frozen 5 μm-thick lung tissue sections via a Biotin-Streptavidin detection system using Alexa-488 or -594 fluorochromes according to manufacturer's manual (Molecular Probes/Invitrogen, Frederick, MD). Stained sections were mounted with VectaShield embedding medium with DAPI (Vector Labs, Burlingame, CA), and examined under a Zeiss fluorescent microscope. Images were acquired using AxioVision digital imaging system.

Immunohistochemical (IHC) staining with CtBP1 antibodies was performed on formalin-fixed paraffin-embedded (FFPE) lung tissue sections using DAB detection system (Dako, Carpinteria, CA).

RNA Sequencing (RNA-Seq)

RNA from bovine CO-Fibs (n=6) and PH-Fibs (n=6) were used to perform RNA-Sequencing analysis. Total RNA was purified using Qiagen Mini Kit (Qiagen, Valencia, CA). Quality was evaluated using RNA Integrity Number (RIN) value from the Experion automated electrophoresis system (BioRad, Hercules, CA). The RIN values were near 10 in all the samples. mRNA was purified, fragmented, and converted to cDNA [13]. Adapters were ligated to the ends of double-stranded cDNA and PCR amplified to create libraries. Sequencing libraries were executed with the TruSeq RNA Sample Preparation kit (Illumina, San Diego, CA) [14]. RNA-sequencing was performed on a HiSeq 2000 sequencer analyzer. Sequence reads (100bp) were assembled to the annotated UMD3.1 bovine reference genome (http://www.ncbi.nlm.nih.gov/genome/?term=bos+taurus). Quality control analysis was performed using the CLC Genomics workbench software (CLC Bio, Aarhus, Denmark) [15, 16]. This tool assess sequence quality indicators based on the FastQC-project (http:// www.bioinformatics.babraham.ac.uk/projects/fastqc/). Quality was measured taking into account sequence-read lengths and base-coverage, nucleotide contributions and base ambiguities, quality scores as emitted by the base caller and over-represented sequences [14]. All the samples analyzed passed all the QC parameters, indicating a very good quality.

Data was normalized by calculating the 'reads per kilo base per million mapped reads' (RPKM) for each gene [17]. The statistical analysis was performed using the total exon reads as expression values by the empirical analysis of differential gene expression (EDGE) tool of CLC

Bio Genomic workbench software. This tool is based on the EdgeR Bioconductor package [18] and uses count data (i.e. total exon reads) for the statistical analysis. Genes were filtered based on minimum expression greater than 0.2 RPKM [19, 20]. False discovery rate (FDR) was used for multiple testing corrections. Finally, differentially expressed genes were selected based on fold-change (equal or higher to 2), P-value ($p<0.01$), and FDR value ($q<0.1$).

Western Blotting

The procedure was performed as previously described[1]. GLUT1-specific antibodies were purchased from Novus Biologicals (Littleton, CO) and used at 1: 200 dilution.

Real-Time RT-PCR

Total RNA from cultured cells was isolated using Qiagen Mini Kit (Qiagen, Valencia, CA). Total RNA from tissues was isolated with Trizol. First-strand cDNA synthesis and real-time RT-PCR were performed as described previously [11]. The sequences for all primers are listed in Suppl. Table 1. Results are presented as fold change using delta-delta Ct method.

Quantitative Multinuclear Magnetic Resonance (NMR) Metabolomics and steady-state ^{13}C-glucose uptake and metabolism

Fibroblasts were cultured in 150 mm tissue culture dishes until 90% confluent, and then were incubated with 10 mM of $^{13}C_1$-glucose (glucose with ^{13}C at C_1 position, Cambridge Isotope Laboratories, Tewksbury, MA) as the exclusive glucose source and otherwise under standard growth conditions for 24 hrs prior to perchloric acid extraction, as per a previously published extraction protocol [21, 22]. Cells from five plates were pooled per condition for fibroblasts.

After extractions, both hydrophilic and lipophilic extracts were lyophilized overnight and reconstituted in deuterated solvents for NMR analysis. Collected culture media were lyophilized as well for glucose uptake/lactate export analysis. High-resolution ^{1}H-, ^{31}P- and ^{13}C-NMR

experiments were performed using Bruker 400 MHz Avance III spectrometer (Bruker BioSpin, Fremont, CA) as described previously [22]. Trimethylsilyl propionic-2,2,3,3,-d4 acid (TSP) and diphosphoric acid (DPA) in sealed capillaries were used as external standards for metabolite quantification in ^{1}H- and ^{31}P-NMR, respectively. The $^{13}C_3$-lactate peak at 21 ppm was used as an internal reference (calculated from ^{1}H-NMR) for quantification of ^{13}C spectra. All spectra acquisition and metabolite integration was performed using Bruker TopSpin software. Intracellular ^{13}C-glucose and its ^{13}C-labeled products from glycolysis and the TCA cycle were calculated from ^{13}C-NMR spectra. All metabolite identification and multivariate partial least squares-discriminant analysis (PLS-DA) were performed using the Human Metabolome Data Base (HMDB). NMR data are normalized to cell mass.

Ultra-high Pressure Liquid Chromatography-Mass Spectrometry-Based direct NADH measurements and Metabolomics Analyses: steady-state and tracing experiments with U-^{13}C-glucose

Metabolomics analyses were performed as previously reported [23]. Briefly, CO and PH fibroblasts (n=3) were extracted in ice-cold lysis/extraction buffer (methanol:acetonitrile: water 5:3:2, 2x10^6 cells/ml buffer). After discarding protein pellets, water and methanol soluble fractions were run through a C18 reversed phase column (phase A: water, 0.1% formic acid; B: acetonitrile, 0.1% formic acid - Phenomenex, Torrance, CA) through an ultra-high performance chromatographic system (UHPLC - Ultimate 3000, Themo Fisher). UHPLC was coupled in line with a high resolution quadrupole Orbitrap instrument run in either polarity modes (QExactive, Thermo Fisher) at 70,000 resolution (at 200 m/z). Metabolite assignment and peak integration for relative quantitation were performed through the software Maven (Princeton), against the KEGG pathway database and an in-house validated standard library, including NADH (product

no. N8129 - SIGMA Aldrich, St Louis, MO; >650 compounds; IROATech). To determine linearity (r^2 >0.99 – Suppl Fig. 2C) and sensitivity of the approach (LOD and LOQ), NADH was weighed and progressively diluted (from 0.5 to 5000 injected pmol range – 4 orders of magnitude) before injection through UHPLC-MS. Integrated peak areas were exported into Excel (Microsoft, Redmond, CA) for statistical analysis (T-Test, ANOVA) through supervised partial least square-discriminant analysis with the software Multibase and MetaboAnalyst 3.0.

Alternatively, CO and PH fibroblasts were cultured in 60mm petri dish in duplicate (for experiment and cell counting) until 90% confluent, and then were incubated with 10 mM of U-^{13}C-glucose (glucose with all ^{13}C carbon atoms at positions 1 through 6, Cambridge Isotope Laboratories, Tewksbury, MA) as the exclusive glucose source and otherwise under standard growth conditions for 5 min, 1, 8 and 24 hrs. Extractions were performed as described above, by normalizing lysis buffer volume to cell counts at each time point ($2x10^6$ cell/ml of lysis buffer). Isotopologue distributions from U-^{13}C-glucose in tracing experiments were determined through the software Maven, as previously reported [23, 24].

Frozen mouse whole lung tissues were snap-frozen by liquid nitrogen as soon as they were isolated. The tissues were powdered in the presence of liquid nitrogen to make the tissue uniform. Some tissues were weighed in the presence of liquid nitrogen and dry ice in a cold room and lysis buffer (10mg tissue /ml buffer) was added. Samples were extracted at 4°C for 30min, centrifuged, and the supernatants were used for metabolomics analysis as described above.

Assessment of NADH/NAD$^+$ Ratio

NADH/NAD$^+$ ratio was determined using modified methods of DH Williamson *et al* [25] based on the enzymatic cycling reaction (Pyruvate + NADH + H^+ ↔ Lactate + NAD^+) and was performed as previously described [26]. Briefly, cells were cultured in 100 mm Petri dish in growth

medium to 80% confluence and all medium was replaced with fresh growth medium. After 24hrs, cells were washed with cold PBS and homogenized with 100 μl of cold acid-extraction buffer (1 M $HClO_3$) and then neutralized with 50 μl of cold 2 M $KHCO_3$. The pH of $HCLO_3$ and $KHCO_3$ mixture was 7.0. The absorbance of NADH at 340nM was measured before and after the enzymatic cycling reaction. The difference of NADH absorbance was used to determine the concentration of lactate or pyruvate. Standard curves for lactate and pyruvate concentration were generated for every set of experiments. The ratio of [lactate]: [pyruvate] was used to calculate the NADH:NAD^+ ratio according to the following equation: NADH: NAD^+ = K(lactate)/(pyruvate)(H^+), where K is the equilibrium constant for lactate dehydrogenase.

Frozen mouse whole lung tissues were snap-frozen by liquid nitrogen as soon as they were isolated. The tissues were powdered in the presence of liquid nitrogen to make the tissue uniform. Some tissues were weighed in the presence of liquid nitrogen and dry ice in a cold room, put in 1.5ml Eppendorf tubes and extracted with 200 μl of acid-extraction buffer (1 M $HClO_3$) and neutralized with 100 μl of 2 M $KHCO_3$ at the pH of 7.0. Samples were centrifuged and the supernatant were used for enzymatic cyclin reaction and the result were normalized by tissue mass.

Fluorescence Lifetime Imaging (FLIM)

FLIM of two-photon excited NADH was performed at the UCD Advanced Light Microscopy Core as previously described [27, 28] to directly visualize NADH level in cells. Measurements were carried out on a Zeiss LSM780 (Carl Zeiss, Jena, Germany) confocal microscope equipped with ISS Fast FLIM technology and a titanium:sapphire Chameleon Ultra II (Coherent, Santa Clara, CA). Briefly, the intrinsic NADH fluorescence was observed through a 40x water-immersion objective (Zeiss Korr C-Apochromat NA 1.2, Carl Zeiss, Jena, Germany)

for a monolayer cell culture. The NADH fluorescence was isolated using a 488nm long pass dichroic mirror (Semrock Di02-R488-25-D) and a bandpass filter with the spectral range 415nm-485nm (Semrock FF01-450/70-25) and detected with a Hamamatsu H7422p-40 photon-counting PMT connected to a ISS A320 FastFLIM box (ISS, Champaign, IL). Lifetime calibration was done using a 30nM fluorescein aqueous solution with a lifetime of 4 ns. Calibration and NADH imaging of the live cells were done using the same acquisition parameters. All FLIM images show pixels with free-NADH in red and pixels with bound NADH in green, defined by the red or green circles respectively on the phasor plot. The positioning of the red circle encloses the majority of the free-NADH signal. Even though the fluorescent properties of the nicotinamide ring of NADPH are identical to those of NADH [29], a recent study demonstrated that FLIM can separate free-NADH and NADPH fluorescence in live cells and tissues when they are bound to proteins [30]. Another important consideration is that the dissociation constant (Kd) of CtBP is much higher for NADH (1nM) than NADPH (10^4nM) [26], which indicate that the relative contribution of free NADPH to CtBP activation would have been minimal.

Inhibition of CtBP1

CtBP1 was inhibited genetically by siRNA or pharmaceutically by 4-Methylthio 2-oxobutyric acid (*MTOB*). Briefly, transfection assay was performed as follows: Fibroblast cells (at 60% confluency) were transfected with scrambled siRNA (control) or siCTBP1 (50 nM) using Lipofectamine 2000 (Invitrogen, Grand Island, NY) as previously described [31-33]. Transfection efficiencies were 75% and 82% for bovine and human cells respectively based on RT-PCR results (Suppl Fig. 1). CtBP transcriptional repression is dependent on active regulation by the dehydrogenase domain [34, 35]. MTOB is a substrate for CtBP dehydrogenase. At high

concentrations it may inhibit the dehydrogenase, impacting repression function [36]. It was also reported that MTOB can displace CtBP from the Bik promoter and induce Bik expression [5].

Cell Proliferation Assay

Equal numbers of cells were plated onto 24-well plates in full DMEM supplemented with 10% calf serum (CS, bovine cells) or with 10% fetal calf serum (FCS, human cells), and then treated with 2-deoxy-glucose (2-DG, 10 mM), pyruvate (20 mM), 4-Methylthio 2-oxobutyric acid (*MTOB*, 2.5 mM), CtBP1 siRNA (25 nM), scrambled siRNA, or left untreated. Cells in triplicate wells were counted on days 1, 2, and 3. In parallel, cells from each treatment type were collected for RT-PCR.

Chromatin Immunoprecipitation (ChIP) Assay

ChIP assay was used to study CtBP1 protein interaction with its target gene. Human fibroblast cells were cross-linked with ice cold 1% formaldehyde for 15min and the reaction quenched with addition of 0.125M glycine. Cells were scrapped off the plates, centrifuged and the pellets sonicated in lysis buffer to shear DNA. Fragmented DNA was precipitated with CtBP1 antibody (EMD Millipore, Billerica MA) using immobilized recombinant protein A affinity resins (RepliGen. Waltham, MA). Unbound DNA fragments were washed off and beads were removed with elution buffer. Precipitated protein/DNA complex were reverse cross-linked by adding 350mM NaCl and incubated for 6hrs at 65℃. DNA were then purified and used for PCR analysis.

Statistical Analysis

Prism software version 5 (GraphPad, Software, Inc, www.graphpad.com) was used for t-test or ANOVA followed by Bonferroni post-test analysis.

Values were expressed as mean ± SEM. For basic comparisons of two gaussian distributed sample sets, we used student t-tests. When comparing multiple groups, the respective ANOVA Analysis (one way when comparing one characteristic, or two way if two dependent variables where involved) was performed. P-values were subject to multiple testing adjustment using Bonferroni correction. Supervised partial least square-discriminant analysis (PLS-DA, Simca, Umetrics, San Jose, CA) were used to determine the variance of metabolic phenotypes in CO- and PH-Fibs, as determined via NMR and MS analyses and were sufficient to discriminate biological samples. To validate partial least square-discriminant analysis in MS, random permutations were performed through MetaboAnalyst and Multibase (20 random permutations were selected (significance threshold 0.05, <100 variables tested). False discovery rate (Benjamin Hochberg) was <0.1 for all significant metabolites. Power analysis was performed to make sure that the number of replicates was sufficient to ensure >80% probability to have a FDR<0.1 for all the significant observations (tested through MetaboAnalyst 3.0). Differences with *P* values less than 0.05 were considered statistically significant.

Supplemental References

1. Li M, Riddle SR, Frid MG, El Kasmi KC, McKinsey TA, Sokol RJ, Strassheim D, Meyrick B, Yeager ME, Flockton AR, McKeon BA, Lemon DD, Horn TR, Anwar A, Barajas C and Stenmark KR. Emergence of fibroblasts with a proinflammatory epigenetically altered phenotype in severe hypoxic pulmonary hypertension. *Journal of immunology*. 2011;187:2711-22.

2. Das M, Burns N, Wilson SJ, Zawada WM and Stenmark KR. Hypoxia exposure induces the emergence of fibroblasts lacking replication repressor signals of PKCzeta in the pulmonary artery adventitia. *Cardiovascular research*. 2008;78:440-8.

3. Brown RD, Ambler SK, Li M, Sullivan TM, Henry LN, Crossno JT, Jr., Long CS, Garrington TP and Stenmark KR. MAP kinase kinase kinase-2 (MEKK2) regulates hypertrophic remodeling of the right ventricle in hypoxia-induced pulmonary hypertension. *American journal of physiology Heart and circulatory physiology*. 2013;304:H269-81.

4. Clambey ET, McNamee EN, Westrich JA, Glover LE, Campbell EL, Jedlicka P, de Zoeten EF, Cambier JC, Stenmark KR, Colgan SP and Eltzschig HK. Hypoxia-inducible factor-1 alpha-dependent induction of FoxP3 drives regulatory T-cell abundance and function during inflammatory hypoxia of the mucosa. *Proceedings of the National Academy of Sciences of the United States of America*. 2012;109:E2784-93.

5. Straza MW, Paliwal S, Kovi RC, Rajeshkumar B, Trenh P, Parker D, Whalen GF, Lyle S, Schiffer CA and Grossman SR. Therapeutic targeting of C-terminal binding protein in human cancer. *Cell cycle*. 2010;9:3740-50.

6. Savai R, Al-Tamari HM, Sedding D, Kojonazarov B, Muecke C, Teske R, Capecchi MR, Weissmann N, Grimminger F, Seeger W, Schermuly RT and Pullamsetti SS. Pro-proliferative

and inflammatory signaling converge on FoxO1 transcription factor in pulmonary hypertension. *Nature medicine*. 2014;20:1289-300.

7. El Kasmi KC, Pugliese SC, Riddle SR, Poth JM, Anderson AL, Frid MG, Li M, Pullamsetti SS, Savai R, Nagel MA, Fini MA, Graham BB, Tuder RM, Friedman JE, Eltzschig HK, Sokol RJ and Stenmark KR. Adventitial fibroblasts induce a distinct proinflammatory/profibrotic macrophage phenotype in pulmonary hypertension. *Journal of immunology*. 2014;193:597-609.

8. Savai R, Pullamsetti SS, Kolbe J, Bieniek E, Voswinckel R, Fink L, Scheed A, Ritter C, Dahal BK, Vater A, Klussmann S, Ghofrani HA, Weissmann N, Klepetko W, Banat GA, Seeger W, Grimminger F and Schermuly RT. Immune and inflammatory cell involvement in the pathology of idiopathic pulmonary arterial hypertension. *American journal of respiratory and critical care medicine*. 2012;186:897-908.

9. Wang D, Zhang H, Li M, Frid MG, Flockton AR, McKeon BA, Yeager ME, Fini MA, Morrell NW, Pullamsetti SS, Velegala S, Seeger W, McKinsey TA, Sucharov CC and Stenmark KR. MicroRNA-124 controls the proliferative, migratory, and inflammatory phenotype of pulmonary vascular fibroblasts. *Circulation research*. 2014;114:67-78.

10. Frid MG, Brunetti JA, Burke DL, Carpenter TC, Davie NJ, Reeves JT, Roedersheimer MT, van Rooijen N and Stenmark KR. Hypoxia-induced pulmonary vascular remodeling requires recruitment of circulating mesenchymal precursors of a monocyte/macrophage lineage. *The American journal of pathology*. 2006;168:659-69.

11. Frid MG, Li M, Gnanasekharan M, Burke DL, Fragoso M, Strassheim D, Sylman JL and Stenmark KR. Sustained hypoxia leads to the emergence of cells with enhanced growth,

migratory, and promitogenic potentials within the distal pulmonary artery wall. *American journal of physiology Lung cellular and molecular physiology*. 2009;297:L1059-72.

12. Jones PL and Rabinovitch M. Tenascin-C is induced with progressive pulmonary vascular disease in rats and is functionally related to increased smooth muscle cell proliferation. *Circulation research*. 1996;79:1131-42.

13. Canovas A, Rincon G, Islas-Trejo A, Wickramasinghe S and Medrano JF. SNP discovery in the bovine milk transcriptome using RNA-Seq technology. *Mamm Genome*. 2010;21:592-8.

14. Canovas A, Reverter A, DeAtley KL, Ashley RL, Colgrave ML, Fortes MR, Islas-Trejo A, Lehnert S, Porto-Neto L, Rincon G, Silver GA, Snelling WM, Medrano JF and Thomas MG. Multi-tissue omics analyses reveal molecular regulatory networks for puberty in composite beef cattle. *PloS one*. 2014;9:e102551.

15. Canovas A, Rincon G, Islas-Trejo A, Jimenez-Flores R, Laubscher A and Medrano JF. RNA sequencing to study gene expression and single nucleotide polymorphism variation associated with citrate content in cow milk. *J Dairy Sci*. 2013;96:2637-48.

16. Canovas A, Rincon G, Bevilacqua C, Islas-Trejo A, Brenaut P, Hovey RC, Boutinaud M, Morgenthaler C, VanKlompenberg MK, Martin P and Medrano JF. Comparison of five different RNA sources to examine the lactating bovine mammary gland transcriptome using RNA-Sequencing. *Sci Rep*. 2014;4:5297.

17. Mortazavi A, Williams BA, McCue K, Schaeffer L and Wold B. Mapping and quantifying mammalian transcriptomes by RNA-Seq. *Nature methods*. 2008;5:621-8.

18. Robinson MD, McCarthy DJ and Smyth GK. edgeR: a Bioconductor package for differential expression analysis of digital gene expression data. *Bioinformatics*. 2010;26:139-40.

19. Wickramasinghe S, Canovas A, Rincon G and Medrano JF. RNA-sequencing: a tool to explore new frontiers in animal genetics. *Livestock Science*. 2014;166:206-216.

20. Wickramasinghe S, Rincon G, Islas-Trejo A and Medrano JF. Transcriptional profiling of bovine milk using RNA sequencing. *BMC genomics*. 2012;13:45.

21. Kominsky DJ, Klawitter J, Brown JL, Boros LG, Melo JV, Eckhardt SG and Serkova NJ. Abnormalities in glucose uptake and metabolism in imatinib-resistant human BCR-ABL-positive cells. *Clinical cancer research : an official journal of the American Association for Cancer Research*. 2009;15:3442-50.

22. Serkova NJ and Glunde K. Metabolomics of cancer. *Methods in molecular biology*. 2009;520:273-95.

23. D'Alessandro A, Nemkov T, Kelher M, West FB, Schwindt RK, Banerjee A, Moore EE, Silliman CC and Hansen KC. Routine storage of red blood cell (RBC) units in additive solution-3: a comprehensive investigation of the RBC metabolome. *Transfusion*. 2015;55:1155-68.

24. D'Alessandro A, Amelio I, Berkers CR, Antonov A, Vousden KH, Melino G and Zolla L. Metabolic effect of TAp63alpha: enhanced glycolysis and pentose phosphate pathway, resulting in increased antioxidant defense. *Oncotarget*. 2014;5:7722-33.

25. Williamson DH, Lund P and Krebs HA. The redox state of free nicotinamide-adenine dinucleotide in the cytoplasm and mitochondria of rat liver. *The Biochemical journal*. 1967;103:514-27.

26. Zhang Q, Piston DW and Goodman RH. Regulation of corepressor function by nuclear NADH. *Science*. 2002;295:1895-7.

27. Stringari C, Cinquin A, Cinquin O, Digman MA, Donovan PJ and Gratton E. Phasor approach to fluorescence lifetime microscopy distinguishes different metabolic states of germ

cells in a live tissue. *Proceedings of the National Academy of Sciences of the United States of America*. 2011;108:13582-7.

28. Stringari C, Nourse JL, Flanagan LA and Gratton E. Phasor fluorescence lifetime microscopy of free and protein-bound NADH reveals neural stem cell differentiation potential. *PloS one*. 2012;7:e48014.

29. De Ruyck J, Fameree M, Wouters J, Perpete E, Preat J and Jacquemin D. Towards the understanding of the absorption spectra of NAD(P)H/NAD(P)+ as a common indicator of dehydrogenase enzymatic activity. *Chemical Physics Letters*. 2007;450:119-122.

30. Blacker TS, Mann ZF, Gale JE, Ziegler M, Bain AJ, Szabadkai G and Duchen MR. Separating NADH and NADPH fluorescence in live cells and tissues using FLIM. *Nature communications*. 2014;5:3936.

31. Bergman LM, Birts CN, Darley M, Gabrielli B and Blaydes JP. CtBPs promote cell survival through the maintenance of mitotic fidelity. *Molecular and cellular biology*. 2009;29:4539-51.

32. Zhang Q, Wang SY, Fleuriel C, Leprince D, Rocheleau JV, Piston DW and Goodman RH. Metabolic regulation of SIRT1 transcription via a HIC1:CtBP corepressor complex. *Proceedings of the National Academy of Sciences of the United States of America*. 2007;104:829-33.

33. Zhang Q, Yoshimatsu Y, Hildebrand J, Frisch SM and Goodman RH. Homeodomain interacting protein kinase 2 promotes apoptosis by downregulating the transcriptional corepressor CtBP. *Cell*. 2003;115:177-86.

34. Balasubramanian P, Zhao LJ and Chinnadurai G. Nicotinamide adenine dinucleotide stimulates oligomerization, interaction with adenovirus E1A and an intrinsic dehydrogenase activity of CtBP. *FEBS letters*. 2003;537:157-60.

35. Kumar V, Carlson JE, Ohgi KA, Edwards TA, Rose DW, Escalante CR, Rosenfeld MG and Aggarwal AK. Transcription corepressor CtBP is an NAD(+)-regulated dehydrogenase. *Molecular cell*. 2002;10:857-69.

36. Achouri Y, Noel G and Van Schaftingen E. 2-Keto-4-methylthiobutyrate, an intermediate in the methionine salvage pathway, is a good substrate for CtBP1. *Biochemical and biophysical research communications*. 2007;352:903-6.

Supplemental Figure Legend:

Supplemental Figure 1: CtBP1 siRNA successfully decreased *CTBP1* mRNA level in adventitial fibroblast cells.

Bovine and human pulmonary artery adventitial fibroblast cells from both control (CO-Fibs) and hypoxic-induced hypertensive groups (PH-Fibs) were transfected with *CTBP1* siRNA (siCtBP1: 50nM) or scrambled RNA (SCR) when they were 60% confluent for 72hrs and cells were collected, CtBP1 mRNA levels were determined by qPCR. siRNA significantly inhibited CtBP1 level by 75% and 82% for bovine and human cells respectively (Ux=untreated, n=3. *, $P<0.05$; **, $P < 0.01$, ***, $P < 0.001$, compared to scrambled cells within each group)

Supplemental Figure 2. Aerobic glycolysis and its correlated metabolites are among the top metabolism pathway and top metabolites in PH-Fibs detected through RNA sequencing (RNA-Seq), mass spectrometry (MS) and Nuclear magnetic resonance (NMR).

(A) Most significant pathways identified by RNA-Seq (*Bonferroni analysis of Gene Ontology in* Blast2GO of PH-Fibs compared to CO-Fibs with stringency of RPKM $p<0.01$, fold change > 2), correlate with aerobic glycolysis reprograming in PH-Fibs. More detailed information presented in Table 1. Steady-state experiments were performed via nuclear magnetic resonance (NMR) and Ultra-High Pressure Liquid Chromatography-Mass Spectrometry (UHPLC-MS) by incubating bovine CO and PH-Fibs either with $^{13}C_1$ or U-^{13}C-glucose, respectively. (B) Top metabolites analyzed by MS analysis ($p<0.05$, fold change > 2 in PH-Fibs compared to CO-Fibs, n=3) are indicative of aerobic glycolysis reprograming in PH-Fibs. The important metabolites correlated with aerobic glycolysis are highlighted in red. (C) Variable Importance in Projection (VIP) scores (from NMR data) identify increased glycolytic metabolites (highlighted in red) and processes as key for separation of PH-Fibs from CO-Fibs by PLS-DA. Phospholipid metabolism,

consistent with rapidly dividing cells, and hydroxybutyrate, a metabolite associated with altered redox status also differentiate the populations ($P< 0.05$, n=4).

Supplemental Figure 3. Nuclear magnetic resonance (NMR) and mass spectrometry (MS) analysis confirm PH-Fibs have different overall metabolic profile compared to CO-Fibs and PH-Fibs exhibit aerobic glycolysis.

(A, B)Statistical elaborations, Partial Least Square Discriminant Analysis (PLS-DA, from NMR: n=4 and MS: n=3) indicate that PH-Fibs (green) can be clearly differentiated from CO-Fibs (pink) by metabolic analysis. (C) Carbon tracing strategy of NMR analysis shows different isotopes of carbon in the cellular fractions. Open circle: ^{12}C, red circle: ^{13}C, pink circle: ^{13}C, but the quantity is too low for NMR detection. The flow chart shows the pathway of glucose metabolism: glucose is metabolized to pyruvate and either enters the TCA cycle or is converted to lactate by glycolysis, or converted into alanine. Glucose entering glycolysis (or glycolytic signature) is determined by carbon tracing and calculated by the sum of ^{13}C-Glucose-6-PO_4, ^{13}C-Fructose-6-PO_4, ^{13}C-lactate and ^{13}C-alanine. Glucose entering the TCA cycle is calculated by the sum of ^{13}C-Glutamate and ^{13}C-Glutamine generated via pyruvate dehydrogenase and pyruvate carboxylase. $^{13}C_1$-glucose loses ^{13}C at position 1 and enters pentose phosphate pathway. LDH-Lactate dehydrogenase; Glu-Glutamate; Gln-Glutamine; ALT-Alanine transaminase; PDH-Pyruvate dehydrogenase; PC-Pyruvate carboxylase; OAA-Oxaloacetate; a-KG- alpha ketoglutarate; PPP-pentose phosphate pathway. (D) As demonstrated by ^{13}C-glucose incubation NMR experiments, PH-Fibs (green) exhibit increases in intracellular glucose uptake, glucose consumption by glycolysis, and glucose entering glycolysis versus TCA cycle compared to CO-Fibs (pink) at steady state. (n=3, * $P < 0.05$, **, $P < 0.01$, compared to CO-Fibs)

Supplemental Figure 4. NADH/NAD$^+$ ratio measured by the Ultra-high Pressure Liquid Chromatography-Mass Spectrometry (UHPLC-MS) and enzymatic cycling reaction method showed an increased ratio in bovine and human PH-Fibs compared to CO-Fibs and 2-deoxy-glucose (2DG) decreased the NADH/NAD$^+$ ratio in PH-Fibs.

(A) Linearity of the NADH detection down to a LOQ of 500 fmol injected, over four orders of magnitude, was performed through a targeted UHPLC-MS method in order to measure NADH directly. (B) Mass spectrometry-based analysis showed significant increased NADH/NAD$^+$ in bovine PH-Fibs compared to CO-Fibs (n=3, *, $P < 0.05$, compared to CO-Fibs, NS, non-statistic significant). (C) Both bovine and human PH-Fibs have a significantly higher NADH/NAD$^+$ ratio (as indicated by the ratio of [lactate]/[pyruvate]) compared to CO-Fibs. (n=3-5. *, $P<0.05$; **, $P < 0.01$, compared to CO-Fibs). (D) 2DG decreased the NADH/NAD$^+$ ratio, as extrapolated from the ratio of lactate to pyruvate concentration. (n=3. ***, $P < 0.001$, compared to untreated PH-Fibs).

Supplement Figure 5. Bovine and human PH-Fibs, as well as vessels from IPAH patients exhibited decreased expression of pro-proliferative and anti-apoptotic genes

qPCR analysis showed decreased expression of pro-proliferative (p21, p15) and anti-apoptotic (NOXA, PERP) genes in bovine and human PH-Fibs as well as vessels isolated from IPAH patients. (n=3-8, *, $P <0.05$; **, $P <0.01$, compared to PH-Fibs or IPAH vessels)

Supplement Figure 6. mRNA expression profile for normoxic and hypoxic mouse whole lung tissue.

(A)Genes involved in proliferation (CDK1), vascular remodeling (tenascin C, TN-C), and inflammation (MCP1, SDF1, HMOX1, IL6, IL1β) were analyzed by qPCR in normoxia (Nx) and hypoxia exposed (Hx, day 4, 14 and 28) mouse whole lung tissue and revealed that most

genes peaked at day 4 hypoxia. (n=5, *, P <0.05; **, P <0.01; ***, P <0.001, compared to normoxic lungs). (B) MTOB has no significant effect on CDK1, TN-C and MCP1 mRNA expression in normoxic mice lungs (n=5).

Supplement Figure 7. MTOB attenuates perivascular inflammation and vascular remodeling in the hypoxic mouse lung at 4 days.

(A) Hematoxylin and Eosin (H&E) staining demonstrates initiation of vascular inflammation at 4 days of hypoxia. MTOB treatment attenuates this response. (B) alpha-smooth muscle actin (α-SMA) expression is increased in distal vessels at 4 days of hypoxia. This response is mitigated in MTOB-treated animals. (SL: sea level; 4d-Hx: hypoxia, 4 days; Scale bars: H&E, 500μm and α-SMA, 200μm; α-SMA: red color; DAPI: blue color).

Supplemental Table 1. Bovine, human and mouse primer sequences for real-time RT-PCR		
Bovine Gene	**Forward 5'-3'**	**Reverse 5'-3'**
HPRT	CTGGCTCGAGATGTGATGAA	CAACAGGTCGGCAAAGAACT
CTBP1	CGAGCACAACCACCACCTCATC	TGTTCACCAGGAAAGCCCCTTG
GLUT1	GCTCATGGGCTTCTCAAAAC	CACGTACATGGGCACAAAAC
HEXOKINASE 2 (HK2)	CGGAGCTCAACCACGACCAA	TGGTGGCTCCAAGCCCTTTC
LDHA	GGTACCACTGCCCATGTTGC	TTGGACTAGGCACCTTGGCT
HMOX1	CCCTCAGCACTCACCCCTTCC	TGGCTACATCTTCTGGGCTCTGC
p21	TGGGTGTTACGAAGTCCTGC	GGCCCCCTTCAAAGTGCTAT
p15/CDKN2B	AGTTCGCCACCCCAACTTA	CTTCGCTGCCGGGAATCTA
NOXA	GGTTGCATCCCTGAGTTGCC	CGCTCTTACGAGCCCTCCTT
PERP	CTGCCGCTGCTACTGCTTA	ATACGTCATGAGGCTGTCGC
Human Gene	**Forward 5'-3'**	**Reverse 5'-3'**
18S	GAATTCCCAGTAAGTGCGGG	GGGCAGGGACTTAATCAACG
CTBP1	GGACCTGCTCTTCCACAGCGACT	CCTTGTCTCATCTGCTTGACGGTGA
GLUT1	TGCCACCATTGGCTCCGGTA	AGCAGTGCTAGCGCGATGGT
HEXOKINASE 2 (HK2)	CCTTCCCTGAACCTTTTCCA	TGCTAGACACCAGACTCCAA
LDHA	AGCTGTTCCACTTAAGGCCC	AATGAGATCCGGAATCGGCG
HMOX1	AGAGGGGGCGAAGGGGTCAG	GGGCTTTTGGAGGTTTGAGACAGC
p21	AGCAGCTGCCGAAGTCAGTT	ACATGGCGCCTCCTCTGAGT
p15/CDKN2B	ACTAGTGGAGAAGGTGCGAC	ATCATCATGACCTGGATCGC
NOXA	GCTGGAAGTCGAGTGTGCTA	GGAGTCCCCTCATGCAAGTT
PERP	TTGCAACCCCATCAGTCGAT	ACTGCACACTGTATCCAGGC
Mouse Gene	**Forward 5'-3'**	**Reverse 5'-3'**
HPRT	TGGGCTTACCTCACTGCTTT	CTAATCACGACGCTGGGACT
CDK1	AAGTGTGGCCAGAAGTCGAG	TCGTCCAGGTTCTTGACGTG
MCP1	CACCAGCACCAGCCAACTCT	ATGCTCCAGCCGGCAACTGT
SDF1	ATCGGTGGCTGCGAGCTGAA	ACATGCCTGGGATGCTGCGT
IL6	CCGGAGAGGAGACTTCACAG	TCCACGATTTCCCAGAGAAC
HMOX1	CCTCACAGATGGCGTCACTT	GCTGATCTGGGGTTTCCCTC

Supplemental Figure 1

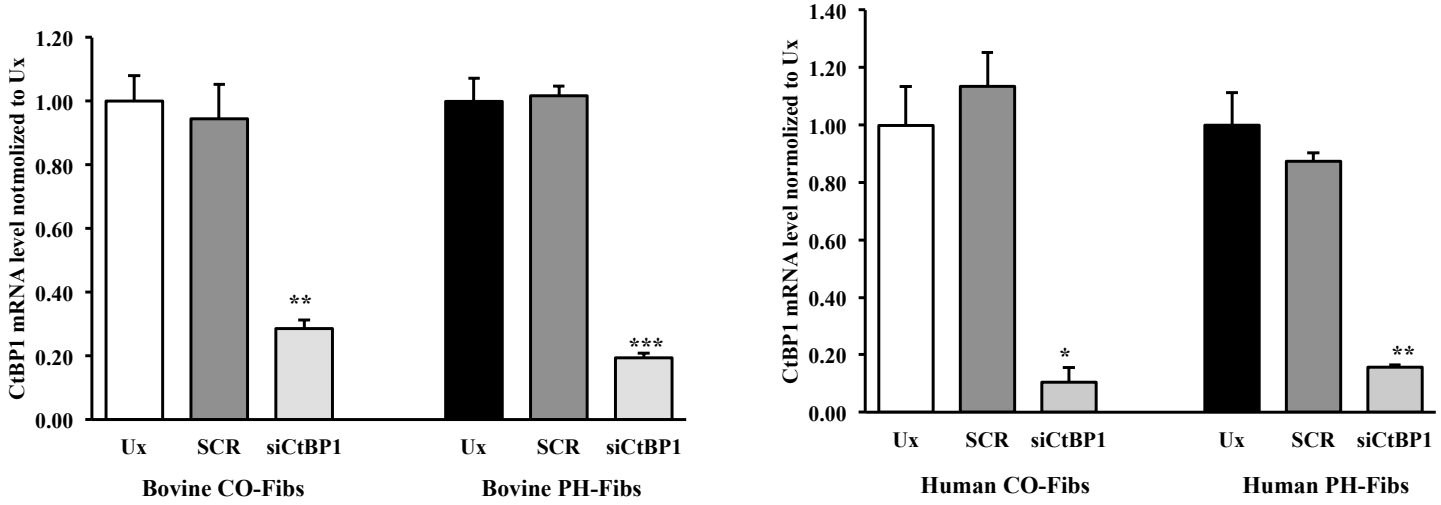

Supplemental Figure 2

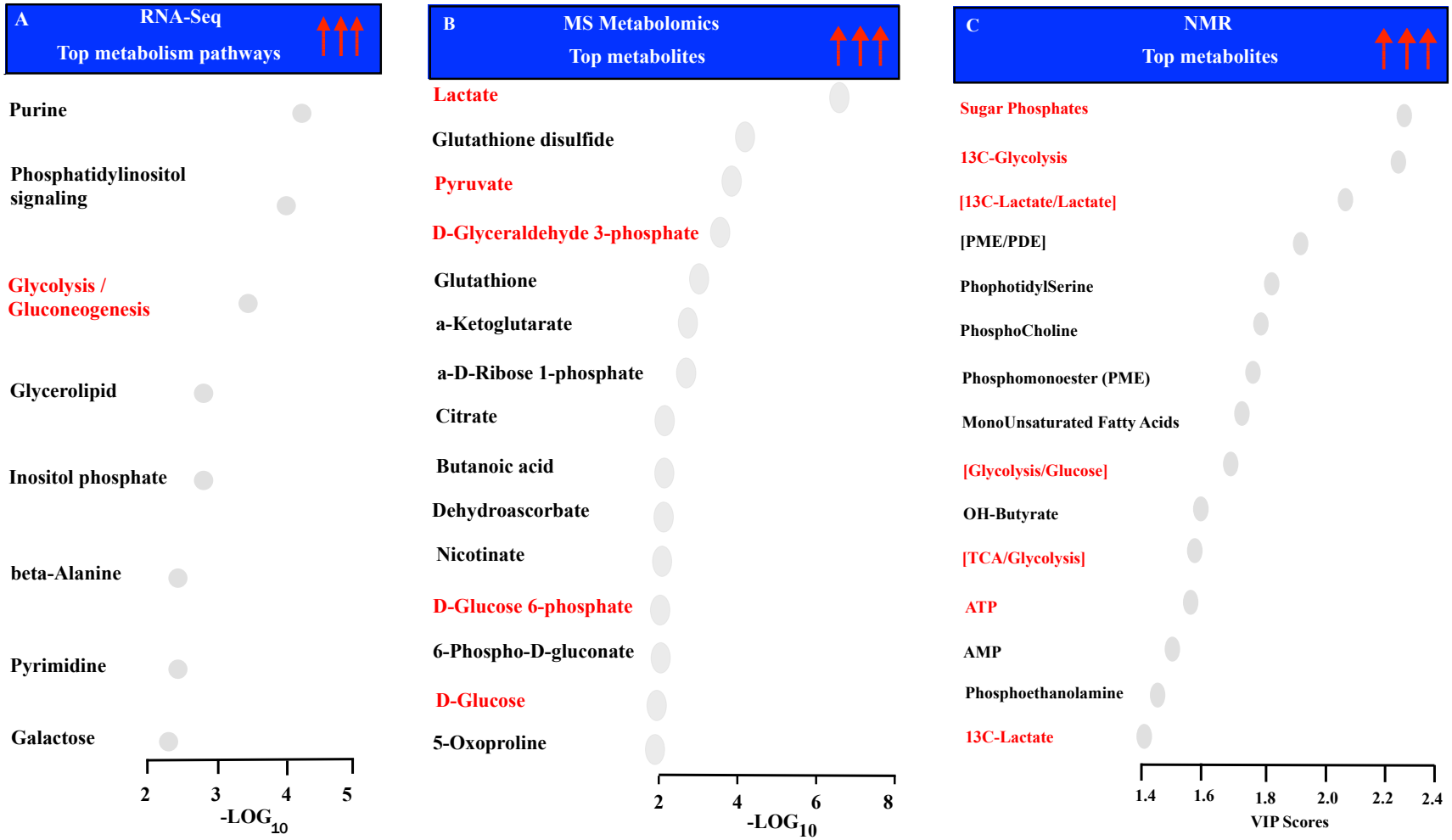

Supplemental Figure 3

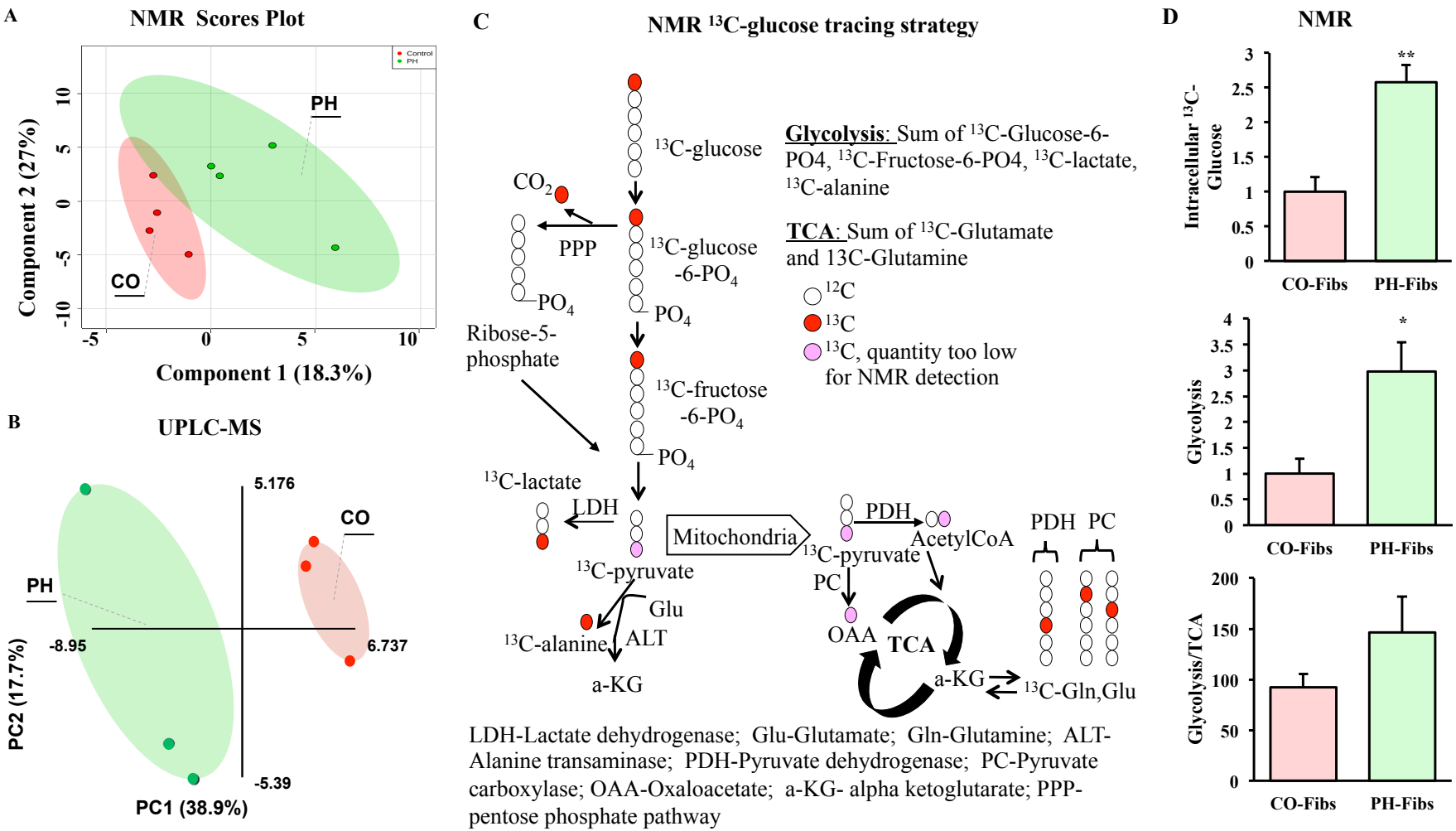

Supplemental Figure 4

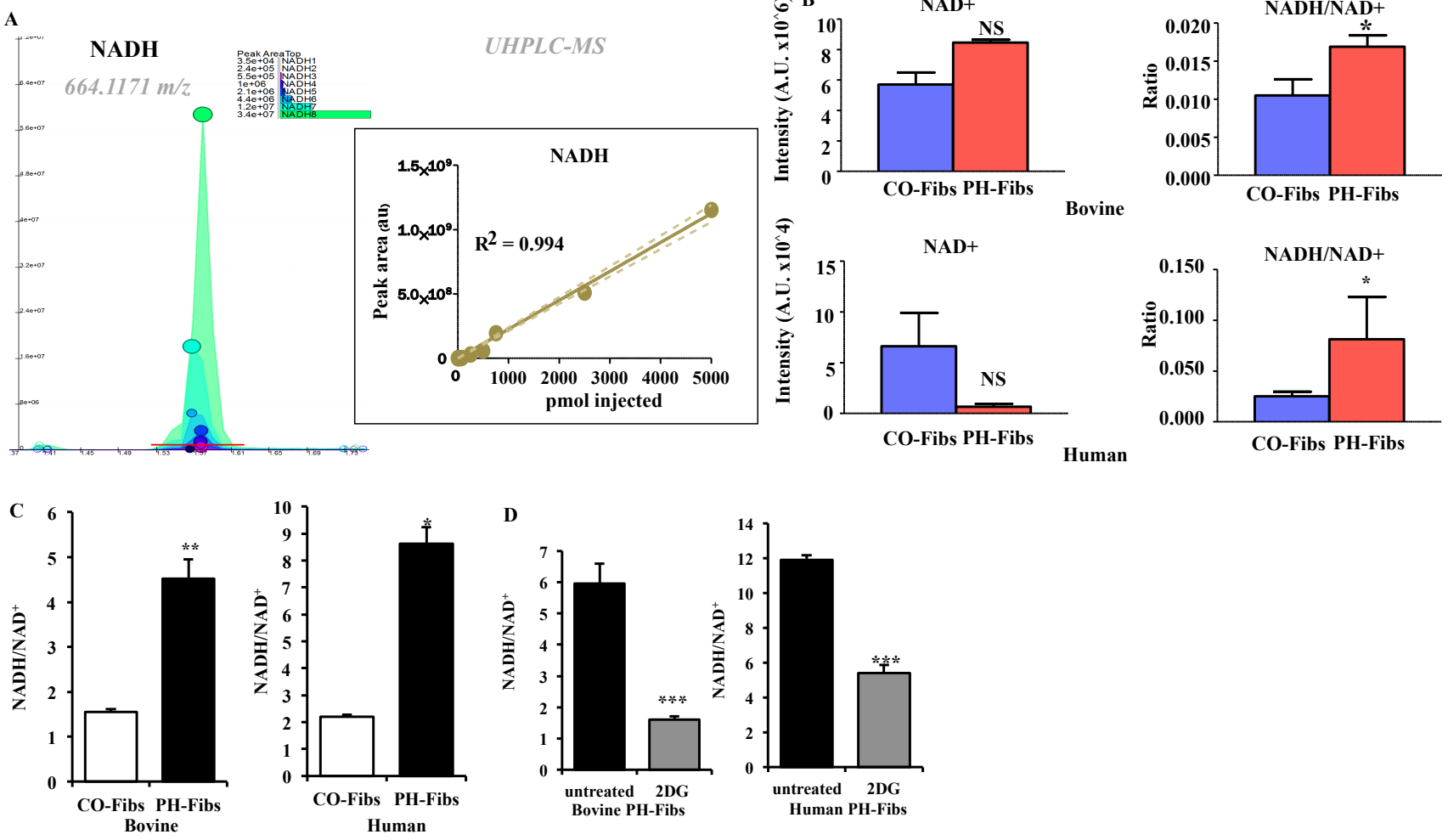

Supplemental Figure 5

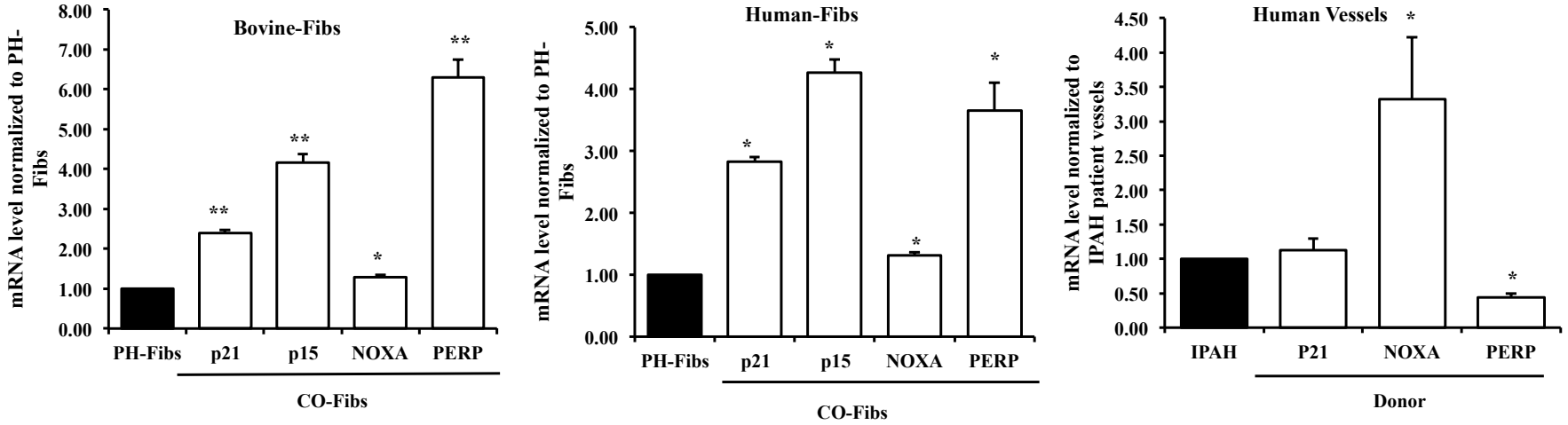

Supplemental Figure 6

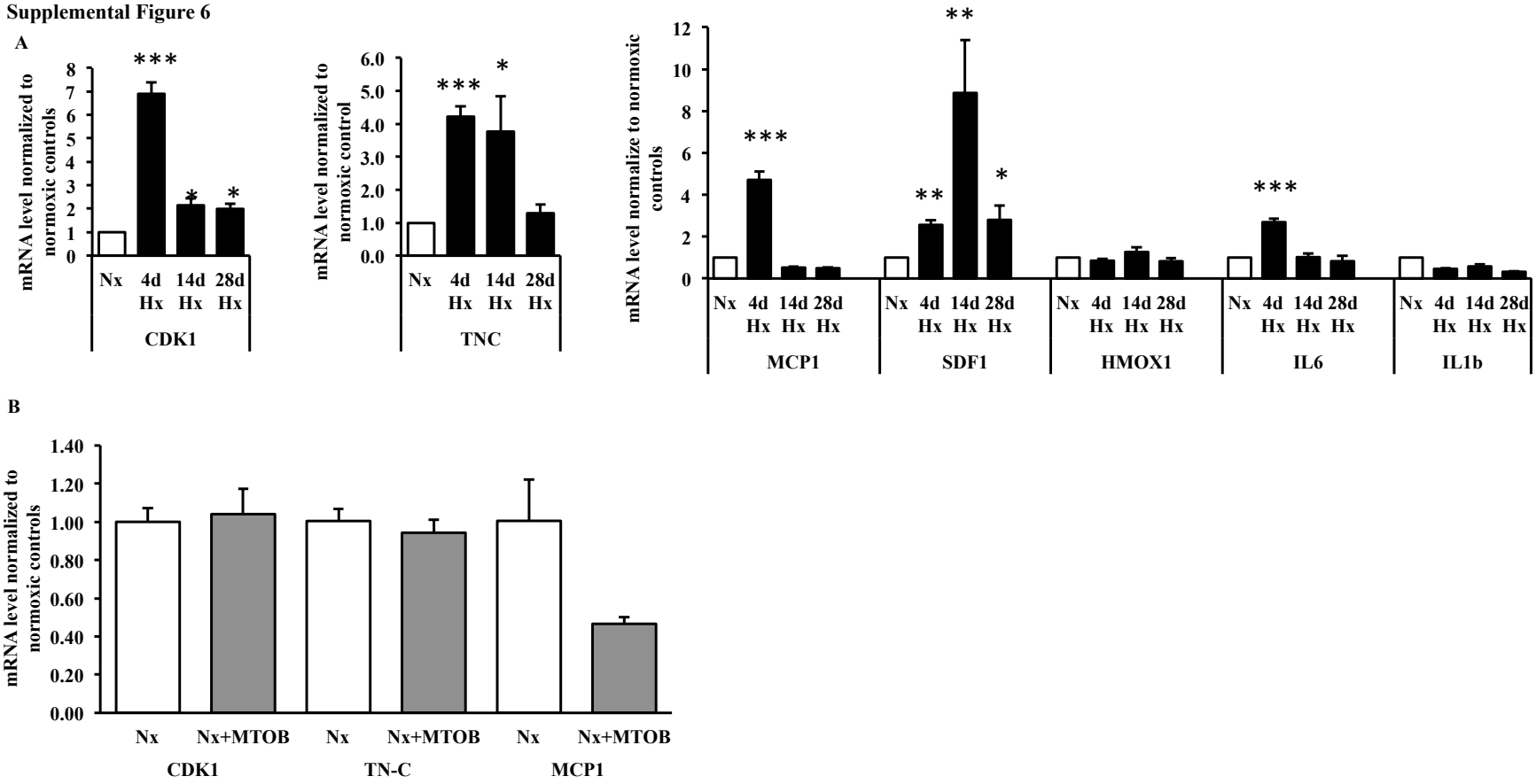

Supplemental Figure 7

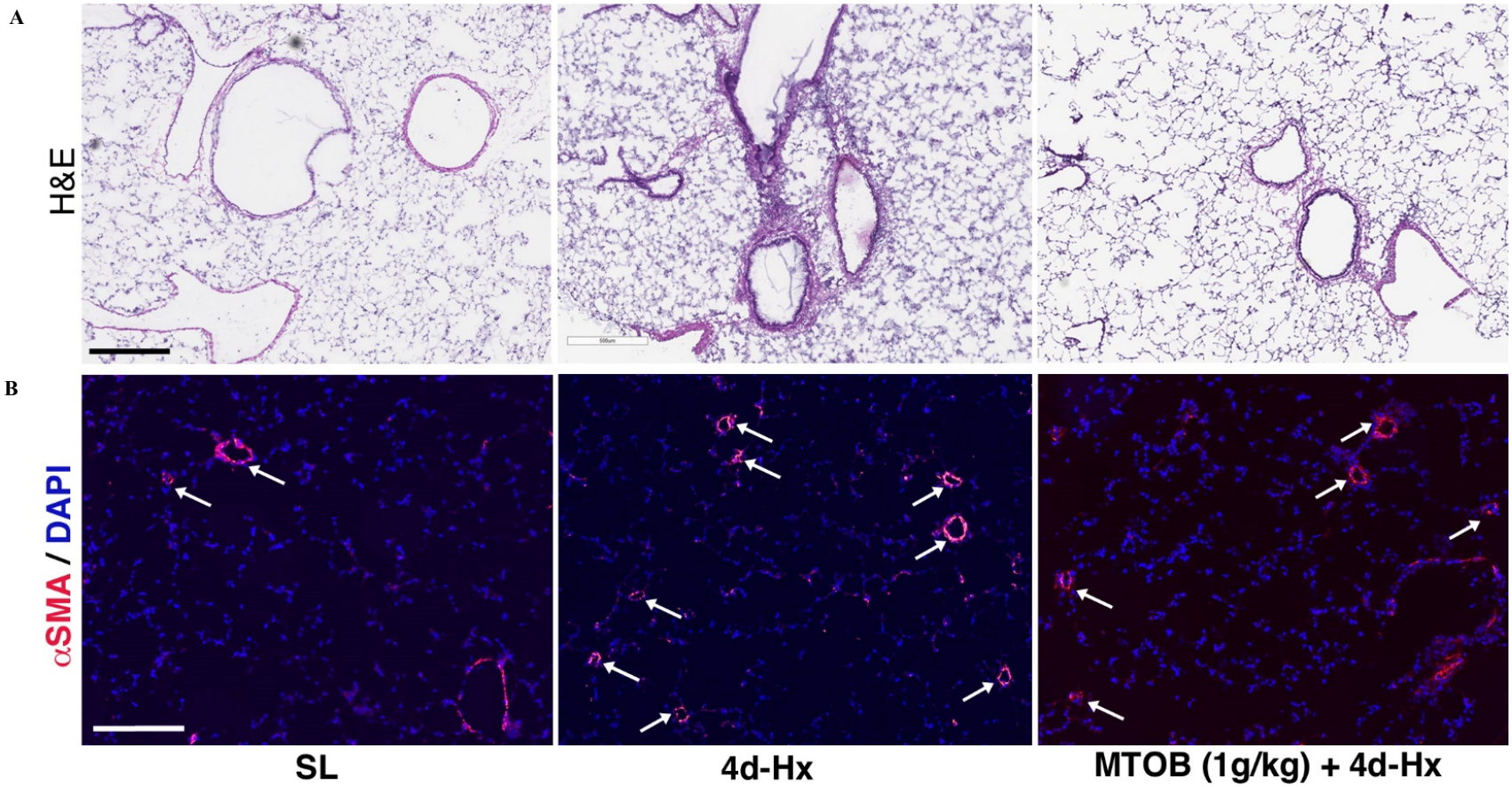

J Appl Physiol 119: 1164–1172, 2015.
First published April 30, 2015; doi:10.1152/japplphysiol.00283.2015.

HIGHLIGHTED TOPIC | *Hypoxia 2015*

Metabolic reprogramming and inflammation act in concert to control vascular remodeling in hypoxic pulmonary hypertension

Kurt R. Stenmark,[1,3] Rubin M. Tuder,[4] and Karim C. El Kasmi[2]

[1]*Division of Critical Care Medicine, Department of Pediatrics, University of Colorado, Anschutz Medical Campus, Denver, Colorado;* [2]*Division of Gastroenterology, Department of Pediatrics, University of Colorado, Anschutz Medical Campus, Denver, Colorado;* [3]*Cardiovascular Pulmonary Research Laboratories, Department of Medicine, University of Colorado, Anschutz Medical Campus, Denver, Colorado; and* [4]*Program in Translational Lung Research, Department of Medicine, Division of Pulmonary Sciences, University of Colorado, Anschutz Medical Campus, Denver, Colorado*

Submitted 6 April 2015; accepted in final form 28 April 2015

Stenmark KR, Tuder RM, El Kasmi KC. Metabolic reprogramming and inflammation act in concert to control vascular remodeling in hypoxic pulmonary hypertension. *J Appl Physiol* 119: 1164–1172, 2015. First published April 30, 2015; doi:10.1152/japplphysiol.00283.2015.—Pulmonary hypertension (PH) is a complex, multifactorial syndrome that remains poorly understood despite decades of research. PH is characterized by profound pulmonary artery (PA) remodeling that includes significant fibro-proliferative and inflammatory changes of the PA adventitia. In line with the emerging concept that PH shares key features with cancer, recent work centers on the idea that PH results from a multistep process driven by reprogramming of gene-expression patterns that govern changes in cell metabolism, inflammation, and proliferation. Data demonstrate that in addition to PA endothelial cells and smooth muscle cells, adventitial fibroblasts from animals with experimental hypoxic PH and from humans with PH (hereafter, termed PH-Fibs) exhibit proinflammatory activation, increased proliferation, and apoptosis resistance, all in the context of metabolic reprogramming to aerobic glycolysis. PH-Fibs can also recruit, retain, and activate naïve macrophages (Mϕ) toward a proinflammatory/proremodeling phenotype through secretion of chemokines, cytokines, and glycolytic metabolites, among which IL-6 and lactate play key roles. Furthermore, these fibroblast-activated Mϕ (hereafter, termed FAMϕ) exhibit aerobic glycolysis together with high expression of *arginase 1*, *Vegfa*, and *Il1b*, all of which require hypoxia-inducible factor 1α and STAT3 signaling. Strikingly, in situ, the adventitial Mϕ phenotype in the remodeled PA closely resembles the Mϕ phenotype induced by fibroblasts in vitro (FAMϕ), suggesting that FAMϕ crosstalk involving metabolic and inflammatory signals is a critical, pathogenetic component of vascular remodeling. This review discusses metabolic and inflammatory changes in fibroblasts and Mϕ in PH with the goal of raising ideas about new interventions to abrogate remodeling in hypoxic forms of PH.

glycolysis; HIF; IL-6; fibroblast; macrophage

PEOPLE WITH PULMONARY HYPERTENSION (PH), due to lung diseases and/or hypoxemia, comprise a distinct group (Group 3) in the World Health Organization (WHO) clinical classification system (80). WHO Group 3 comprises a heterogeneous set of diseases sharing the common feature of hypoxia-induced pulmonary vascular remodeling. The presence of PH in these patients, who include survivors of acute lung injury and those with pulmonary fibrosis or chronic obstructive pulmonary disease (COPD), significantly worsens morbidity and mortality. Furthermore, recent data demonstrate that in these patients, PH is markedly underdiagnosed and is specifically associated with substantial mortality (19, 45, 53). Unfortunately, all therapies currently approved for use in PH have been designed for patients with WHO Group 1 PH [so-called pulmonary arterial hypertension (PAH), e.g., idiopathic PAH (iPAH), scleroderma PAH, human immunodeficiency virus-related PAH, etc.], and to date, no clinical trial with these drugs has shown benefit in patients with WHO Group 3 disease (78). Furthermore, whereas oxygen supplementation attenuates PH and improves overall survival in patients with COPD, it remains unclear whether these effects are mediated by improved pulmonary vascular modeling or why some patients with COPD develop severe pulmonary vascular disease despite oxygen therapy (1, 10). Thus the identification of underlying pathogenic mecha-

Address for reprint requests and other correspondence: K. R. Stenmark, Univ. of Colorado Denver, 12700 E. 19th Ave., B131, Aurora, CO 80045 (e-mail: kurt.stenmark@ucdenver.edu).

nisms, which may instruct the development of novel and improved treatment strategies for PH in these patients, is of paramount importance. The goal of this mini-review is to examine evidence supporting the hypothesis that chronic hypoxia can induce adaptations in metabolism of both mesenchymal cells (specifically fibroblasts) and immune cells [macrophages (Mϕ)], particularly in genetically susceptible individuals, who induce and maintain signaling networks that drive sustained increases in cell proliferation and inflammatory activation/phenotype (Fig. 1). This cell-proliferation/inflammation nexus is therefore critical to the pathogenesis of PH.

METABOLIC THEORY OF PH: RELATIONSHIP TO CANCER

Lung tissue hypoxia, to a variable extent, is common to all of the conditions encountered in patients with Group 3 PH. As the lung cells, including the pulmonary vasculature, react to hypoxia, PH develops; this paradigm is particularly relevant in patients with COPD, sleep-disordered breathing, and fibrosing interstitial lung diseases and those living in altitude (80, 83). Oxygen therapy alone, in these patients, is usually not sufficient to normalize pulmonary arterial pressure, suggesting the involvement of cellular growth mechanisms, which cannot wholly be explained by hypoxic vasoconstriction responses (45). Importantly, in all of these conditions, PH is also consistently associated with early and persistent perivascular inflammation and pulmonary arterial remodeling (87, 93). A striking feature is the predominance of perivascular Mϕ surrounding remodeled pulmonary arteries (27, 49, 77). This remodeling involves an imbalance of cell proliferation vs. cell death, which taken in conjunction with inflammation and Mϕ activation, has led to the hypothesis that the cellular and molecular features of PH resemble hallmark characteristics of cancer monoclonal behavior (18, 39, 93, 95). It is increasingly recognized that changes in cell metabolism in cancer cells, as well as in cells in the surrounding stroma, including Mϕ, are essential for cancer cells to proliferate, migrate, and exhibit proinflammatory characteristics (22, 55, 101). As such, there is an intense effort in the cancer field to define the molecular mechanisms that underlie the coordinated response of cancer cells with their immediate cellular microenvironment, made of cancer-associ-

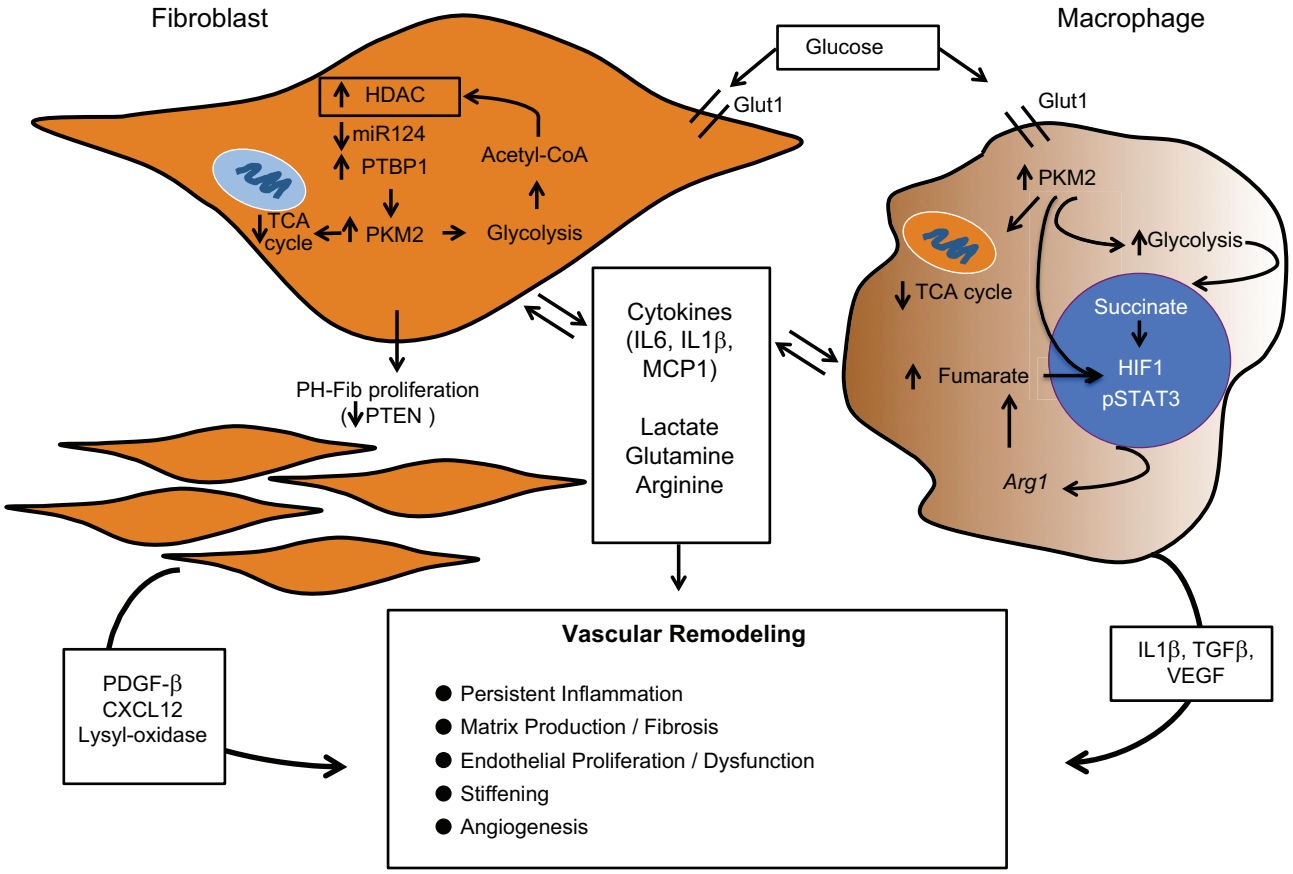

Fig. 1. In line with the emerging concept that pulmonary hypertension (PH) shares key features with cancer, increasing evidence supports the idea that PH results from a multistep process driven by reprogramming genes that govern changes in cell metabolism, inflammation, and proliferation. Pulmonary artery adventitial fibroblasts from animals with experimental hypoxic PH and from humans with pulmonary arterial hypertension exhibit proinflammatory activation, increased proliferation, and apoptosis resistance, all in the context of metabolic reprogramming to aerobic glycolysis. These activated adventitial fibroblasts can recruit, retain, and activate macrophages (Mϕ) toward a distinct proinflammatory/proremodeling phenotype through the secretion of chemokines, cytokines, and other metabolites, including lactate. This fibroblast-activated Mϕ (FAMϕ) also exhibits a switch to aerobic glycolysis, which is regulated through a STAT3-hypoxia-inducible factor 1 (HIF1) signaling axis. Collectively, this fibroblast-FAMϕ signaling unit plays a critical role in the persistent inflammation and fibrosis that characterize certain forms of PH. HDAC, histone deacetylase; miR-124, microRNA 124; PTBP1, polypyrimidine tract-binding protein 1; TCA, tricarboxylic acid; PKM2, M2 isoform of pyruvate kinase; Glut1, glucose importer typically up-regulated in cells adapted to high glycolysis; PH-Fib, adventitial fibroblasts from animals with experimental hypoxic PH and from humans with PH; PTEN, phosphatase and tensin homolog; MCP1, monocyte chemoattractant protein 1; pSTAT3, phosphorylated STAT3; *Arg1*, arginine 1; TGFβ, transforming growth factor β.

ated fibroblasts (CAFs) and Mϕ. The basis of this interaction relates to changes in metabolism, growth, and inflammation. These pathogenic nodes may offer new opportunities for therapy.

Strikingly, a metabolic adaptation akin to aerobic glycolysis ("Warburg-like"), historically assigned to cancer cells, has also recently been reported in PH (18, 32, 67, 93, 105). These changes have been described to occur in smooth muscle cells (SMCs), endothelial cells, and fibroblasts (34, 67). Additional strong data in support of the importance of this metabolic adaptation are supported by 18-fluorodeoxyglucose (^{18}FDG) PET imaging, which has demonstrated increased glucose uptake and metabolism in PAH patients as well as in the monocrotaline rat model of PH (54, 105). Furthermore, ^{18}FDG uptake and gene-expression studies in pulmonary arterial fibroblasts, isolated from iPAH patients, lend support to the concept that a proliferative and inflammatory pulmonary vascular pathology contributes to the lung ^{18}FDG PET signal (105). This study also showed that ^{18}FDG uptake occurs in perivascular mononuclear cells, which accumulate in the adventitial perivascular regions. In vivo studies in the monocrotaline model demonstrated a close correlation between lung ^{18}FDG uptake and pulmonary vascular remodeling. Importantly, enhancement of oxidative glycolysis with dichloroacetate-mediated inhibition of the enzyme pyruvate dehydrogenase kinase attenuated PH and vascular remodeling in this model and also reduced expression of the glucose transporter (Glut1) typically upregulated in cells exhibiting high glycolysis. These findings correlated with reduced ^{18}FDG PET signals, which were associated with decreased peripheral vascular muscularization and inflammatory cell accumulation. Collectively, these in vivo and ex vivo observations support a "metabolic hypothesis" for the pathogenesis of PH, whereby a rearrangement of the mitochondrial and cytosolic metabolism, known as the "Warburg effect," might explain, at least partially, the molecular and functional abnormalities seen in PH cells, including excessive proliferation, apoptosis resistance, and inflammatory activation (67).

METABOLIC AND INFLAMMATORY CHANGES IN FIBROBLASTS AND Mϕ IN CANCER

Our laboratory has been particularly focused on fibroblasts and Mϕ in PH, based on observations of inflammation occurring largely in the perivascular regions in PH (which harbor fibroblasts and Mϕ) in humans and animal models of PH (9, 77, 85, 87). Interestingly, similar observations of largely adventitial inflammatory responses, mostly involving Mϕ, are observed in systemic circulation in response to changes in blood flow and are necessary for remodeling (89). It seems that despite marked cytokine and chemokine production by medial SMCs, Mϕ accumulation occurs largely in the adventitia (48, 108). These observations are consistent with the idea that under most circumstances, the vascular media of almost all arteries appear to be an immune-privileged site (91). Here again, the cancer paradigm is appropriate: consistent with the hypothesis put forth by Dvorak (26), almost 30 years ago—that a "tumor is a wound that never heals"—an ever-increasing body of evidence demonstrates that the fibroblasts and Mϕ in tumors, often referred to as CAFs and tumor-associated Mϕ (TAMs), are key players in the process of tumorigenesis (39, 62). Several recent studies have shown that in many cancers, the cancer-promoting and therapy-resistant properties of the tumor stroma largely reside in the activity of fibroblasts and Mϕ (61, 62). CAFs have been shown to play roles in many aspects of tumor initiation, progression, and metastasis. CAFs are now implicated in the following: *1*) modulating the tumor and microenvironment through the secretion of a large variety of soluble factors; *2*) modifying tumor metabolism; *3*) remodeling the extracellular matrix of the tumor; *4*) regulating cancer stemness; *5*) modulating the immune response (and affecting Mϕ phenotype); *6*) promoting cancer cell migration and metastasis; and *7*) altering therapeutic responses in a variety of tumors (12, 13). Of particular relevance to the hypothesis that PH exhibits a critical relationship to cancer is the ability of fibroblasts to secrete cytokines and growth factors, their ability to modify tumor metabolism, and their role in modulating immune responses and Mϕ phenotype. A wide variety of growth factors and cytokines has been documented to be produced and released into the tumor microenvironment by fibroblasts (75). The CAF secretome also regulates angiogenesis. VEGF-A as well as CXCL12, CXCL14, and connective tissue growth factor are induced in CAFs by neoplastic cells (4). Interestingly, CAFs also show important metabolic changes that probably promote their own survival as well as promote tumorigenesis. CAFs demonstrate increased autophagy in concert with upregulation of members of the glycolytic pathway, including phosphoglycerate kinase 1 (PGK1). Overexpression of PGK1 in normal fibroblasts results in a myofibroblastic phenotype and an ability to promote tumor cell growth (13, 99). Furthermore, in many tumors, CAFs express glycolytic enzymes related to the Warburg effect, such as the M2 isoform of pyruvate kinase (PKM2), as well as lactate dehydrogenase. This metabolic adaptation toward increased aerobic glycolysis in CAFs is hypothesized to generate lactate and ketones, which are secreted into the intracellular space and can act as paracrine oncometabolites that fuel the oxidative mitochondrial metabolism in neoplastic cells. This phenomenon is often referred to as the "reverse" Warburg effect (68). In addition, lactate and ketones have been recognized to modulate Mϕ activation (16).

As noted, chronic inflammation is a prominent risk factor for many cancers. An inflammatory environment, especially in the context of the metabolic environment described above, is known to promote error-prone, high-rate proliferation, thereby facilitating tumorigenesis (37). CAFs mediate tumor-enhancing inflammation by expressing a proinflammatory gene signature, which creates a microenvironment that attracts myeloid cells and supports tumor growth and angiogenesis (92). Importantly, carcinoma cells can induce normal surrounding fibroblasts to turn on a proinflammatory gene signature. Furthermore, accumulating evidence shows that the tumor stroma and CAFs, in particular, actively participate in modulating the immune response to help neoplastic cells escape detection, thereby supporting tumor progression (43). Recent studies have shown that depletion of fibroblast-activating protein α-positive cells restored immunologic detection and destruction of the tumor, indicating that presumably fibroblasts can act as immunosuppressant cells in the tumor microenvironment (31). Additionally, reports suggest that at least within the pancreas, fibroblast-like cells induce the differentiation of peripheral blood mononuclear cells into immune-suppressive,

myeloid-derived suppressor cells, contributing to T cell inhibition (51). In summary, CAFs possess the ability to manipulate the innate (i.e., Mϕ, natural killer cells) and the adaptive immune system (i.e., T cells) to maintain an aberrant inflammatory environment tailored to promoting tumorigenesis.

METABOLIC AND INFLAMMATORY CHANGES IN PULMONARY ARTERIAL ADVENTITIAL FIBROBLASTS: PARALLELS TO CAFS

Fibroblasts are also recognized to play a critical role within the vasculature and its innate immune system in the absence of oncogenic transformation by acting as "sentinel" cells (8, 25, 44, 79, 86, 87), which detect and respond to a variety of local environmental stresses and thereby initiate and coordinate pathophysiological responses (5, 6, 8, 33, 41, 63, 81, 82, 96, 102). We have documented that in both experimental hypoxic PH and human PAH, the pulmonary artery (PA) adventitia harbors activated fibroblasts (hereafter, termed PH-Fibs) with a hyperproliferative, apoptosis-resistant, and proinflammatory phenotype that persists ex vivo over numerous passages in culture (2, 20, 49, 66, 98). This particular phenotype would be centrally involved in cell signaling, shaping the surrounding inflammation-prone microenvironment. Indeed, in line with the cancer paradigm—that stromal cells play a critical role in initiation and perpetuation of inflammation (7, 40, 81, 84, 86, 87, 96, 102)—we have recently shown that PH-Fibs potently recruit, retain, and activate naïve Mϕ (27, 49). Bovine PH-Fibs exhibit an intriguingly similar cytokine profile to that described for CAFs. We have recently established that these fibroblast-activated Mϕ (FAMϕ) are polarized to a very distinct, heretofore undescribed, proinflammatory/proremodeling phenotype, in which STAT3 and hypoxia-inducible factor 1α (HIF1α) signaling promote expression of genes implicated in chronic, nonresolving tissue responses in PH [e.g., *Pim1*; *nuclear factor of activated T cells, cytoplasmic 2*; *Arginase-1* (*Arg1*); *VEGF*] (27). This fibroblast-driven polarization of Mϕ into a distinct phenotype is similar to that recently described for hypoxic tumor-driven Mϕ polarization (16, 51). In addition, expression of *Arg1*, *Hif1*, and *Vegfa* is characteristic of wound-healing Mϕ (26, 58). Thus Mϕ activation and expression of HIF1α, Arg1, and Vegfa appear to not only be a functional requirement for Mϕ to promote physiological wound healing but also can be "high jacked" to shape an environment, not only conducive to tumor growth but also importantly, to promote pathological tissue remodeling. These observations highlight the idea that hypoxia signaling, inflammation, and remodeling and ultimately, PH are linked through stromal cell (fibroblast)/Mϕ interactions, driven specifically by local changes in a hypoxic or hypoxic-like vascular microenvironment.

Data also show that similar to cancer cells, which reprogram metabolic pathways to support high proliferation (Warburg effect) (3, 23, 24, 57, 71, 88, 93), highly proliferative PH-Fibs exhibit a marked and persistent change in their metabolism toward aerobic glycolysis (i.e., Warburg effect), which is maintained ex vivo (105). However, the mechanisms controlling the metabolic, molecular, and functional changes in the fibroblast phenotype in PH have only recently begun to be investigated. Importantly, observations from our laboratory (49, 66, 87, 93, 95, 98, 106) have documented that cells (including SMCs, endothelial cells, and fibroblasts), derived from the PH vessel wall, exhibit durable ex vivo changes in their metabolic state (aerobic glycolysis), as well as in their proliferative and inflammatory capabilities and in their "molecular phenotype". Stable, "imprinted" changes in the functional phenotype of cell observations strongly support the idea that these stable changes in cells, especially as they relate to metabolism and cell signaling, could arise from acquired somatic mutations and/or epigenetic change.

Here again, there is a striking parallel to observations in cancer. It is now well accepted that signal transduction regulates metabolism (101). Cancer cells exploit signaling-dependent regulation of metabolism. For example, oncogenic activation of signal transduction pathways drives nutrient uptake and metabolism to support continuous macromolecular biosynthesis and cell proliferation (46, 101). Reciprocally, signaling pathways have been shown to be regulated by metabolism through intracellular nutrient-sensing molecules, such as AMP-activated protein kinase (AMPK) and mammalian target of rapamycin complex 1. In addition, metabolites may serve as indicators of the metabolic status of the cell and through metabolite-sensitive protein modifications, modulate the activity of signaling proteins, metabolic enzymes, and transcriptional regulators (101). Modifications, including acetylation, methylation, glycosylation, and phosphorylation, are all generated from metabolites (56). Acetylation, a protein modification involving the addition of an acetyl group obtained from the metabolite acetyl-CoA, is controlled by the combined activities of acetyltransferases and deacetylases (38). There is evidence that both acetylation and deacetylation can be influenced by nutrient availability, suggesting that protein acetylation could serve as a sensitive indicator of cellular metabolic resources (101). It is also recognized that metabolism itself can be regulated by acetylation. A growing body of evidence indicates that nearly all enzymes involved in glucose and fatty acid metabolism are acetylated (107). For some of these enzymes, such as the critically important PKM2, acetylation seems to modulate their activity in a nutrient-responsive, biologically meaningful way (15, 50, 107). The acetylation status of PKM2 was shown to be relevant to tumor growth, as expression of an acetylation mimetic mutant version of PKM2 enhanced the growth of xenograft tumors (50).

Similarities to this concept of reciprocal regulation of metabolism and signaling have been raised in PH. We recently documented that the highly proliferative, apoptotic-resistant, and proinflammatory [high expression of IL-6, CCL2/monocyte chemoattractant protein 1 (MCP-1), CCL12/stromal cell-derived factor 1, IL-1β] phenotype of PH-Fibs, isolated from the pulmonary circulation of humans and calves with severe PH, is mediated, at least in part, by a marked decrease in the expression of microRNA 124 (miR-124) and the increased expression of its direct target, the alternative splicing factor polypyrimidine tract-binding protein 1 (PTBP1), as well as increased expression of class I histone deacetylases (HDACs), a specific subgroup of the deacetylase mentioned above (98). With the use of miR-124 inhibitors and mimics in human and bovine fibroblasts, we demonstrated that overexpression of miR-124 decreased the proliferation and migration rates of PH-Fibs. Similarly, inhibition of miR-124 (via anti-miR-124) in normal control fibroblasts (CO-Fibs) augmented cell proliferation and migration, demonstrating that miR-124 regulates

proliferative and migratory characteristics of fibroblasts. It should be noted that with the use of both miR array analysis and real-time PCR, we noted decreased expression of several other miRs (including miR-184; miR-21, miR-155) in PH-Fibs (from calves and humans) compared with corresponding controls. We made miR mimics of each of these miRs and transfected them into PH-Fibs, as we did for miR-124. In no case did overexpression of these miRs decrease proliferation, migration, or inflammatory cytokine expression. Collectively, these data suggest that loss of miR-124 in PH-Fibs is a major contributor to their "constitutively" activated phenotype.

To elucidate the mechanisms by which miR-124 regulates cell proliferation and migration, we screened transcript levels of cell cycle-related genes and found that miR-124 positively regulates *Notch1*, *phosphatase and tensin homolog* (*PTEN*), *forkhead box O3* (*FOXO3*), *p21/Cip1*, and *p27/Kip1*, all of which were reduced in PH-Fibs. Next, we sought to determine the target of miR-124 upstream of the cell cycle regulator genes, knowing that these genes would have to increase, since miR-124 was decreased, as it suppresses cell cycle genes. Previously published data identified PTBP1 as a direct target of miR-124 and showed that PTBP1 can suppress Notch1 signaling (14, 52). Therefore, we focused on PTBP1, which is an abundantly expressed RNA-binding protein involved in several post-transcriptional regulation events, including repression of RNA alternative-splicing events, activation of internal ribosomal entry site-driven translation, and RNA localization and stability. It is overexpressed in a variety of cancer cells in response to oncogenes, such as cMyC and the transcription factor STAT3. We found that PTBP1 expression is increased in bovine and human PH-Fibs (in vitro), as well as in vivo in PA adventitia of humans and calves with severe PH (98). Overexpression of miR-124 (using miR-124 mimics) in human and bovine PH-Fibs inhibited PTPB1 expression, whereas inhibition of miR-124 (using anti-miR-124) in CO-Fibs upregulated PTBP1 expression. We conducted luciferase/PTPB1 3′ untranslated region assays and proved that PTBP1 is a direct target of miR-124 (98). We also showed that PTBP1 acts upstream of Notch1 and negatively regulates the cell cycle-related genes *Notch1*, *PTEN*, *FOXO3*, *p21*, and *p27*. Importantly, it is also known that PTBP1 controls splicing of pyruvate kinase, and its increased expression leads to overexpression of the PKM2 isoform, which as noted above, is an important regulator of the metabolic state of cells. These novel findings demonstrate that miR-124 expression is markedly attenuated in PH-Fibs and results in an increase of an RNA-binding protein, PTBP1, which post-transcriptionally regulates expression of several genes controlling cell proliferation, metabolism, and inflammation.

Given the importance of PTBP1 in regulating the proliferative, metabolic, and inflammatory phenotype of PH-Fibs, we performed experiments elucidating the mechanism controlling expression of miR-124. Since it has previously been shown that miR-124 itself is subject to epigenetic modifications (36, 100), we interrogated whether miR-124 is epigenetically silenced in PH-Fibs. Perhaps not unexpectedly, given the significant change in metabolic status of PH cells (aerobic glycolysis) and the increase in class I HDAC expression, we found that treatment of PH-Fibs with the HDAC inhibitors, suberoylanilide hydroxamic acid and Apidicin, led to a significant increase in miR-124 expression with concurrent decreases in expression of its direct targets, PTBP1 and CCL2/MCP-1 (98). These observations support our previously published data, showing increased class I HDAC activity in cultured PH-Fibs and in hypoxic lungs (11, 106). Furthermore, this suggested that decreased miR-124 expression in PH-Fibs occurred through epigenetic modifications, likely through the removal of acetylation marks on histones, resulting in a more condensed chromatin structure and inhibition of transcription. Such an epigenetic event would explain the constitutively activated phenotype of PH-Fibs, which we have shown to be "reversible" (close to normal) through the application of HDAC inhibitors (11, 106).

In summary, it seems increasingly clear that a fibroblast (fibroblast-like cell) emerges in the adventitia of humans and animals with severe PH that bears a striking resemblance to CAFs. These cells exhibit a Warburg-like glycolytic phenotype and are characterized by excessive proliferation, apoptosis resistance, and a proinflammatory phenotype. Metabolism and signaling pathways in these cells are intimately linked and driven by epigenetic changes that are intimately linked to the metabolic state of the cell (Fig. 1).

METABOLIC AND INFLAMMATORY CHANGES IN PA FAMϕ

We propose that the synchronized and mutually interactive signaling between pulmonary perivascular fibroblasts and Mϕ is central in PH pulmonary vascular remodeling. There is evidence that Mϕ accumulation in the remodeled PA is largely restricted to the adventitia, where Mϕ are in close proximity to adventitial fibroblasts and that Mϕ critically contribute to the vascular remodeling process (27, 35, 73, 77, 86). Importantly, there is evidence for adventitial Mϕ progenitor cells (at least in the systemic circulation in the setting of atherosclerosis) that can serve as a durable pool for adventitial Mϕ populations (72). As outlined for fibroblasts above, rapidly increasing evidence supports a role for the Warburg effect in immune activation (65), specifically, in Mϕ and dendritic cells (DCs). Initial reports by the Pearce lab (29, 30, 47, 69) have demonstrated that Toll-like receptor-activated DCs undergo a metabolic adaptation from oxidative phosphorylation to aerobic glycolysis and that this metabolic switch is critical for DC maturation and function, while it also regenerates NADP oxidase and citric acid cycle intermediates to support fatty acid production. In DCs, this metabolic switch to aerobic glycolysis is promoted by phosphatidylinositol 3 kinase/Akt signaling and is inhibited by the AMPK, a central regulator of catabolic metabolism that is also displayed by cancer cells (29). More recent reports by the O'Neill lab (64, 90) have similarly shown that increased aerobic glycolysis and reduced oxidative phosphorylation are critical events required for innate Mϕ activation in response to LPS. These studies have also identified PKM2 as the critical molecular switch to turn on aerobic glycolysis in LPS-activated Mϕ (64). Conversely, the alternatively activated Mϕ phenotype (induced by IL-4) depends on increased oxidative phosphorylation and lipolysis (42, 60, 76, 97). It is, however, unresolved which metabolic adaptations occur in and are critical for the functional phenotype of Mϕ associated with chronic tissue remodeling and fibrosis, especially because these Mϕ often resist categorization into the extremes of M1 (LPS-activated) vs. M2 (IL-4-activated) phenotypes (27); their functional phenotype may be in flux, chang-

ing due to local environmental signaling and metabolic conditions. In addition, in chronic tissue-remodeling conditions, there may be absence of IFN-γ and/or LPS (the M1-defining stimuli) and IL-4/IL-13 (the M2-defining stimuli) but presence of tissue-derived danger signals and cytokines, such as IL-6 (27), which drive Mϕ activation toward displaying a considerable overlap between M1 and M2 phenotypic gene-expression markers and thus Mϕ function (27); conceivably, these Mϕ, including FAMϕ, in vascular remodeling associated with PH, may therefore exhibit metabolic features overlapping with those typically observed in and defining the M1 (LPS-activated) and M2 (IL-4-activated) Mϕ phenotypes. Whereas they express HIF1 and features of increased aerobic glycolysis, they also express increased mRNA and protein for Arg1. Importantly, this fibroblast-activated phenotype is critically dependent on STAT3 signaling, which clearly and distinctly differentiates it from M1 and M2 (27).

The major consequence of metabolic adaptation toward aerobic glycolysis in LPS-activated Mϕ is generation of increased concentrations of the citric acid cycle intermediate succinate (90), which is a potent prolyl hydroxylase (PHD) inhibitor and thus stabilizer of HIF1. The functional consequence of this LPS-mediated HIF1 stabilization through metabolic reprogramming in Mϕ is increased transcriptional activation of the proinflammatory gene *Il1b*. In addition, in LPS-activated Mϕ, increased activity of PKM2 further promotes HIF1-mediated transcriptional induction of IL-1β and other cytokines in colorectal cancer cells (104). PKM2 is also critical for enhancing STAT3 signaling (through increased phosphorylation) (21, 103, 104), whereas STAT3, in turn, increases HIF1 signaling and expression of Glut1, which is important for glucose uptake and maintenance of increased glycolysis, enhancing the anaerobic metabolism (Warburg effect). Thus this PKM2-STAT3-HIF feedforward may be a critical signaling pathway in tissue Mϕ associated with areas of remodeling and fibrosis that typically lack strong M1-inducing signals and is not associated with IL-4 and canonical M2 Mϕ but instead, exhibits STAT3 and HIF1 signaling (27, 104). Moreover, PKM2 can drive expression of Arg1 through activation of STAT3, which as we have reported, is highly upregulated in FAMϕ (27). Increased activity of Arg1 through metabolism of arginine can have profound effects on restricting arginine availability to "client cells" (e.g., adventitial fibroblasts) (70). Under arginine-limiting conditions, Mϕ initiate a salvage pathway (74) that consumes aspartate and generates fumarate, thus directly affecting concentrations of citric acid cycle intermediates that are capable of inhibiting PHDs and thus stabilizing HIF1. Moreover, increased aerobic glycolysis produces increased amounts of lactate. Importantly, because FAMϕ does display evidence of both aerobic glycolysis and citric acid cycle activity (unpublished observations), akin to activated T cells (59), pyruvate is excreted as lactate but also entered into the citric acid cycle; in this regard, lactate has been shown to be a potent activator of Mϕ toward expression of HIF1 and Arg1 (16). Together, these metabolic pathways make these cells glutamine-dependent, whereas the arginine metabolism through Arg1 may provide glutamate and help replenish the citric acid cycle (unpublished observations).

As such, activation of STAT3, HIF1, and PKM2 in the molecular crosstalk between Mϕ and fibroblasts through bidirectional generation and consumption of metabolites downstream and upstream of aerobic glycolysis may perpetuate rather than attenuate inflammatory activation (Fig. 1).

Intriguingly, inhibition of this PKM2 activity has been shown to convert the LPS-activated phenotype toward a Mϕ with anti-inflammatory features, as indicated by increased expression of IL-10 (64). Interestingly, in DCs, IL-10 antagonizes DC maturation through inhibition of metabolic adaptation to aerobic glycolysis (47). Thus Mϕ phenotypic conversion toward generation of anti-inflammatory mediators and simultaneously increasing responsiveness of inflammatory Mϕ to anti-inflammatory IL-10 might be achieved by interfering with PKM2 activity. However, the ability of IL-10 to inhibit LPS-induced IL-1β transcription in Mϕ depends, to some degree, on Arg1, a PKM2-STAT3 target gene (unpublished observations). Precisely how PKM2, HIF1, and aerobic glycolysis affect IL-10 production and IL-10 responsiveness requires further analysis.

The aggregate of these findings demonstrates that functional Mϕ plasticity depends on discrete metabolic adaptions and suggests that Mϕ can be functionally re-educated through manipulating metabolism. However, whether a similar phenotypic conversion/re-education of Mϕ from proinflammatory to a less-inflammatory or even reparative Mϕ phenotype can be achieved by inhibition of HIF1 alone or by inhibition of aerobic glycolysis alone awaits further studies. Intriguingly, PKM2 might turn out to play a critical role as a "master regulator" in driving and/or fine-tuning Mϕ polarization and phenotypic reprogramming/re-education of Mϕ away from proinflammatory or proremodeling phenotypes, because it regulates HIF1 activity and glycolysis, and it also affects STAT3 phosphorylation and signaling (21).

In summary, CAFs and TAMs display considerable overlap with the phenotypes described for PH-Fibs and PH-Fib-activated Mϕ associated with vascular remodeling in PH. Therefore, similar molecular and metabolic mechanisms may govern fibroblast-Mϕ crosstalk in the process of tumorigenesis and vascular remodeling. PKM2 may prove to be a critical driver of the metabolic and functional crosstalk between CAFs and TAMs, as well as between PH-Fibs and FAMϕ. Thus PKM2 targeting may turn out to attenuate tumorigenesis and vascular remodeling through similar mechanisms. Interestingly, small molecule activators of PKM2 that enhance tetramerization activity have been shown to compromise the proglycolytic and pro-HIF signaling functions (64), and it is conceivable that these molecules also interfere with the ability of PKM2 to phosphorylate STAT3; they may thus prove to be potent inhibitors of the uncontrolled PKM2-STAT3-HIF feedforward signal but may also increase generation of and responsiveness to endogenous anti-inflammatory mediators, such as IL-10.

GRANTS

Support for this study was provided, in part, by the National Heart, Lung, and Blood Institute [Grants HL114887 (Axis), HL014985 (PPG), and HL125827 (R01)].

DISCLOSURES

No conflicts of interest, financial or otherwise, are declared by the authors.

AUTHOR CONTRIBUTIONS

Author contributions: K.R.S. and K.C.E.K. conception and design of research; K.R.S. and K.C.E.K. prepared figures; K.R.S. and K.C.E.K. drafted

manuscript; K.R.S., R.M.T., and K.C.E.K. edited and revised manuscript; K.R.S., R.M.T., and K.C.E.K. approved final version of manuscript.

REFERENCES

1. Continuous or nocturnal oxygen therapy in hypoxemic chronic obstructive lung disease: a clinical trial. Nocturnal Oxygen Therapy Trial Group. *Ann Intern Med* 93: 391–398, 1980.
2. **Anwar A, Li M, Frid MG, Kumar B, Gerasimovskaya EV, Riddle SR, McKeon BA, Thukaram R, Meyrick BO, Fini MA, Stenmark KR.** Osteopontin is an endogenous modulator of the constitutively activated phenotype of pulmonary adventitial fibroblasts in hypoxic pulmonary hypertension. *Am J Physiol Lung Cell Mol Physiol* 303: L1–L11, 2012.
3. **Archer SL, Fang YH, Ryan JJ, Piao L.** Metabolism and bioenergetics in the right ventricle and pulmonary vasculature in pulmonary hypertension. *Pulm Circ* 3: 144–152, 2013.
4. **Augsten M, Hagglof C, Olsson E, Stolz C, Tsagozis P, Levchenko T, Frederick MJ, Borg A, Micke P, Egevad L, Ostman A.** CXCL14 is an autocrine growth factor for fibroblasts and acts as a multi-modal stimulator of prostate tumor growth. *Proc Natl Acad Sci USA* 106: 3414–3419, 2009.
5. **Baglole CJ, Ray DM, Bernstein SH, Feldon SE, Smith TJ, Sime PJ, Phipps RP.** More than structural cells, fibroblasts create and orchestrate the tumor microenvironment. *Immunol Invest* 35: 297–325, 2006.
6. **Barone F, Nayar S, Buckley CD.** The role of non-hematopoietic stromal cells in the persistence of inflammation. *Front Immunol* 3: 416, 2012.
7. **Barron L, Smith AM, El Kasmi KC, Qualls JE, Huang X, Cheever A, Borthwick LA, Wilson MS, Murray PJ, Wynn TA.** Role of arginase 1 from myeloid cells in Th2-dominated lung inflammation. *PloS One* 8: e61961, 2013.
8. **Buckley CD, Pilling D, Lord JM, Akbar AN, Scheel-Toellner D, Salmon M.** Fibroblasts regulate the switch from acute resolving to chronic persistent inflammation. *Trends Immunol* 22: 199–204, 2001.
9. **Burke DL, Frid MG, Kunrath CL, Karoor V, Anwar A, Wagner BD, Strassheim D, Stenmark KR.** Sustained hypoxia promotes the development of a pulmonary artery-specific chronic inflammatory microenvironment. *Am J Physiol Lung Cell Mol Physiol* 297: L238–L250, 2009.
10. **Carlsen J, Hasseriis Andersen K, Boesgaard S, Iversen M, Steinbruchel D, Bogelund Andersen C.** Pulmonary arterial lesions in explanted lungs after transplantation correlate with severity of pulmonary hypertension in chronic obstructive pulmonary disease. *J Heart Lung Transplant* 32: 347–354, 2013.
11. **Cavasin MA, Demos-Davies K, Horn TR, Walker LA, Lemon DD, Birdsey N, Weiser-Evans MC, Harral J, Irwin DC, Anwar A, Yeager ME, Li M, Watson PA, Nemenoff RA, Buttrick PM, Stenmark KR, McKinsey TA.** Selective class I histone deacetylase inhibition suppresses hypoxia-induced cardiopulmonary remodeling through an antiproliferative mechanism. *Circ Res* 110: 739–748, 2012.
12. **Chaffer CL, Weinberg RA.** A perspective on cancer cell metastasis. *Science* 331: 1559–1564, 2011.
13. **Chaudhri VK, Salzler GG, Dick SA, Buckman MS, Sordella R, Karoly ED, Mohney R, Stiles BM, Elemento O, Altorki NK, McGraw TE.** Metabolic alterations in lung cancer-associated fibroblasts correlated with increased glycolytic metabolism of the tumor. *Mol Cancer Res* 11: 579–592, 2013.
14. **Cheung HC, Corley LJ, Fuller GN, McCutcheon IE, Cote GJ.** Polypyrimidine tract binding protein and Notch1 are independently re-expressed in glioma. *Mod Pathol* 19: 1034–1041, 2006.
15. **Christofk HR, Vander Heiden MG, Harris MH, Ramanathan A, Gerszten RE, Wei R, Fleming MD, Schreiber SL, Cantley LC.** The M2 splice isoform of pyruvate kinase is important for cancer metabolism and tumour growth. *Nature* 452: 230–233, 2008.
16. **Colegio OR, Chu NQ, Szabo AL, Chu T, Rhebergen AM, Jairam V, Cyrus N, Brokowski CE, Eisenbarth SC, Phillips GM, Cline GW, Phillips AJ, Medzhitov R.** Functional polarization of tumour-associated macrophages by tumour-derived lactic acid. *Nature* 513: 559–563, 2014.
18. **Cottrill KA, Chan SY.** Metabolic dysfunction in pulmonary hypertension: the expanding relevance of the Warburg effect. *Eur J Clin Invest* 43: 855–865, 2013.
19. **Cuttica MJ, Kalhan R, Shlobin OA, Ahmad S, Gladwin M, Machado RF, Barnett SD, Nathan SD.** Categorization and impact of pulmonary hypertension in patients with advanced COPD. *Respir Med* 104: 1877–1882, 2010.
20. **Das M, Burns N, Wilson SJ, Zawada WM, Stenmark KR.** Hypoxia exposure induces the emergence of fibroblasts lacking replication repressor signals of PKCzeta in the pulmonary artery adventitia. *Cardiovasc Res* 78: 440–448, 2008.
21. **Demaria M, Poli V.** PKM2, STAT3 and HIF-1alpha: The Warburg's vicious circle. *JAKSTAT* 1: 194–196, 2012.
22. **Doherty JR, Cleveland JL.** Targeting lactate metabolism for cancer therapeutics. *J Clin Invest* 123: 3685–3692, 2013.
23. **Dromparis P, Michelakis ED.** Mitochondria in vascular health and disease. *Annu Rev Physiol* 75: 95–126, 2013.
24. **Dromparis P, Paulin R, Sutendra G, Qi AC, Bonnet S, Michelakis ED.** Uncoupling protein 2 deficiency mimics the effects of hypoxia and endoplasmic reticulum stress on mitochondria and triggers pseudohypoxic pulmonary vascular remodeling and pulmonary hypertension. *Circ Res* 113: 126–136, 2013.
25. **Duffield JS, Lupher M, Thannickal VJ, Wynn TA.** Host responses in tissue repair and fibrosis. *Annu Rev Pathol* 8: 241–276, 2013.
26. **Dvorak HF.** Tumors: wounds that do not heal. Similarities between tumor stroma generation and wound healing. *N Engl J Med* 315: 1650–1659, 1986.
27. **El Kasmi KC, Pugliese SC, Riddle SR, Poth JM, Anderson AL, Frid MG, Li M, Pullamsetti SS, Savai R, Nagel MA, Fini MA, Graham BB, Tuder RM, Friedman JE, Eltzschig HK, Sokol RJ, Stenmark KR.** Adventitial fibroblasts induce a distinct proinflammatory/profibrotic macrophage phenotype in pulmonary hypertension. *J Immunol* 193: 597–609, 2014.
29. **Everts B, Amiel E, Huang SC, Smith AM, Chang CH, Lam WY, Redmann V, Freitas TC, Blagih J, van der Windt GJ, Artyomov MN, Jones RG, Pearce EL, Pearce EJ.** TLR-driven early glycolytic reprogramming via the kinases TBK1-IKKε supports the anabolic demands of dendritic cell activation. *Nat Immunol* 15: 323–332, 2014.
30. **Everts B, Amiel E, van der Windt GJ, Freitas TC, Chott R, Yarasheski KE, Pearce EL, Pearce EJ.** Commitment to glycolysis sustains survival of NO-producing inflammatory dendritic cells. *Blood* 120: 1422–1431, 2012.
31. **Feig C, Jones JO, Kraman M, Wells RJ, Deonarine A, Chan DS, Connell CM, Roberts EW, Zhao Q, Caballero OL, Teichmann SA, Janowitz T, Jodrell DI, Tuveson DA, Fearon DT.** Targeting CXCL12 from FAP-expressing carcinoma-associated fibroblasts synergizes with anti-PD-L1 immunotherapy in pancreatic cancer. *Proc Natl Acad Sci USA* 110: 20212–20217, 2013.
32. **Fijalkowska I, Xu W, Comhair SA, Janocha AJ, Mavrakis LA, Krishnamachary B, Zhen L, Mao T, Richter A, Erzurum SC, Tuder RM.** Hypoxia inducible-factor1alpha regulates the metabolic shift of pulmonary hypertensive endothelial cells. *Am J Pathol* 176: 1130–1138, 2010.
33. **Flavell SJ, Hou TZ, Lax S, Filer AD, Salmon M, Buckley CD.** Fibroblasts as novel therapeutic targets in chronic inflammation. *Br J Pharmacol* 153, *Suppl* 1: S241–S246, 2008.
34. **Freund-Michel V, Khoyrattee N, Savineau JP, Muller B, Guibert C.** Mitochondria: roles in pulmonary hypertension. *Int J Biochem Cell Biol* 55: 93–97, 2014.
35. **Frid MG, Brunetti JA, Burke DL, Carpenter TC, Davie NJ, Reeves JT, Roedersheimer MT, van Rooijen N, Stenmark KR.** Hypoxia-induced pulmonary vascular remodeling requires recruitment of circulating mesenchymal precursors of a monocyte/macrophage lineage. *Am J Pathol* 168: 659–669, 2006.
36. **Furuta M, Kozaki KI, Tanaka S, Arii S, Imoto I, Inazawa J.** miR-124 and miR-203 are epigenetically silenced tumor-suppressive microRNAs in hepatocellular carcinoma. *Carcinogenesis* 31: 766–776, 2010.
37. **Grivennikov SI, Greten FR, Karin M.** Immunity, inflammation, and cancer. *Cell* 140: 883–899, 2010.
38. **Haigis MC, Sinclair DA.** Mammalian sirtuins: biological insights and disease relevance. *Annu Rev Pathol* 5: 253–295, 2010.
39. **Hanahan D, Weinberg RA.** Hallmarks of cancer: the next generation. *Cell* 144: 646–674, 2011.
40. **Hassoun PM, Mouthon L, Barbera JA, Eddahibi S, Flores SC, Grimminger F, Jones PL, Maitland ML, Michelakis ED, Morrell NW, Newman JH, Rabinovitch M, Schermuly R, Stenmark KR, Voelkel NF, Yuan JX, Humbert M.** Inflammation, growth factors, and pulmonary vascular remodeling. *J Am Coll Cardiol* 54: S10–S19, 2009.
41. **Holt AP, Haughton EL, Lalor PF, Filer A, Buckley CD, Adams DH.** Liver myofibroblasts regulate infiltration and positioning of lymphocytes in human liver. *Gastroenterology* 136: 705–714, 2009.

42. **Huang SC, Everts B, Ivanova Y, O'Sullivan D, Nascimento M, Smith AM, Beatty W, Love-Gregory L, Lam WY, O'Neill CM, Yan C, Du H, Abumrad NA, Urban JF Jr, Artyomov MN, Pearce EL, Pearce EJ.** Cell-intrinsic lysosomal lipolysis is essential for alternative activation of macrophages. *Nat Immunol* 15: 846–855, 2014.
43. **Iijima J, Konno K, Itano N.** Inflammatory alterations of the extracellular matrix in the tumor microenvironment. *Cancers (Basel)* 3: 3189–3205, 2011.
44. **Kaufman J, Graf BA, Leung EC, Pollock SJ, Koumas L, Reddy SY, Blieden TM, Smith TJ, Phipps RP.** Fibroblasts as sentinel cells: role of the CDcd40-CDcd40 ligand system in fibroblast activation and lung inflammation and fibrosis. *Chest* 120: 53S–55S, 2001.
45. **Kessler R, Faller M, Weitzenblum E, Chaouat A, Aykut A, Ducolone A, Ehrhart M, Oswald-Mammosser M.** "Natural history" of pulmonary hypertension in a series of 131 patients with chronic obstructive lung disease. *Am J Respir Crit Care Med* 164: 219–224, 2001.
46. **Koppenol WH, Bounds PL, Dang CV.** Otto Warburg's contributions to current concepts of cancer metabolism. *Nat Rev Cancer* 11: 325–337, 2011.
47. **Krawczyk CM, Holowka T, Sun J, Blagih J, Amiel E, DeBerardinis RJ, Cross JR, Jung E, Thompson CB, Jones RG, Pearce EJ.** Toll-like receptor-induced changes in glycolytic metabolism regulate dendritic cell activation. *Blood* 115: 4742–4749, 2010.
48. **Kuang SQ, Geng L, Prakash SK, Cao JM, Guo S, Villamizar C, Kwartler CS, Peters AM, Brasier AR, Milewicz DM.** Aortic remodeling after transverse aortic constriction in mice is attenuated with AT1 receptor blockade. *Arterioscler Thromb Vasc Biol* 33: 2172–2179, 2013.
49. **Li M, Riddle SR, Frid MG, El Kasmi KC, McKinsey TA, Sokol RJ, Strassheim D, Meyrick B, Yeager ME, Flockton AR, McKeon BA, Lemon DD, Horn TR, Anwar A, Barajas C, Stenmark KR.** Emergence of fibroblasts with a proinflammatory epigenetically altered phenotype in severe hypoxic pulmonary hypertension. *J Immunol* 187: 2711–2722, 2011.
50. **Lv L, Li D, Zhao D, Lin R, Chu Y, Zhang H, Zha Z, Liu Y, Li Z, Xu Y, Wang G, Huang Y, Xiong Y, Guan KL, Lei QY.** Acetylation targets the M2 isoform of pyruvate kinase for degradation through chaperone-mediated autophagy and promotes tumor growth. *Mol Cell* 42: 719–730, 2011.
51. **Mace TA, Ameen Z, Collins A, Wojcik S, Mair M, Young GS, Fuchs JR, Eubank TD, Frankel WL, Bekaii-Saab T, Bloomston M, Lesinski GB.** Pancreatic cancer-associated stellate cells promote differentiation of myeloid-derived suppressor cells in a STAT3-dependent manner. *Cancer Res* 73: 3007–3018, 2013.
52. **Makeyev EV, Zhang J, Carrasco MA, Maniatis T.** The microRNA miR-124 promotes neuronal differentiation by triggering brain-specific alternative pre-mRNA splicing. *Mol Cell* 27: 435–448, 2007.
53. **Maron BA, Choudhary G, Khan UA, Jankowich MD, McChesney H, Ferrazzani SJ, Gaddam S, Sharma S, Opotowsky AR, Bhatt DL, Rocco TP, Aragam JR.** Clinical profile and underdiagnosis of pulmonary hypertension in US veteran patients. *Circ Heart Fail* 6: 906–912, 2013.
54. **Marsboom G, Wietholt C, Haney CR, Toth PT, Ryan JJ, Morrow E, Thenappan T, Bache-Wiig P, Piao L, Paul J, Chen CT, Archer SL.** Lung ^{18}F-fluorodeoxyglucose positron emission tomography for diagnosis and monitoring of pulmonary arterial hypertension. *Am J Respir Crit Care Med* 185: 670–679, 2012.
55. **Martinez-Outschoorn UE, Lisanti MP, Sotgia F.** Catabolic cancer-associated fibroblasts transfer energy and biomass to anabolic cancer cells, fueling tumor growth. *Semin Cancer Biol* 25: 47–60, 2014.
56. **Metallo CM, Vander Heiden MG.** Metabolism strikes back: metabolic flux regulates cell signaling. *Genes Dev* 24: 2717–2722, 2010.
57. **Michelakis ED, McMurtry MS, Wu XC, Dyck JR, Moudgil R, Hopkins TA, Lopaschuk GD, Puttagunta L, Waite R, Archer SL.** Dichloroacetate, a metabolic modulator, prevents and reverses chronic hypoxic pulmonary hypertension in rats: role of increased expression and activity of voltage-gated potassium channels. *Circulation* 105: 244–250, 2002.
58. **Murray PJ, Wynn TA.** Protective and pathogenic functions of macrophage subsets. *Nat Rev Immunol* 11: 723–737, 2011.
59. **O'Sullivan D, Pearce EL.** Targeting T cell metabolism for therapy. *Trends Immunol* 36: 71–80, 2015.
60. **Odegaard JI, Chawla A.** Alternative macrophage activation and metabolism. *Annu Rev Pathol* 6: 275–297, 2011.
61. **Ohlund D, Elyada E, Tuveson D.** Fibroblast heterogeneity in the cancer wound. *J Exp Med* 211: 1503–1523, 2014.
62. **Ostuni R, Kratochvill F, Murray PJ, Natoli G.** Macrophages and cancer: from mechanisms to therapeutic implications. *Trends Immunol* 36: 229–239, 2015.
63. **Otranto M, Sarrazy V, Bonte F, Hinz B, Gabbiani G, Desmouliere A.** The role of the myofibroblast in tumor stroma remodeling. *Cell Adh Migr* 6: 203–219, 2012.
64. **Palsson-McDermott EM, Curtis AM, Goel G, Lauterbach MA, Sheedy FJ, Gleeson LE, van den Bosch MW, Quinn SR, Domingo-Fernandez R, Johnston DG, Jiang JK, Israelsen WJ, Keane J, Thomas C, Clish C, Vanden Heiden M, Xavier RJ, O'Neill LA.** Pyruvate kinase M2 regulates Hif-1alpha activity and IL-1beta induction and is a critical determinant of the Warburg effect in LPS-activated macrophages. *Cell Metab* 21: 65–80, 2015.
65. **Palsson-McDermott EM, O'Neill LA.** The Warburg effect then and now: from cancer to inflammatory diseases. *Bioessays* 35: 965–973, 2013.
66. **Panzhinskiy E, Zawada WM, Stenmark KR, Das M.** Hypoxia induces unique proliferative response in adventitial fibroblasts by activating PDGFbeta receptor-JNK1 signalling. *Cardiovasc Res* 95: 356–365, 2012.
67. **Paulin R, Michelakis ED.** The metabolic theory of pulmonary arterial hypertension. *Circ Res* 115: 148–164, 2014.
68. **Pavlides S, Whitaker-Menezes D, Castello-Cros R, Flomenberg N, Witkiewicz AK, Frank PG, Casimiro MC, Wang C, Fortina P, Addya S, Pestell RG, Martinez-Outschoorn UE, Sotgia F, Lisanti MP.** The reverse Warburg effect: aerobic glycolysis in cancer associated fibroblasts and the tumor stroma. *Cell Cycle* 8: 3984–4001, 2009.
69. **Pearce EJ, Everts B.** Dendritic cell metabolism. *Nat Rev Immunol* 15: 18–29, 2015.
70. **Pesce JT, Ramalingam TR, Mentink-Kane MM, Wilson MS, El Kasmi KC, Smith AM, Thompson RW, Cheever AW, Murray PJ, Wynn TA.** Arginase-1-expressing macrophages suppress Th2 cytokine-driven inflammation and fibrosis. *PLoS Pathog* 5: e1000371, 2009.
71. **Piao L, Marsboom G, Archer SL.** Mitochondrial metabolic adaptation in right ventricular hypertrophy and failure. *J Mol Med (Berl)* 88: 1011–1020, 2010.
72. **Psaltis PJ, Puranik AS, Spoon DB, Chue CD, Hoffman SJ, Witt TA, Delacroix S, Kleppe LS, Mueske CS, Pan S, Gulati R, Simari RD.** Characterization of a resident population of adventitial macrophage progenitor cells in postnatal vasculature. *Circ Res* 115: 364–375, 2014.
73. **Pugliese SC, Poth JM, Fini MA, Olschewski A, El Kasmi KC, Stenmark KR.** The role of inflammation in hypoxic pulmonary hypertension: from cellular mechanisms to clinical phenotypes. *Am J Physiol Lung Cell Mol Physiol* 308: L229–L252, 2015.
74. **Qualls JE, Subramanian C, Rafi W, Smith AM, Balouzian L, DeFreitas AA, Shirey KA, Reutterer B, Kernbauer E, Stockinger S, Decker T, Miyairi I, Vogel SN, Salgame P, Rock CO, Murray PJ.** Sustained generation of nitric oxide and control of mycobacterial infection requires argininosuccinate synthase 1. *Cell Host Microbe* 12: 313–323, 2012.
75. **Rasanen K, Vaheri A.** Activation of fibroblasts in cancer stroma. *Exp Cell Res* 316: 2713–2722, 2010.
76. **Rodriguez-Prados JC, Traves PG, Cuenca J, Rico D, Aragones J, Martin-Sanz P, Cascante M, Bosca L.** Substrate fate in activated macrophages: a comparison between innate, classic, and alternative activation. *J Immunol* 185: 605–614, 2010.
77. **Savai R, Pullamsetti SS, Kolbe J, Bieniek E, Voswinckel R, Fink L, Scheed A, Ritter C, Dahal BK, Vater A, Klussmann S, Ghofrani HA, Weissmann N, Klepetko W, Banat GA, Seeger W, Grimminger F, Schermuly RT.** Immune and inflammatory cell involvement in the pathology of idiopathic pulmonary arterial hypertension. *Am J Respir Crit Care Med* 186: 897–908, 2012.
78. **Seeger W, Adir Y, Barbera JA, Champion H, Coghlan JG, Cottin V, De Marco T, Galie N, Ghio S, Gibbs S, Martinez FJ, Semigran MJ, Simonneau G, Wells AU, Vachiery JL.** Pulmonary hypertension in chronic lung diseases. *J Am Coll Cardiol* 62: D109–D116, 2013.
79. **Servais C, Erez N.** From sentinel cells to inflammatory culprits: cancer-associated fibroblasts in tumour-related inflammation. *J Pathol* 229: 198–207, 2013.
80. **Simonneau G, Gatzoulis MA, Adatia I, Celermajer D, Denton C, Ghofrani A, Gomez Sanchez MA, Krishna Kumar R, Landzberg M, Machado RF, Olschewski H, Robbins IM, Souza R.** Updated clinical

classification of pulmonary hypertension. *J Am Coll Cardiol* 62: D34–D41, 2013.

81. **Sivakumar P, Ntolios P, Jenkins G, Laurent G.** Into the matrix: targeting fibroblasts in pulmonary fibrosis. *Curr Opin Pulm Med* 18: 462–469, 2012.
82. **Smith RS, Smith TJ, Blieden TM, Phipps RP.** Fibroblasts as sentinel cells. Synthesis of chemokines and regulation of inflammation. *Am J Pathol* 151: 317–322, 1997.
83. **Stenmark KR, Fagan KA, Frid MG.** Hypoxia-induced pulmonary vascular remodeling: cellular and molecular mechanisms. *Circ Res* 99: 675–691, 2006.
84. **Stenmark KR, Frid MG, Yeager M, Li M, Riddle S, McKinsey T, El Kasmi KC.** Targeting the adventitial microenvironment in pulmonary hypertension: a potential approach to therapy that considers epigenetic change. *Pulm Circ* 2: 3–14, 2012.
85. **Stenmark KR, Meyrick B, Galie N, Mooi WJ, McMurtry IF.** Animal models of pulmonary arterial hypertension: the hope for etiological discovery and pharmacological cure. *Am J Physiol Lung Cell Mol Physiol* 297: L1013–L1032, 2009.
86. **Stenmark KR, Nozik-Grayck E, Gerasimovskaya E, Anwar A, Li M, Riddle S, Frid M.** The adventitia: essential role in pulmonary vascular remodeling. *Compr Physiol* 1: 141–161, 2011.
87. **Stenmark KR, Yeager ME, El Kasmi KC, Nozik-Grayck E, Gerasimovskaya EV, Li M, Riddle SR, Frid MG.** The adventitia: essential regulator of vascular wall structure and function. *Annu Rev Physiol* 75: 23–47, 2013.
88. **Sutendra G, Bonnet S, Rochefort G, Haromy A, Folmes KD, Lopaschuk GD, Dyck JR, Michelakis ED.** Fatty acid oxidation and malonyl-CoA decarboxylase in the vascular remodeling of pulmonary hypertension. *Sci Transl Med* 2: 44ra58, 2010.
89. **Tang PC, Qin L, Zielonka J, Zhou J, Matte-Martone C, Bergaya S, van Rooijen N, Shlomchik WD, Min W, Sessa WC, Pober JS, Tellides G.** MyD88-dependent, superoxide-initiated inflammation is necessary for flow-mediated inward remodeling of conduit arteries. *J Exp Med* 205: 3159–3171, 2008.
90. **Tannahill GM, Curtis AM, Adamik J, Palsson-McDermott EM, McGettrick AF, Goel G, Frezza C, Bernard NJ, Kelly B, Foley NH, Zheng L, Gardet A, Tong Z, Jany SS, Corr SC, Haneklaus M, Caffrey BE, Pierce K, Walmsley S, Beasley FC, Cummins E, Nizet V, Whyte M, Taylor CT, Lin H, Masters SL, Gottlieb E, Kelly VP, Clish C, Auron PE, Xavier RJ, O'Neill LA.** Succinate is an inflammatory signal that induces IL-1beta through HIF-1alpha. *Nature* 496: 238–242, 2013.
91. **Tellides G, Pober JS.** Inflammatory and immune responses in the arterial media. *Circ Res* 116: 312–322, 2015.
92. **Torres S, Bartolome RA, Mendes M, Barderas R, Fernandez-Acenero MJ, Pelaez-Garcia A, Pena C, Lopez-Lucendo M, Villar-Vazquez R, de Herreros AG, Bonilla F, Casal JI.** Proteome profiling of cancer-associated fibroblasts identifies novel proinflammatory signatures and prognostic markers for colorectal cancer. *Clin Cancer Res* 19: 6006–6019, 2013.
93. **Tuder RM, Archer SL, Dorfmuller P, Erzurum SC, Guignabert C, Michelakis E, Rabinovitch M, Schermuly R, Stenmark KR, Morrell NW.** Relevant issues in the pathology and pathobiology of pulmonary hypertension. *J Am Coll Cardiol* 62: D4–D12, 2013.
95. **Tuder RM, Davis LA, Graham BB.** Targeting energetic metabolism: a new frontier in the pathogenesis and treatment of pulmonary hypertension. *Am J Respir Crit Care Med* 185: 260–266, 2012.
96. **van Nieuwenhoven FA, Turner NA.** The role of cardiac fibroblasts in the transition from inflammation to fibrosis following myocardial infarction. *Vascul Pharmacol* 58: 182–188, 2013.
97. **Vats D, Mukundan L, Odegaard JI, Zhang L, Smith KL, Morel CR, Wagner RA, Greaves DR, Murray PJ, Chawla A.** Oxidative metabolism and PGC-1beta attenuate macrophage-mediated inflammation. *Cell Metab* 4: 13–24, 2006.
98. **Wang D, Zhang H, Li M, Frid MG, Flockton AR, McKeon BA, Yeager ME, Fini MA, Morrell NW, Pullamsetti SS, Velegala S, Seeger W, McKinsey TA, Sucharov CC, Stenmark KR.** MicroRNA-124 controls the proliferative, migratory, and inflammatory phenotype of pulmonary vascular fibroblasts. *Circ Res* 114: 67–78, 2014.
99. **Wang J, Ying G, Wang J, Jung Y, Lu J, Zhu J, Pienta KJ, Taichman RS.** Characterization of phosphoglycerate kinase-1 expression of stromal cells derived from tumor microenvironment in prostate cancer progression. *Cancer Res* 70: 471–480, 2010.
100. **Wang P, Chen L, Zhang J, Chen H, Fan J, Wang K, Luo J, Chen Z, Meng Z, Liu L.** Methylation-mediated silencing of the miR-124 genes facilitates pancreatic cancer progression and metastasis by targeting Rac1. *Oncogene* 33: 514–524, 2014.
101. **Wellen KE, Thompson CB.** A two-way street: reciprocal regulation of metabolism and signalling. *Nat Rev Mol Cell Biol* 13: 270–276, 2012.
102. **Wynn TA.** Cellular and molecular mechanisms of fibrosis. *J Pathol* 214: 199–210, 2008.
103. **Yang P, Li Z, Fu R, Wu H, Li Z.** Pyruvate kinase M2 facilitates colon cancer cell migration via the modulation of STAT3 signalling. *Cell Signal* 26: 1853–1862, 2014.
104. **Yang P, Li Z, Li H, Lu Y, Wu H, Li Z.** Pyruvate kinase M2 accelerates pro-inflammatory cytokine secretion and cell proliferation induced by lipopolysaccharide in colorectal cancer. *Cell Signal* 27: 1525–1532, 2015.
105. **Zhao L, Ashek A, Wang L, Fang W, Dabral S, Dubois O, Cupitt J, Pullamsetti SS, Cotroneo E, Jones H, Tomasi G, Nguyen QD, Aboagye EO, El-Bahrawy MA, Barnes G, Howard LS, Gibbs JS, Gsell W, He JG, Wilkins MR.** Heterogeneity in lung (18)FDG uptake in pulmonary arterial hypertension: potential of dynamic (18)FDG positron emission tomography with kinetic analysis as a bridging biomarker for pulmonary vascular remodeling targeted treatments. *Circulation* 128: 1214–1224, 2013.
106. **Zhao L, Chen CN, Hajji N, Oliver E, Cotroneo E, Wharton J, Wang D, Li M, McKinsey TA, Stenmark KR, Wilkins MR.** Histone deacetylation inhibition in pulmonary hypertension: therapeutic potential of valproic acid and suberoylanilide hydroxamic acid. *Circulation* 126: 455–467, 2012.
107. **Zhao S, Xu W, Jiang W, Yu W, Lin Y, Zhang T, Yao J, Zhou L, Zeng Y, Li H, Li Y, Shi J, An W, Hancock SM, He F, Qin L, Chin J, Yang P, Chen X, Lei Q, Xiong Y, Guan KL.** Regulation of cellular metabolism by protein lysine acetylation. *Science* 327: 1000–1004, 2010.
108. **Zhou J, Tang PC, Qin L, Gayed PM, Li W, Skokos EA, Kyriakides TR, Pober JS, Tellides G.** CXCR3-dependent accumulation and activation of perivascular macrophages is necessary for homeostatic arterial remodeling to hemodynamic stresses. *J Exp Med* 207: 1951–1966, 2010.

HHS Public Access

Author manuscript

Semin Immunol. Author manuscript; available in PMC 2016 October 09.

Published in final edited form as:

Semin Immunol. 2015 August ; 27(4): 267–275. doi:10.1016/j.smim.2015.09.001.

Contribution of Metabolic Reprogramming to Macrophage Plasticity and Function

Karim C. El Kasmi[1,*] and **Kurt R. Stenmark**[2]

[1]University of Colorado Denver, School of Medicine, Department of Pediatrics, Section of Pediatric Gastroenterology, Hepatology and Nutrition, Aurora Colorado, USA.

[2]University of Colorado Denver, School of Medicine, Section of Pediatric Critical Care and Cardiovascular Pulmonary Research, Department of Medicine, Aurora Colorado, USA.

Abstract

Macrophages display a spectrum of functional activation phenotypes depending on the composition of the microenvironment they reside in, including type of tissue/organ and character of injurious challenge they are exposed to. Our understanding of how macrophage plasticity is regulated by the local microenvironment is still limited. Here we review and discuss the recent literature regarding the contribution of cellular metabolic pathways to the ability of the macrophage to sense the microenvironment and to alter its function. We propose that distinct alterations in the microenvironment induce a spectrum of inducible and reversible metabolic programs that might form the basis of the inducible and reversible spectrum of functional macrophage activation/polarization phenotypes. We highlight that metabolic pathways in the bidirectional communication between macrophages and stromals cells are an important component of chronic inflammatory conditions. Recent work demonstrates that inflammatory macrophage activation is tightly associated with metabolic reprogramming to aerobic glycolysis, an altered TCA cycle, and reduced mitochondrial respiration. We review cytosolic and mitochondrial mechanisms that promote initiation and maintenance of macrophage activation as they relate to increased aerobic glycolysis and highlight potential pathways through which anti-inflammatory IL-10 could promote macrophage deactivation. Finally, we propose that in addition to their role in energy generation and regulation of apoptosis, mitochondria reprogram their metabolism to also participate regulating macrophage activation and plasticity.

Keywords

inflammation; aerobic glycolysis; mitochondria; fibroblast; nitric oxide; arginase1; IL-10; Krebs cycle

[*]Correspondence to Karim.Elkasmi@ucdenver.edu.

Disclosure statement

The authors declare no financial interests in any of the work submitted here.

The authors are not aware of any affiliations, memberships, funding, or financial holdings that might be perceived as influencing the objectivity of this review.

1. Sensing of the microenvironment through metabolic adaptation

Macrophages are present in abundant numbers in all tissues of the body where they are regarded as critical in both monitoring and regulating the local tissue microenvironment, including the coordination of organ specific functions of tissue resident cells, such as fibroblasts and parenchymal cells [1, 2]. It is increasingly recognized that the composition of the local tissue microenvironment (e.g. the composition of metabolites, cytokines, oxygen tension, inflammatory signals) including signals from other tissue cells are critical determinants of macrophage metabolism and functional plasticity [3–11]. Considering that macrophages are highly sensitive to variations in concentrations of metabolites [3, 7, 8, 10, 12–15], substrates [10, 12, 16], toxins [17], oxygen tension [5, 18–21], acidification [9], osmolality [22], and other molecular components associated with alterations within the microenvironment (e.g. cytokines) [11, 23, 24], changes in cellular metabolism in macrophages can function as an important primary indicator of altered tissue homeostasis and thus as a critical regulator of macrophage functional responses [25]. Cellular metabolism in turn may directly affect the microenvironment through generation and/or depletion of metabolites [12]. Furthermore, organ specific differences in availability of substrates, metabolites, or oxygen tension, together with base-line differences in macrophage expression levels of genes that encode for proteins that regulate metabolic and transcriptional processes might account for specificity in macrophage responsiveness across tissues. It follows that the functional phenotype of tissue macrophages may be in near constant flux, continuously changing in response to local environmental cues and local metabolic conditions. This versatility of tissue macrophages (i.e. functional plasticity) is reflected by a vast variety, maybe infinite, number of transcriptional, and possibly metabolic phenotypes [4–6, 8, 26]. For example, during normal homeostasis (e.g. absence of pro-inflammatory stimuli), the resident macrophage must exhibit a functional phenotype that promotes and maintains homeostasis. In contrast, in the presence of tissue stimulation or injury (e.g. pro-inflammatory stimuli), macrophages must detect microenvironmental alterations and actively change from a “base-line” transcriptional and metabolic program that promoted homeostasis into one that is compatible with mounting a pro-inflammatory response, which must return to baseline, once the inciting stimulus has been cleared. Thus, transcriptional and metabolic programs within the macrophage must be inducible and reversible on demand and responsive to environmental cues such that macrophage activation occurs in a regulated fashion with regard to amplitude and duration of activation. These programs must further be tailored to the challenge and to the specific organ/tissue to preserve the integrity and specific organ function [9, 27–29]. Thus, a spectrum of inducible and reversible metabolic programs might form the basis of the inducible and reversible spectrum of functional macrophage activation/polarization phenotypes [1, 2, 30–32]. Here, we review recent evidence that suggests that macrophage function is indeed directly and tightly associated with alterations in cellular metabolism and that macrophage plasticity is directly linked to the ability of the macrophage to alter or reprogram cellular metabolism.

2. Metabolic adaptations associated with inflammatory macrophage activation

ATP production to provide energy for cellular function is essential for cells, including macrophages in both homeostatic conditions and under stress. Glucose is the principal source that can be used for ATP production through two directly linked pathways. The upstream pathway involves metabolism of glucose to pyruvate in the cytosol, where phosphates are transferred from glycolytic intermediates to generate ATP (yielding a net production of 2 ATP molecules). The downstream pathway is the mitochondrial tricarboxylic cycle (TCA cycle, also known as Krebs cycle or citric acid cycle) which is directly linked to glycolysis because pyruvate is converted into acetyl-CoA, which then enters the TCA cycle to generate the reducing equivalents nicotin-amide adenine dinucleotide (NADH) and flavin adenine dinucleotide (FADH2), which donate electrons to the electron transport chain in the mitochondrial oxidative phosphorylation (OXPHOS), in which oxygen serves a electron acceptor to support ATP generation by ATP synthase (yielding a net production of 36 ATP molecules) (Figure 1). Because complex 2 of the respiratory chain (SDH, succinate dehydrogenase) is part of the TCS cycle, a fully functional TCA cycle is tightly linked to fully functional oxidative phosphorylation, and mitochondrial function. When pyruvate becomes limiting due to reduced glycolysis, cells can also metabolize glutamine or fatty acids to replenish the TCA cycle and maintain OXPHOS. In contrast, when oxygen becomes limiting or the TCA cycle becomes interrupted (see below) cells reprogram metabolism to produce ATP by diverting glycolytic pyruvate to lactate instead of acetyl-CoA. Although glycolysis yields less ATP than OXPHOS (2 vs. 36 ATP molecules), the speed of ATP generation in the former is quicker than in the latter, which is potentially critical to maintain energy levels.

It is believed that under homeostatic conditions macrophages exhibit a metabolic profile (or base line metabolism) consistent with utilizing glucose mainly through the TCA cycle and utilization of oxygen for mitochondrial oxidative phosphorylation (OXPHOS) to generate ATP [5–7, 10, 33, 34] (Figure 1). In contrast, the hallmark metabolic adjustment observed in the inflammatory macrophage (macrophages activated with LPS or the combination of LPS and IFNγ that produce pro-inflammatory mediators and cytokines [4, 10, 35, 36]) at least *in vitro*, is decreased utilization of the TCA cycle and decreased OXPHOS together with increased metabolism of glucose to lactate (glycolysis) [4, 5, 8, 33] (Figure 2). Importantly, this metabolic adaptation occurs without lack of oxygen, and has thus been referred to as “aerobic glycolysis” [4, 8, 34, 37–41]. Reduction in mitochondrial oxidative phosphorylation is associated with accumulation of mitochondrial TCA intermediates, such as citrate, succinate, and fumarate (Figure 2) and increased consumption of glutamine and arginine [3, 8, 12, 42–45]. Importantly, this metabolic adaptation is required for pro-inflammatory activation (e.g. in response to LPS) and expression of proper effector function [3–8, 33, 36–41, 46, 47]. Intriguingly, the anti-inflammatory cytokine IL-10 limits glycolysis and blocks activation of dendritic cells in response to Toll-like receptor (TLR) activation [41].

In contrast, the metabolic phenotype observed in IL-4 activated macrophages (so called alternatively activated, M2 macrophages [48]) exhibits absence of aerobic glycolysis and presence of OXPHOS [35, 36]. In addition, it has been demonstrated that IL-4 activated macrophages are very dependent on glutamine together with up-regulated expression of a particular nucleotide sugar, Uridine diphosphate *N*-acetylglucosamine (UDP-GlcNAc) [36]. Because UDP-GlcNAc is required for protein glycosylation, the authors hypothesized that this process might be important for functioning of alternatively activated macrophages, because typical M2 macrophage receptors are glycosylated, although the exact functional relevance of UDP-GlcNAc in M2 macrophages remains elusive [4, 35, 36]. Certain chronic conditions that involve IL-4 signaling (e.g. parasite infestation, allergy, asthma) might be associated with continuous maintenance of macrophages in an OXPHOS state, while on the other hand chronic inflammatory conditions might be associated with macrophages arresting in aerobic glycolysis [29]. The metabolic phenotypes of resident macrophages across tissues under normal homeostatic conditions or under stress conditions and exactly how local metabolic cues promote and regulate distinct metabolic phenotypes of tissue macrophages, especially in vivo, remains unclear [36]. Moreover, whether reprogramming of metabolism can be harnessed to interfere with macrophage function awaits future analysis [4, 12, 29].

3. Functional consequences of metabolic adaptation in macrophages

An important question is why do inflammatory macrophages switch to aerobic glycolysis in addition to altering mitochondrial metabolism and reducing mitochondrial respiration? This seemingly paradoxical metabolic phenomenon of an increase in glycolysis with increased production of lactate at the cost of repressed mitochondrial respiration (reduced OXPHOS) despite presence of oxygen was first described almost a century ago in cancer cells by the Nobel Laureate Otto Warburg and is now commonly referred to as “Warburg effect” or “Warburg metabolism” [49]. The metabolic adaptations in tumor cells are thought to be driven largely by somatic mutations, whereas those in inflammatory cells likely occur independent of somatic mutations. Therefore, as opposed to cancer cells, metabolic reprogramming in inflammatory macrophages may have evolved as a quickly inducible, adaptable and potentially reversible cellular process that can quickly relay the sensing of the microenvironment to the transcriptional machinery and evoke, as well as terminate, effector functions. Considering that inflammatory macrophages as opposed to cancer cells, are likely not proliferating at all or if so at a very slow rate, metabolic reprogramming to aerobic glycolysis must serve cellular functions other than proliferation. Among those, biosynthetic activities for the synthesis and secretion of a broad panel of immune mediators are likely candidates.

It is believed that increased aerobic glycolysis “makes up” for the reduced ATP synthesis in the face of attenuated mitochondrial respiration (due to inhibition of OXPHOS) as a survival response that serves to maintain cellular ATP levels. But perhaps most importantly, glycolytic ATP is thought to be a critical contributor to the maintenance of the mitochondrial membrane potential (and thus mitochondrial integrity) referred to as $\Delta\psi m$ [50]. In the presence of reduced mitochondrial respiration, the $\Delta\psi m$ would collapse over time, provoking cytochrome C release, and apoptosis with ensuing cell death. However, it has been demonstrated that $\Delta\psi m$ can be preserved by a mechanism that involves reversal of

ATP synthase, which under these conditions hydrolyses glycolytic ATP, concomitantly extruding protons from the mitochondrial matrix. As such, the mitochondria become ATP consumers (ATP provided by aerobic glycolysis) rather than ATP generators [50, 51] (Figure 2). This mechanism of ATP synthase reversal to maintain mitochondrial integrity has been observed in various pathologies [50, 51]. Moreover, this suggests that competence for aerobic glycolysis is a critical prerequisite in inflammatory macrophages to maintain $\Delta\Psi_m$ and thereby prevent apoptosis. At the same time, preserving mitochondrial integrity allows for continued accumulation of TCA cycle intermediates, which are important in promoting macrophage activation (e.g. succinate and citrate) (Figure 2). A principally similar metabolic adaptation may allow inflammatory macrophages to survive and maintain function in oxygen-deprived environments (e.g. inflammatory hypoxia).

Metabolites that accumulate in the presence of a decreased TCA cycle (e.g. succinate and citrate) and gene products that are upregulated to drive increased glycolysis such as hypoxia-inducible factor 1 (HIF1) can directly increase inflammatory gene transcription [8]. Moreover, reactive oxygen species (ROS) that are increased in the presence of reduced mitochondrial function can also increase inflammatory gene expression (see below) [52, 53]. In addition, metabolites generated downstream of aerobic glycolysis (e.g. lactate) can affect paracrine signaling with other tissue cells and other macrophages (as has been demonstrated in cellular crosstalk between cancer cells and macrophages within tumors [9, 14, 42]). In addition, by reallocating their cellular bioenergetics in favor of glycolytic metabolism, inflammatory macrophages are increasingly reliant on glucose and other nutrients, such as glutamine, for survival and function and if not counteracted become more sensitive to death by nutrient deprivation and local acidification (e.g. lactate). Thus, metabolic programs might also determine macrophage lifespan. Alternatively, akin to cancer cells, macrophages can become autotroph (i.e. independent on external sources) for certain substrates, nutrients and metabolites by inducing specific metabolic salvage pathways (e.g. L-Arginine recovery from citrulline and aspartate), which can maintain function and prolong survival despite nutrient depletion in the microenvironment [44]. In addition, neighboring parenchymal cells might generate metabolites that can be utilized for metabolic and inflammatory pathways in macrophages in auxotroph ways (e.g. lactate, succinate) [9]. Sustained availability of substrates and metabolites through autotrophic and auxotrophic pathways might be a prerequisite for the inflammatory macrophage to remain in aerobic glycolytic metabolism and allow ongoing generation of pro-inflammatory mediators (i.e. chronic inflammatory activation). This hypothesis is further supported by the observation of increased succinate levels in synovial fluid from patients with rheumatoid arthritis (RA) and in stool from animals and patients with inflammatory bowel disease (IBD) [13, 54, 55]. Succinate, which accumulates in cells exhibiting an aerobic glycolytic phenotype due to decreased TCA cycle function, has been shown to promote dendritic cell activation in paracrine ways, especially when combined with TLR activators [13, 52, 54, 56–58]. In addition, increased lactate production by glycolytic cancer cells has been shown to promote macrophage activation towards a phenotype that in turn promoted cancer growth. Lactate activated macrophages that genetically lacked Arginase1 expression no longer supported cancer growth [9]. This finding suggests that Arginase1 induced by paracrine (potentially also autocrine) lactate can

operate as part of a feed forward pathway in the bidirectional communication between macrophages and cancer cells and possible other tissue cells [9, 11, 29].

Yet another important reason to reprogram metabolism to increased glycolysis has been discovered recently by Haschemi et al. The authors demonstrated that LPS promoted the flow of glucose through both the glycolytic pathway and the PPP [33]. This is an important finding because glucose that is shunted through the PPP can reenter glycolysis upstream of pyruvate and continue to contribute to lactate production or enter the TCA [33]. At the same time, shunting glucose through the PPP, generates NADPH, which is required for oxidative reactions (NADPH oxidase-dependent respiratory burst) and glutathione biosynthesis to buffer reactive oxygen species (ROS), which are increased in the activated macrophage (Figure 2). In addition, utilization of the PPP generates substrates for nucleotide metabolism. Haschemi et al. discovered that LPS suppressed carbohydrate kinase-like (CARKL) protein which results in increased glucose flow through the PPP. Forced expression of CARKL antagonized glucose flux through the PPP and attenuated glycolytic flux, as well as LPS-induced cytokine and ROS production [33]. These findings indicate that CARKL is an important regulator of the ability of macrophages to reprogram cellular metabolism in order to equip macrophages with the necessary machinery to sustain mediator production.

4. Linking metabolic reprogramming with inflammatory macrophage activation

Based on above-mentioned Warburg phenotype in cancer cells, it has often been inferred that mitochondrial metabolism, that is the TCA cycle, was attenuated in macrophages that exhibit reprogramming to aerobic glycolysis. However, recent reports suggest that mitochondrial metabolism is not specifically attenuated but rather coordinately reprogrammed [36, 59]. It was found that TCA cycle reprogramming involved down-regulation of two important enzymatic steps, functionally interrupting the TCA cycle flow in LPS and interferon gamma (IFNγ) activated macrophages [36].

The first interruption involves significantly decreased expression of the enzyme isocitrate dehydrogenase (IDH), which results in substantial increases in citrate[36]. The proposed functional consequence is that citrate can be withdrawn from the TCA cycle and transported into the cytosol (by the mitochondrial citrate carrier in exchange for malate [3, 60]) and used for at least three important purposes; 1) the production of itaconic acid, which has been shown to have anti-microbial properties [14, 42] ; 2) the generation of large amounts of fatty acids that are required for the synthesis of new membrane lipids, arachidonic acid, and prostaglandins[3]; 3) the production of oxaloacetate, which produces NADPH (required to generate ROS through NADPH oxidase, and NO through inducible nitric oxide synthase (iNOS), which is typically highly induced in LPS/IFNγ activated macrophages) [3] (Figure 1). These data demonstrate a critical role for citrate derived from a disrupted TCA cycle in LPS and IFNγ activated macrophage function.

The second interruption of the TCA cycle occurs at the level of conversion of succinate to fumarate due to inhibition of succinate dehydrogenase (SDH) [36]. This SDH inhibition not only results in increased levels of succinate but also in reduced mitochondrial respiration

(because SDH constitutes complex II of the respiratory chain) [3]. Mitochondrial succinate transporters facilitate transport of accumulated succinate into the cytosol. Within the cytosol, succinate has been shown to inhibit prolyly-hydroxylases (PHDs), which normally facilitate the degradation of HIF1. The functional consequence of PHD inhibition is therefore accumulation of HIF1 protein [8]. Accumulated HIF1 protein directly promotes transcription of the proinflammatory cytokine IL-1β [8] and positively regulates expression of key enzymes (e.g. hexokinase1) and transporters (e.g. glucose transporter1, GLUT1) in the glycolytic pathway [8]. In the mitochondria, accumulated succinate can inhibit activity of complex I of the respiratory chain. This results in increased ROS production [61]. ROS can also inhibit PHDs in the cytosol [61, 62], which further stabilizes HIF1. ROS mediated PHD inhibition also positively affects NFκB signaling. In addition, succinate can accumulate in the extracellular space, as has been reported for a number of inflammatory conditions, including RA [13], IBD, and even cancer [55–57]. There, it can bind to a receptor (SUCNR1) on the cell surface and synergize with TLRs in the induction of inflammatory macrophage activation and potentiate production of inflammatory cytokines [58]. Succinate can also mediate dendritic cell chemotaxis and promote presentation of autoantigens and stimulation of autoimmunity [58]. Thus, succinate generated by a disrupted TCA cycle in metabolically reprogrammed macrophages appears to be an intracellular and paracrine metabolic signal that can initiate and maintain inflammatory macrophage activation.

A recent study has demonstrated that mitochondrial accumulation of succinate is not restricted to inflammatory macrophages [52]. Using a mouse model of ischemia and reperfusion injury in kidney, heart and brain, the authors demonstrated that a universal metabolic signature of ischemia is succinate accumulation. This succinate accumulation was also related to dysfunction of SDH. However, in contrast to the inhibition of SDH in LPS/IFNγ activated macrophages, the authors discovered that during ischemia SDH was not inhibited, but instead operated “in reverse” and reduced accumulated fumarate to succinate [52]. The reason for this “in reverse” operation of SDH is believed to be due increased accumulation of fumarate, which typically occurs under ischemic conditions. The most important finding of this study was that the accumulated succinate was causing damage once the tissues were re-perfused, and thus oxygen restored. The authors could show, that upon reperfusion, succinate is quickly re-oxidized by SDH (which now operates in its conventional forward fashion), which drives extensive ROS generation through reverse electron transport at mitochondrial complex I [52]. Collectively, these findings provide a mechanistic and teleological explanation for the observation that certain TCA cycle intermediates accumulate and also suggest that alterations in mitochondrial TCA activity are required for enabling inflammatory macrophage activation and constitute a means of paracrine signaling. Intriguingly, cancer cell metabolism is also associated with increased generation of TCA intermediates, such as succinate [59]. The implication of these findings is that hypothetically, in any situation of mitochondrial succinate accumulation and sufficient presence of oxygen, ROS production might substantially be increased at Complex I (Figure 2). Considering that ROS have also been recognized as an important activator of the inflammasome [63], TCA cycle disruption in LPS/IFNγ activated macrophages might promote inflammasome signaling. Whether SHD operation “in reverse” also underlies macrophage activation in inflammatory conditions during which oxygen becomes limiting

(i.e. inflammatory hypoxia) awaits further analysis. Furthermore, if the above-mentioned TCA cycle reprogramming also occurs in conditions in which macrophages are activated by LPS alone or by cytokines other than IFNγ remains further analysis.

The reprogramming of the TCA cycle towards inhibition of IDH and SDH requires that the precursors of succinate and citrate be fueled into the TCA cycle. This replenishing of the TCA cycle is referred to as anerplerosis. It has recently been proposed that in LPS/IFNγ activated macrophages coordinated increases in the activity of the aspartate-arginosuccinate cycle together with a modified aspartate-malate shuttle are an important metabolic adjustment to provide the disrupted TCA cycle with the intermediates fumarate and malate [36] (Figure 2). Importantly, upregulation of aspartate-arginosuccinate cycle together with the modified aspartate-malate shuttle has several additional potential consequences on inflammatory macrophage function in the presence of a disrupted TCA cycle:

(i) increased fumarate availability can further inhibit SDH activity and intensify succinate accumulation or promote operation of SDH “in reverse” (see above) [52].

(ii) malate is important within the malate-aspartate shuttle which usually regenerates NAD^+ within the cytosol to be used in glycolysis and promotes mitochondrial NADH synthesis for ATP generation; however, in LPS/IFNγ activated macrophages increased expression of iNOS results in high citrulline levels[44]; aspartate can now be used for the reaction with citrulline which generates argininosuccinate (Figure 2). Argininosuccinate is further metabolized to Arginine (which is the substrate for iNOS and so maintains the flux between arginine-succinate and citrulline-arginine cycle) and fumarate, which replenishes the TCA cycle (Figure 2).

What is the functional consequence of utilizing the argininosuccinate pathway in LPS/IFNγ activated macrophages?

The argininosuccinate pathway forms the molecular interface with the citrulline-arginine cycle to regenerate Arginine which allows continued NO production by iNOS [36, 44]. The ability to maintain NO generation has recently been shown to be a critical metabolic adaptation in macrophages to allow killing of intracellular mycobacteria [44, 64, 65]. In addition, IL-1β has also been shown to be critical in mycobacterial control in infected macrophages [66]. On the other hand, continuous activity of iNOS and generation of NO is also critical in inhibiting IL-1β generation through the inflammasome [67]. Thus, context dependent fine-tuning of macrophage function might be regulated through activity of the argininosuccinate pathway and thus also through arginine availability in the microenvironment.

NO also promotes inhibition of complex II (which is SDH) [68], re-reinforcing the above-mentioned break-point in the TCA cycle (Figure 2). This important role of the citrulline-arginine cycle is further supported by studies that show that in blood monocyte-derived DCs that express iNOS and are TLR activated , mitochondrial dysfunction coincided with the expression of iNOS and metabolic reprogramming to aerobic glycolysis occurred only in DC subsets that made NO [47]. Similar observations have been made in macrophages,

where NO promotes glycolysis [43, 47, 69]. NO also promotes electron leakiness resulting in increased ROS generation through inhibition of the respiratory chain, which further promotes PHD inhibition leading to HIF1 stabilization and subsequent cytokine generation [47, 68].

Regenerated arginine can also be used by arginase1 to promote glutamate synthesis from ornithine, which can replenish the disrupted TCA cycle. It has been suggested that the metabolism of glutamine through the gamma-amino-butyric acid (GABA) shunt is responsible for TCA anerplerosis in LPS activated macrophages [8], however it is unclear if the enzymes required for the GABA shunt are expressed in macrophages [36]. Therefore, TCA cycle anerplerosis might occur through glutamate derived from the metabolism of Arginine to ornithine by Arginase1. Considering the proposed inability to metabolize ornithine in the urea cycle in macrophages (because of the lack of expression of ornithine transcarbamylase [44]), ornithine to glutamate metabolism through Arginase1 poses an attractive alternative or additional source of TCA cycle anerplerosis [36].

Finally, through regeneration of arginine from citrulline and aspartate, inflammatory macrophages become autotroph for arginine [44]; this metabolic adaptation could be especially relevant for maintaining macrophage functionality at inflammatory sites where arginine concentrations may become quickly limiting [44]. In addition, T-cell proliferation in granulomatous responses (where M2 macrophage activation with high expression of Arginase1 predominates) might not only be linked to availability of arginine to fuel T cell proliferation [12] but also be linked to the regulation of metabolic programs in M2 macrophages that are necessary for provision of cytokines and other factors that support T cell proliferation.

Considering that Arginase1 is a HIF1 regulated gene [9, 11], these data support the hypothesis that metabolic adaptation towards a coordinated expression of HIF1 and Arginase1 together with a coordinated expression of the malate-aspartate, argininosuccinate, and citrulline arginine pathways might be critical to maintain anerplerosis of the TCA cycle in metabolically reprogrammed inflammatory macrophages. Evidently, these metabolic adaptations are potentially more important under the aspect of strong inflammatory activation of macrophages in response to LPS and IFNγ because this combination strongly induces expression of iNOS, and argininosuccinate synthase (ASS) and argininosuccinate lyase (ASL) (key enzymes within the argininosuccinate cycle) [44] (Figure 2). Whether reprogramming of the TCA cycle with inhibition of SDH and IDH and increasing the argininosuccinate cycle is a general metabolic adaptation in macrophages associated with a variety of inflammatory conditions awaits further experimentation. Considering that arginine concentrations can become very limiting in inflamed tissues, activity of the argininosuccinate shunt and arginine availability may turn out to be a critical determinant of metabolic adaption and ability to produce inflammatory cytokines in inflammatory macrophages[44, 45, 65]. Moreover, the relevance of this metabolic program in less inflammatory and chronic inflammatory conditions with low or absent LPS and IFNγ needs to be resolved. It is intriguing to speculate that in a manner analogous to cytochrome *c* release from the mitochondria in apoptosis, and analogous to the role of mitochondrial nucleotides in induction of inflammation [44], generation of inflammatory cytokines

regulated by mitochondrial metabolic reprogramming and subsequent generation of ROS and accumulation and release of TCA cycle intermediates such as succinate is yet another critical mitochondrial feature that has evolved to coordinate macrophage activation.

Finally, direct alteration of functional programs through epigenetic mechanisms that involve HIF1 can contribute to prolonged inflammatory activation and/or facilitate responses to subsequent challenge (a response which has been referred to as innate immune memory or trained immunity) [29, 46, 70].

5. Regulation of metabolic adaptation in inflammatory macrophages

Understanding the mechanisms that regulate metabolic reprogramming and that link metabolism to inflammatory activation and deactivation of macrophages is a critical aspect in macrophage biology. The concrete mechanisms that regulate metabolic reprogramming in macrophages have not yet been elucidated in detail.

Recent evidence in cancer cells shows that pyruvate kinase isoform M2 is upregulated relative to isoform M1 (PKM1), which has been proposed to plays an important role in the Warburg metabolism because PKM2 promotes metabolism of pyruvate to lactate [4]. The PKM2 and PKM1 isoforms are produced by alternative splicing from the *Pkm2* gene [71, 72]. PKM2 exists as a monomer or dimer, both of which have far lower enzymatic activity than the alternatively spliced PKM1, which results in metabolism of glucose to lactate instead of entry into the TCA cycle. PKM2 dimers can enter the nucleus and regulate gene transcription while tetramers are retained in the nucleus [71, 72]. Intriguingly, as recently shown in a seminal study by the Semenza lab, PKM2 can also act as a co-activator for HIF1, greatly increasing the transcriptional activity of HIF1 and thus transcription of key glycolytic enzymes, thereby enhanicng the glycolytic metabolic profile [71, 73]. Moreover, *PKM2* is in turn a target of HIF1, indicating a positive feed forward loop between PKM2 and HIF1 signaling [74]. A recent study by the O'Neill lab has further advanced our understanding of the role of PKM2 in regulation of metabolic adaptation and inflammatory activation of macrophages. This study shows that LPS promotes phosphorylation of PKM2 [4]. This event has also been shown to be important for the Warburg effect in hypoxia and cancer [72]. The LPS mediated phosphorylation event prevents tetramerization and also promotes formation of a PKM2/HIF1 complex within the nucleus. This PKM2/HIF1 complex can directly bind to the *IL1β* promoter and drive *IL1β* expression. Importantly, in isoform-specific *Pkm2* knockout macrophages, LPS failed to promote HIF1 stabilization and *IL1β* transcription. Highly specific small-molecule activators that force PKM2 tetramer formation also impaired LPS-induced PKM2/HIF1 complex formation and *IL1β* transcription. Importantly, enhancing tetramer formation attenuated S. *typhimurium*-in*duced* IL-1β and boosted IL-10 *in vivo*, associated with impaired clearance of infection [4]. These results are largely consistent with an earlier study by Yang et al., who demonstrated that inhibition of PKM2 prevented lethality in a mouse model of septic shock [75]. Intriguingly, dimeric PKM2 that localizes to the nucleus can also facilitate nuclear localization of STAT3 and act as a protein kinase that directly phosphorylates (on tyrosine 705) and activates nuclear STAT3 [76]. Importantly, it has been shown that constitutively active STAT3 induces chronically enhanced HIF1 protein levels and promotes aerobic glycolysis [77, 78].

This is consistent with *Hif1* being a known STAT3 target gene [11], and also demonstrates that STAT3 is sufficient to induce metabolic reprogramming in macrophages. Considering that un-phosphorylated STAT3 is continuously shuttling between the cytoplasm generating a nuclear reservoir of STAT3 available for activation [79], PKM2 mediated STAT3 activation could contribute to macrophage activation upon metabolic reprogramming [76, 80]. Because IL-6 is an external signal that induces phosphorylation of STAT3 [81], increased tissue IL-6 levels, as observed in chronic inflammatory conditions, and certain forms of fibrosis, and vascular remodeling associated with pulmonary hypertension [11, 82, 83] may be sufficient to promote metabolic reprogramming in tissue macrophages and thus initiate and maintain macrophage activation [11]. Intriguingly, Arginase1 is a known STAT3 and HIF1 target gene [9, 11, 29, 44, 45, 65] and genetic absence of *Hif1* or STAT3 prevents Arginase1 induction in response to IL-6 and paracrine lactate [9, 11]. We have previously reported that fibroblasts isolated from the perivascular space of animals with hypoxic pulmonary hypertension display an activated phenotype (high proliferation rate and ability to activate macrophages) [11]. Macrophages are activated by these fibroblasts by paracrine IL6 signaling. Fibroblast-activated macrophages have increased phosphorylated STAT3 and increased HIF1 signaling and increased Arginase1 expression. This Arginase1 expression is dependent on both STAT3 and HIF [11]. Thus, a hypothetical PKM2-STAT3-HIF1-Arginase1 signaling axis could be a critical regulator of metabolic reprogramming in macrophages in certain environmental conditions [77]. Specifically, intercellular signaling between fibroblasts and macrophages in the context of metabolic reprogramming to aerobic glycolysis in association with STAT3, HIF1 and Arginase1 activation can be an important component of chronic inflammatory processes [11].

Considering that coordinated increases in glycolysis and PPP alter the redox status of the cell and increase the NADH/NAD ratio [33], one question that arises is if transcription factor activity involved in metabolic reprogramming, macrophage activation, or macrophage deactivation (e.g. NFκB, STAT1, STAT3) is regulated by the redox status of the cell (i.e. NADH/NAD ratio). Indeed, certain transcriptional repressors (e.g. CtBP1) can “sense” the NADH/NAD ratio in cancer cells and affect expression of genes involved in cellular proliferation [84]. If an altered NADH/NAD ratio in inflammatory cells, including macrophages and fibroblasts with reprogrammed metabolism, regulates expression of pro-inflammatory genes through altering CtBP1 activity is currently being investigated in our laboratory. In addition, it was recently reported that in TLR activated macrophages, certain histonedeacetylases (HDACs) can promote inflammatory signaling and that this ability depended on direct cooperation with HIF1 [85, 86]. Moreover, interactions of HDACs with CtBP1 prevented pro-inflammatory activation, which is in keeping with the hypothesis that in macrophages the NADH/NAD ratio can be sensed and directly relayed to the regulation of pro-inflammatory macrophage activation [85]. These findings are also consistent with the emerging literature on the ability of histone modifying enzymes to affect macrophage function and polarization [85]. Considering that metabolites derived from the TCA cycle, such as acetyl-CoA (derived from citrate) and alpha-ketoglurate, can affect a host of epigenetic mechanisms, including jmjd3, a histone demethylase, which has been shown to promote macrophage responses to LPS but also to be important for alternative macrophage activation in response to IL-4 [87], metabolic reprogramming might co-operate directly with

epigenetic mechanisms to regulate macrophage plasticity[88]. Moreover, as reviewed previously by us, metabolic pathways could emerge as a critical regulator of epigenetic mechanisms that underlie cellular cross-talk between macrophages and fibroblasts in chronic inflammatory vascular remodeling and possibly other conditions associated with chronic inflammatory activation [20].

6. Metabolic pathways in macrophage de-activation

Our understanding of metabolic mechanisms that deactivate macrophages and contribute to resolution of inflammation is still very limited [20]. IL-10 is considered a master signal to promote deactivation of macrophages [89, 90]. All of IL-10's anti-inflammatory properties depend on STAT3 signaling [89, 91]. Through the activation of STAT3, IL-10 suppresses a subset of LPS induced genes, including pro-inflammatory cytokines, such as *Il12*, *Tnfa*, and *Il6* [89, 91]. An open question has been how IL-10 and STAT3 down-regulate a huge variety of inflammatory targets [89, 91, 92], especially in light of the above findings that suggest HIF1, STAT3, and PKM2 interactions in inflammation.

Considering that OXPHOS metabolism has been proposed to be a feature of resting macrophages and considering that prevention of transitioning towards increased aerobic glycolysis is associated with attenuation or even prevention of inflammatory activation of macrophages [89, 91, 92], one hypothesis is that anti-inflammatory IL-10 deactivates macrophages through suppression of the metabolic adaptation to aerobic glycolysis. Alternatively, anti-inflammatory IL-10 might deactivate macrophages only once the macrophage has transitioned back to OXPHOS (e.g. upon substrate depletion and inability to maintain aerobic glycolysis). In dendritic cells, TLR-initiated glycolytic metabolism was inhibited in the presence of concomitant IL-10, suggesting that IL-10 negatively regulates glycolytic metabolism in dendritic cells and that IL-10 generated a metabolic profile that was incompatible with pro-inflammatory activation [4, 41]. These findings indicate that IL-10 deactivates macrophages at least in part through enhancing OXPHOS metabolism in the presence of LPS. On the other hand, when PKM2 was enforced into a tetramer in LPS activated macrophages cellular metabolism exhibited increased OXPHOS, together with attenuated *IL1b* transcription and increased *Il10* transcription [4]. This finding suggests that OXPHOS metabolism enables generation of anti-inflammatory IL-10 in the presence of LPS [4]. Of note, in dendritic cells activated through TLR signaling by LPS, the metabolic adaptation to increased aerobic glycolysis is promoted by PI3K/Akt signaling and is inhibited by the adenosine monophosphate (AMP)–activated protein kinase (AMPK), and by the anti-inflammatory cytokine IL-10, when given concomitantly with LPS [41]. The hypothesis that IL-10 induced STAT3 can only exert anti-inflammatory properties when LPS is concomitantly present needs to be investigated; in favor of this hypothesis is the observation that PKM2 (LPS induced) can cooperate with STAT3 (IL-10 induced) [76, 77].

How IL-10 induced STAT3 would execute metabolic reprogramming towards OXPHOS in inflammatory macrophages remains unclear. Interestingly, macrophage autocrine IL-10 has been shown to induce Arginase1 expression in infected macrophages and this correlated with attenuated antimicrobial effector mechanisms in macrophages [4]. If IL-10 can affect metabolic adaptations to attenuate macrophage activation through induction of Arginase1

requires further investigation. Intriguingly, PKM2 has also been shown to bind and activate (phosphorylate) STAT3 [76, 77]. Thus, STAT3 availability or size of phosphorylated pool of nuclear STAT3 might determine responsiveness of LPS activated macrophages to anti-inflammatory IL-10. Alternatively, IL-10 might selectively block the ability of macrophages to adapt their metabolism to aerobic glycolysis by driving expression of genes that antagonize metabolic reprogramming to aerobic glycolysis or by inducing genes that contribute to depletion of essential substrates, such as glutamine or arginine. Precisely how PKM2, HIF1, and aerobic glycolysis affect both IL-10 production and IL-10 responsiveness requires further analysis.

Conclusions

Metabolic reprogramming with increased glycolysis and a coordinately re-arranged TCA cycle together with reduced mitochondrial oxidative phosphorylation promotes generation of intermediates (e.g. succinate, citrate) and ROS/NO that fulfill specific functions in terms of increasing the ability of the macrophage to mount the inflammatory response and to engage in paracrine signaling. In addition to increasing glycolysis and reprogramming the TCA cycle, cooperation between a modified malate-aspartate, an upregulated argininosuccinate-citrulline-arginine cycle appears to be critical for enabling inflammatory macrophage activation. Competence for increased aerobic glycolysis also appears to be a critical prerequisite to maintain mitochondrial membrane potential ($\Delta\Psi_m$) and thereby prevents apoptosis and allow for continuous generation of ROS/NO, succinate and other metabolites. It is therefore intriguing to speculate that in a manner analogous to cytochrome *c* release from the mitochondria in apoptosis, and analogous to the role of mitochondrial nucleotides in induction of inflammation [15], reprogramming of mitochondrial metabolism is yet another critical mitochondrial feature that has evolved to regulate macrophage activation and plasticity. An increased understanding of how flexibility in metabolic programs in macrophages is controlled and how external (i.e. microenvironmental) and internal signals regulate inducible and reversible metabolic programs and how metabolism and transcriptional networks are linked in macrophages in the course of inflammatory activation and resolution of inflammation is critical for a better understanding of macrophage plasticity and macrophage biology. If phenotypic conversion/re-education of macrophages from pro-inflammatory to a less inflammatory or even reparative macrophage phenotype can be achieved by manipulating metabolic sensors, such as CtBP1, or regulators such as PKM2 or CARKL awaits further studies.

Acknowledgements

This work was supported by National Institutes of Health Grants 1R01 HL125827, 1R01HL114887, and 5P01 HL014985. The authors would like to thank the members of their laboratories and other collaborators for work discussed in this review.

Figures were designed and prepared by Karen E. Rawlinson.

References

1. Kotas ME, Medzhitov R. Homeostasis, inflammation, and disease susceptibility. Cell. 2015; 160:816–827. [PubMed: 25723161]

2. Chovatiya R, Medzhitov R. Stress, inflammation, and defense of homeostasis. Mol Cell. 2014; 54:281–288. [PubMed: 24766892]
3. O'Neill LA. A critical role for citrate metabolism in LPS signalling. Biochem J. 2011; 438:e5–e6. [PubMed: 21867483]
4. Palsson-McDermott EM, Curtis AM, Goel G, Lauterbach MA, Sheedy FJ, Gleeson LE, et al. Pyruvate kinase M2 regulates Hif-1alpha activity and IL-1beta induction and is a critical determinant of the warburg effect in LPS-activated macrophages. Cell Metab. 2015; 21:65–80. [PubMed: 25565206]
5. Kelly B, O'Neill LA. Metabolic reprogramming in macrophages and dendritic cells in innate immunity. Cell Res. 2015
6. Galvan-Pena S, O'Neill LA. Metabolic reprograming in macrophage polarization. Front Immunol. 2014; 5:420. [PubMed: 25228902]
7. McGettrick AF, O'Neill LA. How metabolism generates signals during innate immunity and inflammation. J Biol Chem. 2013; 288:22893–22898. [PubMed: 23798679]
8. Tannahill GM, Curtis AM, Adamik J, Palsson-McDermott EM, McGettrick AF, Goel G, et al. Succinate is an inflammatory signal that induces IL-1beta through HIF-1alpha. Nature. 2013; 496:238–242. [PubMed: 23535595]
9. Colegio OR, Chu NQ, Szabo AL, Chu T, Rhebergen AM, Jairam V, et al. Functional polarization of tumour-associated macrophages by tumour-derived lactic acid. Nature. 2014; 513:559–563. [PubMed: 25043024]
10. Rodriguez-Prados JC, Traves PG, Cuenca J, Rico D, Aragones J, Martin-Sanz P, et al. Substrate fate in activated macrophages: a comparison between innate, classic, and alternative activation. J Immunol. 2010; 185:605–614. [PubMed: 20498354]
11. El Kasmi KC, Pugliese SC, Riddle SR, Poth JM, Anderson AL, Frid MG, et al. Adventitial fibroblasts induce a distinct proinflammatory/profibrotic macrophage phenotype in pulmonary hypertension. J Immunol. 2014; 193:597–609. [PubMed: 24928992]
12. Pesce JT, Ramalingam TR, Mentink-Kane MM, Wilson MS, El Kasmi KC, Smith AM, et al. Arginase-1-expressing macrophages suppress Th2 cytokine-driven inflammation and fibrosis. PLoS Pathog. 2009; 5:e1000371. [PubMed: 19360123]
13. Kim S, Hwang J, Xuan J, Jung YH, Cha HS, Kim KH. Global metabolite profiling of synovial fluid for the specific diagnosis of rheumatoid arthritis from other inflammatory arthritis. PLoS One. 2014; 9:e97501. [PubMed: 24887281]
14. Strelko CL, Lu W, Dufort FJ, Seyfried TN, Chiles TC, Rabinowitz JD, et al. Itaconic acid is a mammalian metabolite induced during macrophage activation. J Am Chem Soc. 2011; 133:16386–16389. [PubMed: 21919507]
15. Kuck JL, Obiako BO, Gorodnya OM, Pastukh VM, Kua J, Simmons JD, et al. Mitochondrial DNA damage-associated molecular patterns mediate a feed-forward cycle of bacteria-induced vascular injury in perfused rat lungs. Am J Physiol Lung Cell Mol Physiol. 2015; 308:L1078–L1085. [PubMed: 25795724]
16. Campbell L, Saville CR, Murray PJ, Cruickshank SM, Hardman MJ. Local arginase 1 activity is required for cutaneous wound healing. J Invest Dermatol. 2013; 133:2461–2470. [PubMed: 23552798]
17. El Kasmi KC, Anderson AL, Devereaux MW, Vue PM, Zhang W, Setchell KD, et al. Phytosterols promote liver injury and Kupffer cell activation in parenteral nutrition-associated liver disease. Sci Transl Med. 2013; 5:206ra137.
18. Fumagalli S, Perego C, Pischiutta F, Zanier ER, De Simoni MG. The ischemic environment drives microglia and macrophage function. Front Neurol. 2015; 6:81. [PubMed: 25904895]
19. Labiano S, Palazon A, Melero I. Immune Response Regulation in the Tumor Microenvironment by Hypoxia. Semin Oncol. 2015; 42:378–386. [PubMed: 25965356]
20. Pugliese SC, Poth JM, Fini MA, Olschewski A, El Kasmi KC, Stenmark KR. The role of inflammation in hypoxic pulmonary hypertension: from cellular mechanisms to clinical phenotypes. Am J Physiol Lung Cell Mol Physiol. 2015; 308:L229–L252. [PubMed: 25416383]

21. Ugocsai P, Hohenstatt A, Paragh G, Liebisch G, Langmann T, Wolf Z, et al. HIF-1beta determines ABCA1 expression under hypoxia in human macrophages. Int J Biochem Cell Biol. 2010; 42:241–252. [PubMed: 19828131]
22. Ip WK, Medzhitov R. Macrophages monitor tissue osmolarity and induce inflammatory response through NLRP3 and NLRC4 inflammasome activation. Nat Commun. 2015; 6:6931. [PubMed: 25959047]
23. Hashimoto-Kataoka T, Hosen N, Sonobe T, Arita Y, Yasui T, Masaki T, et al. Interleukin-6/interleukin-21 signaling axis is critical in the pathogenesis of pulmonary arterial hypertension. Proc Natl Acad Sci U S A. 2015; 112:E2677–E2686. [PubMed: 25941359]
24. Idzko M, Ferrari D, Eltzschig HK. Nucleotide signalling during inflammation. Nature. 2014; 509:310–317. [PubMed: 24828189]
25. Shalova IN, Lim JY, Chittezhath M, Zinkernagel AS, Beasley F, Hernandez-Jimenez E, et al. Human monocytes undergo functional re-programming during sepsis mediated by hypoxia-inducible factor-1alpha. Immunity. 2015; 42:484–498. [PubMed: 25746953]
26. Menon D, Coll R, O'Neill LA, Board PG. Glutathione transferase omega 1 is required for the lipopolysaccharide-stimulated induction of NADPH oxidase 1 and the production of reactive oxygen species in macrophages. Free Radic Biol Med. 2014; 73:318–327. [PubMed: 24873723]
27. Davies LC, Jenkins SJ, Allen JE, Taylor PR. Tissue-resident macrophages. Nat Immunol. 2013; 14:986–995. [PubMed: 24048120]
28. Murray PJ, Wynn TA. Protective and pathogenic functions of macrophage subsets. Nat Rev Immunol. 2011; 11:723–737. [PubMed: 21997792]
29. Stenmark KR, Tuder RM, El Kasmi KC. Metabolic Reprogramming and Inflammation Act in Concert to Control Vascular Remodeling in Hypoxic Pulmonary Hypertension. J Appl Physiol. 1985:2015. jap 00283 02015.
30. Sica A, Mantovani A. Macrophage plasticity and polarization: in vivo veritas. J Clin Invest. 2012; 122:787–795. [PubMed: 22378047]
31. Okabe Y, Medzhitov R. Tissue-specific signals control reversible program of localization and functional polarization of macrophages. Cell. 2014; 157:832–844. [PubMed: 24792964]
32. Medzhitov R, Horng T. Transcriptional control of the inflammatory response. Nat Rev Immunol. 2009; 9:692–703. [PubMed: 19859064]
33. Haschemi A, Kosma P, Gille L, Evans CR, Burant CF, Starkl P, et al. The sedoheptulose kinase CARKL directs macrophage polarization through control of glucose metabolism. Cell Metab. 2012; 15:813–826. [PubMed: 22682222]
34. Weinberg SE, Sena LA, Chandel NS. Mitochondria in the regulation of innate and adaptive immunity. Immunity. 2015; 42:406–417. [PubMed: 25786173]
35. Ganeshan K, Chawla A. Metabolic regulation of immune responses. Annu Rev Immunol. 2014; 32:609–634. [PubMed: 24655299]
36. Jha AK, Huang SC, Sergushichev A, Lampropoulou V, Ivanova Y, Loginicheva E, et al. Network integration of parallel metabolic and transcriptional data reveals metabolic modules that regulate macrophage polarization. Immunity. 2015; 42:419–430. [PubMed: 25786174]
37. Pearce EJ, Everts B. Dendritic cell metabolism. Nat Rev Immunol. 2015; 15:18–29. [PubMed: 25534620]
38. Everts B, Pearce EJ. Metabolic control of dendritic cell activation and function: recent advances and clinical implications. Front Immunol. 2014; 5:203. [PubMed: 24847328]
39. Pearce EL, Pearce EJ. Metabolic pathways in immune cell activation and quiescence. Immunity. 2013; 38:633–643. [PubMed: 23601682]
40. Everts B, Amiel E, Huang SC, Smith AM, Chang CH, Lam WY, et al. TLR-driven early glycolytic reprogramming via the kinases TBK1-IKKvarepsilon supports the anabolic demands of dendritic cell activation. Nat Immunol. 2014; 15:323–332. [PubMed: 24562310]
41. Krawczyk CM, Holowka T, Sun J, Blagih J, Amiel E, DeBerardinis RJ, et al. Toll-like receptor-induced changes in glycolytic metabolism regulate dendritic cell activation. Blood. 2010; 115:4742–4749. [PubMed: 20351312]

42. Michelucci A, Cordes T, Ghelfi J, Pailot A, Reiling N, Goldmann O, et al. Immune-responsive gene 1 protein links metabolism to immunity by catalyzing itaconic acid production. Proc Natl Acad Sci U S A. 2013; 110:7820–7825. [PubMed: 23610393]
43. Albina JE, Mastrofrancesco B. Modulation of glucose metabolism in macrophages by products of nitric oxide synthase. Am J Physiol. 1993; 264:C1594–C1599. [PubMed: 7687412]
44. Qualls JE, Subramanian C, Rafi W, Smith AM, Balouzian L, DeFreitas AA, et al. Sustained generation of nitric oxide and control of mycobacterial infection requires argininosuccinate synthase 1. Cell Host Microbe. 2012; 12:313–323. [PubMed: 22980328]
45. Qualls JE, Neale G, Smith AM, Koo MS, DeFreitas AA, Zhang H, et al. Arginine usage in mycobacteria-infected macrophages depends on autocrine-paracrine cytokine signaling. Sci Signal. 2010; 3:ra62. [PubMed: 20716764]
46. Cheng SC, Quintin J, Cramer RA, Shepardson KM, Saeed S, Kumar V, et al. mTOR- and HIF-1alpha-mediated aerobic glycolysis as metabolic basis for trained immunity. Science. 2014; 345:1250684. [PubMed: 25258083]
47. Everts B, Amiel E, van der Windt GJ, Freitas TC, Chott R, Yarasheski KE, et al. Commitment to glycolysis sustains survival of NO-producing inflammatory dendritic cells. Blood. 2012; 120:1422–1431. [PubMed: 22786879]
48. Mills CD, Kincaid K, Alt JM, Heilman MJ, Hill AM. M-1/M-2 macrophages and the Th1/Th2 paradigm. J Immunol. 2000; 164:6166–6173. [PubMed: 10843666]
49. Warburg O, Wind F, Negelein E. The Metabolism of Tumors in the Body. J Gen Physiol. 1927; 8:519–530. [PubMed: 19872213]
50. Chinopoulos C, Adam-Vizi V. Mitochondria as ATP consumers in cellular pathology. Biochim Biophys Acta. 2010; 1802:221–227. [PubMed: 19715757]
51. Beltran B, Mathur A, Duchen MR, Erusalimsky JD, Moncada S. The effect of nitric oxide on cell respiration: A key to understanding its role in cell survival or death. Proc Natl Acad Sci U S A. 2000; 97:14602–14607. [PubMed: 11121062]
52. Chouchani ET, Pell VR, Gaude E, Aksentijevic D, Sundier SY, Robb EL, et al. Ischaemic accumulation of succinate controls reperfusion injury through mitochondrial ROS. Nature. 2014; 515:431–435. [PubMed: 25383517]
53. Pan Y, Mansfield KD, Bertozzi CC, Rudenko V, Chan DA, Giaccia AJ, et al. Multiple factors affecting cellular redox status and energy metabolism modulate hypoxia-inducible factor prolyl hydroxylase activity in vivo and in vitro. Mol Cell Biol. 2007; 27:912–925. [PubMed: 17101781]
54. Dawiskiba T, Deja S, Mulak A, Zabek A, Jawien E, Pawelka D, et al. Serum and urine metabolomic fingerprinting in diagnostics of inflammatory bowel diseases. World J Gastroenterol. 2014; 20:163–174. [PubMed: 24415869]
55. Stephens NS, Siffledeen J, Su X, Murdoch TB, Fedorak RN, Slupsky CM. Urinary NMR metabolomic profiles discriminate inflammatory bowel disease from healthy. J Crohns Colitis. 2013; 7:e42–e48. [PubMed: 22626506]
56. Ariake K, Ohkusa T, Sakurazawa T, Kumagai J, Eishi Y, Hoshi S, et al. Roles of mucosal bacteria and succinic acid in colitis caused by dextran sulfate sodium in mice. J Med Dent Sci. 2000; 47:233–241. [PubMed: 12160236]
57. Baysal BE, Ferrell RE, Willett-Brozick JE, Lawrence EC, Myssiorek D, Bosch A, et al. Mutations in SDHD, a mitochondrial complex II gene, in hereditary paraganglioma. Science. 2000; 287:848–851. [PubMed: 10657297]
58. Rubic T, Lametschwandtner G, Jost S, Hinteregger S, Kund J, Carballido-Perrig N, et al. Triggering the succinate receptor GPR91 on dendritic cells enhances immunity. Nat Immunol. 2008; 9:1261–1269. [PubMed: 18820681]
59. Saqcena M, Mukhopadhyay S, Hosny C, Alhamed A, Chatterjee A, Foster DA. Blocking anaplerotic entry of glutamine into the TCA cycle sensitizes K-Ras mutant cancer cells to cytotoxic drugs. Oncogene. 2015; 34:2672–2680. [PubMed: 25023699]
60. Infantino V, Convertini P, Cucci L, Panaro MA, Di Noia MA, Calvello R, et al. The mitochondrial citrate carrier: a new player in inflammation. Biochem J. 2011; 438:433–436. [PubMed: 21787310]

61. Drose S. Differential effects of complex II on mitochondrial ROS production and their relation to cardioprotective pre- and postconditioning. Biochim Biophys Acta. 2013; 1827:578–587. [PubMed: 23333272]
62. Brunelle JK, Bell EL, Quesada NM, Vercauteren K, Tiranti V, Zeviani M, et al. Oxygen sensing requires mitochondrial ROS but not oxidative phosphorylation. Cell Metab. 2005; 1:409–414. [PubMed: 16054090]
63. Wen H, Gris D, Lei Y, Jha S, Zhang L, Huang MT, et al. Fatty acid-induced NLRP3-ASC inflammasome activation interferes with insulin signaling. Nat Immunol. 2011; 12:408–415. [PubMed: 21478880]
64. Morris SM Jr. Enzymes of arginine metabolism. J Nutr. 2004; 134:2743S–2747S. discussion 2765S-2767S. [PubMed: 15465778]
65. El Kasmi KC, Qualls JE, Pesce JT, Smith AM, Thompson RW, Henao-Tamayo M, et al. Toll-like receptor-induced arginase 1 in macrophages thwarts effective immunity against intracellular pathogens. Nat Immunol. 2008; 9:1399–1406. [PubMed: 18978793]
66. Mayer-Barber KD, Barber DL, Shenderov K, White SD, Wilson MS, Cheever A, et al. Caspase-1 independent IL-1beta production is critical for host resistance to mycobacterium tuberculosis and does not require TLR signaling in vivo. J Immunol. 2010; 184:3326–3330. [PubMed: 20200276]
67. Mishra BB, Rathinam VA, Martens GW, Martinot AJ, Kornfeld H, Fitzgerald KA, et al. Nitric oxide controls the immunopathology of tuberculosis by inhibiting NLRP3 inflammasome-dependent processing of IL-1beta. Nat Immunol. 2013; 14:52–60. [PubMed: 23160153]
68. Brown GC. Nitric oxide and mitochondrial respiration. Biochim Biophys Acta. 1999; 1411:351–369. [PubMed: 10320668]
69. Mateo RB, Reichner JS, Mastrofrancesco B, Kraft-Stolar D, Albina JE. Impact of nitric oxide on macrophage glucose metabolism and glyceraldehyde-3-phosphate dehydrogenase activity. Am J Physiol. 1995; 268:C669–C675. [PubMed: 7534983]
70. Saeed S, Quintin J, Kerstens HH, Rao NA, Aghajanirefah A, Matarese F, et al. Epigenetic programming of monocyte-to-macrophage differentiation and trained innate immunity. Science. 2014; 345:1251086. [PubMed: 25258085]
71. Luo W, Semenza GL. Emerging roles of PKM2 in cell metabolism and cancer progression. Trends Endocrinol Metab. 2012; 23:560–566. [PubMed: 22824010]
72. Yang W, Lu Z. Nuclear PKM2 regulates the Warburg effect. Cell Cycle. 2013; 12:3154–3158. [PubMed: 24013426]
73. Luo W, Semenza GL. Pyruvate kinase M2 regulates glucose metabolism by functioning as a coactivator for hypoxia-inducible factor 1 in cancer cells. Oncotarget. 2011; 2:551–556. [PubMed: 21709315]
74. Luo W, Hu H, Chang R, Zhong J, Knabel M, O'Meally R, et al. Pyruvate kinase M2 is a PHD3-stimulated coactivator for hypoxia-inducible factor 1. Cell. 2011; 145:732–744. [PubMed: 21620138]
75. Yang L, Xie M, Yang M, Yu Y, Zhu S, Hou W, et al. PKM2 regulates the Warburg effect and promotes HMGB1 release in sepsis. Nat Commun. 2014; 5:4436. [PubMed: 25019241]
76. Yang P, Li Z, Fu R, Wu H, Li Z. Pyruvate kinase M2 facilitates colon cancer cell migration via the modulation of STAT3 signalling. Cell Signal. 2014; 26:1853–1862. [PubMed: 24686087]
77. Demaria M, Poli V. PKM2, STAT3 and HIF-1alpha: The Warburg's vicious circle. JAKSTAT. 2012; 1:194–196. [PubMed: 24058770]
78. Demaria M, Giorgi C, Lebiedzinska M, Esposito G, D'Angeli L, Bartoli A, et al. A STAT3-mediated metabolic switch is involved in tumour transformation and STAT3 addiction. Aging (Albany NY). 2010; 2:823–842. [PubMed: 21084727]
79. Pranada AL, Metz S, Herrmann A, Heinrich PC, Muller-Newen G. Real time analysis of STAT3 nucleocytoplasmic shuttling. J Biol Chem. 2004; 279:15114–15123. [PubMed: 14701810]
80. Gao X, Wang H, Yang JJ, Liu X, Liu ZR. Pyruvate kinase M2 regulates gene transcription by acting as a protein kinase. Mol Cell. 2012; 45:598–609. [PubMed: 22306293]
81. El Kasmi KC, Holst J, Coffre M, Mielke L, de Pauw A, Lhocine N, et al. General nature of the STAT3-activated anti-inflammatory response. J Immunol. 2006; 177:7880–7888. [PubMed: 17114459]

82. Fielding CA, Jones GW, McLoughlin RM, McLeod L, Hammond VJ, Uceda J, et al. Interleukin-6 signaling drives fibrosis in unresolved inflammation. Immunity. 2014; 40:40–50. [PubMed: 24412616]

83. Manresa MC, Godson C, Taylor CT. Hypoxia-sensitive pathways in inflammation-driven fibrosis. Am J Physiol Regul Integr Comp Physiol. 2014; 307:R1369–R1380. [PubMed: 25298511]

84. Deng Y, Liu J, Han G, Lu SL, Wang SY, Malkoski S, et al. Redox-dependent Brca1 transcriptional regulation by an NADH-sensor CtBP1. Oncogene. 2010; 29:6603–6608. [PubMed: 20818429]

85. Shakespear MR, Hohenhaus DM, Kelly GM, Kamal NA, Gupta P, Labzin LI, et al. Histone deacetylase 7 promotes Toll-like receptor 4-dependent proinflammatory gene expression in macrophages. J Biol Chem. 2013; 288:25362–25374. [PubMed: 23853092]

86. Shakespear MR, Halili MA, Irvine KM, Fairlie DP, Sweet MJ. Histone deacetylases as regulators of inflammation and immunity. Trends Immunol. 2011; 32:335–343. [PubMed: 21570914]

87. Satoh T, Takeuchi O, Vandenbon A, Yasuda K, Tanaka Y, Kumagai Y, et al. The Jmjd3-Irf4 axis regulates M2 macrophage polarization and host responses against helminth infection. Nat Immunol. 2010; 11:936–944. [PubMed: 20729857]

88. Kruidenier L, Chung CW, Cheng Z, Liddle J, Che K, Joberty G, et al. A selective jumonji H3K27 demethylase inhibitor modulates the proinflammatory macrophage response. Nature. 2012; 488:404–408. [PubMed: 22842901]

89. Murray PJ. Understanding and exploiting the endogenous interleukin-10/STAT3-mediated anti-inflammatory response. Curr Opin Pharmacol. 2006; 6:379–386. [PubMed: 16713356]

90. Murray PJ, Smale ST. Restraint of inflammatory signaling by interdependent strata of negative regulatory pathways. Nat Immunol. 2012; 13:916–924. [PubMed: 22990889]

91. Murray PJ. STAT3-mediated anti-inflammatory signalling. Biochem Soc Trans. 2006; 34:1028–1031. [PubMed: 17073743]

92. Murray PJ. The primary mechanism of the IL-10-regulated antiinflammatory response is to selectively inhibit transcription. Proc Natl Acad Sci U S A. 2005; 102:8686–8691. [PubMed: 15937121]

Highlights

- Cellular metabolism links sensing of microenvironment with macrophage plasticity
- Metabolic adaptation towards aerobic glycolysis is a hallmark of inflammatory macrophage activation
- TCA cycle reprogramming and inhibition of mitochondrial respiration promote macrophage activation
- Argininosuccinate cycle is critical for sustaining macrophage activation
- Mitochondria are important in macrophage activation and deactivation

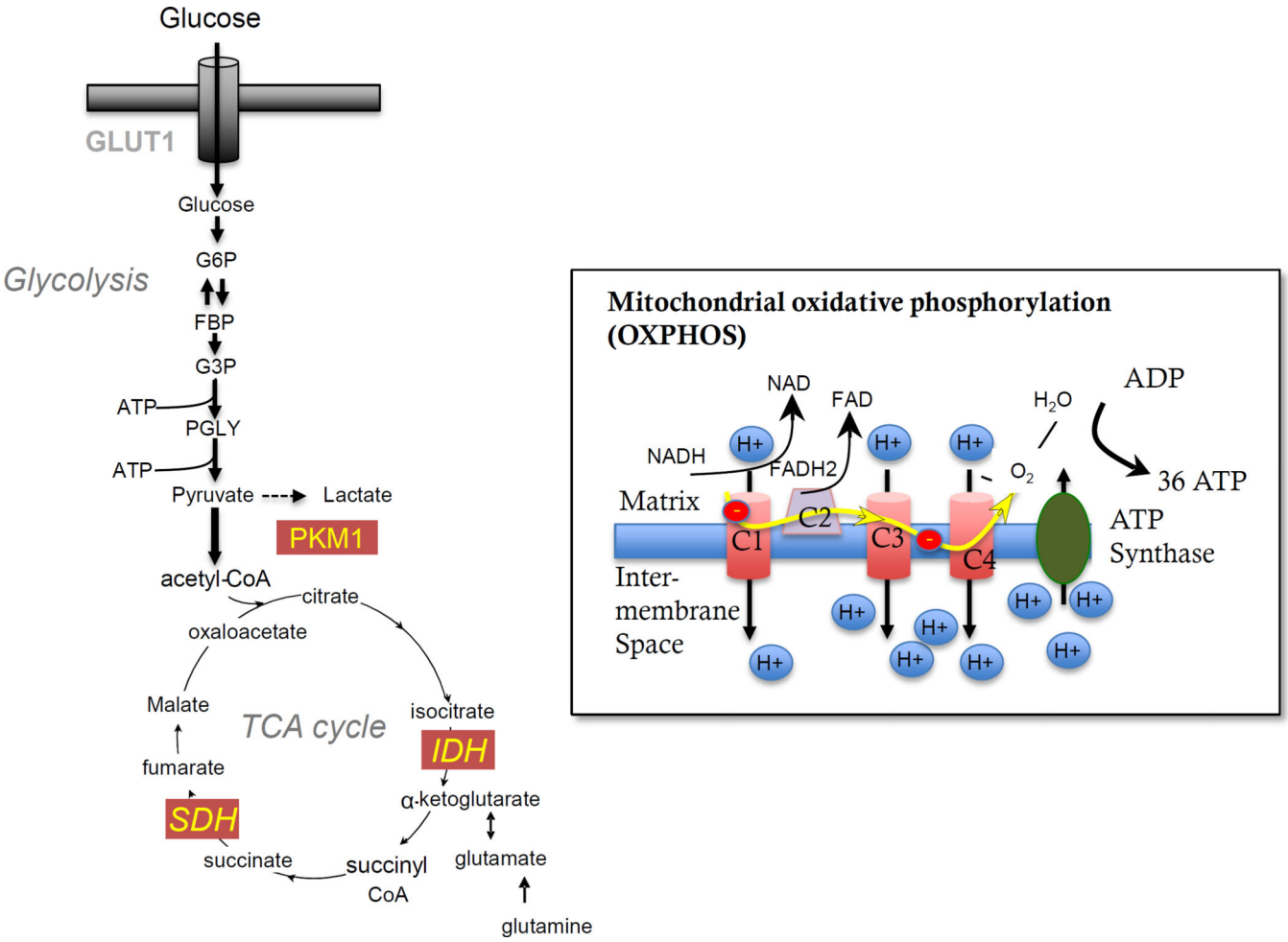

Figure 1. Integration of glycolysis with TCA cycle and mitochondrial oxidative phosphorylation

Shown are the glycolytic pathway and the mitochondrial TCA cycle. Also show is the mitochondrial respiratory chain when operating in oxphos. Electron transport (yellow line) enables proton gradient, which is used to generate ATP by ATP synthase after oxygen has served as the terminal electron acceptor at complex 4.

G6P: glose-6-phosphate; FBP: Fructose bisphosphatase; G3P: Glyceraldehyde 3-phosphate; PGLY: 3-phosphoglycerolphopsphate; Trnasort chin complexes (C-C4).

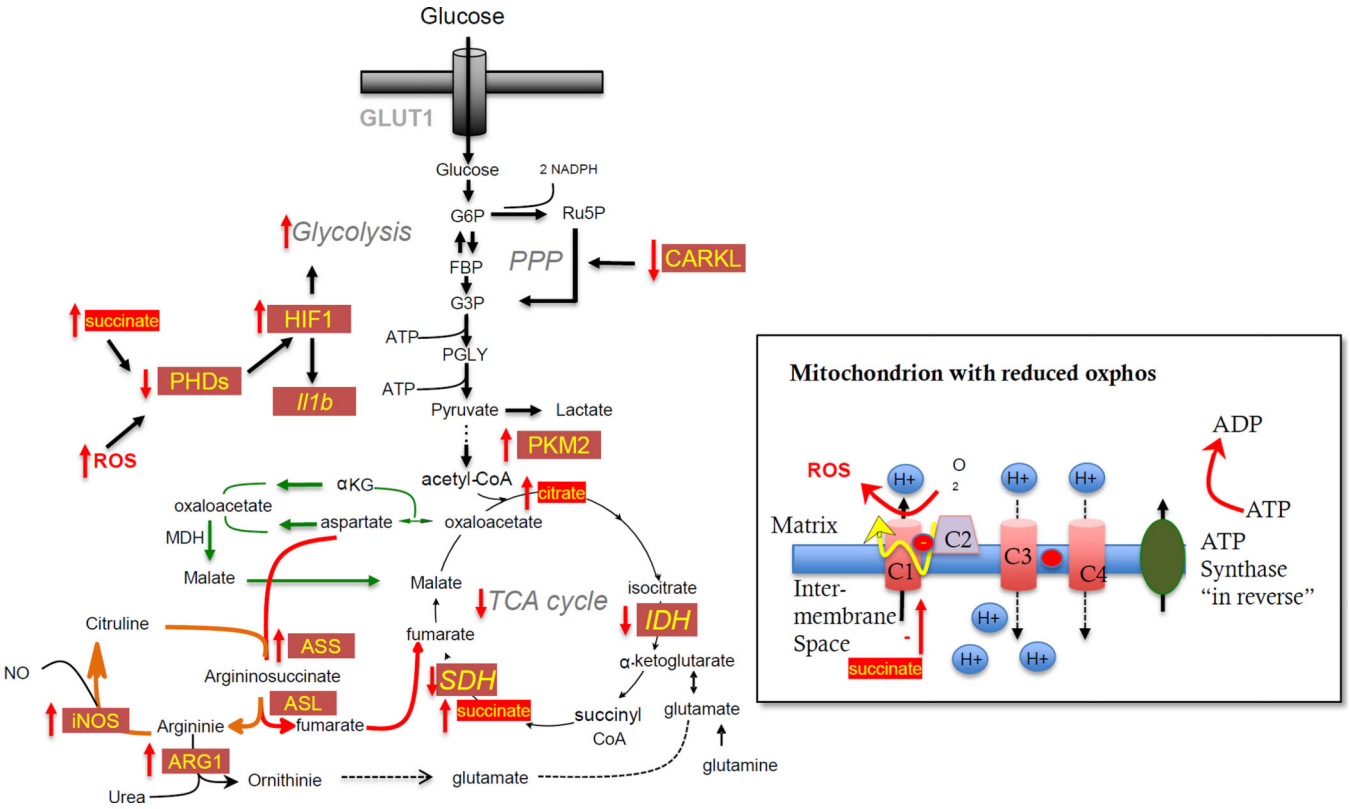

Figure 2. Metabolic adaptations in the inflammatory macrophage

Metabolic reprogramming of the inflammatory (LPS/IFNγ activated) macrophage involves increased expression of HIF1 and PKM2 protein, which increases glycolysis. Concomitant suppression of CARKL increases the pentose phosphate pathway (PPP), providing antioxidants reducing equivalents (NADPH). ATP generated by glycolysis is used to maintain energy demands in the face of concomitantly reduced mitochondrial respiration (reduced oxphos), which occurs secondary to inhibition of SDH (which is complex II, C2). Glycolysis derived ATP is also used to fuel "in reverse" operating ATP synthase in the mitochondria in order to maintain membrane potential and mitochondrial integrity. The inhibition of SDH promotes accumulation of succinate, which inhibits cytosolic prolylhydroxylases (PHDs) which usually mediate HIF1 degradation, thus increasing HIF1 stabilization and thus increased transcription of *Il1b* and glycolytic enzymes, and Arginase1. Succinate also inhibits complex I in the mitochondria which promotes ROS generation, which in turn enhances PHD inhibition and cytokine generation through stabilization of HIF1. In addition, expression of IDH is suppressed, resulting in citrate accumulation. To maintain anerplerosis of TCA cycle intermediates, inflammatory macrophages upregulate the argininosuccinate and citrulline-arginine cycle (orange), modify the malate aspartate shuttle (green) towards utilization of the argininiosuccinate cycle (red). This maintains fumarate anerplerosis and regenerates arginine for NO synthesis by iNOS. Furthermore, Arginine can be used for glutamate synthesis to replenish the TCA cycle in order to maintain succinate generation. Upregulation of the argininosuccinate and citrulline-arginine cycle also makes cells less sensitive to extracellular arginine limitation. NO also inhibits the respiratory chain further enhancing ROS production and succinate accumulation (not

depicted). In the mitochondria, disruption of electron transport chain (inhibition of SDH that is Complex2, and production of NO) promotes reverse electron transport on complex 1 (yellow line), which increase ROS formation. Reduced proton gradient reduced membrane potential (not shown), which is prevented from breaking down completely by ATP synthase operating in reverse.

ASS: Argininosuccinate synthase; ASL: Argininosuccinate lyase; a-KG: alpha-ketoglutarate; C1-C4: complexes of the mitochondrial respiratory electron transport chain 1–4. PHDs: prolyl hydroxylases; iNOS: inducible nitric oxide synthase; OXPHOS: oxidative phosphorylation; NO: nitric oxide; Glut1: glucose transporter1; HIF: hypoxia inducible factor; IDH: isocitrate dehydrogenase; SDH: succinate dehydrogenase; CARKL: carbohydrate kinase-like protein